Master's thesis

NTNU
Norwegian University of Science and Technology
Faculty of Natural Sciences
Department of Physics

Halvor Sæther

Neutron and Quark Stars

From Non-Interacting Matter to Dense QCD

Master's thesis in Applied Physics and Mathematics
Supervisor: Jens Oluf Andersen
June 2020

NTNU
Norwegian University of
Science and Technology

Halvor Sæther

Neutron and Quark Stars

From Non-Interacting Matter to Dense QCD

Master's thesis in Applied Physics and Mathematics
Supervisor: Jens Oluf Andersen
June 2020

Norwegian University of Science and Technology
Faculty of Natural Sciences
Department of Physics

NTNU
Norwegian University of
Science and Technology

Abstract

In this master's thesis we study many of the key features in determining the structure and upper mass limit of compact stars, in particular neutron stars and strange quark stars. We start off with an introduction to the Tolman–Oppenheimer–Volkoff equation of hydrostatic equilibrium and solve it for a few different equations of state describing non-interacting matter: uniform energy density, linear equation of state, polytropes and an ideal Fermi gas of neutrons. The last of these resulted in an upper mass limit of approximately 0.71 solar masses. Next we examine in detail some of the most important approximations and assumptions applied in this field of research: the use of a flat spacetime metric in quantum field theoretical calculations, the zero temperature approximation, chemical equilibrium, and the assumption of local electric charge neutrality. In the final chapter we study strange matter and strange stars in the framework of perturbative quantum chromodynamics. With leading-order quantum corrections to the grand potential and a running mass for the strange quark, we find an upper mass limit of approximately 1.52 solar masses. By comparing this to the case of completely massless strange matter we learn that the running of the strange quark mass is crucial for the structure of strange stars; the upper mass limit is reduced by approximately 22%.

Sammendrag

I denne masteroppgaven tar vi for oss mange av hovedtrekkene knyttet til det å bestemme strukturen og den øvre massegrensen til kompakte stjerner, spesielt nøytronstjerner og kvarkstjerner. Vi begynner med en innføring i TOV-ligningen for hydrostatisk likevekt og løser den for en rekke tilstandsligninger som beskriver ikke-vekselvirkende materie: uniform energitetthet, lineær tilstandsligning, polytroper og en ideell Fermi-gass av nøytroner. Sistnevnte tilstandsligning gir en øvre massegrense på omtrent 0.71 solmasser. Deretter følger en detaljert gransking av noen av de aller viktigste approksimasjonene og antagelsene som anvendes i forskningsfeltet: bruken av Minkowski-metrikken i kvantefeltberegniner, null-temperatureapproksimasjonen, kjemisk likevekt og antagelsen om lokal elektrisk nøytralitet. I det avsluttende kapittelet studerer vi kvarkstjerner bestående av opp, ned og s-kvarker i sammenheng med perturbativ kvantekromodynamikk. Med ledende ordens kvantekorreksjoner til det termodynamiske potensialet og løpende masse for s-kvarkene finner vi en øvre massegrense på omtrent 1.52 solmasser. Ved å sammenligne dette med tilfellet hvor alle kvarkene er masseløse lærer vi at en løpende masse for s-kvarkene er helt avgjørende for strukturen til kvarkstjernene; den øvre massegrensen reduseres med omtrent 22%.

Acknowledgements

I would like to thank my supervisor Professor Jens O. Andersen for providing me with very valuable guidance and feedback throughout my work with this master's thesis. I would also like to thank my close friend Martin Aria Mojahed for all the support and the fruitful discussions on quantum field theory. Lastly, I would like to thank all my friends and classmates for creating a wonderful and supportive environment throughout my years as a student.

Contents

1 Introduction

Since the dawn of our existence, humans have gazed upon the night sky with humility and wonder. Thanks to modern science, we now have answers to many of the questions asked by our ancestors, from our position in the solar system to the scale of the entire observable universe. But the more we learn about the Universe, the more peculiar it becomes, and new questions emerge. Soon after James Chadwick's discovery of the neutron in 1932, theoretical physicists discussed the possible existence of stellar remnants consisting almost entirely of neutrons. The first discovery of such a star was made in 1967 by Jocelyn Bell, almost three decades after the first theoretical publication on the subject. With the later advancements in particle physics, particularly the discovery of quarks, it was natural to ask if even more exotic stars exist out there, hidden away in the dark corners of the Universe.

We start off this introductory chapter by outlining the birth and death of a high-mass star, basing our presentation on [1, 2]. The end of this life cycle marks the birth of a compact star — the type of star whose structure will be studied in this master's thesis. We then give a brief overview of the research field of neutron and quark stars, followed by an introduction to general relativity, Einstein's field equation and the equation of hydrostatic equilibrium. Finally, we describe the structure of this thesis. (Note that Section 1.1 and 1.2 were written as part of a project the author did in the fall semester of 2019.)

1.1 Stellar Evolution

The formation of a star begins with the formation of a sufficiently massive, dense and cold cloud of gas and dust, consisting mainly of hydrogen and helium. Such a cloud will have an inward force of gravity that exceeds its outward thermal pressure. Inevitably, the cloud contracts, resulting in an increase in density. The temperature, on the other hand, remains low because the increase in thermal energy is radiated away into space. At some point the cloud becomes so dense that the photons carrying the radiant energy will have trouble escaping. The temperature and thermal pressure quickly rise, and the contraction is considerably slowed down. The cloud has now become a *protostar*, the next stage of stellar evolution. From here, the temperature inside the star will gradually rise over a duration of several million years. Eventually the temperature in the center of the star reaches about 10 million kelvin, at which point the temperature is high enough for hydrogen to fuse into helium. The gravitational contraction comes to a halt, and with that, we say that a star is born. It is no longer a protostar, but a *main-sequence star*.

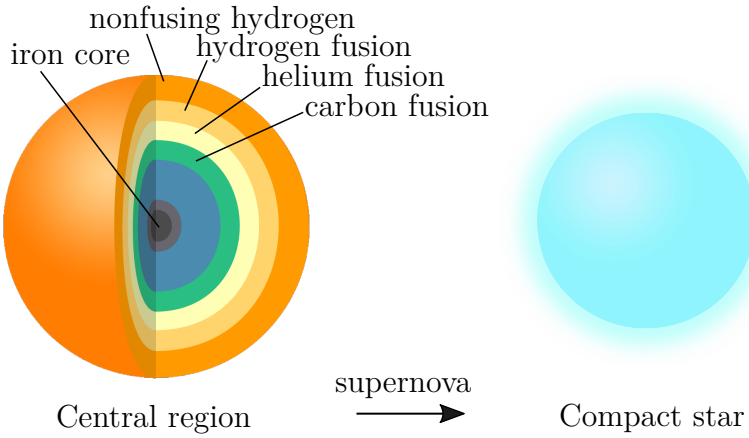

Figure 1.1: To the left is the central region of a star whose life is nearing its end. The core collapses into a compact star when it becomes rich with iron. The figure is not to scale.

The overwhelming majority of stars in the Universe are classified as main-sequence stars, and they are all characterized by the fact that they only fuse hydrogen into helium. The fusion process occurs exclusively in the central region of the star, where the temperature is the highest. After millions of years, the hydrogen fuel will become exhausted, leaving behind a central volume of almost pure helium. We refer to this central volume as the *core*. The outer layer, on the other hand, still consists of nearly pure hydrogen and is called the *envelope*. With the lack of energy output from fusion, both the core and the envelope will contract. Soon, hydrogen will start to fuse in a shell around the core, adding more helium to it. This amplifies the inward gravitational pull. At the same time, energy is released into the outer layer, causing it to expand. The core and the shell will continue to contract while the star as a whole grows larger until the temperature in the core is high enough for helium to fuse into carbon. When this happens, equilibrium is again restored, and the star has become a *red giant*.

For sufficiently massive stars, the process described above involving hydrogen and helium will repeat for successively heavier elements, creating an onion-like structure with layers upon layers of shells around the core. Each of these shells will be fusing a different element. Helium fuses with carbon to create oxygen, with oxygen to create neon, and so on, see Figure 1.1 for a rough sketch. But when the innermost regions of the star experience a buildup of iron, something dramatic is about to happen. The process of fusing iron does not release energy, neither does fission; on the contrary, they both require it. Thus, gravity completely gets the upper hand. Not even the electron degeneracy pressure resulting from the Pauli exclusion principle will be able to resist the pull of gravity. Electrons are therefore forced to combine with protons to form neutrons and neutrinos. The electron degeneracy pressure instantly vanishes, and in a fraction of a second, the core collapses. The collapse releases an inconceivable amount of energy in a spectacular explosion called a supernova, blowing the outer layers off at a speed of 10,000 kilometers per second; an event that can outshine an entire galaxy.

What happens next depends heavily on the core's mass. A core with a mass of around 1.4–2.2 $M_\odot$ (solar masses) will collapse into a ball of neutrons with a diameter of only a few kilometers. The density becomes extremely high, resulting in a pressure from both neutron degeneracy and the strong force. The combined pressure will be able to withstand gravity and so a *neutron star* is formed; a type of *compact star*. It has long been suggested that for sufficiently massive neutron stars, there is not only degeneracy pressure from neutrons that supports the star against gravity. In the central parts of a neutron star, the density might become so high that the neutron matter undergoes a phase transition to quark matter, resulting in a new degeneracy pressure between the quarks. However, if the mass of the neutron star were to exceed the *upper mass limit* at around 2.2 $M_\odot$, we know that there would be nothing that could resist the pull of gravity. The core would then have to keep collapsing, eventually forming a black hole.

1.2 Neutron and Quark Stars

In 1939, only seven years after the discovery of the neutron, Robert Oppenheimer and his student George Volkoff published the paper "On Massive Neutron Cores", marking the beginning of research on neutron stars. In their paper they assumed that the neutrons form a cold, ideal Fermi gas, therefore neglecting thermal energy and interactions. The upper mass limit of neutron stars was approximated to $\sim 0.7 M_\odot$ [3]. This was done in the very early days of quantum theory. Today the upper mass limit of neutron stars is referred to as the Tolman-Oppenheimer-Volkoff limit, and very recent electromagnetic and gravitational-wave information from a merging neutron star pair along with simulations has placed the limit at $\sim 2.17 M_\odot$ [4–6]. There is no doubt that neutron stars are strange objects. With a mass comparable to that of our own Sun, they have a radius of only about 10 kilometers [7]. The density is therefore extremely high by terrestrial standards, especially in the central regions where it is expected to exceed the nuclear saturation density $\rho_{\text{sat}} = 2.8 \times 10^{14}$ g cm^{-3}.

Because of the inability to reach densities similar to those of neutron star cores in experiments here on Earth, advancements on the subject of neutron stars heavily rely on astrophysical observations combined with theoretical calculations. A major challenge is to find the correct equation of state describing the matter, with the search being led by QCD calculations and effective models. One of many open questions regarding neutron stars is whether and how the matter in the central regions should be described as individual quarks rather than as nucleons [7]. With the use of general relativity, a given equation of state yields a specific mass-radius relation that must agree with observations if it is to be the correct one. Looking at it the other way around: measurements of neutron stars place strong constraints on the properties of matter at very high densities. Thus, the motivation for studying neutron star lies not only in our interest to understand the objects themselves, but also because they are essentially giant laboratories suited for probing matter under extreme conditions.

The possible existence of quark matter (matter whose degrees of freedom are those of quarks and gluons) in the central regions of certain astronomical objects

was hypothesized by Ivanenko and Kurdgelaidze as early as in 1965 [8]. If such objects exist, they are most likely neutron stars with a quark-matter core, which we refer to as hybrid stars. The existence of quark-matter cores in the most massive neutron stars is highly probable [9, 10]. Since the early 2000s, several neutron stars that might actually happen to be hybrid stars have been observed, but no observations have been conclusive. It could also be that there exists stars out there that are completely made of quark matter called quark stars. This could be the case if nuclear matter is not the absolute ground state of matter after all, but quark matter is. In 2016 it was suggested that the extremely luminous supernova ASASSN-15lh might have been the signature of a newborn quark star [11]. Although many neutron stars have been observed, as of now, hybrid and quark stars are yet to be discovered.

1.3 General Relativity and Hydrostatic Equilibrium

> "I was sitting in a chair in the patent office in Bern when all of a sudden a thought occurred to me: If a person falls freely he will not feel his own weight. I was startled. This simple thought made a deep impression on me. It impelled me toward a theory of gravitation." —Albert Einstein

In 1905, Einstein presented his theory of special relativity, and its consequences shook physics to its foundation. Our new reality included time dilation, length contraction, mass-energy equivalence, relativity of simultaneity, and speed of light as the universal speed limit. Einstein had successfully accomplished his goal of making Newtonian mechanics compatible with electromagnetism. The success of special relativity had major implications on other fields of physics as well, most notably on gravitation; Newton's theory of gravity is not Lorentz covariant and does therefore not yield the same physics in all inertial frames. This inconsistency with the principle of relativity made it clear that Newton's theory did not tell the whole story of gravity [12, p. 107].

In 1907, Einstein had what he called the happiest thought of his life: "If a person falls freely he will not feel his own weight." This seemingly simple thought became the origin of what we now call the Einstein equivalence principle (EEP)—the foundational principle that led Einstein to a new theory of gravity. To formulate the EEP, we start with a simple thought experiment in the context of Newtonian gravity: imagine finding yourself in a spaceship far into deep space and far away from any source of gravitational field. The spaceship is traveling with constant velocity. If you drop an apple, it just floats in place. But the same would happen if the spaceship was in free fall in a gravitational field of a massive object (with no atmosphere). Unfortunately, there are no windows on the spaceship. How then can you truly know that you are deep into empty space rather than falling freely in some gravitational field? The two situations are perfectly equivalent.

We can imagine a similar scenario but this time the spaceship's engine is throttled so that it provides a constant acceleration g equal to the local gravitational acceleration on, say, the surface of the Moon. If you drop an apple, the floor accelerates towards it with acceleration g. This situation is perfectly equivalent to the

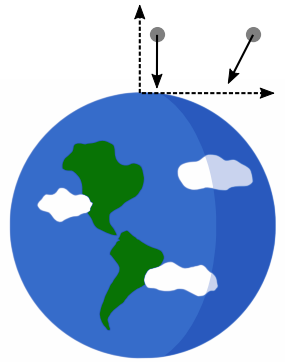

Figure 1.2: The Einstein equivalence principle holds only locally.

rocket standing still at the surface of the Moon. One cannot differentiate between a gravitational field and uniform acceleration by watching the trajectories of freely falling objects. Einstein took this principle a step further by suggesting that there is no way whatsoever to distinguish between uniform acceleration and a gravitational field, no matter the experiment [13, p. 50]. One very crucial detail must be added to this statement, however: it only applies to small enough regions of space. If, for example, we constructed a Lorentz frame at the North Pole and followed a tangent far enough out into space, then objects would fall on an incline with respect to the vertical axis, see Figure 1.2. Thus, we would know that we are in a gravitational field. The EEP can therefore be formulated as follows: *In small enough regions of spacetime, the laws of physics reduce to those of special relativity; it is impossible to detect the existence of a gravitational field by means of local experiments* [13, p. 50].

Let us now consider a phenomenon that was predicted by the EEP — gravitational redshift. We briefly summarize the discussion in [13, p. 52]. Imagine two spaceships far away from any source of gravitational field. They both travel with the same constant acceleration g, one in front of the other. The trailing spaceship sends out a beam of light with wavelength λ_0, which is redshifted by the conventional Doppler effect (assuming the acceleration is not too high) to λ_1 by the time it reaches the leading spaceship. Now, the EEP tells us that this situation is perfectly equivalent to two observers on Earth, one located at the top of a tall tower and the other beneath it. The observer beneath the tower sends out a beam of light with wavelength λ_0, and since this situation is equivalent to the one with the spaceships, we can immediately conclude that the light received by the observer in the tower is redshifted to λ_1. This is called gravitational redshift.

Since the frequencies measured by the two observers differ, the time they measure between the start of a wavelength to its end also differ. Note that we still assume Newtonian gravity, and in particular that spacetime is flat. The observer on the ground emits the beam of light at a height z_0 and measures Δt_0 as the period of a wavelength, while the observer in the tower measures the light at z_1 with a wave period of Δt_1. Since we assume the gravitational field and everything but the light to be static, the leading and trailing edge of an emitted wave must follow congruent paths through spacetime, as illustrated in Figure 1.3. Looking at the figure, this seems to indicate that the time intervals measured by the two observers are equal, which, from the above discussion, they are clearly not. The issue must lie

in our assumption that spacetime is flat — the spacetime through which the photons traveled must be curved.

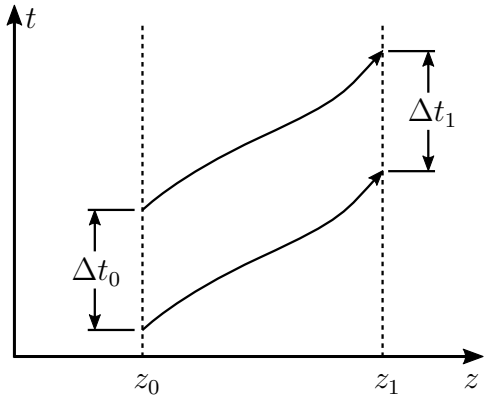

Figure 1.3: A spacetime diagram illustrating the breakdown of Euclidean geometry in the gravitational redshift experiment: whatever spacetime paths the photons take must be congruent, and thus the time intervals must be equal according to this diagram, but the observed time intervals are different [13, p. 54].

The appropriate mathematical structure for describing curved spaces is a differentiable manifold. An n-dimensional manifold is very loosely defined as a set of points with the property that every point has a neighborhood homeomorphic to $\mathbb{R}^n$. Einstein defined spacetime as a four-dimensional differentiable manifold with a Lorentzian metric tensor. An important property is that at every point p we can find a local coordinate system in which the metric components equal those of the flat Minkowski metric, and, furthermore, that all first-order derivatives of the metric vanish [13, p. 73],

$$g_{\mu\nu}(p) = \eta_{\mu\nu}, \qquad \partial_\rho g_{\mu\nu}(p) = 0. \tag{1.1}$$

The second-order derivatives, however, can not all be made to vanish. This property resonates with the EEP: in small enough regions of spacetime, the laws of physics reduce to those of special relativity.

If the curvature of spacetime is what we perceive as gravity and gravity as we know it from Newtonian mechanics depends on the distribution of matter, then it should be possible to find an equation of motion relating the matter distribution of spacetime to its curvature. This equation is called Einstein's field equation,

$$R_{ab} - \tfrac{1}{2}Rg_{ab} = 8\pi G T_{ab}. \tag{1.2}$$

It is an equation between tensor fields defined on the curved spacetime manifold. Alternatively, one can view it as six independent equations between the components of the tensors expressed in any preferable coordinate system. On the right side is the energy-momentum tensor T_{ab}, which contains information about the matter distribution in spacetime. On the left side we find the Ricci tensor, the Ricci scalar and the metric tensor. Both the Ricci tensor and the Ricci scalar are derived from the metric tensor, through products and derivatives up to second order of it, and thus Einstein's equation is really just an equation relating T_{ab} to g_{ab}.

In Appendix C we show how Einstein's field equation can be derived from a variational principle. The beauty of that particular approach lies in the fact that the so-called Einstein-Hilbert action can be shown to be the simplest possible non-trivial action one can construct from the metric tensor. Einstein's field equation can also be derived from a less formal strategy, by trying to generalize the Newtonian field equation through a series of plausibility arguments. The Newtonian field equation reads

$$\nabla^2\Phi = 4\pi G\rho, \tag{1.3}$$

where Φ is the gravitational potential and ρ is the mass density. We will not go over this approach here (see [13] instead), but one could first of all reason that the general relativistic version of Eq. (1.3), i.e., Einstein's equation, should be an equation between tensors to satisfy the requirement of Lorentz covariance. Second, it is quite natural to generalize the right side to be the energy-momentum tensor. Furthermore, since the Newtonian field equation contains second order derivatives of Φ, it is also quite natural to assume that the general relativistic equation should have second order derivatives of the metric.

Einstein's field equation is undoubtedly beautiful. At first glance it appears almost simple, but that is far from the truth; it contains 6 independent, non-linear, partial differential equations. The Ricci scalar is the trace of the Ricci tensor, which is a contraction of the Riemann curvature tensor, which furthermore is composed of products and derivatives of the metric and the inverse metric. Nevertheless, solutions to the equation do exist. The most famous one is the Schwartzschild solution, which can be derived by assuming vacuum, $T_{ab} = 0$, and a static, spherically symmetric metric. The solution is appropriate for describing the exterior of, for example, stars and black holes — matter distributions that are (approximately) spherically symmetric and static. For the interior, one usually assumes a perfect fluid,

$$T_{ab} = \rho u_a u_b + P(g_{ab} + u_a u_b), \tag{1.4}$$

where ρ is the rest-frame energy density, and P is the isotropic rest-frame pressure. With a particular choice of metric, namely a static, spherically symmetric metric, Einstein's field equation reduces to the following equations in Schwarzschild coordinates:

$$\frac{dP}{dr} = -(\rho + P)\frac{Gm(r) + 4\pi Gr^3 P}{r[r - 2Gm(r)]}, \tag{1.5}$$

$$\frac{dm}{dr} = 4\pi r^2 \rho, \tag{1.6}$$

$$\frac{d\alpha}{dr} = -\frac{1}{\rho + P}\frac{dP}{dr}. \tag{1.7}$$

These equations are derived in detail in Appendix D. The first one is the Tolman–Oppenheimer–Volkoff (TOV) equation of hydrostatic equilibrium. It constrains the structure of a static, spherically symmetric star and is without a doubt the most important equation in this thesis and in the study of neutron stars and quark stars in general. The variables m and α specifies the metric, which is of the form

$$ds^2 = -e^{2\alpha(r)}dt^2 + \left[1 - \frac{2Gm(r)}{r}\right]^{-1} dr^2 + r^2 d\Omega. \tag{1.8}$$

Now, the set of equations above are actually not closed. One way to achieve a closed set is to specify an equation of state (EOS) for the matter,

$$P = P(\rho), \tag{1.9}$$

where the entropy is assumed to be small and usually neglected [13, p. 233]. One of the main challenges in the study of compact stars is to determine the appropriate EOS. However, given any EOS, the only independent parameter left is the central pressure of the spherical mass distribution $P_c = P(r = 0)$. If we prescribe this boundary condition, the TOV equation can be solved, yielding a total mass M from integrating Eq. (1.6) and a radius R from the definition $P(r = R) = 0$. By solving the TOV equation for a range of central densities we get a mass-radius relation — a curve of M versus R. Furthermore, in general relativity the curve will have a maximum. This is of central importance in this field of research; if our model of the EOS is realistic, the observed masses and radii of compact stars should lie along the curve, and their masses should also not exceed the maximum.

1.4 Thesis Outline

The purpose of this thesis is to study many of the key features of determining the structure and upper mass limit of neutron and quark stars. The topics we shall cover should be of great interest to someone who are new to the research field.

At the center of it all is the TOV equation. We therefore start off by getting familiar with it in Chapter 2. We discuss the basic criteria that any physically reasonable solution should satisfy, and we explore the differences between general relativity and Newtonian gravity. At this point we only consider quite simple equations of state describing non-interacting matter.

In Chapter 3 we examine in detail some of the most important approximations and assumptions applied in this field of research. The explanations and motivations behind them given in the literature are often quite vague or buried deep. Very important is the zero temperature approximation, because it greatly simplifies calculations. The temperature of neutron stars is actually on the order of 10^6 kelvin, and so it seems rather strange to approximate it as zero. To be able to solve the TOV equation for matter consisting of several particle species we must also discuss local electric charge neutrality and chemical equilibrium; the pressure and the energy density of such matter are generally parameterized by the chemical potentials of all of the different particle species. For the system of equations to be closed, it is important that the number of independent chemical potentials is reduced to one.

In Chapter 4 we study a type of quark star called strange stars. Their matter consist of up, down and strange quarks and electrons. While Chapter 2 was all about non-interacting matter, this chapter covers interactions between quarks in the context of perturbative quantum chromodynamic. Usually, the up and down quarks and the electrons are approximated as massless. The importance of a finite mass for the strange quark will be examined and mass-radius relations for several increasingly complex models will be calculated. This chapter is also where we apply

the results of Chapter 3.

Three of the appendices in this thesis were written as parts of a project of mine during the fall semester of 2019. These are Appendix C, D and E, and **they must not be considered a part of this thesis during evaluation.**

2 Non-Interacting Matter and the TOV Equation

In Appendix D the Tolman–Oppenheimer–Volkoff (TOV) equation of hydrostatic equilibrium is introduced in the form of a detailed derivation. The equation constrains the structure of a static, spherically symmetric mass distribution, and reads

$$\frac{dP}{dr} = -(\rho + P)\frac{Gm(r) + 4\pi G r^3 P}{r[r - 2Gm(r)]}, \tag{2.1}$$

where ρ is the rest frame energy density, P is the isotropic rest frame pressure, and $m(r)$ is given implicitly by the mass continuity equation

$$\frac{dm}{dr} = 4\pi r^2 \rho. \tag{2.2}$$

These two equations are collectively referred to as the structure equations. However, they do not constitute a closed set of equations by themselves. A third equation is needed for that, which is usually taken to be an equation of state (EOS) describing the fluid matter,

$$P = P(\rho). \tag{2.3}$$

We also need two boundary conditions: $m(r = 0) = 0$ and $P(r = 0) = P_c$. The former condition is required for the metric to be smooth at $r = 0$ [14, p. 126], while the latter can be arbitrarily specified. If our chosen EOS is physically reasonable, the pressure will vanish at some finite value of the radial coordinate, which naturally will be defined as the radius of the star $R = r(P = 0)$. We can then define the mass of the star as $M = m(R)$. If we solve the structure equations for a particular P_c, we get a certain mass and radius, which of course will depend on the EOS used. Thus, by solving for a wide range of central pressures we get a mass-radius relation $M(R)$ unique to that EOS. If experimental observations of star masses and radii happen to lie nicely along our calculated $M(R)$ curve, then we can assume that our EOS provides a suitable description of the matter inside the star. We will see that the $M(R)$ curves have a maximum in general relativity, and so, in particular, if our EOS provides a good model for, say, neutron stars, then we should not be able to observe such stars with mass greater than the calculated maximum.

The TOV equation is also often written in the form

$$\frac{dP}{dr} = -\frac{G\rho(r)m(r)}{r^2}\left[1 + \frac{P(r)}{\rho(r)}\right]\left[1 + \frac{4\pi r^3 P(r)}{m(r)}\right]\left[1 - \frac{2Gm(r)}{r}\right]^{-1}. \tag{2.4}$$

This way it becomes more apparent how the equation differs from the corresponding equation of hydrostatic equilibrium from Newtonian gravity, which reads

$$\frac{dP}{dr} = -\frac{G\rho(r)m(r)}{r^2}, \tag{2.5}$$

where $m(r)$ is still defined by Eq. (2.2). The Newtonian equation can easily be derived from either Euler's equation or summation of forces on infinitesimal volume elements. We see that the three bracketed factors in Eq. (2.4) are what constitute the general relativistic corrections. Since the right-hand side of that equation is always more negative than the right-hand side of Eq. (2.5), the central pressure needed to sustain a given mass distribution against gravity is always higher in general relativity than in Newtonian gravity. Both equations of hydrostatic equilibrium appear rather singular at the origin, but they are in fact regular. This is discussed and proven for the TOV equation in [15].

As mentioned by Harko and Mak in [16], there are some criteria that any physically reasonable solution of the structure equations should satisfy:

1. The pressure and the energy density must be finite and positive at the origin.

2. Both the pressure and the energy density must be monotonically decreasing from the origin to the surface.

3. The pressure must vanish at the surface.

4. Causality requires that the speed of sound inside the star cannot be faster than the speed of light.

5. It should be possible to join the resulting interior metric continuously with the exterior Schwarzschild metric.

We can check the causality requirement for a given EOS using the formula for the speed of sound from relativistic hydrodynamics [17, p. 52],

$$v_s = \sqrt{\frac{\partial P}{\partial \rho}}. \tag{2.6}$$

The focus of this chapter will be on solutions involving non-interacting matter. Our goal is to work our way up to the case of an ideal Fermi gas at zero temperature, which must be solved numerically. Our interest in the ideal Fermi gas stems from the fact that it provides the zeroth order term of perturbation expansions in the interacting quantum theories QED and QCD. A few simpler EOS will be considered before we get there, of which some are analytical. Despite the long history of research on the TOV equation, not many analytical solutions exist, and they all assume equations of state that are too simple to be realistic. Nevertheless, it is instructive to study a few of them, and they do indeed provide some physical insight.

2.1 Uniform Energy Density

Perhaps the simplest model of a star is the one where we assume the matter to be an incompressible fluid. This simply means that the energy density is constant all the way from the center to the surface $r = R$,

$$\rho(r) = \begin{cases} \rho_0, & r \leq R \\ 0, & r > R \end{cases}. \tag{2.7}$$

Here $\rho(r)$ simply takes the place of an equation of state. Integrating Eq. (2.2) becomes trivial in this case, yielding

$$m(r) = \begin{cases} \frac{4}{3}\pi r^3 \rho_0, & r \leq R \\ \frac{4}{3}\pi R^3 \rho_0 = M, & r > R \end{cases}. \tag{2.8}$$

Substituting $m(r)$ for $r \leq R$ into the equation of hydrostatic equilibrium, Eq. (2.1), leads to

$$\frac{dP}{dr} = -(\rho_0 + P)\frac{(4\pi/3)G\rho_0 r^3 + 4\pi G r^3 P}{r[r - (8\pi/2)G\rho_0 r^3]} = -\frac{4\pi}{3}G(\rho_0 + P)\frac{(\rho_0 + 3P)r}{1 - 8\pi G\rho_0 r^2/3}. \tag{2.9}$$

We can now separate the variables and integrate from some distance r within the mass distribution to the surface where the pressure is zero,

$$\int_{P(r)}^{0} \frac{dP'}{(\rho_0 + P')(\rho_0 + 3P')} = -\frac{4\pi}{3}G\int_r^R \frac{r'dr'}{1 - 8\pi G\rho_0 r^2/3}. \tag{2.10}$$

Doing the integrals and using $M = (4\pi/3)R^3\rho_0$ results in

$$\frac{1}{2\rho_0}\ln\left(\frac{\rho_0 + P}{\rho_0 + 3P}\right) = \frac{1}{4\rho_0}\ln\left(\frac{1 - 2GM/R}{1 - 2GMr^2/R^3}\right), \tag{2.11}$$

which when solved for P gives

$$P(r) = \rho_0 \frac{\sqrt{1 - 2GM/R} - \sqrt{1 - 2GMr^2/R^3}}{\sqrt{1 - 2GMr^2/R^3} - 3\sqrt{1 - 2GM/R}}. \tag{2.12}$$

Thus, the central pressure required to maintain equilibrium in a star of uniform density is

$$P_c = P(0) = \rho_0 \frac{\sqrt{1 - 2GM/R} - 1}{1 - 3\sqrt{1 - 2GM/R}}. \tag{2.13}$$

We see that the central pressure becomes infinite when

$$3\sqrt{1 - 2GM/R} = 1, \tag{2.14}$$

which is a very interesting result, because it tells us that any static, spherically symmetric star of uniform density with a given mass M will have a lower limit on its radius given by

$$R_{\min} = \frac{9}{4}GM. \tag{2.15}$$

Going below this limit yields no static (real-valued) solution to Einstein's field equation, and therefore, if a star with a fixed mass would somehow shrink to a small enough radius, it would have to keep shrinking, eventually forming a black hole [13, p. 234]. The same would not happen in Newtonian theory, for if we solve Eq. (2.5) with uniform density, which gives

$$P(r) = \frac{2}{3}\pi G\rho_0^2(R^2 - r^2), \tag{2.16}$$

and then consider

$$P_c = P(0) = \frac{2}{3}\pi G\rho_0^2 R^2, \tag{2.17}$$

we see that the central pressure is finite for any values of ρ_0 and R. The existence of a minimum radius, or equivalently maximum mass, in general relativity is actually not unique to mass distributions of uniform density. It can be shown to hold for any static and spherically symmetric mass distribution where the density profile $\rho(r)$ is nonnegative and satisfies $d\rho/dr \leq 0$, see [14, p. 130].

Let us compare the pressure profiles $P(r)$ of general relativity and Newtonian gravity by plotting the two for a few different cases. From Eq. (2.12), we see that a particular general relativistic density profile is given by three parameters: ρ_0, R and M. However, M is related to ρ_0 and R through Eq. (2.8), and thus the number of independent parameters is actually just two. It is more convenient to plot the pressure as a function of the dimensionless variable $x = r/R$ instead of r, so let us write

$$P(r) = \rho_0 \frac{\sqrt{1 - 2GM/R} - \sqrt{1 - 2GMx^2/R}}{\sqrt{1 - 2GMx^2/R} - 3\sqrt{1 - 2GM/R}}. \tag{2.18}$$

This can be simplified further by introducing the *Schwarzschild radius*

$$R_S \equiv 2GM, \tag{2.19}$$

and then writing the radius R as a multiple of it,

$$R = \alpha R_S = 2\alpha GM, \tag{2.20}$$

where $\alpha \equiv R/R_S = R/2GM$ is a dimensionless factor. The pressure now becomes

$$P(r) = \rho_0 \frac{\sqrt{1 - 1/\alpha} - \sqrt{1 - x^2/\alpha}}{\sqrt{1 - x^2/\alpha} - 3\sqrt{1 - 1/\alpha}}. \tag{2.21}$$

From the minimum-radius expression, Eq. (2.15), we get a minimum α-value,

$$\alpha_{\min} = \frac{9}{8} = 1.125. \tag{2.22}$$

No static solution with uniform energy density exists for the equation of hydrostatic equilibrium for α-values below this minimum. Finally, we can get rid of the parameter ρ_0 by choosing to plot the dimensionless ratio P/P_c instead of P, which is more

illustrative anyway. Dividing by the general relativistic central pressure P_c given by Eq. (2.13) leads to

$$\frac{P(r)}{P_c} = \frac{1-3\sqrt{1-1/\alpha}}{\sqrt{1-1/\alpha}-1}\frac{\sqrt{1-1/\alpha}-\sqrt{1-x^2/\alpha}}{\sqrt{1-x^2/\alpha}-3\sqrt{1-1/\alpha}}. \tag{2.23}$$

To plot this expression we only need to specify a value for α. The same steps can be used to simplify the Newtonian pressure, Eq. (2.16), which gives

$$\frac{P(r)}{P_c} = \frac{1}{4\alpha}\frac{1-3\sqrt{1-1/\alpha}}{\sqrt{1-1/\alpha}-1}(1-x^2). \tag{2.24}$$

Be aware that we have divided by the general relativistic central pressure here as well, not the Newtonian central pressure.

Figure 2.1 shows plots of the pressure profiles, Eq. (2.23) and Eq. (2.24), for three different values of α. The first plot, Figure 2.1.a, has $\alpha = 1.15$, which is very close to $\alpha_{\text{min}} = 1.125$. We see that for such extreme conditions, that is, very close to the minimum radius limit, the difference between the pressure profiles is huge. It was mentioned in the introduction to this chapter that the central pressure needed to sustain a mass distribution against gravity in general relativity is always higher than in Newtonian gravity. Here we see that for the Newtonian pressure profile $P(0)/P_c \approx 0.03$, which means that the central pressure is ~ 33 times larger in general relativity.

For the middle plot, Figure 2.1.b, we have chosen $R = 10.0$ km and $M = 2.0M_\odot$, which corresponds to $\alpha = 1.7$. These parameter values are within the range of typical neutron star masses and radii [7]. The difference between the two pressure profiles is again very large. This may not be all that surprising since the chosen parameter values corresponds to extreme objects, and thus we would expect Newtonian gravity to fall short.

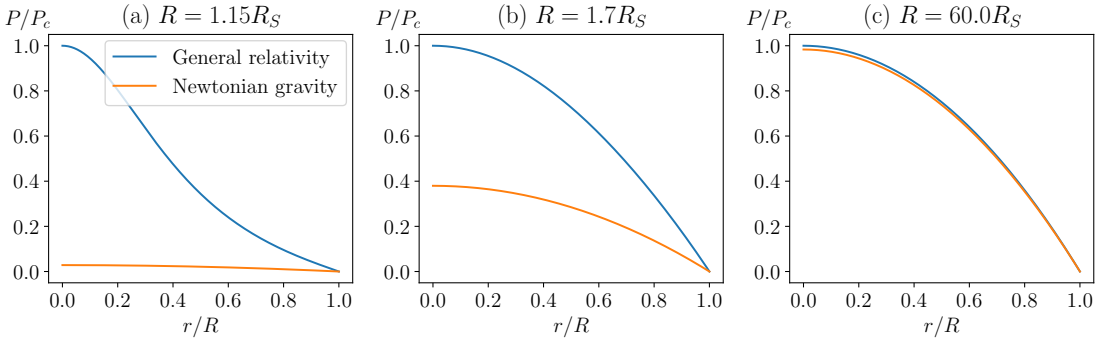

Figure 2.1: Pressure profiles as a function of relative radial coordinate and normalized by the general relativistic central pressure. In all three plots, the blue and the orange line represents the results of general relativistic and Newtonian calculations, respectively.

In the last plot, Figure 2.1.c, $\alpha = 60.0$. This is very large compared to typical values for neutron stars, although very small compared to that of the sun, which has $\alpha_{\text{Sun}} = 235714$. Even white dwarf stars (which are very dense stellar objects) have α-values way beyond 60.0; a typical white dwarf star has parameter values $R = 8835.4$ km and $M = 0.55 M_{\odot}$, corresponding to $\alpha = 5438$ [18]. One way of understanding the difference in α-values between plot b and c is to pretend we took the typical neutron star in plot b and scaled its radius by a factor of 35. It is evident from plot c that the difference between general relativity and Newtonian gravity starts to become negligible at such densities. Thus, we can conclude that the difference between the two theories of gravity when it comes to the equilibrium structure of incompressible fluids is negligible for those stellar objects that are less dense than neutron stars, e.g. white dwarf- and main-sequence stars.

2.2 Nondimensionalization

The problem of solving the TOV equation for more complicated equations of state can be greatly simplified if we rewrite it in terms of dimensionless quantities. This gives the equation a simpler form, which is easier to work with algebraically, and it also ensures numerical accuracy as well as reducing the need to specify input parameters in numerical calculations.

Before we begin to nondimensionalize, we first wish to reinstate the speed of light c for clarity, but only in this section. It is common to see ρ being used interchangeably as the symbol for the rest frame energy density and the rest frame mass density when working with general relativity. The reason is that c is usually set to unity, and thus the mass-energy equivalence then states that

$$\epsilon = \rho c^2 = \rho. \tag{2.25}$$

That is, when $c = 1$, there is no distinction between energy density ϵ and mass density ρ. However, it is important to realize that it is ultimately the energy density ϵ that should appear in the TOV equation, because Einstein's equation tells us that all forms of energy contributes to the curvature of spacetime, not just those forms of energy that correspond to a distribution of mass. Photons, for example, carry energy and therefore curve spacetime although they are massless.

Further confusion might arise when simultaneously working with equations of state were we often see the appearance of the particle number density $\langle n \rangle$; the mass density of a gas of particles with mass m is given by $m\langle n \rangle$, and this is generally not the same as $\rho = \epsilon/c^2$, which we also refer to as the (rest frame) mass density. The reason is that the (rest) mass of a composite system is generally not the same as the sum of the masses of the individual components. To clarify, a system of particles with momenta p_i in the center of momentum frame and masses m_i has total energy given by

$$E_{\text{system}} = \sum_i E_i = \sum_i \sqrt{(p_i c)^2 + (m_i c^2)^2}, \tag{2.26}$$

and since we are in the center of momentum frame, or rest frame of the system, the

mass of the system is given by

$$m_{\text{system}} = E_{\text{system}}/c^2 = \sum_i \sqrt{(p_i c)^2 + (m_i c^2)^2}/c^2 \neq \sum_i m_i. \tag{2.27}$$

Thus, we emphasize that ρ must not be confused with $m\langle n\rangle$, but should rather be viewed as simply defined by the relation $\rho \equiv \epsilon/c^2$. It is what you would get if you observed an infinitesimal fluid element in its rest frame, summed up all the energies of the particles inside and then divided the resulting total energy by c^2 and the volume. It is the rest mass density of the system as a whole.

When c is reinstated and ϵ is used as one of the variables instead of ρ, the structure equations become

$$\frac{dP}{dr} = -\frac{G\epsilon(r)m(r)}{r^2c^2}\left[1+\frac{P(r)}{\epsilon(r)}\right]\left[1+\frac{4\pi r^3P(r)}{m(r)c^2}\right]\left[1-\frac{2Gm(r)}{rc^2}\right]^{-1}, \tag{2.28}$$

$$\frac{dm}{dr} = \frac{4\pi r^2\epsilon(r)}{c^2}. \tag{2.29}$$

To put these into a dimensionless form, we start by defining dimensionless variables $\bar{r}$, $\overline{m}$, $\overline{P}$ and $\bar{\epsilon}$ in terms of scaling factors r_0, m_0, P_0 and ϵ_0,

$$\bar{r} = \frac{r}{r_0}, \qquad \overline{m}(\bar{r}) = \frac{m(r_0\bar{r})}{m_0}, \qquad \overline{P}(\bar{r}) = \frac{P(r_0\bar{r})}{P_0} \qquad \text{and} \qquad \bar{\epsilon}(\bar{r}) = \frac{\epsilon(r_0\bar{r})}{\epsilon_0}. \tag{2.30}$$

As of now, the scaling factors are all arbitrary, but they should later be chosen in a way that simplifies the specific problem at hand. Substituting the above definitions into the TOV equation gives

$$\frac{d\overline{P}}{d\bar{r}} = -\left(\frac{G\epsilon_0 m_0}{P_0 r_0 c^2}\right)\frac{\bar{\epsilon}\,\overline{m}}{\bar{r}^2}\left[1+\left(\frac{P_0}{\epsilon_0}\right)\frac{\overline{P}}{\bar{\epsilon}}\right]\left[1+\left(\frac{4\pi r_0^3 P_0}{m_0c^2}\right)\frac{\bar{r}^3\overline{P}}{\overline{m}}\right]\left[1-2\left(\frac{Gm_0}{r_0c^2}\right)\frac{\overline{m}}{\bar{r}}\right]^{-1}. \tag{2.31}$$

Each of the square bracketed factors are dimensionless, and thus the expressions in parentheses are as well. Let us choose to set the expressions in the parentheses in the first and the second set of brackets equal to 1. This leads to

$$\epsilon_0 = P_0 = \frac{m_0c^2}{4\pi r_0^3}, \tag{2.32}$$

and it essentially means that we have chosen (or constrained) two of the four scaling factors. Let us also define the dimensionless number

$$a = \frac{Gm_0}{r_0c^2} = \frac{4\pi G\epsilon_0 r_0^2}{c^4}. \tag{2.33}$$

We are now left with the freedom to specify two of the four scaling factors (except for the case of specifying both ϵ_0 and P_0 of course), and the other two then follow from Eq. (2.32). One could alternatively specify a and any one of the four scaling

factors. Substituting Eq. (2.32) and Eq. (2.33) into the structure equations leads to their dimensionless form,

$$\frac{d\overline{P}}{d\bar{r}} = -a\frac{\bar{\epsilon}\,\overline{m}}{\bar{r}^2}\left[1+\frac{\overline{P}}{\bar{\epsilon}}\right]\left[1+\frac{\bar{r}^3\overline{P}}{\overline{m}}\right]\left[1-2a\frac{\overline{m}}{\bar{r}}\right]^{-1}, \tag{2.34}$$

$$\frac{d\overline{m}}{d\bar{r}} = \bar{r}^2\bar{\epsilon}. \tag{2.35}$$

Regarding the choice of the two remaining unconstrained scaling factors, it is sometimes convenient to choose $r_0 = R$ and $m_0 = M_\odot$, where R is the radius of the star and $M_\odot$ is the solar mass. This makes it so that the surface of the star is given by $\bar{r} = 1$ and $\overline{m}(1) = M/M_\odot$ gives the mass of the star as a fraction of solar masses. However, unless we actually specify the radius of the star R, this choice of r_0 will only be helpful algebraically or when plotting as a function of $\bar{r}$. Other good choices for r_0 could be 1 km or even 10 km, since $R \sim 10$ km for a typical neutron star.

Given an equation of state, we sometimes wish to compare our solutions of the structure equations from general relativity with the Newtonian solutions. We therefore need dimensionless versions of the Newtonian structure equations as well. By using the same dimensionless variables, scaling factors and constraints on them as earlier, the equations become

$$\frac{d\overline{P}}{d\bar{r}} = -a\frac{\bar{\epsilon}\,\overline{m}}{\bar{r}^2}, \tag{2.36}$$

$$\frac{d\overline{m}}{d\bar{r}} = \bar{r}^2\bar{\epsilon}. \tag{2.37}$$

Not only is it instructive to observe when and by how much Newtonian gravity falls short for different EOS, but comparing the two can sometimes also work as a check to see if our calculations are correct; in light of Section 2.1, we expect the two equilibrium equations to give very similar results for stars that are sufficiently less dense than typical neutron stars.

2.3 Ultra and Non-Relativistic Ideal Fermi Gases

Even though our earlier case of uniform energy density was somewhat instructive, it is not very realistic, because we expect the energy density to increase as we move towards the center of the star. Since neutrons and quarks are fermions, the next logical step towards a more realistic model for neutron- and quark stars would be to consider the equation of state for an ideal Fermi gas, particularly within the zero-temperature approximation. It is shown in appendix E that the pressure, energy density and particle density of an ideal Fermi gas at zero temperature is given by

$$P = \frac{1}{24\pi^2}\left[p_F\sqrt{p_F^2+m^2}\left(2p_F^2-3m^2\right)+3m^4\sinh^{-1}\left(\frac{p_F}{m}\right)\right], \tag{2.38}$$

$$\epsilon = \frac{1}{8\pi^2}\left[p_F\sqrt{p_F^2+m^2}\left(2p_F^2+m^2\right)-m^4\sinh^{-1}\left(\frac{p_F}{m}\right)\right], \tag{2.39}$$

$$\langle n\rangle = \frac{p_F^3}{3\pi^2}, \tag{2.40}$$

where m is the mass of the individual particles and p_F is the Fermi momentum. These expressions can be used to solve the TOV equation numerically. But before we do so, we first consider the non-relativistic (NR) and the ultrarelativistic (UR) limit.

Let us start with the non-relativistic limit, which is given by $p_F \ll m$. For convenience, introduce the variable $x_F = p_F/m$. By inserting the Maclaurin series for the functions $\sqrt{1+x_F^2}$ and $\sinh^{-1}(x_F)$ into Eq. (2.38), we get

$$P = \frac{m^4}{24\pi^2}\Bigg[x_F\Big(1+\frac{1}{2}x_F^2-\frac{1}{8}x_F^4+\mathcal{O}\big(x_F^6\big)\Big)\big(2x_F^2-3\big) + 3\Big(x_F-\frac{1}{6}x_F^3+\frac{3}{40}x_F^5+\mathcal{O}\big(x_F^7\big)\Big)\Bigg] = \frac{m^4}{15\pi^2}x_F^5+\mathcal{O}\big(x_F^6\big). \tag{2.41}$$

Since $x_F \to 0$ in the non-relativistic limit, the pressure becomes dominated by the term with the lowest power of x_F. Thus, the non-relativistic pressure is given by

$$P_{\mathrm{NR}} = \frac{m^4}{15\pi^2}x_F^5 = \frac{1}{15\pi^2}\frac{p_F^5}{m} = \frac{(3\pi^2)^{5/3}}{15\pi^2 m}\langle n\rangle^{5/3}, \tag{2.42}$$

where we have used Eq. (2.40) in the last step.

A similar expansion of the energy density leads to

$$\epsilon = m\frac{p_F^3}{3\pi^2}+\frac{p_F^5}{10\pi^2 m}+\mathcal{O}\big(x_F^7\big) = m\langle n\rangle+\frac{3}{2}P_{\mathrm{NR}}+\mathcal{O}\big(x_F^7\big). \tag{2.43}$$

We see that in the non-relativistic limit, the energy density is completely dominated by the rest mass energy density,

$$\epsilon_{\mathrm{NR}} = m\langle n\rangle. \tag{2.44}$$

By combining Eq. (2.42) and Eq. (2.44) we find the equation of state for an ideal Fermi gas at $T=0$ in the non-relativistic limit:

$$P_{\mathrm{NR}} = \frac{1}{5m^2}\left(\frac{3\pi^2}{m}\right)^{2/3}\epsilon_{\mathrm{NR}}^{5/3}. \tag{2.45}$$

This is an example of a *polytropic* EOS,

$$P = K\epsilon^{(n+1)/n}, \tag{2.46}$$

where the polytropic index n can be any real number between 0 and $+\infty$. The particular case above corresponds to $n=3/2$ and $K=\frac{1}{5m^2}\left(\frac{3\pi^2}{m}\right)^{2/3}$. Solutions to the structure equations for polytropes will be considered in Section 2.5

The ultrarelativistic limit is given by $p_F \gg m$, or equivalently $x_F \to \infty$, and the energy-momentum relation can therefore be written

$$E_F = \sqrt{p_F^2+m^2} = p_F\sqrt{1+\left(\frac{1}{x_F}\right)^2} = p_F\left[1+\frac{1}{2x_F^2}+\mathcal{O}\left(\frac{1}{x_F^4}\right)\right] \approx p_F. \tag{2.47}$$

We also need to investigate the behavior of $\sinh^{-1}(x_F)$ as $x_F \to \infty$. This can be done by calculating the Laurent series of the function $f(y) = \sinh^{-1}(1/y)$ at $y = 0$ and then substitute back $x_F = 1/y$. One would then find that

$$\sinh^{-1}(x_F) = \ln(2x_F) + \frac{1}{4x_F^2} - \frac{3}{32x_F^4} + \mathcal{O}\left(\frac{1}{x_F^6}\right). \tag{2.48}$$

None of these terms will contribute much to the pressure and energy density at large x_F. Instead, the expressions for pressure and energy density, Eq. (2.38) and Eq. (2.39), becomes dominated by the term with the highest power of x_F. By dropping all the terms from $\sinh^{-1}(x_F)$, the pressure now takes the form

$$P \approx \frac{m^4}{24\pi^2}x_F^2\left(2x_F^2 - 3\right) = \frac{m^4}{24\pi^2}\left(2x_F^4 - 3x_F^2\right). \tag{2.49}$$

The fourth order term will dominate for large x_F, and thus the pressure in the ultrarelativistic limit becomes

$$P_{\text{UR}} = \frac{m^4}{12\pi^2}x_F^4 = \frac{p_F^4}{12\pi^2} = \frac{(3\pi^2)^{1/3}}{4}\langle n\rangle^{4/3}. \tag{2.50}$$

Similarly, the energy density becomes

$$\epsilon_{\text{UR}} = \frac{p_F^4}{4\pi^2} = \frac{3(3\pi^2)^{1/3}}{4}\langle n\rangle^{4/3}, \tag{2.51}$$

Combining the two expressions leads to the equation of state for an ideal Fermi gas at zero temperature in the ultrarelativistic limit:

$$P_{\text{UR}} = \frac{1}{3}\epsilon_{\text{UR}}. \tag{2.52}$$

This is an example of a linear EOS,

$$P = \gamma\epsilon, \tag{2.53}$$

where in this case $\gamma = 1/3$. In the next section we consider solutions of the structure equations for such EOS.

2.4 Linear Equation of State

Consider a linear equation of state

$$P(\epsilon) = \gamma\epsilon, \tag{2.54}$$

where γ is a dimensionless constant of proportionality. We found in the previous section that the case $\gamma = 1/3$ corresponds to an ultrarelativistic ideal Fermi gas at zero temperature. Since the speed of sound is given by

$$v_s = \sqrt{\frac{\partial P}{\partial \rho}} = \sqrt{\frac{\partial P}{\partial \epsilon}}c = \gamma c, \tag{2.55}$$

we must have $\gamma \in [0, 1]$ to satisfy the causality requirement $v_s \leq c$. By employing the dimensionless variables defined in Section 2.2, the equation of state can be written as

$$\overline{P} = \gamma \bar{\epsilon}. \tag{2.56}$$

This combined with the structure equations, Eq. (2.34) and Eq. (2.35), constitutes a closed set of equations.

As a natural first step, we seek a solution of the simple form

$$\overline{P}(\bar{r}) = K\bar{r}^n, \tag{2.57}$$

where K and n are constants to be determined. Combining the mass continuity equation (2.35) and the EOS (2.56) yields

$$\overline{m}(\bar{r}) = \frac{K}{\gamma}\int_0^{\bar{r}} s^{n+2} ds = \frac{K}{\gamma(n+3)}\bar{r}^{n+3}. \tag{2.58}$$

Next, inserting the last three equations into the TOV equation (2.34) and then rearranging leads to

$$n\bar{r}^{n-1} + \frac{ak}{\gamma^2(n+3)}\Big\{(1+\gamma)\big[1+\gamma(n+3)\big] - 2n\Big\}\bar{r}^{2n+1} = 0. \tag{2.59}$$

The only non-trivial way to satisfy this equation is if the exponents are equal, implying $n = -2$, and the coefficients in front of $\bar{r}$ are the additive inverse of each other,

$$n = -\frac{aK}{\gamma^2(n+3)}\Big\{(1+\gamma)\big[1+\gamma(n+3)\big] - 2n\Big\}. \tag{2.60}$$

When solved for K, this equation gives

$$K = \frac{2\gamma^2}{a(\gamma^2+6\gamma+1)}. \tag{2.61}$$

Thus, we have found an exact solution to the Tolman-Oppenheimer-Volkoff equation for a linear equation of state,

$$\overline{P}(\bar{r}) = \frac{2\gamma^2}{a(\gamma^2+6\gamma+1)\bar{r}^2}. \tag{2.62}$$

There are, however, two obvious problems with this solution. One is that it is singular at $\bar{r} = 0$, giving an infinite central pressure. The other problem is that the pressure only approaches zero asymptotically as $\bar{r} \to \infty$ and therefore resulting in an infinite radius.

A better solution can be obtained by using a power series ansatz. Following the steps in [16], we first use the EOS and Eq. (2.35) to completely eliminate both P and ϵ from the TOV equation (2.34). This leads to

$$\gamma\left[1 - 2a\frac{\overline{m}}{\bar{r}}\right]\left[\bar{r}\frac{d^2\overline{m}}{d\bar{r}^2} - 2\frac{d\overline{m}}{d\bar{r}}\right] = -a\overline{m}\frac{d\overline{m}}{d\bar{r}}(1+\gamma)\left[\frac{1}{\bar{r}} + \frac{\gamma}{\overline{m}}\frac{d\overline{m}}{d\bar{r}}\right], \tag{2.63}$$

where we have used the chain rule on the left-hand side,

$$\frac{d\overline{P}}{d\bar{r}} = \frac{d\overline{P}}{d\bar{\epsilon}}\frac{d\bar{\epsilon}}{d\bar{r}} = \gamma\left[\frac{1}{\bar{r}^2}\frac{d^2\overline{m}}{d\bar{r}^2} - \frac{2}{\bar{r}^3}\frac{d\overline{m}}{d\bar{r}}\right]. \tag{2.64}$$

Multiplying out the brackets and rearranging leads to what we shall refer to as the relativistic mass equation,

$$\bar{r}\frac{d^2\overline{m}}{d\bar{r}^2} - 2\frac{d\overline{m}}{d\bar{r}} - 2a\overline{m}\frac{d^2\overline{m}}{d\bar{r}^2} + \alpha\frac{\overline{m}}{\bar{r}}\frac{d\overline{m}}{d\bar{r}} + \beta\left(\frac{d\overline{m}}{d\bar{r}}\right)^2 = 0, \tag{2.65}$$

where we have defined $\alpha \equiv a(5 + 1/\gamma)$ and $\beta \equiv a(1 + \gamma)$. The boundary values are

$$\overline{m}(0) = 0 \quad \text{and} \quad \overline{m}'(0) = \frac{d\overline{m}}{d\bar{r}}\Big|_{\bar{r}=0} = 0. \tag{2.66}$$

If we were to find a solution $\overline{m}(\bar{r})$ to this differential equation then it would be easy to obtain both ϵ and P through Eq. (2.35) and Eq. (2.56). Our power series ansatz will be of the form

$$\overline{m}(\bar{r}) = \sum_{n=1}^{\infty} c_{2n+1}\bar{r}^{2n+1}. \tag{2.67}$$

Notice that this automatically satisfies the initial conditions $\overline{m}(0) = \overline{m}'(0) = 0$. The first and second derivatives are given by

$$\frac{d\overline{m}}{d\bar{r}} = \sum_{n=1}^{\infty}(2n+1)c_{2n+1}\bar{r}^{2n} \tag{2.68}$$

and

$$\frac{d^2\overline{m}}{d\bar{r}^2} = \sum_{n=1}^{\infty}2n(2n+1)c_{2n+1}\bar{r}^{2n-1}. \tag{2.69}$$

Our goal is to write each of the terms in Eq. (2.65) as a power series in the variable $\bar{r}$. The entire left-hand side can then be merged together to a single power series where all the coefficients must vanish.

We start by looking at the three nonlinear terms. They can all be rewritten using the Cauchy product, defined for two infinite series $\sum_{i=0}^{\infty} a_i$ and $\sum_{j=0}^{\infty} b_j$ as

$$\left(\sum_{i=0}^{\infty} a_i\right)\cdot\left(\sum_{j=0}^{\infty} b_j\right) = \left(\sum_{k=0}^{\infty} c_k\right) \quad \text{where} \quad c_k = \sum_{l=0}^{k} a_l b_{k-l}. \tag{2.70}$$

This gives

$$\begin{aligned}
\overline{m}\frac{d^2\overline{m}}{d\bar{r}^2} &= \left(\sum_{i=1}^{\infty} c_{2i+1}\bar{r}^{2i+1}\right)\cdot\left(\sum_{j=1}^{\infty} 2j(2j+1)c_{2j+1}\bar{r}^{2j-1}\right) \\
&= \left(\sum_{i=0}^{\infty} c_{2i+3}\bar{r}^{2i+3}\right)\cdot\left(\sum_{j=0}^{\infty} 2(j+1)(2j+3)c_{2j+3}\bar{r}^{2j+1}\right) \\
&= \sum_{n=1}^{\infty}\sum_{k=1}^{n} 2(n-k+1)(2n-2k+3)c_{2k+1}c_{2n-2k+3}\bar{r}^{2n+2}.
\end{aligned} \tag{2.71}$$

Similarly, the two other terms become

$$\frac{\overline{m}}{\bar{r}}\frac{d\overline{m}}{d\bar{r}} = \sum_{n=1}^{\infty}\sum_{k=1}^{n}(2n-2k+3)c_{2k+1}c_{2n-2k+3}\bar{r}^{2n+2} \tag{2.72}$$

and

$$\left(\frac{d\overline{m}}{d\bar{r}}\right)^2 = \sum_{n=1}^{\infty}\sum_{k=1}^{n}(2k+1)(2n-2k+3)c_{2k+1}c_{2n-2k+3}\bar{r}^{2n+2}. \tag{2.73}$$

After substituting this into Eq. (2.65) one gets

$$\begin{aligned} 0 = &\sum_{n=1}^{\infty}2(n-1)(2n+1)c_{2n+1}\bar{r}^{2n} + \sum_{n=1}^{\infty}\sum_{k=1}^{n}(2n-2k+3) \\ &\times\Big[-4a(n-k+1)+\alpha+\beta(2k+1)\Big]c_{2k+1}c_{2n-2k+3}\bar{r}^{2n+2}. \end{aligned} \tag{2.74}$$

We must now shift the dummy index in the first sum to be able to write the complete expression as a single power series. After doing so we can pull out the sum over n, which gives

$$\begin{aligned} 0 = &\sum_{n=1}^{\infty}\Bigg\{2n(2n+3)c_{2n+3} + \sum_{k=1}^{n}(2n-2k+3) \\ &\times\Big[-4a(n-k+1)+\alpha+\beta(2k+1)\Big]c_{2k+1}c_{2n-2k+3}\Bigg\}\bar{r}^{2n+2}. \end{aligned} \tag{2.75}$$

The expression in the curly braces must vanish, and we can then solve for c_{2n+3} before shifting $n \to n-1$ to get c_{2n+1}. This yields the recursive relation

$$\begin{aligned} c_{2n+1} = &-\frac{a}{2(n-1)(2n+1)\gamma}\sum_{k=1}^{n-1}(2n-2k+1) \\ &\times\Big[2\gamma(\gamma+3)k - 4n\gamma + \gamma^2 + 6\gamma + 1\Big]c_{2k+1}c_{2n-2k+1}, \quad n \geq 2. \end{aligned} \tag{2.76}$$

Furthermore, the energy density and the pressure are given by

$$\bar{\epsilon}(\bar{r}) = \frac{1}{\bar{r}^2}\frac{d\overline{m}}{d\bar{r}} = \sum_{n=1}^{\infty}(2n+1)c_{2n+1}\bar{r}^{2n-2} \tag{2.77}$$

and

$$\overline{P}(\bar{r}) = \gamma\bar{\epsilon} = \gamma\sum_{n=1}^{\infty}(2n+1)c_{2n+1}\bar{r}^{2n-2}. \tag{2.78}$$

The first non-zero power series coefficient c_3 gets fixed as soon as we prescribe a central energy density $\epsilon(0) = \epsilon_c$,

$$c_3 = \frac{1}{3}\bar{\epsilon}(0) = \frac{\epsilon_c}{3\epsilon_0}. \tag{2.79}$$

All other coefficients follow from the recursive relation, Eq. (2.76). The next two are

$$c_5 = -\frac{3a}{10\gamma}(3\gamma+1)(\gamma+1)c_3^2 \tag{2.80}$$

and

$$c_7 = -\frac{a}{14\gamma}(15\gamma^2+9\gamma+4)c_3c_5. \tag{2.81}$$

Notice that this exact power series solution is regular at $\bar{r}=0$ and has therefore fixed one of the issues concerning the previous power law solution. However, the power series solution still has the problem of having infinite radius. This can perhaps most easily be shown by employing the criteria for (in)finite radii derived by Rendall and Schmidt [15]. They showed that a star with a finite radius must satisfy

$$\int_0^{P_c} \frac{dP}{\epsilon(P)+P} < \infty, \quad P_c = P(r=0). \tag{2.82}$$

With the linear equation of state (2.54), we get

$$\int_0^{P_c} \frac{dP}{P/\gamma+P} = \frac{\gamma}{1+\gamma}\int_0^{P_c}\frac{dP}{P} = \infty. \tag{2.83}$$

Thus, any solution to the structure equations with a linear equation of state will necessarily have an infinite radius. This of course means that we cannot find a mass-radius relation for this EOS.

A similar power series solution can be obtained for the Newtonian structure equations. The mass equation corresponding to Eq. (2.65) becomes

$$\bar{r}\frac{d^2\overline{m}}{d\bar{r}^2} - 2\frac{d\overline{m}}{d\bar{r}} - 2a\overline{m}\frac{d^2\overline{m}}{d\bar{r}^2} = 0. \tag{2.84}$$

All the terms in this equation is also present in the relativistic mass equation. Therefore, finding the recursive relation for the coefficients becomes easy when using the same ansatz as before, Eq. (2.67). We find

$$c_{2n+1} = -\frac{a}{2(n-1)(2n+1)\gamma}\sum_{k=1}^{n-1}(2n-2k+1)c_{2k+1}c_{2n-2k+1}, \quad n \geq 2, \tag{2.85}$$

and the energy density, the pressure and the coefficient c_3 is of course still given by Eq. (2.77), Eq. (2.78) and Eq. (2.79). The next two non-zero coefficients are

$$c_5 = -\frac{3a}{10\gamma}c_3^2 \qquad \text{and} \qquad c_7 = -\frac{2a}{7\gamma}c_3c_5. \tag{2.86}$$

Figure 2.2 displays the pressure profile and the mass profile for an ultrarelativistic star of non-interacting particles ($\gamma = 1/3$) with central pressure $P_c = 3.60 \times 10^{34}\,\mathrm{J/m^3}$. As we shall see in Section 2.6, this central pressure produces a star of maximum mass in the case of the full ideal Fermi gas EOS. The dashed lines in the plots correspond to the power series solutions with 20 coefficients, while the two solid lines underneath correspond to numerical solutions obtained with the

Runge–Kutta fourth-order method. (More will be said about the numerical calculations in Section 2.6.) The singular solution to the TOV equation has also been plotted. Since the central pressure is infinite for that one, it has been normalized by the same P_c as for the other two. We see that the power series solutions are in perfect agreement with the numerical ones up to certain radii, from which they diverge. Even when including more than 100 coefficients they still diverge heavily at the same radii as for 20 coefficients, and they therefore seem to be the radii of convergence. We see that the difference between the general relativistic solution and the Newtonian solution is very large. By using Eq. (2.50), we find that the central pressure used here corresponds to a central particle number density of $\langle n \rangle_c = 8.3 n_{\text{sat}}$, where $n_{\text{sat}} = 1.7 \times 10^{44}\,/\text{m}^3$ [19, p. 20] is the nuclear saturation density. Since the density is so large, it was nothing more than expected that the two theories deviate a lot.

All of the solutions considered here are of course unphysical if they are assumed to apply for the entire star, because they all give infinite radii. However, if one consider stars with mixed phases, then it could be that the power series solution is applicable to central regions where the particles are expected to be highly relativistic.

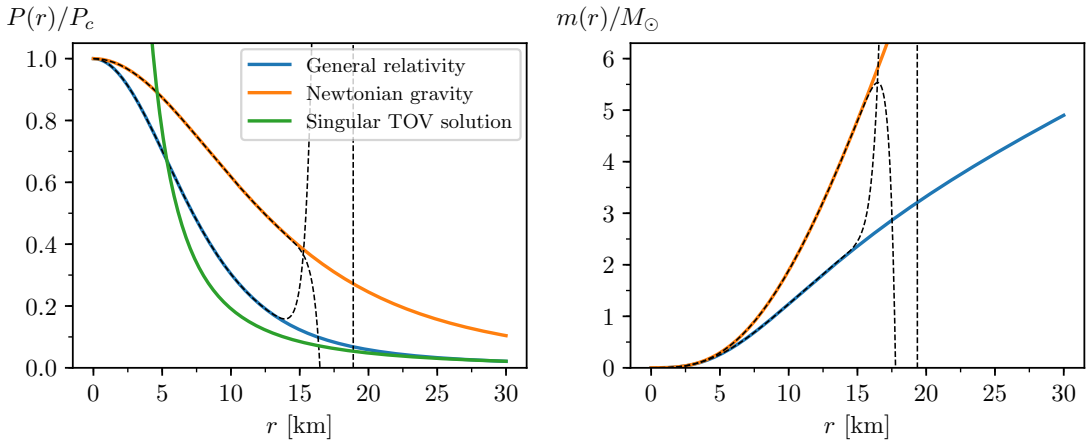

Figure 2.2: Linear EOS solution with $\gamma = 1/3$. The plots show pressure and mass profiles as a function of the radial coordinate and normalized by the central pressure $P_c = 3.60 \times 10^{34}\,\text{J/m}^3$ and the solar mass $M_\odot$. The dashed lines are the power series solutions with 20 coefficients included, while the solid lines underneath are the result of numerical calculations.

2.5 Polytropes

Consider a polytropic equation of state,

$$P(\epsilon) = K\epsilon^{(n+1)/n}, \tag{2.87}$$

where K is some constant of proportionality and the polytropic index n ranges from 0 to $+\infty$. In Section 2.3 we found that the case $n = 3/2$ corresponds to a

non-relativistic ideal Fermi gas at zero temperature. When using our dimensionless variables and scaling factors from Section 2.2, the dimensionless form of the polytropic EOS becomes

$$\overline{P} = \overline{K}\bar{\epsilon}^{1+1/n}, \qquad \text{where} \qquad \overline{K} = K\epsilon_0^{1/n}. \tag{2.88}$$

There exists exact power series solutions to both the TOV equation and the Newtonian equilibrium equation for this EOS as well, see [16, 20]. Furthermore, closed form analytical solutions of the Newtonian equation have been found for the cases $n = 0, 1$ and 5. We will, however, restrict ourselves to numerical calculations this time. When trying to solve the structure equations numerically, one realizes that the TOV equation has an apparent singularity at $\bar{r} = 0$, resulting in a division by zero error. We show how to deal with this issue in Section 2.6.

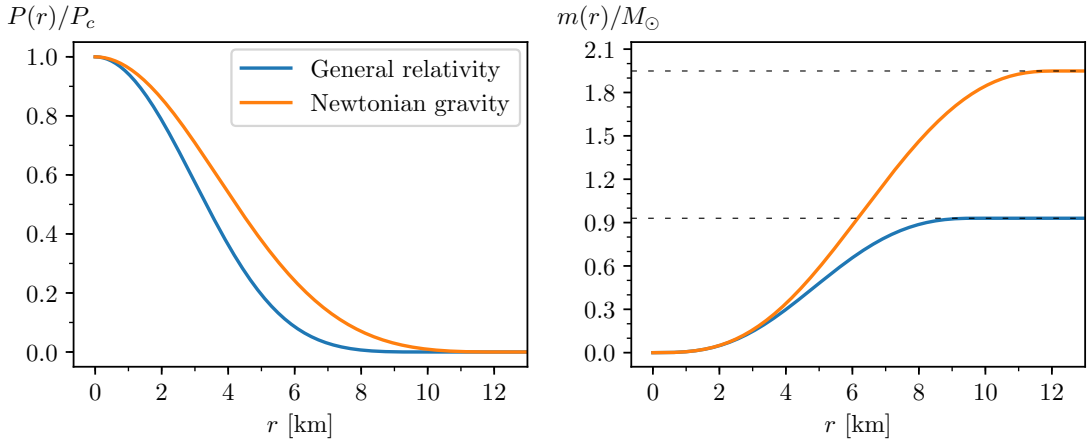

Figure 2.3: Polytropic EOS solution with polytropic index $n = 3/2$ and proportionality constant $K = 2.98 \times 10^{-25}\,\mathrm{m^2 J^{-3/2}}$. The plots show pressure and mass profiles as a function of the radial coordinate and normalized by the central pressure $P_c = 3.60 \times 10^{34}\,\mathrm{J/m^3}$ and the solar mass $M_\odot$. For the general relativistic profiles, $R = 9.68\,\mathrm{km}$ and $M = 0.930 M_\odot$. These plots do not correspond to the maximum mass star for this EOS.

Let us solve the structure equations numerically for the, non-relativistic, degenerate Fermi gas from Section 2.3, meaning we take $n = 3/2$ and

$$K = \frac{1}{5m^2}\left(\frac{3\pi^2}{m}\right)^{2/3}. \tag{2.89}$$

Although this EOS would be more appropriate for white dwarf star (which are a lot less relativistic than neutron stars), take $m = m_n$ regardless, so that we get a star of pure non-interacting, non-relativistic neutrons. The result in the case of a central pressure $P_c = 3.60 \times 10^{34}\,\mathrm{J/m^3}$ can be seen in Figure 2.3. (Like the plotted solution in the previous section, we chose the central pressure that gives the maximum mass for the full ideal Fermi gas EOS, which we shall study in the next section.) This time

we have both regularity at the origin and a finite radius. The difference between general relativity and Newtonian gravity is large for this solution, especially when it comes to the mass profile; the total mass in Newtonian gravity is more than twice as large as for general relativity in this case. From Eq. (2.42) we get that the central particle number density is $\langle n \rangle_c = 11.1 n_{\text{sat}}$. It is nothing more than expected that the difference between the theories is large at such extremely high densities. However, the difference is less compared to the linear EOS solution at the same central pressure, Figure 2.2.

Each choice of central pressure results in a star with a particular mass M and radius R. By solving the structure equations for a range of central pressures we get a mass-radius relation $M(R)$. For a polytropic EOS with $n = 3/2$ and K chosen as in the previous paragraph, Eq. (2.89) with $m = m_n$, the resulting $M(R)$ relation can be seen in Figure 2.4. We see that the general relativistic calculations lead to an upper mass limit $M_{\text{max}} = 0.963 M_\odot$, corresponding to $R = 7.99\,\text{km}$, $P_c = 1.10 \times 10^{35}\,\text{J/m}^3$ and $\langle n \rangle_c = 21.7 n_{\text{sat}}$. No solutions with mass greater than $0.963 M_\odot$ exist for this particular EOS. We shall see in Section 3.5 that the points to the left of the maximum on the $M(R)$ curve correspond to unstable stars, while those to the right are stable.

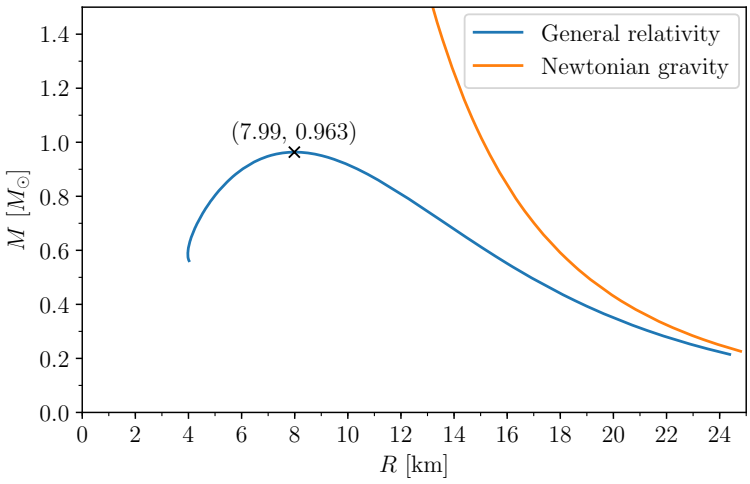

Figure 2.4: Mass-radius relation for a non-relativistic ideal Fermi gas EOS at zero temperature with polytropic index $n = 3/2$ and proportionality constant $K = 2.98 \times 10^{-25}\,\text{m}^2\text{J}^{-3/2}$.

The speed of sound for a polytropic EOS is obtained with Eq. (2.6), giving

$$v_s = \sqrt{\frac{\partial P}{\partial \epsilon}} = \frac{n+1}{n} K \epsilon^{1/n}. \tag{2.90}$$

Since $\epsilon(r)$ is monotonically decreasing, the speed of sound is largest at the center of the star. We find that the speed of sound for the star of maximum mass is $v_s = 0.58c$. Because the central pressure increases towards the left in Figure 2.4, the causality requirement holds for all stars on at least the stable part of the $M(R)$ curve, that is, those to the right of the maximum.

2.6 Ideal Fermi Gas

So far we have covered the ultrarelativistic and the non-relativistic regimes of an ideal Fermi gas at zero temperature. In this section, we solve the structure equations numerically in the case of arbitrary relativity. As mentioned in Section 2.3 and derived in Appendix E, the pressure, energy density and particle density is given by

$$P = \frac{m^4}{24\pi^2}\left[x_F\sqrt{x_F^2+1}\left(2x_F^2-3\right)+3\sinh^{-1}(x_F)\right], \tag{2.91}$$

$$\epsilon = \frac{m^4}{8\pi^2}\left[x_F\sqrt{x_F^2+1}\left(2x_F^2+1\right)-\sinh^{-1}(x_F)\right], \tag{2.92}$$

$$\langle n\rangle = m^3\frac{x_F^3}{3\pi^2}, \tag{2.93}$$

where $x_F = p_F/m$ is dimensionless. We obtain the dimensionless pressure $\overline{P}$ and energy density $\bar{\epsilon}$ by simply dividing the expressions above by ϵ_0, see Section 2.2 and in particular Eq. (2.32). This time we do not have a closed form EOS, and thus we cannot eliminate ϵ in the structure equations. Instead, for each step i in the numerical routine, we must find the $x_{F,i}$ corresponding to the pressure P_i at that step and then substitute $x_{F,i}$ into Eq. (2.92) to find the energy density ϵ_i. This means that at each step we must solve the equation

$$P(x_{F,i}) = P_i, \tag{2.94}$$

where the left-hand side is given by Eq. (2.91).

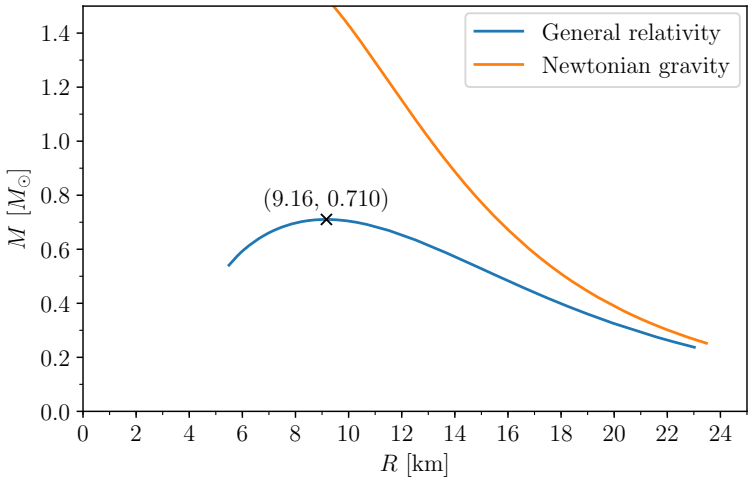

Figure 2.5: Mass-radius relation for an ideal Fermi gas EOS at $T = 0$ and with $m = m_n$. The maximum mass for this EOS is $M = 0.710M_\odot$, with a radius of $R = 9.16\,\text{km}$. Points to the right of this maximum correspond to stable stars, whereas those to the left are unstable.

When trying to numerically solve the structure equations, one immediately notices a problem; even though we know that the TOV equation is regular at the

origin, see [15], we would get a division by zero error if we naively tried to evaluate it there. One must therefore manually specify the appropriate value for $d\overline{P}/d\bar{r}$ at $\bar{r} = 0$. This value can be found by inserting the Taylor expansion of $\overline{m}(\bar{r})$ at the origin into the TOV equation and then taking the limit $\bar{r} \to 0$. To Taylor expand $\overline{m}(\bar{r})$ we need its first few derivatives, which we get by repeatedly differentiating Eq. (2.35),

$$\begin{aligned}
&\overline{m}'(0) = \bar{r}^2 \bar{\epsilon}(\bar{r})\Big|_0 = 0, \\
&\overline{m}''(0) = 2\bar{r}\bar{\epsilon}(\bar{r}) + \bar{r}^2 \bar{\epsilon}'(\bar{r})\Big|_0 = 0, \\
&\overline{m}'''(0) = 2\bar{\epsilon}(\bar{r}) + 2\bar{r}\bar{\epsilon}'(\bar{r}) + 2\bar{r}\bar{\epsilon}'(\bar{r}) + \bar{r}^2 \bar{\epsilon}''(\bar{r})\Big|_0 = 2\bar{\epsilon}(0).
\end{aligned} \tag{2.95}$$

Here we have assumed that the energy density $\bar{\epsilon}(\bar{r})$ is sufficiently smooth such that its derivatives exist and are continuous. Recalling that $\overline{m}(0) = 0$, we get

$$\overline{m}(\bar{r}) = \frac{1}{6}\overline{m}'''(0)\bar{r}^3 + \mathcal{O}(\bar{r}^4) = \frac{1}{3}\bar{\epsilon}(0)\bar{r}^3 + \mathcal{O}(\bar{r}^4). \tag{2.96}$$

Inserting this into Eq. (2.34) and taking the limit $r \to 0$ gives

$$\begin{aligned}
\frac{d\overline{P}}{d\bar{r}}\bigg|_0 = \lim_{\bar{r}\to 0} -a\bar{\epsilon}(\bar{r})\left[\frac{1}{3}\bar{\epsilon}(0)\bar{r} + \mathcal{O}(\bar{r}^2)\right]\left[1 + \frac{\overline{P}(\bar{r})}{\bar{\epsilon}(\bar{r})}\right]\left[1 + \overline{P}(\bar{r})\left(\frac{1}{3}\bar{\epsilon}(0) + \mathcal{O}(\bar{r})\right)^{-1}\right] \\
\times \left[1 - 2a\left(\frac{1}{3}\bar{\epsilon}(0)\bar{r}^2 + \mathcal{O}(\bar{r}^3)\right)\right]^{-1} = 0.
\end{aligned} \tag{2.97}$$

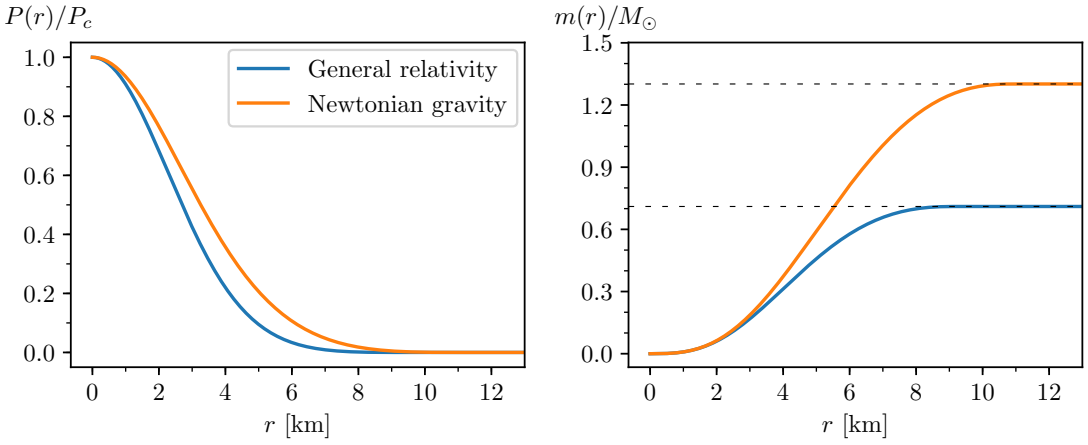

Figure 2.6: Ideal Fermi gas solution at $T = 0$ with $m = m_n$. The plots show the pressure and mass profiles of the maximum mass star as a function of the radial coordinate and normalized by the central pressure $P_c = 3.60 \times 10^{34}\,\mathrm{J/m^3}$ and the solar mass $M_\odot$.

As in the previous section, we consider pure neutron stars, meaning $m = m_n$. Figure 2.5 shows the resulting mass-radius relation. For reference, we chose the

scaling factors $r_0 = 1\,\mathrm{km}$ and $m_0 = M_\odot = 1.988 \times 10^{30}\,\mathrm{kg}$, which gives $a = 1.48$. The maximum mass for this EOS is $M_{\max} = 0.710 M_\odot$, corresponding to a radius $R = 9.16\,\mathrm{km}$, central pressure $P_c = 3.60 \times 10^{34}\,\mathrm{J/m^3}$ and central particle number density $\langle n \rangle_c = 12.5 n_{\mathrm{sat}}$. We have successfully reproduced the upper mass limit of pure neutron stars obtained by Oppenheimer and Volkoff [3]. The pressure and mass profiles for the star of maximum mass is shown in Figure 2.6. We can easily compare this to Figure 2.2 and Figure 2.3, because in all cases the central pressure is the same. As expected, the difference between general relativity and Newtonian gravity is again very large, though less so than for both the linear EOS and the polytrope. So far we have not said anything about the stability of the equilibrium solutions. This will be discussed in Section 3.5, where we will find that the stars to the left of the maximum are unstable with respect to radial oscillations, whereas those to the right are stable.

3 | Theory of Compact Stars

So far we have only combined the structure equations with different single-particle equations of state. More realistic models involve the interplay between several different particle species. Recall from Section E.6 that the pressure P and the energy density ϵ of the ideal Fermi gas is given by the Fermi momentum p_F, which at $T = 0$ is equal to the chemical potential $\mu(T = 0)$ of the given particle species. There is clearly a one-to-one relationship between P and ϵ. However, when multiple particle species are involved, P and ϵ become functions of the chemical potentials of all the particles, and there is generally no longer a one-to-one relationship between them. One can therefore no longer substitute one for the other, as was the whole point of an equations of state: to eliminate a degree of freedom. To fix this, we need to find equations that relate the different chemical potentials to each other. This is where chemical equilibrium and the charge neutrality approximation comes in, which are two of several important subjects to be discussed in this chapter.

We shall also deal with the issue of stability; equilibrium configurations can generally be stable or unstable with respect to some form of perturbations, and the stable ones are the only ones of interest to us. Two criteria for stability will be discussed, one microscopic and one macroscopic. The macroscopic criterion is related to radial perturbations of the star matter and leads to a theorem that lets us determine if a star is stable or not based on the mass-radius relation.

All in all, this chapter is devoted to some of the fundamental theory and considerations of compact stars. But before we get to the subjects mentioned above, we shall briefly justify two approximations of central importance: the use of a flat spacetime metric in quantum field theoretical derivations, and the zero temperature approximation.

3.1 Partial Decoupling of Matter From Gravity

In the previous chapter we used the expressions for the pressure and the energy density of an ideal Fermi gas at zero temperature as the equation of state. In Appendix E, those expressions are seen to emerge from the partition function (a path integral in the imaginary time formalism) for the Dirac Lagrangian, $\mathcal{L}_{\text{Dirac}} = \bar{\psi}(i\gamma^\mu\partial_\mu - m)\psi$. Throughout all the calculations in thermal field theory we used the constant, flat metric of Minkowski space $\eta_{\mu\nu}$. To treat spacetime as flat inside a compact star seems rather strange, since the strength of the gravitational field surrounding such objects is immense, billions of times stronger than on Earth. To justify our use of the flat metric in particle physics, we must show that spacetime

appears flat on the scale of many times the radius of the particles and the interparticle spacing. In doing so, we shall use the same method as Glendenning in [21, p. 66].

Consider a static, spherically symmetric star of mass M close to gravitational collapse. It was mentioned in Section 2.1 that a lower bound on the radius for any star in static spherically symmetric equilibrium is given by $R = \frac{9}{4}GM$. Let us see how much the metric changes across the radius of such a star. The exterior metric is the Schwarzschild metric,

$$ds^2_{\text{ext}} = -\left(1 - \frac{2GM}{r}\right)^{-1} dt^2 + \left(1 - \frac{2GM}{r}\right)^{-1} dr^2 + r^2 d\Omega, \tag{3.1}$$

and thus the rr-component at the surface is

$$g_{rr}(R) = (1 - 2GM/R)^{-1} = (1 - 8/9)^{-1} = 9. \tag{3.2}$$

In Appendix D, we find that the interior metric is given by

$$ds^2_{\text{int}} = -e^{2\alpha(r)} dt^2 + \left[1 - \frac{2Gm(r)}{r}\right]^{-1} dr^2 + r^2 d\Omega. \tag{3.3}$$

The behavior of the rr-component for small r can be seen from Eq. (2.97),

$$g_{rr}(0) = \lim_{r \to 0} \left[1 - \frac{2Gm(r)}{r}\right]^{-1} = 1, \tag{3.4}$$

and so we have

$$\frac{g_{rr}(R)}{g_{rr}(0)} = 9. \tag{3.5}$$

The metric changes by a factor 9 from the center to the surface, which is a lot for macroscopic objects. However, assuming a neutron star, we are rather interested in how much the metric changes across the diameter $2r_n$ of a neutron, which is approximately given by $2r_n/R$ times Eq. (3.5). With a density comparable to the saturation density, such that the particles almost "touch" each other, the total number of neutrons can be approximated as the volume of the star divided by the volume of a neutron,

$$A \approx \left(\frac{R}{r_n}\right)^3. \tag{3.6}$$

By also approximating

$$M = \frac{4R}{9G} \approx A m_n \tag{3.7}$$

and then combining this with Eq. (3.6), we find

$$\frac{g_{rr}(R)}{g_{rr}(0)} \frac{2r_n}{R} = 18A^{-1/3} = 18\left(\frac{4r_n}{9Gm_n}\right)^{-1/2} \approx 10^{-20}, \tag{3.8}$$

which is extremely small. Spacetime is therefore essentially flat over distances spanning many times the diameter of a neturon, and thus the error involved in using the Minkowski metric is negligible.

Notice in Eq. (3.6) that we approximated the volume of the star as the flat space volume. The proper spatial volume of the star is actually

$$\bar{V} = 4\pi \int_0^R \frac{r^2}{\left[1 - \frac{2Gm(r)}{r}\right]} dr. \tag{3.9}$$

The factor in the denominator makes the volume larger compared to flat space, which would only decrease the change in the metric, and it does therefore not take away from our reasoning above.

3.2 The Zero Temperature Approximation

In many calculations on compact stars the temperature is set to zero. This might seem rather strange, since these stars are without a doubt very violent; the temperature of a newborn neutron star is believed to be on the order of 10^{10} K. After a few hundred years they have usually cooled down to 10^6 K, where they remain for at least 10,000 years [22, p. 306]. Still, this is nowhere near absolute zero.

To understand the zero temperature approximation we must take a look at the Fermi–Dirac distribution, Eq. (E.124). The average number of fermions in the single-particle state with momentum $\mathbf{p}$ is given by

$$n_{\mathbf{p}} = \frac{2}{e^{\beta(E_{\mathbf{p}} - \mu)} + 1} = \frac{2}{e^{(\mu/T)(E_p/\mu - 1)} + 1}, \tag{3.10}$$

where μ is the chemical potential of the particle species, $E_p = \sqrt{|\mathbf{p}|^2 + m^2}$ is the energy of the state, and the factor 2 has to do with there being two independent spin states. It is quite easy to convince oneself that when $T \ll \mu$ the distribution function is approximately equal to the Heaviside function,

$$n_{\mathbf{p}} \approx \theta(\mu - E_p) \quad \text{when} \quad T \ll \mu. \tag{3.11}$$

The Fermi gas is then approximately degenerate, and the chemical potential approximately equals the Fermi energy E_F (simply by the definition of the Fermi energy and Eq. (3.11)). But the same effect is achieved by letting $T \to 0$ (that is, $\beta \to \infty$). We can therefore set $T = 0$ in thermodynamic calculations like those in Section E.6 whenever the following degeneracy condition is satisfied [21, p. 82]:

$$T \ll E_F = \sqrt{p_F^2 + m^2} \quad \text{(degeneracy condition)}. \tag{3.12}$$

A lower bound on the Fermi energy of a particle species can be obtained by setting the Fermi momentum to zero [21, p. 82]. The degeneracy condition most definitely holds if T is a lot smaller than this lower bound,

$$T \ll m \quad \text{(sufficient condition for degeneracy)}. \tag{3.13}$$

As mentioned above, the typical temperature of a neutron star is on the order of 10^6 K, while the electron mass is $m_e = 0.511\,\text{MeV} \sim 6 \times 10^9$ K. Thus, the degeneracy condition is easily satisfied for the electrons in a neutron star, and since the masses of the quark flavors and the nucleons are all greater than m_e, the degeneracy condition is satisfied for these as well.

3.3 Electric Charge

A common practice in the literature is to assume electric charge neutrality. This can mean either one of two things: neutrality at a global scale or at a local scale. Usually the latter is assumed, as it makes things a whole lot easier by providing a simple constraint on the chemical potentials of the charged particles. The main goal of this section is to give some justification to the assumption of global and local electric charge neutrality and to consider the constraint equation resulting from the latter.

Let us begin by taking a look at how a star might achieve a net electric charge. We shall do this in the Newtonian framework of gravity by following the arguments of Eddington [23, p. 272]. Consider a gas consisting of several types of particles and maintained at uniform temperature in a gravitational field. As we shall see, a direct result of the Boltzmann distribution law is that the lighter particles will somewhat separate from the heavier ones; the lighter particles will be concentrated more around the surface, while the heavier particles will tend toward the center. Assume, for simplicity, a gas of only two types of particles with masses m_1 and m_2. The probability for a particle to be located in the volume $dxdydz$ with a velocity in the range $dv_x dv_y dv_z$ is given by

$$A_i e^{-\beta m_i \left[\frac{1}{2}(v_x^2+v_y^2+v_z^2)+\phi\right]} dv_x dv_y dv_z dx dy dz, \quad i = 1, 2, \tag{3.14}$$

where the A_i are some constants and ϕ is the gravitational potential satisfying Poisson's equation,

$$\nabla^2 \phi = 4\pi G\rho. \tag{3.15}$$

The solution to Poisson's equation is

$$\phi(\mathbf{r}) = -\int_{\mathbf{R}^3} \frac{G}{|\mathbf{r}-\mathbf{x}|}\rho(\mathbf{x})d^3x, \tag{3.16}$$

but because of spherical symmetry, it is better to combine the shell theorem [24, p. 418] with the definition of the potential in the special case of a point mass to get

$$\phi(r) = \int_\infty^r \mathbf{f}_g \cdot d\mathbf{x} = \int_\infty^r \frac{Gm(x)}{x^2} dx, \tag{3.17}$$

where $m(x)$ is the mass inside a radius x. We see that the potential is everywhere negative and strictly increasing toward zero at infinity. Integrating Eq. (3.14) over velocities and dividing by the volume $dxdydz$ yields the number densities

$$n_i = \left(\frac{2\pi}{\beta m_i}\right)^{\frac{3}{2}} A_i e^{-\beta m_i \phi}, \quad i = 1, 2. \tag{3.18}$$

The densities of the two types of particles relative to each other goes as

$$\frac{n_1}{n_2} \propto e^{\beta(m_1-m_2)|\phi|}. \tag{3.19}$$

If $m_1 > m_2$ this diminishes as we move out toward the surface of the star, where $|\phi|$ is smaller. Thus, we have showed that the lighter particles has a tendency to

rise to the top. Furthermore, lighter particles have a higher average velocity [25]. Combined, this should lead to more frequent escape of lighter particles. If those particles are electrons, the star will be left with a positive net electric charge. Thus, a star can achieve a charge from the diffusion of electrons. This polarizes the star, which eventually causes the diffusion process to stop.

If the net electric charge on a star is very large, a particle whose charge is of the same sign might get expelled out into space. We can obtain a rough estimate of the maximum amount of charge a star can hold by requiring that the coulomb force and the gravitational attraction on a test particle are balanced on the surface (where the pressure is zero) [21, p. 71]. Assuming the particle is a proton, we get

$$\frac{Qe}{R^2} \leq \frac{GMm_p}{R^2}, \tag{3.20}$$

where Q, M and R are the total net charge, mass and radius of the star, and e and m_p are the proton charge and mass. For a compact star with twice the mass of the sun (for example a neutron star) the maximum amount of net charge is estimated to $Q \approx 300\,\mathrm{C}$. On average, this amounts to a deficit of one electron in every two million tons of matter, which is very little.

One might wonder if the picture is different in the general relativistic framework. The gravitational attraction in general relativity is stronger than in Newtonian gravity and should indeed allow for a larger net charge. A non-rotating, static and spherically symmetric body of mass M and charge Q is described in general relativity by the Reissner–Nordström metric. The equilibrium condition for a test particle with mass m and charge q to be at rest in the field of such a star is given by

$$m = \frac{Qqb}{G\big(Mb - Q^2\big)}\sqrt{1 - \frac{2GM}{b} + \frac{GQ^2}{b^2}}, \tag{3.21}$$

where b is the radial distance between the particle and the center of the star [26, 27]. This equation is the general relativistic analog of Eq. (3.20). Thus, the maximum amount of net charge for a compact star with twice the mass of the sun is estimated to $Q \approx 480\,\mathrm{C}$. This is quite a lot more than we get from Newtonian theory, but still very little.

Although the above estimate suggests that the global electric charge on a star is negligible for our purposes, it does not really say much about neutrality at the local scale. It seems unlikely that a star is completely neutral everywhere; however, the work of Bhatia, Bonazzola and Szamosi seems to indicate that abandoning the assumption of local electric charge neutrality has little impact on the maximum mass of a compact star [28]. The same is suggested by the work of Ray, Espíndola and Malheiro [29], where they conclude that to see any appreciable effect on the mass-radius relation of a neutron star consisting of electrons, protons and neutrons, the total charge must be huge $Q \sim 10^{20}\,\mathrm{C}$.

In light of the above discussion, we shall simply assume that local electric charge neutrality is a good approximation and see how this constrains the chemical potentials. The main constituents of a neutron star are neutrons, protons and electrons. If n_p and n_e denote the number densities of protons and electrons, the condition for

local electric charge neutrality reads

$$n_p = n_e. \tag{3.22}$$

With the use of Eq. (E.128), this translates into

$$p_{F,p} = p_{F,e}, \tag{3.23}$$

or in terms of the chemical potentials

$$\sqrt{\mu_p^2 - m_p^2} = \sqrt{\mu_e^2 - m_e^2}. \tag{3.24}$$

This equation is one of several constraints on the μ_i that can be combined to reduce the number of independent chemical potentials to one. The other constraint equations are a consequence of chemical equilibrium, which will be discussed in Section 3.4.

A quark star is generally assumed to consist of mainly electrons and up, down and strange quarks. The reason that the charm, bottom and top flavors are not present is that their chemical potentials are too small compared to their masses at the relevant central densities (more on this in Section 3.4). If n_e, n_u, n_d and n_s denote the number densities of electrons and up, down and strange quarks, the charge neutrality condition becomes

$$\tfrac{2}{3}n_u - \tfrac{1}{3}n_d - \tfrac{1}{3}n_s - n_e = 0, \tag{3.25}$$

since the charges of the down and strange quarks are $-\frac{1}{3}e$, the up quark $\frac{2}{3}e$, and the electron $-e$. These number densities depend on the chemical potentials of the particle species and the above equation therefore let us eliminate one of them. Recall that the number densities of non-interacting particles is generally given by Eq. (E.128), but because there are three colors for each quark flavor, an extra factor $N_c = 3$ must be included in the right-hand side of Eq. (E.124) to account for the extra degeneracy [30, p. 14]. This factor is carried along into Eq. (E.128), and thus the number density of quark flavor $f = u, d, s$ becomes

$$n_f = \frac{p_{F,f}^3}{\pi^2}. \tag{3.26}$$

Inserting this along with the number density for electrons, Eq. (E.128), into the charge neutrality condition above gives

$$2p_{F,u}^3 - p_{F,d}^3 - p_{F,s}^3 - p_{F,e}^3 = 0, \tag{3.27}$$

or equivalently

$$2(\mu_u^2 - m_u^2)^{\frac{3}{2}} - (\mu_d^2 - m_d^2)^{\frac{3}{2}} - (\mu_s^2 - m_s^2)^{\frac{3}{2}} - (\mu_e^2 - m_e^2)^{\frac{3}{2}} = 0. \tag{3.28}$$

3.4 Chemical Equilibrium

All stars are composed of a variety of different particles. These collide with each other, in which different particles can be created and destroyed. For a static star, such processes must necessarily be in some form of equilibrium. If not, the composition of the star would change with time; hence, the star would not be static. This section, inspired by [22], is devoted to the discussion of equilibrium with respect to particle reactions. We shall see that the requirement of chemical equilibrium puts heavy constraints on the chemical potentials of the different particle species.

Consider some fluid flowing through spacetime. For each fluid element we can imagine constructing a local Lorentz frame moving with the same velocity. All thermodynamic quantities will describe measurements made with respect to these frames. When we talk about, for example, the pressure P at some position r, that coordinate location has a fluid element, and $P(r)$ is the pressure one would measure in that fluid element when comoving with it. This is exactly how ϵ and P were defined earlier, namely as the rest-frame energy density and the isotropic rest-frame pressure.

Let us carry over the general setup from Section B.1 on the second law of thermodynamics in the context of stars. Specifically, assume that the star is not too far from equilibrium and approximate it as an isolated thermodynamic system. This effectively means that we neglect thermal radiation and the possibility for particles to escape the star. We shall view a fluid element as a thermodynamic system that can exchange heat and volume with the surrounding fluid elements, but not particles. However, the chemical composition can change due to particle reactions. Let n and ϵ be the baryon density and the energy density in a fluid element. Then ϵ/n is the energy per baryon. In light of Section B.1, the first law of thermodynamics for a fluid element undergoing quasistatic processes reads

$$Tds = d\left(\frac{\epsilon}{n}\right) + Pd\left(\frac{1}{n}\right) + \sum_i \mu_i dY_i, \tag{3.29}$$

where s is the amount of entropy per baryon, $1/n$ is the volume per baryon, μ_i and Y_i are the chemical potential and the relative amount of the i-th particle species,

$$Y_i \equiv \frac{n_i}{n}, \tag{3.30}$$

and, of course, T and P are the temperature and pressure. Among all of these thermodynamic quantities, the chemical potential μ_i is probably the least familiar one. It can be interpreted as the change in energy density for a unit change in the given species, while all other state variables are kept constant,

$$\mu_i = \frac{\partial(\epsilon/n)}{\partial Y_i} = \frac{\partial \epsilon}{\partial n_i}. \tag{3.31}$$

The second law of thermodynamics tells us that the total entropy of the star will tend to increase with time, in accordance with Eq. (3.29), until it reaches a maximum whereupon equilibrium is reached. When the fluid elements are very, very close to equilibrium, their chemical composition is more or less set, and we can

therefore assume that the subsequent particle processes do not change the volume much. Neither do they change the energy, since energy is conserved in particle processes. Technically, energy could of course escape as photons and neutrinos, but we tactically assume the energy loss to be negligible so close to equilibrium. Since particle processes do not change the energy or volume at this point, the chemical aspect of the entropy can be treated independently. For simplicity, assume that thermal and mechanical equilibrium is reached and that the star is very close to chemical equilibrium. Only particle reactions remain to maximize the total entropy and since these processes do not change the internal energy or volume, the thermal and mechanical equilibrium is kept intact. All that is left is for the star to increase its entropy through the particle reactions alone. This means we can set $d(\epsilon/n) = d(1/n) = 0$ in what remains to reach equilibrium,

$$Tds = \sum_i \mu_i dY_i. \tag{3.32}$$

When equilibrium is reached, the entropy is at a maximum, $ds = 0$, and we get

$$\sum_i \mu_i dY_i = 0 \qquad \text{(in equilibrium)}. \tag{3.33}$$

To proceed from here, we need information about the different processes that take place in the star, but first we must determine what kinds of particles are present. There are probably a lot, but of course, to keep the model simple, we must restrict ourselves to the most relevant ones: those that contribute the most to the pressure. Calculations on neutron stars often assume the chemical composition to be of pure neutrons, but this is a simplification. Above nuclear densities, charge-neutral matter does indeed have neutrons as its main constituent, but protons, leptons and hyperons are also present [21, p.228]. Thus, a step up from the assumption of pure neutron matter is the inclusion of protons and electrons. The main processes that occur on the path to chemical equilibrium is β-decay and inverse β-decay,

$$n \to p + e + \bar{\nu_e}, \tag{3.34}$$

$$p + e \to n + \nu_e. \tag{3.35}$$

In a collapsing core, inverse β-decay is the process that occurs when the electron degeneracy pressure gives out. The neutrinos and antineutrinos produced in the above reactions have a mean free path on the order of the star or larger and will therefore quickly leave the star, carrying energy away with them [30, p.12]. Ideally, the star will reach a lowest energy state, where the matter is completely degenerate. The β-processes then come to a stop, because of so-called Pauli blocking; there is not enough energy for the reactants to produce particles that surpasses the Fermi level of the products. However, infinitely close to equilibrium, we can combine the β-reactions with Eq. (3.33) to obtain constraints on the chemical potentials. For example, Eq. (3.34) tells us that $dY_n = -dY_p = -dY_e = -dY_{\bar{\nu_e}}$, and thus

$$\mu_n = \mu_p + \mu_e + \mu_{\bar{\nu_e}} \tag{3.36}$$

But since the neutrinos immediately leave the star, their chemical potentials must be set to zero [21, p.209],

$$\mu_\nu = \mu_{\bar{\nu}} = 0. \tag{3.37}$$

The two reactions then give the same important constraint on the chemical potentials for a neutron star in equilibrium,

$$\mu_n = \mu_p + \mu_e. \tag{3.38}$$

As mention in Chapter 1, it is believed that a neutron star core with sufficiently high pressure will experience a breakdown of its nucleons into their constituents: up and down quarks. Generally, these can turn into other quark flavors through weak interactions. Each flavor f has its own chemical potential μ_f, and at zero temperature their number densities n_f are determined by Eq. (E.128) (with an extra degeneracy factor $N_c = 3$ to account for the three colors),

$$n_f = \frac{3}{\pi^2}\int_0^\infty dp\, p^2 \theta\left(\mu_f - \sqrt{p^2 + m_f^2}\right), \tag{3.39}$$

where θ is the Heaviside step function. If $\mu_f \leq m_f$, the population of that quark flavor is zero. Now, the requirement of charge neutrality and chemical equilibrium put constraints on the chemical potentials such that the number of independent chemical potentials gets reduced to one [30, p. 20]. When we specify a central pressure, this last independent chemical potential becomes fixed. That is, specifying a central pressure fixes all of the μ_f. For the density ranges typical of neutron stars, the chemical potentials of the charm, bottom and top quark flavors turn out to be far below their respective masses, and thus their average number densities are zero [21, p. 295]. We shall therefore only consider quark matter consisting of up, down and strange quarks (and electrons). Such forms of matter, where strange is the heaviest flavor present, are called strange matter.

The relevant processes to determine chemical equilibrium between the quarks in strange matter are the following:

$$\begin{aligned} d \to u + e + \bar{\nu}_e, \qquad & s \to u + e + \bar{\nu}_e, \\ u + e \to d + \nu_e, \qquad & u + e \to s + \nu_e, \end{aligned} \tag{3.40}$$

and

$$s + u \leftrightarrow d + u, \tag{3.41}$$

[30, p. 15]. When setting the neutrino chemical potentials to zero like before, one can easily see that these processes yield the equilibrium condition

$$\mu_d = \mu_s = \mu_e + \mu_u. \tag{3.42}$$

3.5 Stability

Although we have found several solutions to the TOV equation, we have not yet said anything about the stability of these solutions. Equilibrium can either be stable or unstable. For example, imagine a ball situated on the top of a sinusoidal looking

hill versus a sinusoidal looking valley. Both cases represent equilibrium, but for small perturbations, only the ball in the valley is stable. Now, what are the stability criteria for stars? Two main criteria will be discussed here. The first one has to do with stability of the matter on a microscopic level. It says that the following inequality must be satisfied:

$$\frac{\partial P}{\partial \epsilon} > 0 \quad \text{(microscopic equilibrium)}. \tag{3.43}$$

This one is easy to understand; an increase in density implies an increase in gravitational pull. If an increase in density did not also lead to an increase in pressure, then just a small perturbation in the density in some area of the star would lead to unbounded growth of gravitational pull and cause a total gravitational collapse of that area.

The second stability criterion is considerably more complicated and is related to the normal modes of radial oscillations. Imagine a perfect fluid in static, spherically symmetric equilibrium with energy density $\epsilon_0 = \epsilon_0(r)$ and pressure $P_0 = P_0(r)$. What happens if we perturb the fluid elements slightly in the radial direction and in a spherically symmetric fashion? Any such spherically symmetric perturbation can be described in terms of a small *Lagrangian displacement* $\xi(t, r)$, which is simply the radial displacement of the fluid elements initially located at r in the unperturbed configuration. With an equation of motion for $\xi(t, r)$ we could formally discern if an equilibrium configuration is stable or not; a star would be considered stable with respect to radial perturbations if the Lagrangian displacement is always bounded. On the other hand, if ξ grows without bounds for some initial radial perturbation, the star is considered unstable.

An equation of motion for ξ was first discovered by Chandrasekhar [31] on the basis of linear stability theory, and an outlined derivation can be found in [32]. The starting point is conservation of the energy-momentum tensor, $\nabla^a T_{ab} = 0$, from which one obtains the Euler equation describing the motion of fluid elements,

$$(P + \epsilon)u^a \nabla_a u_b + (g_{ab} + u_a u_b)\nabla^a P = 0. \tag{3.44}$$

All quantities appearing here are time-dependent during radial oscillations. The next step is to write all these quantities, including the metric coefficients, as small perturbations from equilibrium, e.g.,

$$P(t, r) \approx P_0(r) + \delta P(t, r), \tag{3.45}$$

and then find expressions for the small time-dependent parts in terms of ξ. The derivation is somewhat lengthy and shall not be done here. However, the result is the following linear equation of motion governing the stellar pulsations:

$$W\ddot{\zeta} = \left(P\zeta'\right)' + Q\zeta, \tag{3.46}$$

where ζ is just a renormalized version of ξ, and W, Q and P are functions of r that

are fully determined by the unperturbed equilibrium configuration,

$$\zeta \equiv r^2 e^{-\alpha_0} \xi, \tag{3.47}$$

$$W \equiv (\epsilon_0 + P_0) r^{-2} e^{3\beta_0 + \alpha_0}, \tag{3.48}$$

$$P \equiv \Gamma_1 P_0 r^{-2} e^{\beta_0 + 3\alpha_0}, \tag{3.49}$$

$$Q \equiv e^{\beta_0 + 3\alpha_0} \left[\frac{\left(P_0'\right)^2}{\epsilon_0 + P_0} r^{-2} - 4P_0' r^{-3} - 8\pi(\epsilon_0 + P_0) P_0 r^{-2} e^{2\beta_0} \right], \tag{3.50}$$

$$\Gamma_1 = \left(\frac{\partial \ln P}{\partial \ln \epsilon} \right)_s \tag{3.51}$$

[32, p. 694]. The zero subscript refers to the particular configuration in static, spherically symmetric equilibrium that is to be analyzed. The variables α and β are defined in Appendix D, Eq. (D.2). They determine the tt and rr components of the metric, respectively. The boundary conditions for the equation of motion (3.46) is that the displacement is zero at the origin (because of spherical symmetry), and that the fluid elements that make up the unperturbed surface are displaced to the perturbed surface [22, p. 138]. This can be formulated as

$$\xi = 0 \qquad \text{at } r = 0, \tag{3.52}$$

$$\Delta P = 0 \qquad \text{at } r = R. \tag{3.53}$$

Here, ΔP denotes the *Lagrangian perturbation*, defined as

$$\Delta P(t, r) = P(t, r + \xi(t, r)) - P_0(r). \tag{3.54}$$

It is the change in pressure one measures when following a specific fluid element as it moves along. In contrast, the *Eulerian perturbation* is defined as the change in the physical quantity measured at the same coordinate location,

$$\delta P(t, r) = P(t, r) - P_0(r). \tag{3.55}$$

These two notions of change are used extensively throughout the derivation of Eq. (3.46). An intermediate result of the derivation is

$$\Delta P = -\Gamma_1 P_0 r^{-2} e^{\alpha_0} \left(r^2 e^{-\alpha_0} \xi \right)' \tag{3.56}$$

[32, p. 694]. Since P_0 is zero at R, it is generally sufficient to demand

$$\xi \text{ finite at } r = R \tag{3.57}$$

[22, p. 138].

To solve the equation of motion (3.46) we can try separation of variables,

$$\zeta = U(r) T(t). \tag{3.58}$$

Substituting this into Eq. (3.46) leads to the two equations

$$\ddot{T} = -\omega^2 T, \tag{3.59}$$

$$(PU')' + QU = -\omega^2 W U, \tag{3.60}$$

where ω^2 is some constant eigenvalue. The former equation has the general solution

$$T(t) = c_1 e^{i\omega t} + c_2 e^{-i\omega t}, \tag{3.61}$$

where only the real part is physical of course. If ω is real, the fluid oscillates sinusoidally, but if ω has an imaginary part, there can be exponential growth or decay. Eq. (3.60) along with the boundary conditions Eq. (3.52) and (3.57) constitute a *Sturm–Liouville eigenvalue problem*. Such eigenvalue problems have several interesting properties, notably the following [22]:

1. The eigenvalues ω_n^2 are all real.
2. The eigenvalues form a discrete countably infinite sequence,
$$\omega_0^2 < \omega_1^2 < \omega_2^2 < \cdots.$$
3. The n-th eigenfunction U_n has exactly n zeros in the interval $0 < r < R$.
4. The eigenfunctions U_n form a basis for the set of all functions satisfying the boundary conditions (3.52) and (3.57).

Since the eigenfunctions U_n form a basis, their linear combination covers all initial perturbations satisfying the boundary conditions. Hence, the method of separation of variables has led us to the general solution for the equation of motion (3.46): it is the linear combination of all modes $\zeta_n = U_n(r)T_n(t)$.

To determine if a star is stable on the macroscopic level we must investigate the normal modes. Recall that P, Q and W are determined by a specific equilibrium configuration, which in turn is determined by a central pressure P_c. Each star in equilibrium therefore has its own set of eigenvalues (and eigenfunctions). If any of the eigenvalues are negative, $\omega^2 < 0$, the frequency ω of that mode is either positive or negative on the imaginary axis. That mode therefore either decays or grows exponentially. Since ω_0^2 is the smallest eigenvalue, the stability criterion becomes $\omega_0^2 \geq 0$ for a stable star. The onset of instability occurs for the equilibrium configuration that has $\omega_0^2 = 0$. It can be shown that this corresponds to the first maximum we reach on the $M(R)$ curve as we decrease R [17, 22, 33]. More generally, some radial mode changes stability at a stationary point,

$$\frac{\partial M}{\partial R} = 0. \tag{3.62}$$

Therefore, if we assume the low density configurations to be stable, the stars after the first maximum must be unstable. Looking back at Figure 2.4 and Figure 2.5, we conclude that the star configurations to the right of the maximum are stable with respect to radial oscillations, while the ones to the left are unstable.

4 | Strange Stars

Equipped with the constraints that follow from electric charge neutrality and chemical equilibrium, we are finally in a position to study quark matter. It was mentioned in Section 3.4 that the chemical potentials of the charm, bottom and top quarks in typical compact stars are far too low to allow for any population of those flavors. But stars consisting of up, down and strange quarks are still a real possibility. In this chapter we solve the structure equations for a few different, increasingly complex models of interacting strange matter. We discuss the MIT Bag model and QCD perturbation theory, and the chapter will be concluded with the case of leading-order corrections to the grand potential of quarks with running of the strange quark mass and the strong coupling constant.

4.1 The Bag Model and the Strange Matter Hypothesis

The simplest model incorporating the strong interactions between quarks in quark matter is the so-called MIT bag model. The general argument is that at sufficiently low temperature and pressure, confined quark matter should be more stable than deconfined quark matter, since this is indeed what we observe in the world we live in. For example, we observe up and down quarks as confined to form neutrons and protons instead of roaming around freely. Since stability is achieved at a minimum of the energy, we expect that the confined phase has lower energy than the deconfined phase (at sufficiently low T and P). But this is not the case if we use the ideal Fermi gas EOS to describe the deconfined quarks. The bag model tries to correct for this in a phenomenological (and very crude) way by introducing an overall bag constant B into the energy density of the deconfined quarks.

First of all, without the bag constant, Eq. (B.20) gives the energy density in terms of the grand potential Φ and the number densities n_i, $\epsilon = \Phi + \sum_i \mu_i n_i$. The index i runs over all the particle species present in the matter. The pressure is simply $P = -\Phi$. If $\Phi = \sum_i \Phi_i$ and an overall bag constant B is added, we get

$$\epsilon = B + \sum_i \epsilon_i = B + \sum_i (\Phi_i + \mu_i n_i), \tag{4.1}$$

$$P = -B + \sum_i P_i = -B - \sum_i \Phi_i. \tag{4.2}$$

By choosing a large enough B, the energy density of the deconfined phase ϵ becomes larger than the energy density of the confined phase, making the latter more stable. Let us now see how B is chosen, which will also lead us to discuss the strange matter

hypothesis — the hypothesis that strange quark matter is the ultimate ground state of matter. The following discussion will be heavily based on [30, 34].

For simplicity, we consider massless quark matter. For the grand potentials Φ_i we take the ideal Fermi gas result; in Section E.6 we found the pressure of an ideal gas of fermions, Eq. (E.132), and so the grand potential Φ_i is just the negative of that. However, quarks have an extra factor $N_c = 3$ owing to their color degeneracy. We get the number densities by using $n_i = -\partial\Phi/\partial\mu_i$. Thus, for massless quark matter, we have

$$P_f = -\Phi_f = \frac{\mu_f^4}{4\pi^2}, \qquad n_f = -\frac{\partial\Phi_f}{\partial\mu_f} = \frac{\mu_f^3}{\pi^2}, \qquad \epsilon_f = \Phi_f + \mu_f n_f = \frac{3\mu_f^4}{4\pi^2}. \tag{4.3}$$

This immediately implies

$$\epsilon_f = 3P_f. \tag{4.4}$$

As we shall see in Section 4.5, massless strange matter is free of electrons. In two-flavor quark matter, on the other hand, electrons are required to achieve local electric charge-neutrality; with $\mu = \mu_d = \mu_u + \mu_e$ from chemical equilibrium and the number densities given by Eq. (4.3) for the quarks and Eq. (E.128) for the electrons, the electric charge neutrality condition (4.46) for two-flavor quark matter becomes

$$2(\mu - \mu_e)^3 - \mu^3 - \mu_e^3 = 0. \tag{4.5}$$

If there are no electrons, i.e., $\mu_e = 0$, this implies $\mu = 0$ as well. Electrons must therefore be present. However, for simplicity, let us ignore electrons in the discussion that follows. Their contribution is small enough to be rendered unimportant for the following argument [30].

First, let us determine a lower bound on the bag constant B. We do this by requiring that the energy per baryon in two-flavor matter is greater than the energy per nucleon in nuclear matter when both forms of matter are considered at $T = 0$ and $P = 0$,

$$\left.\frac{\epsilon}{n_B}\right|_{N_f=2} > \left.\frac{E}{A}\right|_{\text{neutrons}}, \qquad T = 0, P = 0. \tag{4.6}$$

Here, E and A are the energy and nucleon number in some volume element of pure neutron matter, and we have defined the baryon number density n_B as

$$n_B = \frac{1}{3}\sum_f n_f, \tag{4.7}$$

because a baryon contains three quarks. Ignoring electrons, the charge neutrality condition becomes

$$n_d = 2n_u, \tag{4.8}$$

and thus

$$\mu_d = 2^{1/3}\mu_u. \tag{4.9}$$

The baryon number density of two-flavor quark matter is therefore $n_B = \mu_u^3/\pi^2$. Furthermore, at $P = 0$ we have from Eq. (4.2) that

$$B = \sum_f P_f = \frac{(\mu_u^4 + \mu_d^4)}{4\pi^2} = \frac{\left(1 + 2^{4/3}\right)\mu_u^4}{4\pi^2}. \tag{4.10}$$

Solving this for μ_u lets us write n_B in terms of B. We also want ϵ in terms of B, which we get by combining Eq. (4.10) with Eqs. (4.1) and (4.4),

$$\epsilon = B + 3\sum_f P_f = 4B. \tag{4.11}$$

In total, the energy per baryon for two-flavor quark matter at zero temperature and pressure is given by

$$\left.\frac{\epsilon}{n_B}\right|_{N_f=2} = (4\pi^2)^{1/4}(1+2^{4/3})^{3/4}B^{1/4} = 6.441B^{1/4}. \tag{4.12}$$

On the other hand, the energy per nucleon in pure neutron matter at zero T and P is just the rest energy of a neutron,

$$\left.\frac{E}{A}\right|_{\text{neutrons}} = m_n = 939.6\,\text{MeV}. \tag{4.13}$$

Hence, if the confined phase is to be energetically more favorable, we must have that

$$B^{1/4} > 145.9\,\text{MeV}. \tag{4.14}$$

This will serve as as our lower bound on the bag constant.

Let us now perform the same calculation but this time for strange matter. Chemical equilibrium implies that $\mu = \mu_s = \mu_d = \mu_u + \mu_e$ and the electric neutrality condition yields $\mu_e = 0$. So all the quark chemical potentials are equal, and therefore also all the number densities. The baryon number density is simply $n_B = \mu^3/\pi^2$. At $P = 0$ we have

$$B = \sum_f P_f = \frac{3\mu^4}{4\pi^2}, \tag{4.15}$$

which, again, can be solved for μ to give n_B in terms of B. As for two-flavor quark matter, $\epsilon = 4B$, so the energy per baryon in strange matter at zero temperature and pressure becomes

$$\left.\frac{\epsilon}{n_B}\right|_{N_f=3} = (4\pi^2)^{(1/4)}3^{3/4}B^{1/4} = 5.714B^{1/4}. \tag{4.16}$$

Notice how strange matter has a lower energy per baryon than *ud* matter. The strange matter hypothesis suggests that the true ground state of matter is not that of hadronic matter, but rather strange matter composed of nearly equal amounts of the three quark flavors. It might just be so that ordinary hadronic matter is just a very long-lived state of matter, but not absolutely stable. If this were to be true, then there might exist stars made up entirely of strange matter [21]. A thorough discussion on the strange matter hypothesis and its compatibility with present knowledge can be found in [21]. Here, we shall simply assume it to be valid, whereby we obtain an upper bound on the bag constant. For if strange matter is to be more stable than hadronic matter, we must have that

$$\left.\frac{\epsilon}{n_B}\right|_{N_f=3} < \left.\frac{E}{A}\right|_{^{56}\text{Fe}}, \tag{4.17}$$

because iron ^{56}Fe has the lowest mass per nucleon of all the nuclides. The binding energy of ^{56}Fe is at $\Delta E_b = 8.8\,\mathrm{MeV}$ per nucleon, and thus with 30 neutrons and 26 protons, its energy per nucleon is simply

$$\left.\frac{E}{A}\right|_{^{56}\mathrm{Fe}} = \frac{30m_n + 26m_p - 56\Delta E_b}{56} = 930.2\,\mathrm{MeV}, \tag{4.18}$$

where we have used $m_n = 939.6\,\mathrm{MeV}$ and $m_p = 938.3\,\mathrm{MeV}$. Substituting this and Eq. (4.16) into Eq. (4.17) yields an upper bound on the bag constant at $B^{1/4} = 162.8\,\mathrm{MeV}$. The interval for the bag constant is therefore

$$146\,\mathrm{MeV} < B^{1/4} < 163\,\mathrm{MeV}. \tag{4.19}$$

In Section 4.5, mass-radius relations for several different values of B, from both inside and slightly outside the above interval, will be considered.

4.2 Yang–Mills Theory

In Appendix E on thermal quantum field theory we argued that a quantum system is defined by its Lagrangian. We saw how the Dirac Lagrangian and the path integral formulation gave us Fermi–Dirac statistics describing non-interacting fermions. To describe a system where the particles are actually interacting, one has to add so-called interaction terms to the Lagrangian. The Dirac Lagrangian is the result of a series of minimal and reasonable assumptions. The same can be said for the QCD Lagrangian describing the strong interactions between quarks; QCD is a form of Yang–Mills theory, which can be seen as a generalization of quantum electrodynamics (QED). Therefore, let us begin by seeing how QED emerges from symmetry considerations and then how this is generalized to give QCD. The main purpose of this section is to justify and discuss the QCD Lagrangian since it is what defines the theory and therefore the interactions between quarks, which is what we ultimately seek a description of.

The free Dirac Lagrangian is given by $\mathcal{L}_{\mathrm{Dirac}} = \bar{\psi}(i\gamma^\mu\partial_\mu - m)\psi$, see the beginning of Section E.5. It has a global $U(1)$ symmetry under the transformation $\psi \to e^{-i\alpha}\psi$, where α is a real number. Quantum electrodynamics emerges when we promote this global symmetry to a local one, $\alpha \to \alpha(x)$. When trying to make the symmetry local, one can easily show that we are forced to add a new field A_μ (called a gauge field) to the Lagrangian, and in such a way that it can be absorbed into the definition of the derivative, resulting in a covariant derivative $\partial_\mu \to D_\mu \equiv \partial_\mu + ieA_\mu$. The gauge field must transform as $A_\mu(x) \to A_\mu(x) + e^{-1}\partial_\mu\alpha(x)$ under the gauge transformation. The constant e is the (bare) elementary charge and determines the strength of the interaction. If we want the gauge field to be dynamical we need to add a kinetic term. The most general kinetic term for the gauge field we can add to the Lagrangian that preserves the newly constructed gauge invariance is the square of the electromagnetic field strength tensor $F_{\mu\nu}$ [35]. Therefore, the QED Lagrangian is given by

$$\mathcal{L}_{\mathrm{QED}} = -\frac{1}{4}F_{\mu\nu}^2 + \bar{\psi}(i\gamma^\mu D_\mu - m)\psi. \tag{4.20}$$

Like the free Dirac Lagrangian can be shown to describe non-interacting fermions, the kinetic term for the gauge field can be shown to describe non-interacting, massless, spin-1 bosons, specifically photons. The photon is therefore also referred to as a gauge boson.

Yang–Mills theory can be viewed as a generalization of QED. The Dirac Lagrangian has in fact not only a global $U(1)$ symmetry, but also a global $SU(n)$ symmetry if we take ψ to be an n-component object of n fermionic fields $\psi \to \vec{\psi} = (\psi_1, \ldots, \psi_n)^T$. By considering linear transformations on these $\vec{\psi}$, one realizes that the Lagrangian is invariant when acting on them with a special unitary matrix of degree n. That is, the Lagrangian is invariant under the global gauge transformation $\vec{\psi} \to U\vec{\psi}$, where U is a special unitary $n \times n$ matrix. For QED the symmetry group was $U(1)$ and there was only one fermionic field. The group elements were $U = e^{-i\alpha}$ and we claimed that we had to add one gauge field to the Lagrangian to make the symmetry local. In Yang–Mills theory, however, we must add $n^2 - 1$ gauge fields. Let us briefly see why this is so.

The $SU(n)$ matrices are just representations of elements of the more abstract Lie group $SU(n)$. A Lie group G is also a differentiable manifold and from it we can construct a Lie algebra $\mathfrak{g}$ by using the tangent space to G at its identity element $U = \mathbf{1}_G$ as the underlying vector space of the algebra. This particular algebra is very useful when studying the Lie group, because a neighborhood of 0 of the algebra is mapped smoothly and bijectively onto a neighborhood of the group's identity element via the exponential map $\exp : \mathfrak{g} \to G$. The Lie algebra can therefore be said to capture the local structure of the Lie group. For $SU(n)$, we write $\mathfrak{su}(n)$ for its corresponding Lie algebra, and in this case the exponential map $\exp : \mathfrak{su}(n) \to SU(n)$ maps onto the entire group. Thus, any group element U of SU(n) can be written as $U = \exp\{i\alpha^a T^a\}$, where α^a are real numbers and T^a are the *generators* of $\mathfrak{su}(n)$. Generators are just a minimal set of elements of an algebra such that by using the operations of the algebra on them we can construct any element of the algebra. One can easily show that when the global $SU(n)$ symmetry of the Lagrangian is promoted to a local symmetry, we are forced to add a gauge field A^a_μ for each generator T^a of the symmetry group, resulting in the covariant derivative

$$D_\mu \vec{\psi} = \partial_\mu \vec{\psi} - igA^a_\mu T^a \vec{\psi} \tag{4.21}$$

where g, the coupling constant, is a real number that determines the strength of the interaction. That is why we had to add exactly one gauge field in QED; The group $U(1)$ has only one generator. For $SU(n)$, on the other hand, there are $n^2 - 1$ generators, and that is why we must add $n^2 - 1$ gauge fields in Yang–Mills theory.

The gauge fields in Yang–Mills theory must transform as

$$A^a_\mu(x) \to A^a_\mu(x) + \frac{1}{g}\partial_\mu \alpha^a(x) - f^{abc}\alpha^b(x)A^c_\mu(x), \tag{4.22}$$

where f^{abc} are the structure constants for $\mathfrak{su}(n)$. These are defined by the commutation relations for the generators,

$$\left[T^a, T^b\right] = if^{abc}T^c. \tag{4.23}$$

In fact, the structure constants are what defines the Lie algebra. If all the generators of a Lie algebra commute, $f^{abc} = 0$, the Lie groups constructed from the algebra are commutative, also called Abelian. Since the generators of $SU(n)$ do not commute, Yang–Mills theory is also referred to as non-Abelian gauge theory.

All that is missing are kinetic terms for the gauge fields to make them dynamic. The unique kinetic term we can add that preserves the gauge symmetry is

$$\mathcal{L}_{\text{YM}} = -\frac{1}{4}\sum_a (F^a_{\mu\nu})^2 = -\frac{1}{4}\sum_a \left(\partial_\mu A^a_\nu - \partial_\nu A^a_\mu + g f^{abc} A^b_\mu A^c_\nu\right)^2, \tag{4.24}$$

where $F^a_{\mu\nu}$ is obviously a generalization of the electromagnetic field strength tensor [35]. Finally, putting everything together yields the locally $SU(n)$ invariant Lagrangian

$$\boxed{\mathcal{L} = -\frac{1}{4}\sum_a (F^a_{\mu\nu})^2 + \sum_{i,j=1}^{n} \bar{\psi}_i(\delta_{ij} i\gamma^\mu \partial_\mu + g\gamma^\mu A^a_\mu T^a_{ij} - m\delta_{ij})\psi_j.} \tag{4.25}$$

The QCD Lagrangian is a special case of the above, corresponding to $n = 3$. That is, the symmetry group of QCD is $SU(3)$, for the reason that there are 3 colors. The generators for $SU(3)$ are often written in a standard basis $T^a = \frac{1}{2}\lambda^a$, where λ^a are the Gell-Mann matrices, see for example [35, p. 485]. Also, the field strength tensors $F^a_{\mu\nu}$ for the gauge/gluon fields are often denoted by $G^a_{\mu\nu}$ instead.

4.3 Perturbative QCD

In the previous section we arrived at the expression for the Lagrangian describing quarks that interact via the strong force. The next step toward a description of interacting quark matter would be to calculate the system's partition function Z from its definition, similar to what we did for the free scalar field and the free Dirac Lagrangian in Appendix E. However, the QCD Lagrangian is miles more complicated, and thus the path integral that defines the partition function is impossible to evaluate in closed form. We must therefore use approximation techniques, namely perturbation theory. The path integral is expanded as a perturbation series in the interaction, and for every order we get several new integrals that must be evaluated. These are, of course, a lot less complex than the original path integral, but they do rise very quickly in complexity as the order increases and are by no means easy to evaluate. The expansion is expected to converge when the interaction is weak, but the convergence properties of such expansions are not really established yet in terms of rigorous mathematics [36, p. 33]. Also, the interaction can not really be regarded as weak at the energy scales applicable for compact stars. However, results from perturbative QCD seems to agree reasonably well with other methods [37]. In this section we shall discuss how perturbative QCD is performed, and we will also take a look at the lowest-order correction to the partition function for quarks that interact via the strong force.

For simplicity, let us consider a single scalar field ϕ, basing our discussion on [36]. The main idea is the same for more physical theories like QED, QCD and the

Glashow–Weinberg–Salam theory. The general Lagrangian for a neutral scalar field is given by Eq.(E.45). It has a kinetic term and a mass term that both are quadratic in the field, and it has an unspecified number of interaction terms collectively denoted by $U(\phi)$. The partition function is given by Eq. (E.58),

$$Z = C' \int \mathcal{D}\phi \, e^{S}. \tag{4.26}$$

Note that the action S houses the Euclidean version of the Lagrangian $\mathcal{L}_E$, as seen in Eq. (E.58). We already know from Section E.4 how to integrate the quadratic terms; it is the higher order interaction terms that are causing trouble. The trick is therefore to decompose the action into two parts,

$$S = S_0 + S_I, \tag{4.27}$$

where S_0 contains the quadratic terms and S_I the higher order interaction terms. We can then expand the factor e^{S_I} as a power series,

$$\begin{aligned} Z &= C' \int \mathcal{D}\phi \, e^{S_0} \left(1 + \sum_{k=1}^{\infty} \frac{1}{k!} S_I^k \right) \\ &= C' \int \mathcal{D}\phi e^{S_0} + \sum_{k=1}^{\infty} \frac{1}{k!} C' \int \mathcal{D}\phi e^{S_0} S_I^k \\ &= \left(C' \int \mathcal{D}\phi e^{S_0} \right) \left(1 + \sum_{k=1}^{\infty} \frac{1}{k!} \frac{\int \mathcal{D}\phi e^{S_0} S_I^k}{\int \mathcal{D}\phi e^{S_0}} \right). \end{aligned} \tag{4.28}$$

Taking the logarithm on both sides gives

$$\begin{aligned} \ln Z &= \ln \left(C' \int \mathcal{D}\phi e^{S_0} \right) + \ln \left(1 + \sum_{k=1}^{\infty} \frac{1}{k!} \frac{\int \mathcal{D}\phi e^{S_0} S_I^k}{\int \mathcal{D}\phi e^{S_0}} \right) \\ &= \ln Z_0 + \ln Z_I. \end{aligned} \tag{4.29}$$

The partition function has effectively been split into two parts. One that we have already calculated and one interaction part of which we can only hope to calculate up to a few orders in the coupling constant g.

If the interaction S_I is small, the leading order corrections might be a good approximation. The smallness of S_I is heavily dependent on the coupling constant. Generally the coupling constant "runs" with the energies of the particles, i.e., it depends on the energy scale of the system. In QCD we have asymptotic freedom; the strong coupling constant is small at high energies and the particles interact weakly. This regime is ideal for perturbation theory. At low energies the coupling constant is large and the quarks interact strongly and become confined to hadrons.

The integrals that must be evaluated order by order are

$$\langle S_I^k \rangle_0 \equiv \frac{\int \mathcal{D}\phi e^{S_0} S_I^k}{\int \mathcal{D}\phi e^{S_0}} \tag{4.30}$$

For easier communication, such integrals are translated into a diagrammatic form, namely Feynman diagrams, which also serve as visualizations of the different particle interactions. The rules for translating such diagrams to mathematical expressions are called Feynman rules. Each Lagrangian or field theory has its own set of Feynman rules. This is a standard technique covered in any regular QFT book, for example [35, 38]. The Feynman rules for thermal QCD can be found in [36]. Evaluating Feynman diagrams usually leads to divergent terms. These divergences are taken care of by renormalization methods. The essence of such methods is to absorb the infinities into the bare, unmeasurable quantities appearing in the Lagrangian, like m and g, yielding quantum corrections that solely depend on physically measurable (renormalized) versions of these quantities. It is these physical quantities (observables) that we actually measure that depend on the energy of the interacting particles and are said to "run" with the energy of the system.

The lowest-order correction to the partition function for quark matter is the following two-loop diagram:

$$\ln Z_1 = -\frac{1}{2} \tag{4.31}$$

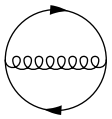

It translates into the following integral expression:

$$\begin{aligned}\frac{\ln Z_1}{\beta V} = -2\pi\alpha_s \frac{N_c^2-1}{2} \int \frac{d^3p}{(2\pi)^3}\frac{d^3q}{(2\pi)^3}\frac{d^3k}{(2\pi)^3}(2\pi)^3\delta(\mathbf{p}-\mathbf{q}-\mathbf{k}) \\ \times T^3 \sum_{n_p,n_q,n_k} \beta\delta_{n_p,n_q+n_k} \frac{\mathrm{Tr}\big[\gamma^\mu(\not{p}+m_f)\gamma_\mu(\not{q}+m_f)\big]}{k^2(p^2-m_f^2)(q^2-m_f^2)},\end{aligned} \tag{4.32}$$

where $N_c = 3$ for QCD and $\alpha_s = g^2/4\pi$ [36, 37]. From here on, we refer to α_s as the strong coupling constant. There are actually three more diagrams at the same order in α_s in addition to this one, but they all vanish at zero temperature. It is not our intention to calculate this diagram; instead, we shall simply quote the result. But first we mention that it is slightly more convenient to work with the grand potential Φ rather than $\ln Z$. They are related by

$$\Phi = -\frac{\ln Z}{\beta V}, \tag{4.33}$$

see Section B.2. So to make the switch we just take the negative of Eq. (4.32). The calculation of Eq. (4.32) is outlined in [36]; the leading order, zero temperature correction to the grand potential of quark flavor f with mass m_f and chemical potential μ_f in the $\overline{\mathrm{MS}}$ renormalization scheme is

$$\begin{aligned}\Phi_f^{(1)} = \frac{\alpha_s\big(N_c^2-1\big)}{16\pi^3}\Bigg[3\bigg(m_f^2\ln\frac{\mu_f+u_f}{m_f} - \mu_f u_f\bigg)^2 - 2u_f^4 \\ + m_f^2\bigg(6\ln\frac{\bar{\Lambda}}{m_f}+4\bigg)\bigg(\mu_f u_f - m_f^2\ln\frac{\mu_f+u_f}{m_f}\bigg)\Bigg],\end{aligned} \tag{4.34}$$

where $u_f = \sqrt{\mu_f^2 - m_f^2}$ is the Fermi momentum [37]. The quantity $\bar{\Lambda}$ is called the renormalization scale. In theory, it is arbitrary; if we could somehow sum all orders of the perturbation expansion, $\bar{\Lambda}$ would in fact vanish. But since we cannot do that, we should choose $\bar{\Lambda}$ such that the importance of the neglected terms of the expansion are minimized [36, p. 149]. More on this in Section 4.6, where we also introduce the running of the mass and the coupling constant, $m_f = m_f(\bar{\Lambda})$ and $\alpha_s = \alpha_s(\bar{\Lambda})$.

4.4 Equation of State for Strange Matter

In this section we briefly summarize the equations that define the model we shall use for strange matter. For the pressure and energy density we use the basic thermodynamic relations for a grand canonical ensemble, and we shall generally allow those equations to be modified by a bag constant,

$$P = -B - \sum_i \Phi_i, \tag{4.35}$$

$$\epsilon = B + \sum_i (\Phi_i + \mu_i n_i), \tag{4.36}$$

where $i = e, u, d, s$, and the particle number densities are given by

$$n_i = -\left.\frac{\partial \Phi}{\partial \mu_i}\right|_{\mu_{j\neq i}}. \tag{4.37}$$

The long, vertical bar emphasises that the other chemical potentials are to be kept constant while taking the derivative, a notation that will be useful later. Parentheses are more often used for this instead of a vertical bar, but in this case that would clutter up the equations too much. Note that we use the index i to mean both quarks and electrons, and we use the index f (for flavor) when we refer solely to the quarks.

The quark grand potential Φ_f will be taken to leading order in the strong coupling constant α_s. The zeroth-order term $\Phi_f^{(0)}$ is the negative of the pressure of an ideal gas of fermions, given by Eq. (E.132), multiplied by the color degeneracy factor $N_c = 3$,

$$\Phi_f^{(0)} = -\frac{1}{4\pi^2}\left[\mu_f u_f\left(\mu_f^2 - \frac{5}{2}m_f^2\right) + \frac{3}{2}m_f^4 \ln\frac{\mu_f + u_f}{m_f}\right], \tag{4.38}$$

where $f = u, d, s$ and $u_f = \sqrt{\mu_f^2 - m_f^2}$. The leading-order correction $\Phi_f^{(1)}$ (first order in α_s) in the $\overline{\text{MS}}$ renormalization scheme is given by Eq. (4.34),

$$\begin{aligned}\Phi_f^{(1)} = \frac{\alpha_s}{2\pi^3}\Bigg[3\left(m_f^2 \ln\frac{\mu_f + u_f}{m_f} - \mu_f u_f\right)^2 - 2u_f^4 \\ + m^2\left(6\ln\frac{\bar{\Lambda}}{m_f} + 4\right)\left(\mu_f u_f - m_f^2 \ln\frac{\mu_f + u_f}{m_f}\right)\Bigg].\end{aligned} \tag{4.39}$$

The grand potential of the quark flavor f to first order in the strong interaction coupling constant α_s and renormalized at the scale $\bar{\Lambda}$ is given by the sum of the above,

$$\Phi_f = \Phi_f^{(0)} + \Phi_f^{(1)}, \qquad f = u, d, s. \tag{4.40}$$

As mentioned in Section 4.3, the renormalization scale $\bar{\Lambda}$ must be chosen in such a way that the importance of the neglected terms of the perturbation expansion are minimized. Furthermore, the mass m_f and the coupling constant α_s are functions of $\bar{\Lambda}$ in perturbation theory. In the next section, however, we approximate the quarks as massless and the coupling constant as fixed. The running of the parameters will be discussed in Section 4.6.

Note that the expression used for the quark grand potential in the much cited article on strange matter [39] by Farhi and Jaffe was calculated in a different renormalization scheme. The expression used here and the expression found in that article differ simply by a factor in the definition of the renormalization scale, $\rho \approx 1.94773\bar{\Lambda}$. (There is also a + that should be a − in their expression: the one in front of the last of three terms on the second line in Ω_s. This is corrected for in Glendenning's book [21].)

Electrons, being leptons, do not interact through the strong force and will therefore be modeled as an ideal Fermi gas. The pressure of an ideal Fermi gas is given by Eq. (E.132), and thus the electron grand potential Φ_e is the negative of that equation (without N_c this time, of course). However, we shall always approximate the electrons as massless; inserting $m_e = 0$ for m in Eq. (E.132) and recalling that $p_{F,e} = \sqrt{\mu_e^2 - m_e^2}$ yields

$$\Phi_e = -\frac{\mu_e^4}{12\pi^2}. \tag{4.41}$$

Since the quark grand potentials Φ_f do not explicitly depend on μ_e, the number density of electrons is computed from the electron grand potential alone,

$$n_e = -\frac{\partial \Phi_e}{\partial \mu_e} = \frac{\mu_e^3}{3\pi^2}. \tag{4.42}$$

Note that Eq. (4.41) and Eq. (4.42) will hold all throughout this chapter. In other words, the expressions we use for Φ_e and n_e will not change across the various models. Contrarily, the quark grand potentials and number densities will change as a result of assuming either massless or massive quarks and running or constant coupling and mass.

In Section 3.3 and Section 3.4 we found that the local electric charge neutrality condition and chemical equilibrium reduce the number of independent chemical potentials to one. Let us therefore define a new chemical potential simply as $\mu \equiv \mu_s$. Chemical equilibrium, Eq. (3.42), then implies

$$\mu_s = \mu, \tag{4.43}$$

$$\mu_d = \mu, \tag{4.44}$$

$$\mu_u = \mu - \mu_e. \tag{4.45}$$

To eliminate μ_e we need to solve the equation of electric charge neutrality (3.25),

$$\tfrac{2}{3}n_u - \tfrac{1}{3}n_d - \tfrac{1}{3}n_s - n_e = 0, \tag{4.46}$$

but this must generally be done numerically at each step when solving the structure equations. With these relations, the grand potentials Φ_i and the number densities n_i become functions of μ alone, and so do the pressure and the energy density. Solving the structure equations then becomes in principle the same as for the ideal Fermi gas of neutrons in Section 2.6, although the numerical implementation is slightly more involved.

4.5 The Massless Quark Approximation

We start off with perhaps the simplest model of strange stars, where all of the flavors involved (u, d, s) are approximated as massless and the coupling constant is assumed to be independent of the particle energies,

$$m_u = m_d = m_s = 0 \qquad \text{and} \qquad \alpha_s \text{ fixed.} \tag{4.47}$$

The quark grand potentials are then considerably simplified,

$$\Phi_f = -\frac{\mu_f^4}{4\pi^2}\left(1 - \frac{2\alpha_s}{\pi}\right), \qquad f = u, d, s. \tag{4.48}$$

So too is the quark number densities, because we do not have to worry about the derivatives of α_s and the quark masses with respect to μ_f. Also, n_f reduces to the derivative of Φ_f alone (instead of the total grand potential Φ),

$$n_f = -\frac{\partial \Phi_f}{\partial \mu_f} = \frac{\mu_f^3}{\pi^2}\left(1 - \frac{2\alpha_s}{\pi}\right), \qquad f = u, d, s. \tag{4.49}$$

In this case, the electric neutrality equation becomes simple enough to be solved analytically; substituting the electron and quark number densities, Eq. (4.42) and Eq. (4.49), into the electric charge neutrality condition, Eq. (4.46), gives

$$\begin{aligned} 2\mu_u^3\eta - \mu_d^3\eta - \mu_s^3\eta - \mu_e^3 = 0, \quad \eta \equiv \left(1 - \frac{2\alpha_s}{\pi}\right), \\ \left[(1+2\eta)\mu_e^2 - 6\eta\mu\mu_e + 6\eta\mu^2\right]\mu_e = 0. \end{aligned} \tag{4.50}$$

By using the quadratic formula one finds that the non-trivial solutions are complex. We must therefore take $\mu_e = 0$, which by Eq. (4.42) implies that massless quark matter with fixed coupling is free of electrons. This makes the quark chemical potentials particularly symmetric,

$$\mu_u = \mu_d = \mu_s = \mu. \tag{4.51}$$

The pressure and energy density are now easily calculated from (4.35) and (4.36). Since Φ_e and n_e vanish and the μ_f are all equal, we get

$$P = -B + \frac{3\mu^4}{4\pi^2}\left(1 - \frac{2\alpha_s}{\pi}\right), \tag{4.52}$$

$$\epsilon = B + \frac{9\mu^4}{4\pi^2}\left(1 - \frac{2\alpha_s}{\pi}\right). \tag{4.53}$$

Combining the equations by eliminating μ results in the very simple equation of state

$$\epsilon = 3P + 4B. \tag{4.54}$$

Notice that in this case we would get the exact same if we had not included the leading-order corrections at all.

Figure 4.1 shows the mass-radius relation for massless strange matter with fixed coupling for several different values of B. The values are picked from both inside and outside the interval (4.19). The low density stars are the ones located all the way to the left in the plot, and the density increases along the lines toward their respective maximum mass indicated by a cross $\times$. The low-density stars are the ones that are stable, and thus the stars after the maximum are unstable [40], as discussed in Section 3.5. We quickly notice that these MR-relations look quite different from the ones we found for neutron stars in Chapter 2; for neutron stars, the mass increased with decreasing radius. Here it is the opposite (until we really start to close in on the maximum). The maximum masses and corresponding radii for the different choices of $B^{1/4}$ are shown in Table 4.1. Interestingly, the masses and radii for these strange stars are very similar to typical masses and radii of observed neutron stars. We also notice that the maximum mass stars all lie along a straight line. For every 1 km increase in maximum radius (as a result of decreasing the bag constant B), the maximum mass increases by 0.18 $M_\odot$.

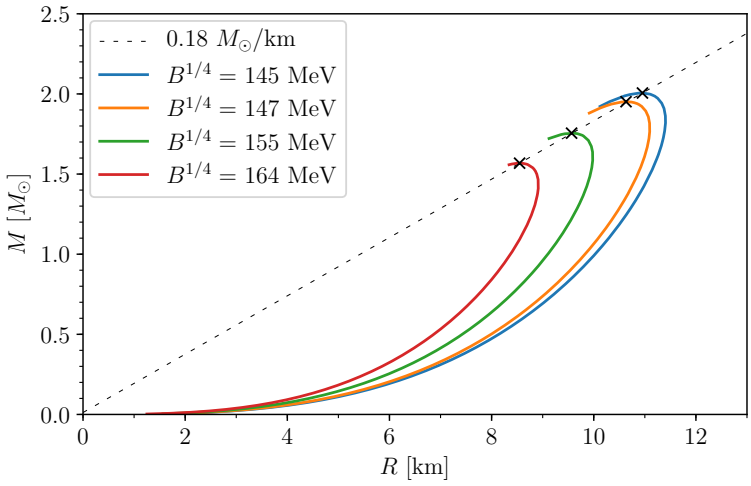

Figure 4.1: Mass-radius relations for massless strange matter with constant coupling. The higher the value of the bag constant B, the lower the maximum mass and radius.

4.6 Running Mass and Coupling

In this section we introduce running of the strong coupling constant α_s and the strange quark mass m_s. We adopt the expressions for their dependence on the

$B^{1/4}$ [MeV]	$M_{\max}$ $[M_\odot]$	R [km]
145	2.01	10.95
147	1.95	10.63
155	1.76	9.57
164	1.57	8.55

Table 4.1: Maximum masses and corresponding radii for the plots in Figure 4.1

renormalization scale $\bar{\Lambda}$ from [37];

$$\alpha_s(\bar{\Lambda}) = \frac{4\pi}{\beta_0 L}\left(1 - 2\frac{\beta_1}{\beta_0^2}\frac{\ln L}{L}\right), \tag{4.55}$$

$$m_s(\bar{\Lambda}) = \hat{m}_s\left(\frac{\alpha_s}{\pi}\right)^{4/9}\left(1 + 0.895062\frac{\alpha_s}{\pi}\right), \tag{4.56}$$

where $L = 2\ln\left(\bar{\Lambda}/\Lambda_{\overline{\text{MS}}}\right)$, $\beta_0 = 11 - 2N_f/3$, and $\beta_1 = 51 - 19N_f/3$. Recall that $N_f = 3$. The scale $\Lambda_{\overline{\text{MS}}}$ is fixed by requiring $\alpha_s \simeq 0.3$ and $m_s \simeq 100$ MeV at $\bar{\Lambda} = 2$ GeV [37]. This yields $\Lambda_{\overline{\text{MS}}} \simeq 380$ MeV and $\hat{m}_s \simeq 262$ MeV. All that remains to have a closed system is to specify the dependence of $\bar{\Lambda}$ on the chemical potentials of the quarks. However, the exact form of this dependence is not completely known [41], but we choose it as in [37],

$$\bar{\Lambda} = \frac{2}{3}(\mu_u + \mu_d + \mu_s). \tag{4.57}$$

The quark grand potentials are still given by Eq. (4.38) and (4.39), but α_s, m_s and $\bar{\Lambda}$ in those expressions are now given by Eq. (4.55), (4.56) and (4.57). This makes computing n_f considerably more tedious, partially because taking the derivative of the individual grand potentials Φ_f is more involved, but also because each of the Φ_f now depend on all of the quark chemical potentials through its dependence on $\bar{\Lambda}$. This means that Eq. (4.37) does not reduce to only the derivative of one grand potential anymore.

Calculating n_i, although technically straightforward, can be quite a mess. To make the procedure more organized, we follow [41] and split up Φ_i into its zeroth- and first-order terms,

$$\Phi_i = \omega_i^{(0)} + \alpha_s\omega_i^{(1)}, \tag{4.58}$$

where neither of $\omega_i^{(0)}$ or $\omega_i^{(1)}$ depend on α_s. We will refer to these as the ω-functions. Notice that $\omega_i^{(0)}$ is just $\Phi_i^{(0)}$, and $\omega_i^{(1)}$ is just $\Phi_i^{(1)}$ without the explicit α_s factor. Notice also that by using i as the index we split up the electron grand potential Φ_e in this way as well, whereby

$$\omega_e^{(0)} = \Phi_e = -\frac{\mu_e^4}{12\pi^2} \quad \text{and} \quad \omega_e^{(1)} = 0. \tag{4.59}$$

Writing the total grand potential as $\Phi = \sum_k \omega_k^{(0)} + \alpha_s \omega_k^{(1)}$ (the sum running over $k = e, u, d, s$) and substituting this into Eq. (4.37) yields

$$n_i = -\left.\frac{\partial \Phi}{\partial \mu_i}\right|_{\mu_{j\neq i}} = -\sum_k \left[\left.\frac{\partial \omega_k^{(0)}}{\partial m_k}\right|_{\mu_k} \frac{\partial m_k}{\partial \mu_i} + \left.\frac{\partial \omega_k^{(0)}}{\partial \mu_k}\right|_{m_k} \frac{\partial \mu_k}{\partial \mu_i} \right. \tag{4.60}$$

$$\left. + \left(\left.\frac{\partial \omega_k^{(1)}}{\partial \mu_k}\right|_{m_k,\bar{\Lambda}} \frac{\partial \mu_k}{\partial \mu_i} + \left.\frac{\partial \omega_k^{(1)}}{\partial m_k}\right|_{\mu_k,\bar{\Lambda}} \frac{\partial m_k}{\partial \mu_i} + \left.\frac{\partial \omega_k^{(1)}}{\partial \bar{\Lambda}}\right|_{\mu_k,m_k} \frac{\partial \bar{\Lambda}}{\partial \mu_i} \right) \alpha_s + \omega_k^{(1)} \frac{\partial \alpha_s}{\partial \mu_i} \right], \tag{4.61}$$

where we have used the chain rule formula for multivariable functions

$$\frac{d}{dx} f\big(g_1(x), \ldots, g_k(x)\big) = \sum_{i=1}^{k} \left(\frac{d}{dx} g_i(x) \right) \frac{\partial f}{\partial g_i}. \tag{4.62}$$

Again, the vertical bars in Eq. (4.60) denote which variables (or functions) to be held fixed when it might not be so obvious. By applying the regular chain rule formula to $\partial m_k / \partial \mu_i$ and $\partial \alpha_s / \partial \mu_i$, a general number density n_i can be written as

$$n_i = n_i^* + n_0 \frac{\partial \bar{\Lambda}}{\partial \mu_i}, \tag{4.63}$$

$$n_i^* = -\left.\frac{\partial \omega_i^{(0)}}{\partial \mu_i}\right|_{m_i} - \left.\frac{\partial \omega_i^{(1)}}{\partial \mu_i}\right|_{m_i,\bar{\Lambda}} \alpha_s, \tag{4.64}$$

$$n_0 = -\sum_f \left(\left.\frac{\partial \omega_f^{(0)}}{\partial m_f}\right|_{\mu_f} \frac{dm_f}{d\bar{\Lambda}} + \left.\frac{\partial \omega_f^{(1)}}{\partial m_f}\right|_{\mu_f,\bar{\Lambda}} \frac{dm_f}{d\bar{\Lambda}} \alpha_s + \left.\frac{\partial \omega_f^{(1)}}{\partial \bar{\Lambda}}\right|_{\mu_f,m_f} \alpha_s + \omega_f^{(1)} \frac{d\alpha_s}{d\bar{\Lambda}} \right), \tag{4.65}$$

where the sum in n_0 now runs over the quarks only ($f = u, d, s$), because the term corresponding to $k = e$ is zero. Notice that n_i^* is the same as the number density in the case of constant coupling and mass, while the other term is the correction due to the running. Since $\bar{\Lambda}$ is independent of μ_e, the number density of electrons is simply

$$n_e = n_e^* = -\left.\frac{\partial \omega_e^{(0)}}{\partial \mu_e}\right|_{m_e} = \frac{\mu_e^3}{3\pi^2}, \tag{4.66}$$

which we already knew from Section 4.4.

4.7 Massless Quarks Revisited

Let us once again consider massless strange matter, but this time with running mass and coupling constant. We already know the grand potential and number density of electrons, Eq. (4.41) and (4.42), and the quark grand potentials are given by Eq. (4.48). To find the quark number densities we evaluate Eq. (4.63). For that we need the ω-functions of the quarks defined by Eq. (4.58). They are simply

$$\omega_f^{(0)} = -\frac{\mu_f^4}{4\pi^2} \quad \text{and} \quad \omega_f^{(1)} = \frac{\mu_f^4}{2\pi^3}, \quad f = u, d, s. \tag{4.67}$$

The first term n_f^* in Eq. (4.63) is easily evaluated. It is equivalent to the right-hand side of Eq. (4.49). Next, consider n_0. Since the quarks are approximated as massless, most of the terms vanish and we are left with

$$n_0 = -\sum_f \frac{\mu_f^4}{2\pi^3}\frac{d\alpha_s}{d\bar{\Lambda}}, \tag{4.68}$$

where the derivative of α_s evaluates to

$$\frac{d\alpha_s}{d\bar{\Lambda}} = -\frac{2}{\bar{\Lambda}L}\left[\alpha_s + \frac{8\pi}{L^2}\frac{\beta_1}{\beta_0^3}\left(1 - \frac{\ln L}{L}\right)\right]. \tag{4.69}$$

Lastly, with $\bar{\Lambda}$ defined as in Eq. (4.57), we get $\partial\bar{\Lambda}/\partial\mu_f = 2/3$; hence, the number densities of the massless quarks become

$$n_f = \frac{\mu_f^3}{\pi^2}\left(1 - \frac{2\alpha_s}{\pi}\right) + \frac{\mu_u^4 + \mu_d^4 + \mu_s^4}{\pi^3\bar{\Lambda}L}\left[\alpha_s + \frac{8\pi}{L^2}\frac{\beta_1}{\beta_0^3}\left(1 - \frac{\ln L}{L}\right)\right]. \tag{4.70}$$

When combined with the usual constraints on the chemical potentials, we now have all we need to compute the pressure and energy density from Eq. (4.35) and (4.36) and to solve the structure equations. This time we set the bag constant to zero; the energy per baryon at $P = 0$ for the case $B = 0$ is $\epsilon/n_B = 911\,\mathrm{MeV}$, barely lower than the energy per nucleon in iron ^{56}Fe. Thus, with no bag constant, we assume the strange matter hypothesis to hold. Note that there are no electrons in massless strange matter. We showed this for fixed coupling in Section 4.5, but it holds for running coupling as well. One can easily verify this by either solving the electric neutrality equation numerically or simply just assume $\mu_e = 0$ and see that the equation holds.

The mass-radius relation is shown in Figure 4.3 together with the mass-radius relation for the model we shall discuss in the next section (running strange quark mass). The maximum mass is $M_{\max} = 1.95M_\odot$ and corresponds to the radius $R = 10.33\,\mathrm{km}$. In Figure 4.2 the pressure P, the energy density ϵ and the strong coupling constant α_s are plotted as functions of the chemical potential μ. Both P and ϵ are normalized by the massless, ideal Fermi gas result. The pressure is zero for $\mu \sim 300\,\mathrm{MeV}$ at which the energy density is $\epsilon \sim 1.4\epsilon_F$. Looking at the plot of the coupling constant, we see that the value of α_s is generally very high, far beyond what can be considered small for perturbation theory, especially when μ is small. This is the reason the energy density takes such a sharp upward turn for low values of μ.

4.8 Finite Strange Quark Mass

The next logical step is to allow for m_s to be finite and let it run according to Eq. (4.56); the strange quark mass has the biggest effect on the EOS since it is by far the most massive among the three flavors and the electron. We still, however, keep the up and down quarks and the electrons massless. As usual, the electron grand potential Φ_e and number density n_e are given by Eq. (4.41) and (4.42). The

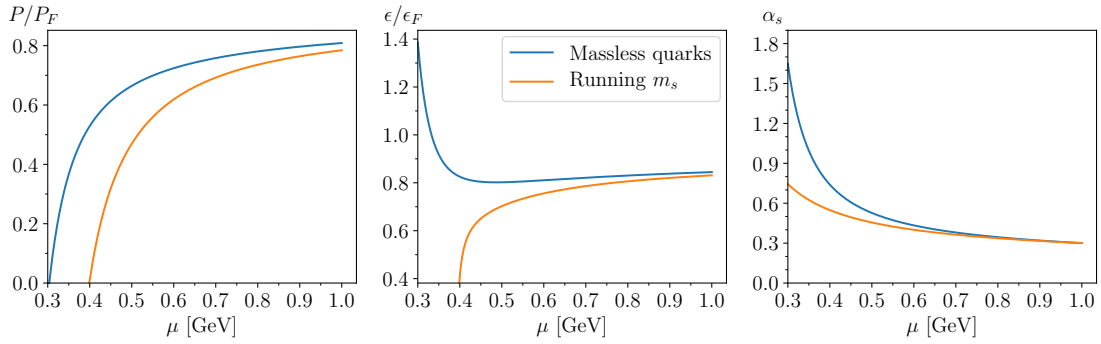

Figure 4.2: Pressure, energy density and coupling constant

grand potentials of the up and down quarks $\Phi_{u,d}$ are given by Eq. (4.48), with corresponding ω-functions as in Eq. (4.67). Lastly, Φ_s is given by Eq. (4.38) and (4.39) and its corresponding ω-functions become

$$\omega_s^{(0)} = -\frac{1}{4\pi^2}\left[\mu_s u_s\left(\mu_s^2 - \frac{5}{2}m_s^2\right) + \frac{3}{2}m_s^4 \ln\left(\frac{\mu_s + u_s}{m_s}\right)\right], \tag{4.71}$$

$$\omega_s^{(1)} = \frac{1}{2\pi^3}\left[3\left(m_s^2 \ln\frac{\mu_s + u_s}{m_s} - \mu_s u_s\right)^2 - 2u_s^4\right. \tag{4.72}$$

$$\left. + m_s^2\left(6\ln\frac{\bar{\Lambda}}{m_s} + 4\right)\left(\mu_s u_s - m_s^2 \ln\frac{\mu_s + u_s}{m_s}\right)\right], \tag{4.73}$$

where $u_s = \sqrt{\mu_s^2 - m_s^2}$ is the Fermi momentum. Next we need the number densities of the quarks. Looking at Eq. (4.63) for the number density n_f, the first term n_f^* is just the derivative of the grand potential Φ_f with the coupling and mass held fixed. For the massless up and down quarks it simply equals the right-hand side of Eq. (4.49). For the strange quarks, we get

$$n_s^* = -\left.\frac{\partial \Phi_s}{\partial \mu_s}\right|_{m_s,\bar{\Lambda},\alpha_s} = \frac{u_s^3}{\pi^2} - \frac{2\alpha_s u_s}{\pi^3}\left(2m_s^2 + \mu_s u_s + 3m_s^2 \ln\frac{\bar{\Lambda}}{\mu_s + u_s}\right). \tag{4.74}$$

If we were to consider the case of fixed coupling constant and mass, as in [40, 42], this would be all we needed. For running coupling and mass, however, we need the last part of n_f; regarding the second term in the equation for n_f (4.63), we have $\partial\bar{\Lambda}/\partial\mu_f = 2/3$ for all of the flavors as before, and n_0 reduces to

$$n_0 = -\left(\left.\frac{\partial\omega_s^{(0)}}{\partial m_s}\right|_{\mu_s} + \left.\frac{\partial\omega_s^{(1)}}{\partial m_s}\right|_{\mu_s,\bar{\Lambda}}\alpha_s\right)\frac{dm_s}{d\bar{\Lambda}} - \left.\frac{\partial\omega_s^{(1)}}{\partial\bar{\Lambda}}\right|_{\mu_s,m_s}\alpha_s - \left(\omega_u^{(1)} + \omega_d^{(1)} + \omega_s^{(1)}\right)\frac{d\alpha_s}{d\bar{\Lambda}}. \tag{4.75}$$

What we are missing here are the first four derivatives. Calculating all of these, writing them down and combining everything is straightforward but quite tedious if done by hand. It is much more convenient to utilize a computer program that can

handle symbolic calculations. We use Wolfram Mathematica, and the calculations along with the resulting expressions can be found in Appendix F.

As mentioned in Section 4.7, Figure 4.2 shows the pressure P, the energy density ϵ and the strong coupling constant α_s as functions of the chemical potential μ. Both P and ϵ have been normalized by the pressure P_F and energy density ϵ_F of a three-component, massless, ideal Fermi gas. The pressure is zero for $\mu \sim 400\,\text{MeV}$ at which the energy density is slightly below $0.4\epsilon_F$. Also in this case do we have that α_s is quite large, but the situation is definitely a lot better than for the completely massless quarks.

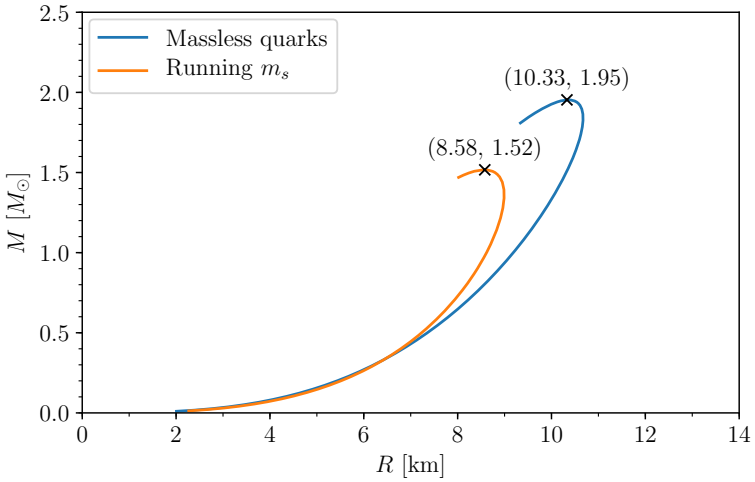

Figure 4.3: Mass-radius relations for massless strange matter and strange matter with running m_s, both with leading-order corrections to the grand potential, running strong coupling constant and $B = 0$.

The mass-radius relation is displayed in Figure 4.3 alongside the mass-radius relation from Section 4.7. We have set $B = 0$ this time as well. The energy per baryon at $P = 0$ is $\epsilon/n_B = 542\,\text{MeV}$, which is quite a lot lower than for ^{56}Fe (see Section 4.1). Therefore, for two-flavor quark matter to be less stable than ^{56}Fe, it would probably be more appropriate to use a finite bag constant here. This is more carefully studied in [41]. The maximum mass is $M_{\text{max}} = 1.52M_\odot$ with a corresponding radius of $R = 8.58\,\text{km}$. This is a lot lower than for the case of completely massless quarks; the maximum mass is reduced by $\sim 22\%$ and the corresponding radius is $\sim 17\%$ smaller. However, for the low density stars with radii $R < 5\,\text{km}$, the mass-radius relations are more or less equal. We note that Fraga and Romatschke obtained very different results for the mass-radius relations of both massless strange matter and strange matter with running m_s in their article [37]. They obtained $M_{\text{max}} = 2.16M_\odot$ at $\sim 12\,\text{km}$ for the case of running m_s, and $M_{\text{max}} = 3.2M_\odot$ at $\sim 17\,\text{km}$ for $m_s = 0$. The reason for the difference is that they found the quark number densities by using $n_f = \partial\Phi_f/\partial\mu_f$ instead of $n_f = \partial\Phi/\partial\mu_f$. That is, they do not use the total grand potential when taking the derivative. This matters because all the grand potentials of the quarks Φ_f depend on $\bar{\Lambda}$, which

further depends on all of the μ_f. So using the total grand potential to find n_f yields a contribution from all of the quark grand potentials, not just Φ_f. Here we use the total grand potential, which is also suggested by [41]. When we only use Φ_f, we get very similar results to those obtained by Fraga and Romatschke. By inspecting Eq. (B.14), it seems strange not to take the derivative of the total grand potential. However, in both cases one can conclude that the running of m_s has a large impact on the maximum mass of strange stars.

Figure 4.4 shows the charge densities of the individual particles species as a function of radial distance from the center of the maximum mass star, i.e., the star with $M = 1.52 M_\odot$ and $R = 8.58\,\mathrm{km}$. The charge densities are given in units of $n_{\mathrm{sat}} e/2$, which is approximately the charge density of nuclear matter consisting of an equal amount of protons and neutrons. At each value of r, the charge densities add up to zero, which is obvious because we required local electric charge neutrality. The density of electrons is seen to be lot lower than the densities of the quarks. We have therefore plotted the charge density of electrons separately to the right. While the densities (and charge densities) of the quarks all approach zero as we move toward the surface of the star, the electron (charge) density is close to zero at the center and builds up toward the surface. This is as expected, because m_s approaches zero at high densities, and we already know that there are no electrons in massless strange matter.

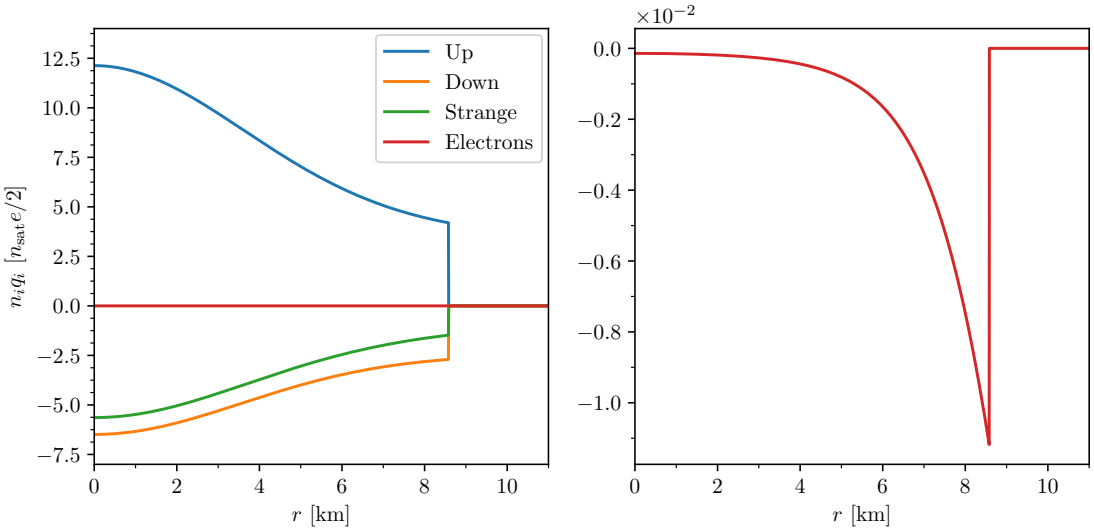

Figure 4.4: Electric charge density profiles for the star of maximum mass, given in units of the charge density of nuclear matter consisting of an equal amount of electrons and protons.

5 | Conclusions and Outlook

In this master's thesis we have studied some of the key features in determining the structure and upper mass limit of compact stars, in particular neutron stars and strange quark stars. We have also discussed a range of different equations of state and their resulting mass-radius relations, ranging from non-interacting matter to dense QCD. The underlying purpose has always been to dissect the foundational theory while taking very little for granted.

Chapter 2 gave an introduction to the TOV equation and the main criteria any physically reasonable solution should satisfy. We learned that the central pressure needed to sustain a mass distribution against gravity is always higher in general relativity than in Newtonian gravity. However, the TOV equation only gives sizable corrections for densities as high as those found in neutron stars and quark stars. Even white dwarf stars are effectively described by the equation of hydrostatic equilibrium from Newtonian gravity. The TOV equation was solved for a series of different equations of state describing non-interacting matter; an ideal Fermi gas of neutrons resulted in an upper mass limit of $\sim 0.71 M_\odot$.

Chapter 3 covered some of the main approximations and assumptions applied in this field of research. Naturally, these are often just briefly stated in research articles without much explanation, making it difficult for someone entering the field. Furthermore, the motivation and justification for these approximations and constraints in the literature are either quite vague or buried deep. Most often overlooked is perhaps the fact that we approximate the spacetime metric as flat in QFT calculations. This was justified in Section 3.1.

In Chapter 4 we considered strange quark stars in the framework of perturbative QCD. Leading-order corrections to the grand potential of interacting quarks with a running mass for the strange quark resulted in an upper mass limit of $M_{\max} = 1.52 M_\odot$ with corresponding radius $R = 8.58\,\mathrm{km}$. Interestingly, these numbers are similar to actual observations of pulsars. We also saw that a running strange quark mass gave a large decrease in the upper-mass limit, $\sim 22\%$. A notable weakness of the model is that the strong coupling constant is very large in the density region applicable to these stars, and we are therefore severely stretching the validity of perturbative QCD. Thus, the upper mass limit obtained here should be taken with a grain of salt and only be seen as suggestive. The large correction due to the running quark mass is probably a bigger take-away. Furthermore, a subtle but important part of the model is the choice of renormalization scale $\bar{\Lambda}$. We followed [37] and chose it as $\bar{\Lambda} = \frac{2}{3}(\mu_u + \mu_d + \mu_s)$. However, in that article, Fraga and Romatschke claims that the results are not greatly affected by other similar choices of $\bar{\Lambda}$. Lastly, we mentioned that there is a difference in the way we calculated the number densities here and the way Fraga and Romatschke did it. We will not examine further which

way is more correct, but the issue is important because it leads to widely different results.

The material covered in this thesis should be a good start for anyone new to this field of research. Below follow a few paths that can be taken to improve upon the models studied here.

Higher-Order Quantum Corrections

An obvious extension of the strange matter model considered in this thesis is to include higher-order corrections to the grand potential. The corrections to order α_s^2 are very complicated, but they have indeed been calculated. This was first done already in 1976, see [43–45], but the effects of the strange quark mass was only included to order α_s, dropping the mass entirely at order α_s^2. More recently, however, the full effects of the strange quark mass have been included all the way to order α_s^2 [46]. These higher-order corrections are expected to modify the structure of strange stars quite a lot [37]. This has been shown to be the case for massless strange matter [37, 47].

Hybrid Stars and Mixed Phases

As mentioned in Chapter 1, the existence of neutron stars with a quark-matter core is highly probable [9, 10]. For such stars, and even neutron stars in general, the use of a single EOS is obviously inadequate. There will be phase transitions at certain densities, for example from quark matter to nuclear matter and then to an iron crust. Furthermore, there are most likely mixed phases as well. For example, it might be that quark matter only exist as a mix between deconfined quarks and confined nuclear matter [21].

Effective Field Theories

The nucleons in nuclear matter interact via the strong nuclear force. Including these interactions is essential for a realistic description of neutron stars. Of course, the strong nuclear force is ultimately a residual effect of the strong force between the quarks that constitute the nucleons. But describing the nucleons and the interactions between them in terms of QCD is highly nontrivial. An alternative is to construct an effective theory where the degrees of freedom are not quarks and gluons but rather baryons and force carrying mesons. Such a theory is essentially "guessed" (often guided by symmetry principles), fitted to experimental results, and then extrapolated [30, p. 27]. A well-known effective field theory in quantum hadrodynamics is the σ–ω model. It describes the protons and neutrons as interacting via the exchange of the scalar σ meson and the vector ω meson [30, p. 28]. The meson fields are often replaced by their mean values. This is called the relativistic mean-field approximation. For more details on the σ–ω model see for example [21, 30].

A | Notation and Conventions

In this appendix, we introduce some notation and conventions used throughout this text.

Units

Unless otherwise stated, we use natural units where the speed of light c, the Planck constant, the Boltzmann constant and the Coulomb constant are all set equal to 1,

$$c = \hbar = k_{\mathrm{B}} = k_{\mathrm{e}} = 1. \tag{A.1}$$

The two exception are in Section 2.2 and E.1, where c and $\hbar$ are reinstated for clarity.

Constants

Here follows a table of some of the constants used throughout this thesis that might not be familiar to the reader.

Solar mass	$M_\odot$	$1.988\,47 \times 10^{30}\,\mathrm{kg}$
Neutron mass	m_n	$1.674\,93 \times 10^{-27}\,\mathrm{kg}$
Nuclear saturation density	n_{sat}	$1.7 \times 10^{44}\,/\mathrm{m}^3$

Acronyms

EOS	Equation Of State
TOV	Tolman–Oppenheimer–Volkoff
QCD	Quantum Chromodynamics
QED	Quantum Electrodynamics

Metric signature

In Appendix C and Appendix D on general relativity we use the metric signature $-+++$ because the standard references on the subject use this signature. In quantum field theory, on the other hand, the most widely used signature is $+---$. Therefore, in appendix Appendix E on thermal quantum field theory, *we will change our metric signature to* $+---$.

Vertical Bar

A vertical bar at the end of an expression usually means that the expression should be evaluated at the value indicated next to the bar, e.g., $x\big|_a = a$. However, in Chapter 4, the bar will also be used to emphasize which variables or functions are to be held constant while taking the derivative. For example, consider some function f that depends explicitly on the variable x but also implicitly through some functions $g_i(x)$, say $f = f\big(x, g_1(x), \ldots, g_k(x)\big) = x + g_1 x + g_1 g_2 \cdots g_k$. Then

$$\left.\frac{\partial f}{\partial x}\right|_{g_i} = 1 + g_1(x). \tag{A.2}$$

That is, all the g_i should be viewed as constants. It is probably more common to see parentheses being used for this purpose instead of a vertical bar. The reason we shall sometimes use a bar instead is to prevent our expressions from being flooded with parentheses.

Tensors

Usually, Greek indices are used to denote space or time components of a tensor, while Latin indices are reserved for spatial components. We call this the component notation. One drawback of this notation is that it is impossible to distinguish a purely tensorial equation from an equation that only holds for the components in a specific basis. We will therefore use the so-called *abstract index notation*, which in practice is just a slight modification of the component notation mentioned above. In the abstract index notation, Latin indices are used merely as a tool to keep track of the different slots of a tensor, while Greek indices are reserved for denoting the actual components of the tensor with respect to some chosen basis. To elaborate, if we have an (r, s) tensor

$$T : \underbrace{V^* \times \cdots \times V^*}_{r \text{ times}} \times \underbrace{V \times \cdots \times V}_{s \text{ times}} \to \mathbb{R}, \tag{A.3}$$

then we introduce the notation

$$T = T^{a_1 \cdots a_r}{}_{b_1 \cdots b_s}. \tag{A.4}$$

Strictly speaking, these Latin indices have nothing to do with components. They should rather be viewed as reminders of how many slots of each type (contravariant and covariant) the tensor has. However, the notation is constructed in a way that mirrors the behaviour of the component notation. For example, the contraction of a tensor is denoted by the same letter as the original tensor, but with a repeated Latin index in the slots that are to be contracted over. Thus, the tensor $T^{abc}{}_{be}$ is the $(2,1)$ tensor one gets from contracting the $(3,2)$ tensor $T^{abc}{}_{de}$ over its second contravariant and first covariant slot. Furthermore, the tensor direct product is denoted by writing the tensors next to each other, omitting the direct product symbol $\otimes$. Thus, $T^{abc}{}_{de}\, S^f{}_g$ is the $(4,3)$ tensor one gets by taking the tensor direct product of $T^{abc}{}_{de}$ and $S^a{}_b$. Given any tensor equation written in the index notation,

by simply replacing the Latin indices with Greek indices, the result is an equation relating the components, which holds true in any basis. Therefore, the index notation distinguishes itself from the component notation mainly in the way we perceive the quantities we write down.

There are additional notational rules related to the metric tensor, which is a $(0,2)$ tensor denoted by g_{ab}. If we were to apply the metric tensor to a vector v^a, we would get the dual vector $g_{ab}v^b$. It is convenient to denote this resulting dual vector as v_a. This is what is meant by "lowering an index". We can also raise indices with the inverse metric $(g^{-1})^{ab}$, which we usually just write as g^{ab}.

One often works with tensors or tensor expression that have certain symmetry properties. We therefore introduce some convenient notation for dealing with such. If T_{ab} is a tensor of type $(0,2)$, we define

$$T_{(ab)} = \frac{1}{2}(T_{ab} + T_{ba}) \tag{A.5}$$

and

$$T_{[ab]} = \frac{1}{2}(T_{ab} - T_{ba}) \tag{A.6}$$

as respectively the totally symmetric and antisymmetric part of the tensor T_{ab}. This generalizes to any number of indices as follows:

$$T_{(a_1,\ldots,a_k)} = \frac{1}{k!}\sum_{\sigma\in S_k} T_{a_{\sigma(1)},\ldots,a_{\sigma(k)}}, \tag{A.7}$$

$$T_{[a_1,\ldots,a_k]} = \frac{1}{k!}\sum_{\sigma\in S_k} \mathrm{sgn}(\sigma) T_{a_{\sigma(1)},\ldots,a_{\sigma(k)}}, \tag{A.8}$$

where σ are permutations of order k and $\mathrm{sgn}(\sigma)$ is $+1$ for even permuations and -1 for odd permutations. To exclude an index from being symmetrized or antisymmetrized, we surround it with vertical bars like so:

$$T^{(a|b|c)} = \frac{1}{2}(T^{abc} + T^{cba}). \tag{A.9}$$

See [14] for more details on the abstract index notation.

B | Thermal Physics

In this appendix we recall a few important concepts and formulas from statistical mechanics and thermodynamics. Most of it, if not all, should already be familiar to the reader.

B.1 The Second Law of Thermodynamics

Consider a single fluid element of a star as a thermodynamic system. The walls of the system are assumed to be closed, such that no particles can flow between neighboring fluid elements. However, volume and heat can generally be exchanged. We assume that our star is not too far from equilibrium and approximate it as an isolated thermodynamic system, neglecting both thermal radiation and the possibility for particles to escape out into space; thus, the energy of the system is constant. This isolated system is composed of many smaller closed systems, namely the fluid elements.

A microstate of a fluid element is a specific arrangement of the particles inside and their momenta, while a macrostate is a collection of microstates that exhibit the same macroscopic properties. If we, for example, specify the internal energy U, volume V and the number of each particle species N_i of a single fluid element, we have specified its macrostate. The multiplicity Ω of a macrostate is the number of microstates corresponding to that particular macrostate. The multiplicity varies with the macrostate, and thus

$$\Omega = \Omega(U, V, N_i) \tag{B.1}$$

We can also talk about states of combined systems, e.g, the star as a whole. A microstate is then a specific arrangement of all the particles in the star and their momenta, while a macrostate is the specification of the macroscopic properties of each and every fluid element. Let the index j label the individual fluid elements of the star. Basic combinatorics tells us that the multiplicity of a macrostate of the combined system is given by the product of the individual multiplicities,

$$\Omega_{\text{total}} = \prod_j \Omega_j. \tag{B.2}$$

Now, the fundamental assumption of statistical mechanics says that all accessible microstates of an isolated system (that is, microstates with the same total energy) are equally probable. However, with combinatorics one can show that there will always be one macrostate with multiplicity (and therefore probability) far, far greater

than the rest. Over time, the star will naturally seek towards this most probable macrostate, increasing the multiplicity until equilibrium is reached. This is the same as saying that the star will tend towards maximum entropy, because the entropy is simply defined as

$$S = k_B \ln \Omega. \tag{B.3}$$

The result of our brief discussion is the second law of thermodynamics:

The total entropy of an isolated system tends to increase.

Recall that the multiplicity (and therefore entropy) of a single fluid element is a function of its internal energy U, volume V and chemical composition N_i. A small change in its entropy S can therefore be written

$$dS = \frac{\partial S}{\partial U} dU + \frac{\partial S}{\partial V} dV + \sum_i \frac{\partial S}{\partial N_i} dN_i. \tag{B.4}$$

The partial derivatives are related to the thermodynamics quantities temperature T, pressure P and chemical potentials μ_i as follows:

$$\frac{1}{T} \equiv \left(\frac{\partial S}{\partial U} \right)_{V,N_i} \tag{B.5}$$

$$P \equiv T \left(\frac{\partial S}{\partial V} \right)_{U,N_i} \tag{B.6}$$

$$\mu_i \equiv -T \left(\frac{\partial S}{\partial N_i} \right)_{U,V,N_{j \neq i}} \tag{B.7}$$

Good motivation for why this should be so can be found in [48]. Substituting these definitions into Eq. (B.4) leads to the thermodynamic identity,

$$TdS = dU + PdV + \sum_i \mu_i dN_i \tag{B.8}$$

For our purposes, it is more convenient to rewrite the thermodynamic identity into a per baryon form. Let N be the total number of baryons in the fluid element. Then $n = N/V$ is the baryon number density. Let also s be the entropy per baryon and n_i the number density of the i-th particle species. Writing $dS = d(sN)$, $dU = d(\epsilon V)$ and $dN_i = d(n_i V)$ and dividing by N in Eq. (B.8) yields

$$Tds = d\left(\frac{\epsilon}{n} \right) + Pd\left(\frac{1}{n} \right) + \sum_i \mu_i dY_i, \tag{B.9}$$

where we also have defined $Y_i = n_i/n$ as the relative amount of the i-th particle species. Notice that we were able to pull the N inside the differential because $dN = 0$; the number of baryons are conserved in particle reactions.

B.2 Grand Canonical Ensemble

In quantum field theory we work with systems where particles can be created and destroyed. The statistics of such systems of variable particle count can be effectively described with a grand canonical ensemble. The chemical potentials μ_i, temperature T and volume V are constants, or parameters, of the ensemble, while the particle numbers N_i, and of course the energy E (also often denoted by U), can vary. All other statistical properties of the system are neatly contained in the grand canonical partition function Z given by

$$Z(\mu_i, T, V) = \operatorname{Tr} e^{(\hat{H} - \mu_i \hat{N}_i)}, \tag{B.10}$$

where $\hat{N}_i$ is the number operator and i is summed over. One can, for example, obtain the pressure P by using

$$P(\mu_i, T) = \frac{1}{\beta} \frac{\partial \ln Z}{\partial V}, \tag{B.11}$$

or the average particle number density of the i-th particle species n_i by using

$$n_i = \frac{1}{\beta V} \frac{\partial \ln Z}{\partial \mu_i} = \frac{\partial P}{\partial \mu_i}. \tag{B.12}$$

The natural state function of the grand canonical ensemble is the grand potential Φ_G, defined as

$$\Phi_G = U - TS - \mu_i N_i. \tag{B.13}$$

Its thermodynamic identity can easily be obtained by taking the differential and using the fundamental relation $dU = TdS - PdV + \mu_i dN_i$, giving

$$d\Phi_G = -PdV - SdT - N_i d\mu_i. \tag{B.14}$$

From this we get the following expressions

$$P = -\frac{\partial \Phi_G}{\partial V}, \tag{B.15}$$

$$S = -\frac{\partial \Phi_G}{\partial T}, \tag{B.16}$$

$$N_i = -\frac{\partial \Phi_G}{\partial \mu_i}. \tag{B.17}$$

The relationship between Z and Φ_G becomes obvious if we compare Eq. (B.11) to Eq. (B.15):

$$\Phi_{\mathrm{G}} = -\frac{\ln Z}{\beta}. \tag{B.18}$$

We usually work with densities, and thus it is convenient to define the grand potential per volume, which we shall denote by the same symbol but without the G,

$$\Phi = \frac{\Phi_{\mathrm{G}}}{V}. \tag{B.19}$$

The grand potential per volume is often referred to as simply the grand potential when what is really meant is obvious from the context.

In our case, the ensembles that the above equations will be applied to are the fluid elements of a star and we usually work in the zero temperature approximation. Dividing Eq. (B.13) by the volume V of the ensemble and setting $T = 0$ gives

$$\Phi = \epsilon - \mu_i n_i. \tag{B.20}$$

If we calculate the partition function using Eq. (B.10), we can easily get the grand potential with Eq. (B.18). Then it is straightforward to calculate the pressure and energy density by using Eq. (B.15) and combining Eq. (B.17) with Eq. (B.20).

C | Einstein's Field Equation

This appendix was written as part of a project of mine during the fall semester of 2019 and **must therefore not be considered a part of this thesis during evaluation.**

In the early 1900s Einstein had an idea that would serve as the foundational principle of perhaps the most beautiful theory in physics: *In small enough regions of space, the laws of physics reduce to those of special relativity; it is impossible to detect the existence of a gravitational field by means of local experiments.* This implies that gravity is inescapable, it affects everything in the universe. Einstein therefore proposed that gravity is not a force, but a feature of spacetime itself, the very fabric on which everything resides. What we experience as gravity is just the manifestation of the curvature of spacetime. From this insight Einstein constructed the theory of general relativity [13, p. 151]. His field equation took its final form in 1915, and that same year David Hilbert showed that it could actually be derived from an action principle. In this chapter, we take Hilbert's approach, starting with the Einstein-Hilbert action and vary the metric. From there we will take a somewhat more elegant approach by considering the so-called Palatini variation, where we vary both the metric and the connection independently.

C.1 The Einstein-Hilbert Action

The principle of least action states that the path taken by a physical system through configuration space is the path for which the action of the system is stationary to first order. Hilbert proposed that the appropriate action in general relativity is

$$S_H = \int \sqrt{-g} R d^n x, \tag{C.1}$$

now known as the **Einstein-Hilbert action**, where g is the determinant of the metric, R is the Ricci scalar and n is the dimension of spacetime. We will only work with the usual four dimensions, but we keep it general for now. In our first approach to deriving the field equation we need to make two assumptions about the covariant derivative:[1]

[1] A torsion-free connection is necessary to ensure that the geodesic paths resulting from the connection coincides with the paths that extremizes the length integral in spacetime [14, p. 45]. Metric compatibility ensures that the inner product of two vectors remain unchanged under parallel transport [14, p. 35].

- Torsion-free: $\Gamma^a_{bc} = \Gamma^a_{cb}$.
- Metric compatibility: $\nabla_c g_{ab} = 0$.

This results in unique connection coefficients when given a metric on our spacetime manifold [13, p. 99]:

$$\Gamma^a_{bc} = \tfrac{1}{2} g^{ad}(\partial_b g_{cd} + \partial_c g_{db} - \partial_d g_{bc}). \tag{C.2}$$

With these assumptions, varying the Einstein-Hilbert action with respect to the metric g_{ab} yields the equation of motion for the metric, namely Einstein's field equation. We will closely follow the steps found in [13].

Before we begin varying the action, we need a relation between the variation of the metric and the variation of the inverse metric. Consider the identity $g^{ab}g_{bc} = \delta^a_c$ and take the variation of both sides,

$$(\delta g^{ab})g_{bc} + g^{ab}(\delta g_{bc}) = 0. \tag{C.3}$$

Multiplication by g_{ad} leads to

$$\delta^b_d(\delta g_{bc}) = \delta g_{cd} = -g_{ad}g_{bc}(\delta g^{ab}). \tag{C.4}$$

By relabeling indices and using the symmetry properties of both g_{ab} and δg^{ab}, we end up with the following useful relation between the variation of the metric and the variation of the inverse metric:

$$\delta g_{ab} = -g_{ac}g_{bd}\delta g^{cd}. \tag{C.5}$$

It turns out that it is easier to do the variation of S_H with respect to the inverse metric g^{ab}. Using $R = g^{ab}R_{ab}$, we have

$$\delta S_H = \int d^n x \Big[\delta(\sqrt{-g})R + \sqrt{-g}(\delta g^{ab})R_{ab} + \sqrt{-g}g^{ab}\delta R_{ab}\Big] = \delta S_1 + \delta S_2 + \delta S_3. \tag{C.6}$$

Fortunately, the δS_2 term is already in the desired form, so let us move on to the δS_1 term, where we need to deal with the variation of $\sqrt{-g}$. By using the chain rule, we get

$$\delta\sqrt{-g} = -\frac{1}{2\sqrt{-g}}\delta g. \tag{C.7}$$

To proceed, we need to compute the variation of the determinant. This can be done quite easily by making use of Jacobi's formula,

$$\frac{d}{dt}\det A(t) = \det A(t)\,\mathrm{Tr}\left(A^{-1}\frac{dA(t)}{dt}\right), \tag{C.8}$$

where A is a differentiable map from the real numbers to $n \times n$ matrices. Applying this to the variation of the metric gives us

$$\delta g = g\,\mathrm{Tr}\Big(g^{ab}\delta g_{bc}\Big) = -gg^{ab}\delta g_{ab} = -gg_{ab}\delta g^{ab}, \tag{C.9}$$

where in the last step we used Eq. (C.5). The first term of the total variation is therefore given by

$$\delta S_1 = \int d^n x \left(-\tfrac{1}{2}\sqrt{-g} g_{ab} \delta g^{ab} R\right). \tag{C.10}$$

Consider now the last term, δS_3. To calculate δR_{ab} we start with the Riemann tensor:

$$R^a{}_{bcd} = 2\partial_{[c}\Gamma^a_{d]b} + 2\Gamma^a_{[c|e|}\Gamma^e_{d]b}. \tag{C.11}$$

Taking the variation yields us

$$\delta R^a{}_{bcd} = 2\partial_{[c}(\delta\Gamma^a_{d]b}) + 2(\delta\Gamma^a_{[c|e|})\Gamma^e_{d]b} + 2\Gamma^a_{[c|e|}(\delta\Gamma^e_{d]b}). \tag{C.12}$$

Since $\delta\Gamma^a_{db}$ is the difference between two connection coefficients, it is itself a proper tensor, see [13, p. 98]. We can therefore take the covariant derivative,[2] before antisymmetrizing,

$$\nabla_{[c}(\delta\Gamma^a_{d]b}) = \partial_{[c}(\delta\Gamma^a_{d]b}) + \Gamma^a_{[c|e|}(\delta\Gamma^e_{d]b}) - \Gamma^e_{[cd]}(\delta\Gamma^a_{eb}) - \Gamma^e_{[c|b|}(\delta\Gamma^a_{d]e}). \tag{C.13}$$

The third term on the right vanishes, attributed to the fact that the connection is torsion free. As for the fourth term, we have

$$\Gamma^e_{[c|b|}(\delta\Gamma^a_{d]e}) = -\Gamma^e_{[d|b|}(\delta\Gamma^a_{c]e}) = -(\delta\Gamma^a_{[c|e|})\Gamma^e_{d]b}. \tag{C.14}$$

Our expression for the covariant derivative now takes the form

$$\nabla_{[c}(\delta\Gamma^a_{d]b}) = \partial_{[c}(\delta\Gamma^a_{d]b}) + \Gamma^a_{[c|e|}(\delta\Gamma^e_{d]b}) + (\delta\Gamma^a_{[c|e|})\Gamma^e_{d]b}. \tag{C.15}$$

Comparing this to Eq. (C.12), we see that

$$\delta R^a{}_{bcd} = 2\nabla_{[c}(\delta\Gamma^a_{d]b}). \tag{C.16}$$

The next step is to find the variation of the Christoffel symbol with respect to the inverse metric. Taking the variation of Eq. (C.2) gives

$$\delta\Gamma^a_{db} = \delta g^{ae}\big(\partial_{(b}g_{d)e} - \tfrac{1}{2}\partial_e g_{bd}\big) + g^{ae}\big(\partial_{(b}\delta g_{d)e} - \tfrac{1}{2}\partial_e \delta g_{bd}\big). \tag{C.17}$$

Notice that

$$g_{fe}\Gamma^f_{bd} = \big(\partial_{(b}g_{d)e} - \tfrac{1}{2}\partial_e g_{bd}\big), \tag{C.18}$$

which is exactly the expression found in the first set of parentheses in Eq. (C.17). Making the substitution and using the relation between the variation of the metric and the variation of the inverse metric, Eq. (C.5), leads to

$$\begin{aligned}\delta\Gamma^a_{db} &= \delta g^{ae} g_{fe}\Gamma^f_{bd} + g^{ae}\big(\cdots\big) = -\delta g_{fe} g^{ae}\Gamma^f_{bd} + g^{ae}\big(\cdots\big) \\ &= g^{ae}\Big(\partial_{(b}\delta g_{d)e} - \tfrac{1}{2}\partial_e\delta g_{bd} - \Gamma^f_{bd}\delta g_{ef}\Big).\end{aligned} \tag{C.19}$$

We now write the partial derivatives in terms of the covariant derivative and the Christoffel symbols. The first term in the parentheses in the above expression becomes

$$\partial_{(b}\delta g_{d)e} = \nabla_{(b}\delta g_{d)e} + \Gamma^f_{b(d}\delta g_{e)f} + \Gamma^f_{d(b}\delta g_{e)f}. \tag{C.20}$$

[2] Here we use the Christoffel symbols with respect to the unperturbed metric g_{ab}, not $g_{ab} + \delta g_{ab}$.

As for the second term, we have

$$-\tfrac{1}{2}\partial_e \delta g_{bd} = -\tfrac{1}{2}\nabla_e \delta g_{bd} - \Gamma^f_{e(b}\delta g_{d)f}. \tag{C.21}$$

When we substitute these expressions into Eq. (C.19), all the terms with connection coefficients will cancel, and we are left with

$$\begin{aligned}\delta\Gamma^a_{db} &= g^{ae}\big(\nabla_{(b}\delta g_{d)e} - \tfrac{1}{2}\nabla_e \delta g_{bd}\big)\\ &= -g_{e(b}\nabla_{d)}\delta g^{ae} + \tfrac{1}{2}g_{bc}g_{de}\nabla^a \delta g^{ce},\end{aligned} \tag{C.22}$$

where we used metric compatibility in the last step.

With all that ground work out of the way, we combine Eq. (C.16) and Eq. (C.22) and turn to the expression for δS_3:

$$\begin{aligned}\delta S_3 &= \int d^n x\sqrt{-g}g^{ab}\delta R^f{}_{afb} = \int d^n x\sqrt{-g}g^{ab}\Big(2\nabla_{[f}\delta\Gamma^f_{b]a}\Big)\\ &= \int d^n x\sqrt{-g}\nabla_c\Big(g^{ab}\delta\Gamma^c_{ab} - g^{ac}\delta\Gamma^f_{fa}\Big).\end{aligned} \tag{C.23}$$

Carrying out the contractions in each of the two terms in the parentheses yields

$$g^{ab}\delta\Gamma^c_{ab} = \tfrac{1}{2}g_{ab}\nabla^c\delta g^{ab} - \nabla_a\delta g^{ac} \tag{C.24}$$

and

$$g^{ac}\delta\Gamma^f_{fa} = -\tfrac{1}{2}g_{ab}\nabla^c\delta g^{ab}, \tag{C.25}$$

resulting in

$$\delta S_3 = \int d^n x\sqrt{-g}\nabla_c\Big(g_{ab}\nabla^c\delta g^{ab} - \nabla_a\delta g^{ac}\Big). \tag{C.26}$$

We can now apply Stokes theorem to this expression, turning it into a boundary contribution. This can be set to zero if we demand that both the metric and its first derivatives are held fixed at the boundary.[3]

Finally, looking back at Eq. (C.6),

$$\delta S_H = \delta S_1 + \delta S_2 = \int d^n x\sqrt{-g}\big(R_{ab} - \tfrac{1}{2}g_{ab}R\big)\delta g^{ab}. \tag{C.27}$$

For this to be zero for any variation δg^{ab}, we must have

$$R_{ab} - \tfrac{1}{2}Rg_{ab} = 0, \tag{C.28}$$

which we know as Einstein's field equation in vacuum.

In general relativity we often deal with large systems comprised of a huge number of particles. It is obviously not feasible to specify momentum vectors for every single particle; instead, we describe the system's mass distribution as a fluid with macroscopic quantities like density, pressure and an overall four-velocity field. All such properties of the fluid can neatly be described by a symmetric $(2,0)$ tensor

[3] To circumvent making this constraint on the metric one could also modify the total action to cancel this boundary contribution, see [14, p. 458].

field called the *energy-momentum tensor* T^{ab}, and we therefore talk about a *matter field*. To add the matter field into Einstein's equation we simply include a matter term S_M and a normalization factor to the total action,

$$S = \frac{1}{16\pi G} S_H + S_M, \tag{C.29}$$

where G is Newton's gravitational constant. Taking again the variation leads to

$$\delta S = \frac{1}{16\pi G}\delta S_H + \delta S_M = \int d^n x \left[\frac{\sqrt{-g}}{16\pi G}(R_{ab} - \tfrac{1}{2}g_{ab}R) + \frac{\delta S_M}{\delta g^{ab}}\right]\delta g^{ab}. \tag{C.30}$$

If we now choose to define the energy-momentum tensor to be

$$T_{ab} \equiv -2\frac{1}{\sqrt{-g}}\frac{\delta S_M}{\delta g^{ab}}, \tag{C.31}$$

we obtain

$$\boxed{R_{ab} - \tfrac{1}{2}Rg_{ab} = 8\pi G T_{ab},} \tag{C.32}$$

which is Einstein's field equation in all its glory.

C.2 The Palatini Variation

In this section we want to take a slightly different approach to deriving Einstein's field equation. The advantage being that there is no need to assume that the connection is metric compatible anymore, because it will turn out to be a requirement for the action to be stationary. We do, however, still assume the connection to be torsion-free. The following derivation will be heavily based upon [14, p. 454].

Consider again the combined Einstein-Hilbert- and matter-action, but now as a functional of both the metric and the covariant derivative,

$$S[g^{ab}, \nabla_a] = \frac{1}{16\pi G} S_H[g^{ab}, \nabla_a] + S_M[g^{ab}]. \tag{C.33}$$

Notice that we assume the matter action to be independent of the choice of covariant derivative. Let $\widetilde{\nabla}_a$ be the covariant derivative compatible with g^{ab} when the action is stationary, and let ∇_a be the covariant derivative we wish to vary. Then, to show that ∇_a is metric compatible equates to showing that $\nabla_a = \widetilde{\nabla}_a$ when the action is stationary. Since any covariant derivative can be expressed in terms of an arbitrary fixed derivative operator and a $(1,2)$ tensor field $C^b{}_{ac}$ symmetric in the last two indices,[4] see [14, p. 33], we can write the following for some tangent vector t^a:

$$\nabla_a t^b = \widetilde{\nabla}_a t^b + C^b{}_{ac} t^c, \tag{C.34}$$

extending to higher rank tensors in the obvious way. Variation of ∇_a is therefore equivalent to variation of $C^b{}_{ac}$.

[4] The symmetry property of the tensor field $C^b{}_{ac}$ need not hold if the derivative operators related by it are not torsion-free.

Let us now first examine S_H. As in the previous section, taking the variation leads to

$$\delta S_H = \int d^n x \Big[\delta(\sqrt{-g})R + \sqrt{-g}(\delta g^{ab})R_{ab} + \sqrt{-g}g^{ab}\delta R_{ab}\Big] = \delta S_1 + \delta S_2 + \delta S_3, \quad \text{(C.35)}$$

but this time the variation of the Ricci tensor is taken with respect to $C^c{}_{ab}$. Luckily, we can still use Eq. (C.16), where the Christoffel symbols Γ^a_{db} of course belongs to ∇_a. But we wish to vary the Ricci tensor with respect to $C^a{}_{db}$, not Γ^a_{db}. To solve this, we write out the relation between ∇_a and $\widetilde{\nabla}_a$, Eq. (C.34), in terms of the Christoffel symbols:

$$\begin{aligned} \partial_a t^b + \Gamma^b_{ac} t^c &= \partial_a t^b + \widetilde{\Gamma}^b_{ac} t^c + C^b{}_{ac} t^c \\ \Gamma^b_{ac} - \widetilde{\Gamma}^b_{ac} &= C^b{}_{ac} \\ \delta\Gamma^b_{ac} &= \delta C^b{}_{ac}. \end{aligned} \quad \text{(C.36)}$$

Using this result together with the fact that δS_1 and δS_2 are exactly the same as before, we get

$$\begin{aligned} \delta S_H &= \int d^n x \Big[\sqrt{-g}R_{ab} - \tfrac{1}{2}\sqrt{-g}g_{ab}R\Big]\delta g^{ab} + 2\int d^n x \sqrt{-g} g^{ab} \nabla_{[f}\delta C^f{}_{b]a} \\ &= \int d^n x \Big[\cdots\Big]\delta g^{ab} - 2\int d^n x \sqrt{-g} g^{ab} \nabla_{[a}\delta C^f{}_{f]b}. \end{aligned} \quad \text{(C.37)}$$

Let us write out the two terms involved in the antisymmetric tensor in the last integral:

$$\nabla_a \delta C^f{}_{fb} = \widetilde{\nabla}_a \delta C^f{}_{fb} + C^f{}_{ae}\delta C^e{}_{fb} - C^e{}_{af}\delta C^f{}_{eb} - C^e{}_{ab}\delta C^f{}_{fe} \quad \text{(C.38)}$$

and

$$\nabla_f \delta C^f{}_{ab} = \widetilde{\nabla}_f \delta C^f{}_{ab} + C^f{}_{fe}\delta C^e{}_{ab} - C^e{}_{fa}\delta C^f{}_{eb} - C^e{}_{fb}\delta C^f{}_{ae}. \quad \text{(C.39)}$$

Substituting this back into Eq. (C.37), we find

$$\begin{aligned} \delta S_H = &\int d^n x \Big[\cdots\Big]\delta g^{ab} - 2\int d^n x \sqrt{-g} g^{ab} \widetilde{\nabla}_{[a}\delta C^f{}_{f]b} \\ &+ \int d^n x \sqrt{-g} g^{ab} \Big(C^e{}_{ab}\delta C^f{}_{fe} + C^f{}_{fe}\delta C^e{}_{ab} - 2C^e{}_{fb}\delta C^f{}_{ae}\Big). \end{aligned} \quad \text{(C.40)}$$

Since $\widetilde{\nabla}_a$ is, by definition, compatible with g^{ab} when the action is stationary, we can move g^{ab} inside $\widetilde{\nabla}_a$. By applying Stoke's theorem, this whole term vanishes, as long as we require $\delta C^c{}_{ab}$ to vanish on the boundary. $\delta C^c{}_{ab}$ can now be pulled outside the parentheses.

Looking now at the variation of the total action, we have

$$\begin{aligned} \delta S = \frac{1}{16\pi G}\delta S_H + \delta S_M = &\int d^n x \left[\frac{\sqrt{-g}}{16\pi G}(R_{ab} - \tfrac{1}{2}g_{ab}R) + \frac{\delta S_M}{\delta g^{ab}}\right]\delta g^{ab} \\ &+ \frac{\sqrt{-g}}{16\pi G}\int d^n x \Big(C^{bd}{}_d\delta^a_c + C^d{}_{dc}g^{ab} - 2C^b{}_c{}^a\Big)\delta C^c{}_{ab}. \end{aligned} \quad \text{(C.41)}$$

To have $\delta S = 0$ for any variation δg^{ab} and $\delta C^{c}{}_{ab}$, we must require that the expression in the square brackets in the first integral and the expression in the parentheses in the second integral vanish independently. The first of the two expressions yields Einstein's field equation like before,

$$\boxed{R_{ab} - \tfrac{1}{2} R g_{ab} = 8\pi G T_{ab},} \tag{C.42}$$

when using our previous definition of T_{ab}, Eq. (C.31). But we do not yet know which connection that goes into this equation. This is where the second expression comes into play. When symmetrizing the expression over a and b, we get

$$C^{bd}{}_{d}\delta^{a}_{c} + C^{ad}{}_{d}\delta^{b}_{c} + 2C^{d}{}_{dc}g^{ab} - 2C^{b\ a}_{\ c} - 2C^{a\ b}_{\ c} = 0. \tag{C.43}$$

By contracting over a and b and using the identity $C^{c\ b}_{\ a} = C^{cb}{}_{a}$, which follows directly from raising either of the last two indices in the previously mentioned symmetry property $C^{c}{}_{ab} = C^{c}{}_{ba}$, we find

$$C^{bd}{}_{d} = 0. \tag{C.44}$$

This gets rid of the first two terms in Eq. (C.43) [49, p. 396]. With these two terms out of the way, we take the trace of what remains of Eq. (C.43) by multiplying with g_{ab}, leading to

$$C^{d}{}_{dc} = 0, \tag{C.45}$$

which gets rid of the middle term. This leaves only

$$C^{b\ a}_{\ c} = -C^{a\ b}_{\ c}, \tag{C.46}$$

which, by lowering a and b and using the symmetry property of the last two indices, equates to

$$C_{bac} = -C_{abc}. \tag{C.47}$$

Thus, C_{bac} is antisymmetric in the first two indices in addition to being symmetric in the last two. Using these properties, we find

$$C_{bac} = C_{bca} = -C_{cba} = -C_{cab} = C_{acb} = C_{abc} = -C_{bac}. \tag{C.48}$$

Thus, by raising b, we finally arrive at

$$C^{b}{}_{ac} = 0 \iff \nabla_a = \widetilde{\nabla}_a, \tag{C.49}$$

when the action is stationary. We can therefore conclude that the connection that goes into Einstein's field equation is nothing but the unique metric compatible connection given by Eq. (C.2).

D The Tolman–Oppenheimer–Volkoff Equation

This appendix was written as part of a project of mine during the fall semester of 2019 and **must therefore not be considered a part of this thesis during evaluation.**

The equations of motion in general relativity differ from those of many other fundamental theories of physics, in ways that make them considerably harder to solve. Not only is Einstein's field equation a set of 10 independent partial differential equations, but it is also nonlinear, unlike Maxwell's equations and the Schrödinger equation; the Christoffel symbols involve both the inverse metric and derivatives of the metric, and products and derivatives of these symbols are what constitutes the Riemann tensor, which in turn is contracted and taken traces of. Luckily, like in most fields of physics, we can make things a lot simpler by assuming symmetries. Not surprisingly, there are quite a few symmetries that are natural to assume when working with celestial objects.

The goal of this chapter is to introduce a reasonable physical model describing the gravitational field generated by the presence of a static and spherically symmetric mass distribution, such as stars. Our main result of interest will be the Tolman–Oppenheimer–Volkoff equation; the equation of hydrostatic equilibrium. Considering that the mass distribution will be modeled as static (unevolving) and spherically symmetric, the solutions to Einstein's field equation should possess the same properties. The first section will define what is actually meant by static and spherically symmetric, resulting in a metric with exactly these properties, expressed in a particularly useful set of coordinates. Next, we consider the energy-momentum tensor, the Ricci tensor and the Ricci scalar, after which we are in position to derive the Tolman–Oppenheimer–Volkoff equation from Einstein's field equation.

D.1 Static, Spherically Symmetric Spacetimes

We say that a spacetime (manifold) is *stationary* if it has a one-parameter group of isometries whose orbits are timelike curves. If these orbits are also orthogonal to some spacelike hypersurface, then we say that the spacetime is *static*. These two conditions ensures that we can find a coordinate system in which all the metric components are independent of the time coordinate and there are no cross terms $dt\,dx^\mu$ [14, p. 119]. This coordinate system results from the construction of so-called

Gaussian normal coordinates, where the Killing vector field ξ^a which generates the isometry is taken to be one of the coordinate basis vector fields.

A spacetime is said to be spherically symmetric if its isometry group contains a subgroup isomorphic to the group SO(3) and the orbits of this subgroup are 2-spheres. Each 2-sphere will then inherit a metric which in spherical coordinates must be a multiple of the metric of a unit 2-sphere [14, p. 119].

If a spacetime is both static and spherically symmetric, these formal definitions ultimately implies that we can always find a coordinate system where the metric takes the simple form

$$ds^2 = -f(r)dt^2 + h(r)dr^2 + r^2(d\theta^2 + \sin^2\theta d\phi^2), \tag{D.1}$$

see [14, p. 121]. Here, f and h are some scalar functions that will later be settled by Einstein's field equation. Despite being the result of rigorous topological definitions, the metric above is no more than an ansatz. Though it is a quite reasonable one; it is independent of the time coordinate and invariant under both time reversal and rotations. To make things even easier we simply assume that the coefficient of dt^2 is negative and the coefficient of dr^2 is positive.[1] This turns out to hold up for stars, but not for black holes [50, p. 258]. Our assumption about the sign of the coefficients can be expressed mathematically by swapping out f and h with exponential functions, leading to

$$ds^2 = -e^{2\alpha(r)}dt^2 + e^{2\beta(r)}dr^2 + r^2 d\Omega, \tag{D.2}$$

where we have written the metric on the unit 2-sphere as $d\Omega$, and we have introduced two new scalar functions α and β that are yet to be pinned down by Einstein's field equation.

D.2 The Energy-Momentum Tensor and the Einstein Tensor

Before we can focus our attention on Einstein's field equation, we need a suitable energy-momentum tensor T_{ab}, as well as expressions for the Ricci scalar and the components of the Ricci tensor.

We choose to model the mass distribution as a perfect fluid, meaning that the energy-momentum tensor takes the form

$$T_{ab} = \rho u_a u_b + P(g_{ab} + u_a u_b), \tag{D.3}$$

where ρ is the rest-frame energy density, and P is the isotropic rest-frame pressure. Note that the energy-momentum tensor for a perfect fluid is diagonal in its rest frame; there are no shear stresses or heat conduction. For the energy-momentum tensor to be compatible with our static spacetime, we must have that the 4-velocity field of the fluid u_a points in the same direction as the timelike Killing vector field ξ^a [14, p. 125]; looking at it the other way around, if the static mass distribution follows

[1] Note that one of the coefficients has to be positive and the other negative, since we are dealing with a Lorentzian metric [13, p. 201].

a certain path through spacetime, the curvature surrounding it should necessary look the same along that path. By working in the coordinate system we used to express the static, spherically symmetric metric tensor in Eq. (D.2), we find

$$u^\mu = (e^{-\alpha}, 0, 0, 0), \tag{D.4}$$

when normalizing such that $u_a u^a = -1$. By lowering the index and using Eq. (D.3), we get that the components of the energy-momentum tensor is given by

$$T_{\mu\nu} = \begin{pmatrix} e^{2\alpha}\rho & & & \\ & e^{2\beta}P & & \\ & & r^2 P & \\ & & & r^2\sin^2\theta P \end{pmatrix}. \tag{D.5}$$

The energy density ρ and pressure P will necessarily depend only on r, since we want everything to be static and spherically symmetric.

To find the Ricci scalar and the components of the Ricci tensor, we first need the Christoffel symbols. The calculations are straightforward, but tedious, so only the results will be presented. By choosing labels (t, r, θ, ϕ) instead of $(0, 1, 2, 3)$ and using the expression for the Christoffel symbols in terms of the metric, Eq. (C.2), we get

$$\begin{aligned} &\Gamma^t_{tr} = \partial_r\alpha, && \Gamma^r_{tt} = e^{2(\alpha-\beta)}\partial_r\alpha, && \Gamma^r_{rr} = \partial_r\beta, \\ &\Gamma^\theta_{r\theta} = \frac{1}{r}, && \Gamma^r_{\theta\theta} = -re^{-2\beta}, && \Gamma^\phi_{r\phi} = \frac{1}{r}, \\ &\Gamma^r_{\phi\phi} = -re^{-2\beta}\sin^2\theta, && \Gamma^\theta_{\phi\phi} = -\sin\theta\cos\theta, && \Gamma^\phi_{\theta\phi} = \cot\theta. \end{aligned} \tag{D.6}$$

All of the other components are either zero or related to the ones above by symmetries. We can now simply contract the Riemann tensor given in Eq. (C.11) to get the components of the Ricci tensor,

$$\begin{aligned} R_{tt} &= e^{2(\alpha-\beta)}\Big[\partial_r^2\alpha + (\partial_r\alpha)^2 - \partial_r\alpha\partial_r\beta + \tfrac{2}{r}\partial_r\alpha\Big], \\ R_{rr} &= -\partial_r^2\alpha - (\partial_r\alpha)^2 + \partial_r\alpha\partial_r\beta + \tfrac{2}{r}\partial_r\beta, \\ R_{\theta\theta} &= e^{-2\beta}\Big[r(\partial_r\beta - \partial_r\alpha) - 1\Big] + 1, \\ R_{\phi\phi} &= \sin^2\theta\, R_{\theta\theta}. \end{aligned} \tag{D.7}$$

Taking the trace of the Ricci tensor yields the Ricci scalar

$$R = -2e^{-2\beta}\left[\partial_r^2\alpha + (\partial_r\alpha)^2 - \partial_r\alpha\partial_r\beta + \frac{2}{r}(\partial_r\alpha - \partial_r\beta)\frac{1}{r^2} + (1 - e^{2\beta})\right]. \tag{D.8}$$

We can take things one step further by introducing the Einstein tensor

$$G_{ab} \equiv R_{ab} - \tfrac{1}{2}Rg_{ab}, \tag{D.9}$$

which is actually just the left hand side of Einstein's field equation, Eq. (C.42). It can be shown that this is a conserved tensor,

$$\nabla^a G_{ab} = 0, \tag{D.10}$$

see [13, p. 131]. This means that the energy-momentum tensor is also conserved,

$$\nabla^a T_{ab} = 0, \tag{D.11}$$

since the two tensors are proportional to each other by Einstein's field equation. The components of the Einstein tensor becomes

$$\begin{aligned} G_{tt} &= \frac{1}{r^2} e^{2(\alpha-\beta)}\big(2r\partial_r\beta - 1 + e^{2\beta}\big), \\ G_{rr} &= \frac{1}{r^2}\big(2r\partial_r\alpha + 1 - e^{2\beta}\big), \\ G_{\theta\theta} &= r^2 e^{-2\beta}\Big[\partial_r^2\alpha + (\partial_r\alpha)^2 - \partial_r\alpha\partial_r\beta + \frac{1}{r}(\partial_r\alpha - \partial_r\beta)\Big], \\ G_{\phi\phi} &= \sin^2\theta\, G_{\theta\theta}. \end{aligned} \tag{D.12}$$

Now that we have expressions for both $G_{\mu\nu}$ and $T_{\mu\nu}$, we can finally focus our full attention on Einstein's field equation.

D.3 Deriving the Tolman–Oppenheimer–Volkoff Equation

In our case, Einstein's field equation, $G_{ab} = 8\pi G T_{ab}$, is diagonal, leaving us with four equations, one for each diagonal entry. But a quick inspection of the equation for the $\phi\phi$ component reveals that it is proportional to the equation for the $\theta\theta$ component. Thus, the number of independent equations is actually three. They are

$$\frac{1}{r^2} e^{-2\beta}\Big(2r\partial_r\beta - 1 + e^{2\beta}\Big) = 8\pi G\rho, \tag{D.13}$$

$$\frac{1}{r^2} e^{-2\beta}\Big(2r\partial_r\alpha + 1 - e^{2\beta}\Big) = 8\pi G P, \tag{D.14}$$

$$e^{-2\beta}\left[\partial_r^2\alpha + (\partial_r\alpha)^2 - \partial_r\alpha\partial_r\beta + \frac{1}{r}(\partial_r\alpha - \partial_r\beta)\right] = 8\pi G P. \tag{D.15}$$

The first thing to notice is that Eq. (D.13) only involves β and ρ. We therefore consider this equation first, following the steps in [13, p. 232-233]. For convenience, we introduce the new function

$$m(r) = \frac{1}{2G} r\big(1 - e^{-2\beta}\big), \tag{D.16}$$

or equivalently

$$e^{2\beta} = \left[1 - \frac{2Gm(r)}{r}\right]^{-1}. \tag{D.17}$$

The metric, Eq. (D.2), now takes the form

$$ds^2 = -e^{2\alpha(r)}dt^2 + \left[1 - \frac{2Gm(r)}{r}\right]^{-1} dr^2 + r^2 d\Omega. \tag{D.18}$$

This motivates the introduction of $m(r)$, because the metric is now starting to look like the static, spherically symmetric vacuum solution (the well-known Schwarzschild solution). The interior solution and the vacuum solution obviously have to be equal at the boundary between the mass distribution and the vacuum, and having them in the same form makes it easier to join them. Next, substituting Eq. (D.17) into Eq. (D.13) gives

$$\frac{1}{r^2}e^{-2\beta}\left(2r\partial_r\beta - 1 + e^{2\beta}\right) = \frac{1}{r^2}\left(-r\partial_r e^{-2\beta} + \frac{2Gm(r)}{r}\right) = \frac{2G}{r^2}\frac{dm}{dr} = 8\pi G\rho, \tag{D.19}$$

or simply

$$\frac{dm}{dr} = 4\pi r^2\rho. \tag{D.20}$$

By integrating, we get

$$m(r) = 4\pi\int_0^r \rho(r')r'^2dr'. \tag{D.21}$$

Imagine now that the mass distribution under consideration extends to a radius $r = R$ and define the parameter M as

$$M = m(R) = 4\pi\int_0^R \rho(r)r^2dr. \tag{D.22}$$

If one were to compare the expression for our metric so far to the static, spherically symmetric vacuum solution, one would find that for the two solutions to agree at $r = R$, then M as we defined it here is the same as the M that appears in the Schwarzschild metric. Furthermore, it can be quite easily shown that the behavior of a test body in a Newtonian gravtitional field of mass M coincides with the behavior of a test body in the weak field regime ($r \to \infty$) of a Schwarzschild gravitational field with parameter value M [14, p. 126]. We will therefore refer to M as the total mass of the Schwarzschild field. However, this can be somewhat misleading, because the integral in Eq. (D.22) is not a proper spatial integral, the reason being that the volume element is incorrect. The total *proper mass* is in fact given by

$$\bar{M} = 4\pi\int_0^R \rho(r)r^2e^{\beta(r)}dr. \tag{D.23}$$

Eq. (D.14) can be easily written in terms of $m(r)$ by using our expression for $e^{2\beta}$, giving

$$\frac{d\alpha}{dr} = \frac{Gm(r) + 4\pi Gr^3P}{r[r - 2Gm(r)]}. \tag{D.24}$$

Instead of using Eq. (D.15), we will consider energy-momentum conservation,

$$\nabla_\mu T^{\mu\nu} = 0. \tag{D.25}$$

Since most of the Christoffel symbols in our case are zero and the energy-momentum tensor is diagonal, it is straightforward to show that the only nontrivial component is when $\nu = r$. In that case we find

$$(\rho + P)\frac{d\alpha}{dr} = -\frac{dP}{dr}, \tag{D.26}$$

which can very easily be combined with Eq. (D.24) to eliminate $\alpha(r)$. The result is the **Tolman-Oppenheimer-Volkoff equation** of hydrostatic equilibrium:

$$\boxed{\frac{dP}{dr} = -(\rho + P)\frac{Gm(r) + 4\pi G r^3 P}{r[r - 2Gm(r)]}.} \tag{D.27}$$

This equation is a relation between $P(r)$ and $\rho(r)$, since $m(r)$ is really just an integral of $\rho(r)$, Eq. (D.21). If we were to have an equation of state for the fluid matter,

$$P = P(\rho), \tag{D.28}$$

we would have a closed system of equations constraining the structure of the entire mass distribution.

By pulling out a factor $G\rho m(r)/r^2$ and doing some dimensional analysis to restore c, the equation of hydrostatic equilibrium can be written as

$$\frac{dP}{dr} = -\frac{G\rho m(r)}{r^2}\left(1 + \frac{P}{\rho c^2}\right)\left(1 + \frac{4\pi r^3 P}{m(r)c^2}\right)\left(1 - \frac{2Gm(r)}{rc^2}\right)^{-1}. \tag{D.29}$$

We would now like to take the Newtonian limit by letting $c \to \infty$. Since ρ is simply defined as the energy density measured in the rest frame of the mass distribution, it does not depend on c. The same must be true for $m(r)$, because it is just the integral of ρ. However, the pressure P goes as v^2 in the non-relativistic limit, where $v \ll c$. Therefore, as $c \to \infty$, the three bracketed factors all reduce to 1, leaving us with

$$\frac{dP}{dr} = -\frac{G\rho m(r)}{r^2}, \tag{D.30}$$

which is the Newtonian hydrostatic equilibrium equation. This equation can be quite easily derived in Newtonian theory by summation of forces on infinitesimal volume elements. Notice that the right-hand side of Eq. (D.29) is always more negative than the right-hand side of Eq. (D.30). With the boundary condition $P(R) = 0$, this implies that the central pressure needed for equilibrium in general relativity is always higher than in Newtonian gravity.

E | Finite-Temperature Field Theory

This appendix was written as part of a project of mine during the fall semester of 2019 and **must therefore not be considered a part of this thesis during evaluation.**

The customary approach to introducing quantum field theory is to start with the notion of canonical quantization. This way of doing quantum field theory closely follows quantum mechanics, and it is also how the theory was developed and understood historically [35, p. 10]. Another common way of doing quantum field theory is through the path integral formalism, developed by Richard Feynman. This is the most popular method of choice for doing calculations on elementary particles these days [36, p. 12]. Therefore, it is the one that will be introduced here. Other than being particularly useful for studying non-perturbative phenomenon, it reveals a beautiful connection to the variational formulation of classical mechanics, explaining why nature chooses to obey the principle of stationary action, see [51, p. 11].

We start off this chapter by considering the path integral for a non-relativistic quantum mechanical system. This will serve to illustrate the general idea behind the formalism. After that, the concept of field operators is introduced, and we will see how the structure of quantum mechanics is generalized to fields before deriving the path integral for bosonic fields. From there, the connection is made between the path integral and the partition function of a statistical ensemble by considering the imaginary time formalism, after which be calculate the partition function for a neutral scalar field. Next, we introduce fermionic fields, which is obviously of great interest to us, since both quarks and neutrons are spin-$\frac{1}{2}$ particles. Like for bosons, the partition function will be calculated as a path integral in imaginary time, from which we will derive a simple model for the equation of state for a cold compact star.

E.1 The Path Integral in Quantum Mechanics

In this section we introduce the path integral in quantum mechanics. That way the generalization to quantum field theory becomes less mysterious. The discussion will be heavily based upon [51]. Note that $\hbar$ will be included for clarity here.

The path integral formulation of quantum mechanics is focused on the so-called *propagator*. It is defined as the matrix elements of the time-evolution operator expressed in the position eigenbasis,

$$K(x,t;x_0,t_0) = \langle x|U(t,t_0)|x_0\rangle\,. \tag{E.1}$$

These matrix elements are referred to as transition amplitudes. If we square them, we get the *probability density* for our system to be in the state $|x\rangle$ at time t given that it was in the state $|x_0\rangle$ at time t_0. Much can be said about the propagator, but the main thing to realize is that knowledge of the propagator implies knowledge of the general solution of the time-dependent Schrödinger equation; assume that $\psi(x, t_0)$ is some initial wave function, then at a later time t the wave function describing our quantum mechanical system is given by

$$\begin{aligned}\psi(x,t) &= \langle x|U(t,t_0)|\psi(t_0)\rangle = \int dx_0 \, \langle x|U(t,t_0)|x_0\rangle \, \langle x_0|\psi(t_0)\rangle \\ &= \int dx_0 \; K(x,t;x_0,t_0)\psi(x_0,t_0).\end{aligned} \tag{E.2}$$

The path integral formulation of quantum mechanics is therefore physically equivalent to the use of the Schrödinger equation.

Consider now a one-dimensional system in non-relativistic quantum mechanics with Hamiltonian

$$\hat{H} = \frac{\hat{p}^2}{2m} + V(\hat{x}) = \hat{T} + \hat{V}. \tag{E.3}$$

We assume for simplicity that $\hat{H}$ has no explicit time dependence. Generalizing to higher dimensions and time-dependent potentials is in fact not very hard. We wish to find the propagator for this system, that is, the matrix elements of the time-evolution operator. Since $\hat{H}$ is time independent, the time-evolution operator takes the simple form

$$U(t) = e^{-i\hat{H}t/\hbar} = e^{-it(\hat{T}+\hat{V})/\hbar}. \tag{E.4}$$

Be aware that this does not equal the product of the two exponentials, $e^{-it\hat{T}/\hbar}e^{-it\hat{V}/\hbar}$, because $\hat{T}$ and $\hat{V}$ do not commute. However, we will see that such a factorization is approximately true for small t. Let us therefore proceed by slicing up the time interval $[0, t]$ into a large number N of small intervals of duration ϵ,

$$\epsilon = \frac{t}{N}. \tag{E.5}$$

According to the composition property of the time-evolution operator, we can write

$$U(t) = \left[U(\epsilon)\right]^N. \tag{E.6}$$

Expanding $U(\epsilon)$ in a Taylor series gives

$$U(\epsilon) = 1 - \frac{i\epsilon}{\hbar}(\hat{T} + \hat{V}) + \mathcal{O}(\epsilon^2). \tag{E.7}$$

If we also Taylor expand the product of the exponentials, we find

$$e^{-it\hat{T}/\hbar}\, e^{-it\hat{V}/\hbar} = \left[1 - \frac{i\epsilon}{\hbar}\hat{T} + \mathcal{O}(\epsilon^2)\right]\left[1 - \frac{i\epsilon}{\hbar}\hat{V} + \mathcal{O}(\epsilon^2))\right] = 1 - \frac{i\epsilon}{\hbar}(\hat{T} + \hat{V}) + \mathcal{O}(\epsilon^2). \tag{E.8}$$

The last two equations imply that

$$U(\epsilon) = e^{-i\epsilon\hat{T}/\hbar}\, e^{-i\epsilon\hat{V}/\hbar} + \mathcal{O}(\epsilon^2), \tag{E.9}$$

which we can raise to the power of N to get

$$U(t) = \left[e^{-i\epsilon\hat{T}/\hbar}\, e^{-i\epsilon\hat{V}/\hbar} + \mathcal{O}(\epsilon^2)\right]^N = \left[e^{-i\epsilon\hat{T}/\hbar}\, e^{-i\epsilon\hat{V}/\hbar}\right]^N + \mathcal{O}(\epsilon^2). \tag{E.10}$$

As $\epsilon \to 0$, $N \to \infty$, and we can therefore write

$$\langle x|\, U(t)\, |x_0\rangle = \lim_{N\to\infty} \langle x| \left[e^{-i\epsilon\hat{T}/\hbar}\, e^{-i\epsilon\hat{V}/\hbar}\right]^N |x_0\rangle\,. \tag{E.11}$$

We now insert $N-1$ resolutions of the identity between the N factors,

$$\begin{aligned}\langle x|U(t)|x_0\rangle = \lim_{N\to\infty} \int dx_1 \ldots dx_{N-1} \\ \times \langle x_N|\, e^{-i\epsilon\hat{T}/\hbar}\, e^{-i\epsilon\hat{V}/\hbar}\, |x_{N-1}\rangle \langle x_{N-1}| \ldots |x_1\rangle \langle x_1|\, e^{-i\epsilon\hat{T}/\hbar}\, e^{-i\epsilon\hat{V}/\hbar}\, |x_0\rangle\,,\end{aligned} \tag{E.12}$$

where we have defined $x_N \equiv x$ for easier manipulation in the equations to come.

Let us now consider one of the matrix elements on the right side of Eq.(E.12). If we insert a resolution of the identity in the momentum eigenbasis, we get

$$\begin{aligned}\left\langle x_{j+1}\right|\, e^{-i\epsilon\hat{T}/\hbar}\, e^{-i\epsilon\hat{V}/\hbar}\, \left|x_j\right\rangle &= \int dp\, \left\langle x_{j+1}\right|\, e^{-i\epsilon\hat{p}^2/2m\hbar}\, |p\rangle\langle p|\, e^{-i\epsilon V(\hat{x})/\hbar}\, \left|x_j\right\rangle \\ &= \int dp\, \left\langle x_{j+1}|p\right\rangle\, e^{-i\epsilon p^2/2m\hbar}\, \left\langle p|x_j\right\rangle\, e^{-i\epsilon V(x_j)/\hbar}.\end{aligned} \tag{E.13}$$

Notice how we freed ourselves from the operators $\hat{p}$ and $\hat{x}$ by letting them act on the eigenkets. If we choose to normalize the states $|p\rangle$ such that $\langle p_1|p_2\rangle = \delta(p_1 - p_2)$, one can easily show that

$$\langle x|p\rangle = \frac{1}{\sqrt{2\pi\hbar}} e^{ipx/\hbar}, \tag{E.14}$$

which when used in Eq. (E.13) leads to

$$\left\langle x_{j+1}\right|\, e^{-i\epsilon\hat{T}/\hbar}\, e^{-i\epsilon\hat{V}/\hbar}\, \left|x_j\right\rangle = \int \frac{dp}{2\pi\hbar} \exp\left\{\frac{i}{\hbar}\left[-\epsilon\frac{p^2}{2m} + p(x_{j+1} - x_j) - \epsilon V(x_j)\right]\right\}. \tag{E.15}$$

This is a Gaussian integral, and it can be easily solved by applying the well-known formula

$$\int_{-\infty}^{\infty} dp\; e^{-\frac{1}{2}ap^2 + Jp} = \sqrt{\frac{2\pi}{a}} e^{J^2/2a}. \tag{E.16}$$

In our case, $a = \frac{i\epsilon}{m\hbar}$ and $J = i(x_{j+1} - x_j)/\hbar$. The result is

$$\left\langle x_{j+1}\right|\, e^{-i\epsilon\hat{T}/\hbar}\, e^{-i\epsilon\hat{V}/\hbar}\, \left|x_j\right\rangle = \sqrt{\frac{m}{2\pi i\epsilon\hbar}} \exp\left\{\frac{i}{\hbar}\left[m\frac{(x_{j+1} - x_j)^2}{2\epsilon} - \epsilon V(x_j)\right]\right\}. \tag{E.17}$$

When substituting this back into Eq. (E.12), we get

$$\begin{aligned}\langle x|U(t)|x_0\rangle = \lim_{N\to\infty} \left(\frac{m}{2\pi i\epsilon\hbar}\right)^{N/2} \int dx_1 \ldots dx_{N-1} \\ \times \exp\left\{\frac{i\epsilon}{\hbar} \sum_{j=0}^{N-1} \left[m\frac{(x_{j+1} - x_j)^2}{2\epsilon^2} - V(x_j)\right]\right\}.\end{aligned} \tag{E.18}$$

This expression will be referred to as the discretized version of the *path integral* in non-relativistic quantum mechanics.

We usually visualize the integration above by identifying the points $(x_0, \ldots, x_N)$ with a path $x(t)$ in configuration space consisting of straight lines between the points, and we think of the path $x(t)$ as passing through the point x_j at time $t_j = j\epsilon$. This makes sense if we go back and study Eq. (E.12). The integrand is a product of transition amplitudes, and the square of each such amplitude is just the probability density of measuring the system (e.g., a particle) to be at position x_{j+1} at time t_{j+1} given that it was at position x_j at time $t_j = j\epsilon$. The square of the whole integrand therefore represent the probability density for the system to end up at the final position $x = x_N$ at time $t = t_N$ given that it was at the initial position x_0 at time $t_0 = 0$ and that it was located at the intermediate positions $(x_1, x_2, \ldots, x_{N-1})$ at the corresponding times $(t_1, t_2, \ldots, t_{N-1})$. A visual representation of the paths is given in Fig. E.1. When the path integral is computed, the intermediate points (being variables of integration) run up and down the dotted lines, all the way from $-\infty$ to ∞. As $N \to \infty$, we end up with a representation of the path for all values of t between the initial time and the final time. We therefore say that we integrate over all paths in configuration space connecting x_0 and x_N.

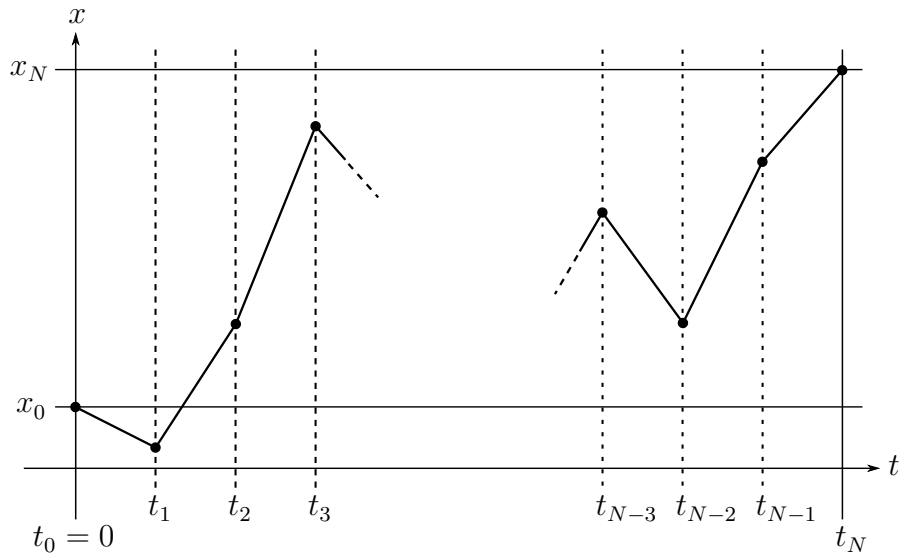

Figure E.1: A spacetime diagram illustrating one of infinitely many discretized paths connecting the initial point (x_0, t_0) and the final point (x_N, t_N). When $N \to \infty$, the spacing between the dotted lines will diminish and we get a representation of the path for all intermediate times. Be aware that the paths are generally not well behaved.

One can easily fall into the trap of thinking of the path integral as merely a sum over all paths connecting x_0 and $x = x_N$, where each path is weighted by the probability of the system to take that particular path through configuration space, but this is not entirely correct. The path integral is indeed a sum over all paths connection the start- and endpoint, but the weights are not the probabilities of the paths, but rather the transition amplitudes. When we eventually square

the propagator to get the probability density of finding the system in the state $|x\rangle$ at time t given the initial condition, the sum of the transition amplitudes of the different paths are squared, resulting in cross terms, that is, interference between the different paths.

The discretized path integral can be put into a nicer form by observing that if we set $\Delta t = \epsilon$ and $\Delta x_j = x_{j+1} - x_j$, then the exponent in Eq. (E.18) looks like $i/\hbar$ times a Riemann sum,

$$\Delta t \sum_{j=0}^{N-1} \left[\frac{m}{2} \left(\frac{\Delta x_j}{\Delta t} \right)^2 - V(x_j) \right], \tag{E.19}$$

It is tempting to think of this as converging to the following Riemann integral in the limit $N \to \infty$:

$$S[x(\tau)] = \int_0^t d\tau \left[\frac{m}{2} \left(\frac{dx}{d\tau} \right)^2 - V(x) \right] = \int_0^t d\tau \; L\left(x(\tau), \dot{x}(\tau)\right), \tag{E.20}$$

where L is the classical Lagrangian,

$$L(x, \dot{x}) = \frac{m\dot{x}^2}{2} - V(x). \tag{E.21}$$

But one must be careful, because the path $x(\tau)$ is generally not well behaved. It can go from $x = -\infty$ to $x = \infty$ from one point to the next. However, it turns out that the paths that actually contribute to the path integral are indeed continuous, though generally not differentiable. See [51] for a more in-depth discussion. Nevertheless, it is convenient to simply introduce a more compact notation for the path integral,

$$\langle x|U(t)|x_0\rangle = C \int d[x(\tau)] \exp\left\{ \frac{i}{\hbar} \int_0^t L \; d\tau \right\}, \tag{E.22}$$

where C is the normalization constant appearing in Eq. (E.18), and $d[x(\tau)]$ means we are integrating over all paths in configuration space having x_0 and x as endpoints. Furthermore, in many applications we choose to regard the action integral (E.20) as any other Riemann integral and allow ourselves to employ the rules of ordinary calculus when manipulating it.

E.2 Path Integrals in Quantum Field Theory

Quantum field theory introduces the concept of field operators $\hat{\phi}(\mathbf{x})$. Just like any other operator in quantum mechanics they act on the Hilbert space of the quantized system, its eigenvalues correspond to the possible outcomes of a measurement, and the eigenkets represents the different states of the field. The eigenvalue equation for a general Schrödinger-picture field operator without explicit time dependence can be written as

$$\hat{\phi}(\mathbf{x})|\phi\rangle = \phi(\mathbf{x})|\phi\rangle \,. \tag{E.23}$$

Here, $\mathbf{x}$ is not an operator, but a parameter of the field representing the position where the measurement is made. A good example is the electromagnetic field operator $\hat{\mathbf{E}}(\mathbf{x})$. Its eigenvalues at parameter value $\mathbf{x}$ are the possible outcomes of a measurement of the electromagnetic field at the point $\mathbf{x}$. There are, however, some subtleties concerning such measurements, because in practice they must be done over a volume, not at a single point in space. See [52] for more details on this.

The path integral formulation of quantum field theory is very similar to the one in quantum mechanics. It too revolves around the matrix elements of the time-evolution operator, but field theory is all about the time-evolution of the state of a field $\phi(\mathbf{x})$, not the position $\mathbf{x}$ of the system as a whole. We are therefore no longer interested in expressing the matrix elements of the time-evolution operator in the position eigenbasis $|\mathbf{x}\rangle$, but rather in the eigenbasis $|\phi\rangle$ of the field operator. Suppose that a system with Hamiltonian $\hat{H}$ is in a state $|\phi_0\rangle$ at time $t = 0$. Then at a later time t the system will be in the state $U(t,0)|\phi_0\rangle = e^{-i\hat{H}t}|\phi_0\rangle$. Thus, the transition amplitude for going from a state $|\phi_0\rangle$ at time $t = 0$ to some other state $|\phi\rangle$ at time t is given by the matrix element $\langle\phi|e^{-i\hat{H}t}|\phi_0\rangle$ of the time-evolution operator. To take this any further, we must consider the Hamiltonian. But what is the Hamiltonian in quantum field theory? It should certainly not be a function of $\hat{\mathbf{x}}$ and $\hat{\mathbf{p}}$, because those operators are obviously not very interesting in regard to field configurations. Instead, we draw the connection between classical field theory and quantum field theory.

Finding the quantum Hamiltonian that best describes a given dynamical system ultimately boils down to making an educated guess. Often in quantum mechanics we start of by considering the Hamiltonian for a classical theory, and then we quantize it by simply reinterpreting the canonical coordinates and conjugate momenta as operators satisfying the canonical commutation relations. The same procedure can be done in quantum field theory. Suppose we have a classical theory describing some field ϕ. At the very base of such a theory lies the Lagrangian density $\mathcal{L}$, which is a function of the field ϕ and its derivatives. For simplicity, let us consider only first derivatives $\partial_\mu\phi$, but in general, higher order derivatives could indeed be generalized coordinates as well. A Hamiltonian description of the classical theory is obtained by a Legendre transformation of the Lagrangian,

$$\mathcal{H} = \pi(\mathbf{x})\dot{\phi}(\mathbf{x}) - \mathcal{L}, \tag{E.24}$$

where the conjugate momentum field $\pi(\mathbf{x})$ is defined as

$$\pi(\mathbf{x}) \equiv \frac{\partial\mathcal{L}}{\partial\dot{\phi}}. \tag{E.25}$$

By solving Eq. (E.25) for $\dot{\phi}$, the *Hamiltonian density* $\mathcal{H}$ can be written purely in terms of the field ϕ and its conjugate momentum π. Furthermore, the Hamiltonian is obtained by integrating the Hamiltonian density over position space,

$$H = \int d^3x\ \mathcal{H}(\pi,\phi). \tag{E.26}$$

To turn this classical theory into a quantum field theory, we simply borrow the classical Hamiltonian above, Eq. (E.26), and reinterpret the fields $\phi(\mathbf{x})$ and $\pi(\mathbf{x})$ as

Schrödinger-picture quantum field operators $\hat{\phi}(\mathbf{x})$ and $\hat{\pi}(\mathbf{x})$ acting on the Hilbert space of the system, and we require them to satisfy the equal-time canonical commutation relations for fields:

$$\begin{aligned}\left[\hat{\phi}(\mathbf{x}), \hat{\pi}(\mathbf{y})\right] &= i\delta^{(3)}(\mathbf{x}-\mathbf{y}),\\ \left[\hat{\phi}(\mathbf{x}), \hat{\phi}(\mathbf{y})\right] &= \left[\hat{\pi}(\mathbf{x}), \hat{\pi}(\mathbf{y})\right] = 0,\end{aligned} \tag{E.27}$$

[38, p. 20]. Notice that we have switched back to natural units, such that $\hbar = 1$.

Now that we have some intuition for what $\hat{\phi}$ and $\hat{\pi}$ are, let us move on to the path integral formulation of quantum field theory. The following derivation is inspired by [35, 36, 51]. Consider a system described by a Schrõdinger-picture Hamiltonian density with no explicit time dependence given by

$$\hat{\mathcal{H}} = \frac{1}{2}\hat{\pi}^2 + \mathcal{V}(\hat{\phi}), \tag{E.28}$$

where $\mathcal{V}$ is some function of the field operator $\hat{\phi}$. Our goal is to derive the path integral for this system. One can of course consider more general Hamiltonians, but we will stick to the above form to make the derivation a little easier and clearer. Assuming we are dealing with complete Hermitian field operators, as we always do, we can write down the orthonormality condition

$$\langle\phi_a|\phi_b\rangle = \prod_{\mathbf{x}} \delta(\phi_a(\mathbf{x}) - \phi_b(\mathbf{x})) \tag{E.29}$$

and the completeness relation

$$\int \mathcal{D}\phi(\mathbf{x})\, |\phi\rangle\langle\phi| = \mathbb{1}. \tag{E.30}$$

The measure $\mathcal{D}\phi(\mathbf{x})$ means that we integrate over all classical field configurations $\phi(\mathbf{x})$. More specifically, we divide position space into a lattice with spacing l and define

$$\mathcal{D}\phi(\mathbf{x}) = \lim_{l\to 0} \prod_i d\phi(\mathbf{x}_i), \tag{E.31}$$

where $\phi(\mathbf{x}_i)$ is a variable representing the value of the field at the i-th lattice location [38, p. 285]. Similar expressions are expected to hold for the conjugate momentum field operator $\hat{\pi}$. Its eigenvalue equation is

$$\hat{\pi}(\mathbf{x})|\pi\rangle = \pi(\mathbf{x})|\pi\rangle\,, \tag{E.32}$$

and the orthogonality condition and the completeness relation are

$$\langle\pi_a|\pi_b\rangle = 2\pi \prod_{\mathbf{x}} \delta(\pi_a(\mathbf{x}) - \pi_b(\mathbf{x})), \tag{E.33}$$

and

$$\int \frac{\mathcal{D}\pi(\mathbf{x})}{2\pi}\, |\pi\rangle\langle\pi| = \mathbb{1}. \tag{E.34}$$

Moreover, the inner product of $|\phi\rangle$ and $|\pi\rangle$ is given by

$$\langle\phi|\pi\rangle = \exp\biggl(i\int d^3x\ \pi(\mathbf{x})\phi(\mathbf{x})\biggr), \tag{E.35}$$

which is the field theory generalization of Eq. (E.14).

The transition amplitudes of greatest interest in field theory are the ones were the system returns to its original state after the time t, and we therefore consider only the matrix elements $\langle\phi_0|e^{-i\hat{H}t}|\phi_0\rangle$. Since the derivation follows more or less the same procedure as in quantum mechanics, we will not go into the same amount of detail here. The first step is to slice up the time interval $[0,t]$ into a large number N of small intervals of duration ϵ such that the time-evolution operator can be written as

$$\begin{aligned} U(t) = e^{-i\hat{H}t} &= \lim_{N\to\infty}\Bigl[e^{-i\epsilon\int d^3x\,\hat{\mathcal{H}}}\Bigr]^N \\ &= \lim_{N\to\infty}\biggl[\exp\biggl(-i\epsilon\int d^3x\ \tfrac{1}{2}\hat{\pi}^2\biggr)\exp\biggl(-i\epsilon\int d^3x\ \mathcal{V}(\hat{\phi})\biggr)\biggr]^N. \end{aligned} \tag{E.36}$$

Next, sandwich this between $\langle\phi_0|$ and $|\phi_0\rangle$ and insert $N-1$ complete sets of intermediate states between the N factors. This leads to

$$\begin{aligned} \langle\phi_0|U(t)|\phi_0\rangle = \lim_{N\to\infty}\int &\mathcal{D}\phi_1(\mathbf{x})\ldots\mathcal{D}\phi_{N-1}(\mathbf{x}) \\ &\times\langle\phi_N|\,e^{-i\epsilon\hat{H}}\,|\phi_{N-1}\rangle\langle\phi_{N-1}|\ldots|\phi_1\rangle\langle\phi_1|\,e^{-i\epsilon\hat{H}}\,|\phi_0\rangle\,, \end{aligned} \tag{E.37}$$

where we have defined $\phi_N = \phi_0$ so that writing down sums and products over subscripts becomes easier. Now look at the N matrix elements on the right-hand side of Eq. (E.37). By writing out the exponential function as the product of two exponentials, like in Eq. (E.36), and inserting a resolution of the identity in the momentum eigenbasis, each matrix element becomes

$$\begin{aligned} &\langle\phi_{k+1}|\,e^{-i\epsilon\hat{H}}\,|\phi_k\rangle \\ &= \int\frac{\mathcal{D}\pi_k(\mathbf{x})}{2\pi}\,\langle\phi_{k+1}|\exp\biggl(-i\epsilon\int d^3x\ \tfrac{1}{2}\hat{\pi}^2\biggr)|\pi_k\rangle\langle\pi_k|\exp\biggl(-i\epsilon\int d^3x\ \mathcal{V}(\hat{\phi})\biggr)|\phi_k\rangle \\ &= \int\frac{\mathcal{D}\pi_k(\mathbf{x})}{2\pi}\,\langle\phi_{k+1}|\pi_k\rangle\exp\biggl(-i\epsilon\int d^3x\ \tfrac{1}{2}\pi_k(\mathbf{x})^2\biggr)\langle\pi_j|\phi_k\rangle\exp\biggl(-i\epsilon\int d^3x\ \mathcal{V}\bigl(\phi_k(\mathbf{x})\bigr)\biggr) \\ &= \int\frac{\mathcal{D}\pi_k(\mathbf{x})}{2\pi}\exp\biggl\{i\epsilon\int d^3x\biggl[\pi_k(\mathbf{x})\biggl(\frac{\phi_{k+1}(\mathbf{x})-\phi_k(\mathbf{x})}{\epsilon}\biggr) - \tfrac{1}{2}\pi_k(\mathbf{x})^2 - \mathcal{V}\bigl(\phi_k(\mathbf{x})\bigr)\biggr]\biggr\}. \end{aligned} \tag{E.38}$$

Substituting this back into Eq. (E.37) leads to

$$\begin{aligned} \langle\phi_0|U(t)|\phi_0\rangle = \lim_{N\to\infty}\Bigl(\frac{1}{2\pi}\Bigr)^N\int &\biggl(\prod_{i=0}^{N-1}\mathcal{D}\pi_i(\mathbf{x})\biggr)\biggl(\prod_{j=1}^{N-1}\mathcal{D}\phi_j(\mathbf{x})\biggr) \\ &\times\exp\biggl\{i\epsilon\sum_{k=0}^{N-1}\int d^3x\biggl[\pi_k(\mathbf{x})\biggl(\frac{\phi_{k+1}(\mathbf{x})-\phi_k(\mathbf{x})}{\epsilon}\biggr) - \mathcal{H}\bigl(\pi_k(\mathbf{x}),\phi_k(\mathbf{x})\bigr)\biggr]\biggr\}. \end{aligned} \tag{E.39}$$

A similar discussion to the one we had in quantum mechanics follows from here, but we will not go into the same amount of detail, because the idea is essentially the same. We identify the "points" $(\phi_0(\mathbf{x}), \ldots, \phi_N(\mathbf{x}))$ with a path $\phi(\mathbf{x}, t)$ in the configuration space of the field, and we think of the path $\phi(\mathbf{x}, t)$ as passing through the point $\phi_j(\mathbf{x})$ at time $t_j = j\epsilon$. As $N \to \infty$, we end up with a representation of the path for all values of t between the initial time and the final time, and we say that we integrate over all paths in the configuration space of the field connecting the initial configuration $\phi_0(\mathbf{x})$ at time $t = 0$ and the final configuration $\phi_N(\mathbf{x})$ at the later time $t = t_N$. A similar interpretation holds for the conjugate momentum field, giving an infinite set of paths $\pi(\mathbf{x}, t)$ to integrate over, but unlike $\phi(\mathbf{x}, t)$, these paths are not restricted at the endpoints. Just like we did in quantum mechanics, we take the limit $N \to \infty$ and write the sum in the exponent of the exponential as a Riemann integral over the time coordinate, even though we know that this is not entirely rigorous. The final and very important result is

$$\langle \phi_0 | U(t) | \phi_0 \rangle = \langle \phi_0 | \, e^{-i\hat{H}t} \, | \phi_0 \rangle = C \int \mathcal{D}\pi(\mathbf{x}, \tau) \int_{\phi(\mathbf{x},0)=\phi_0(\mathbf{x})}^{\phi(\mathbf{x},t)=\phi_0(\mathbf{x})} \mathcal{D}\phi(\mathbf{x}, \tau) \times \exp\left\{ i \int_0^t d\tau \int d^3x \left[\pi(\mathbf{x}, \tau) \frac{\partial \phi(\mathbf{x}, \tau)}{\partial \tau} - \mathcal{H}\big(\pi(\mathbf{x}, \tau), \phi(\mathbf{x}, \tau)\big) \right] \right\}, \tag{E.40}$$

which is the path integral for a scalar field in quantum field theory. Here we have set $C = (1/2\pi)^N$, which obviously diverges as $N \to \infty$. Such constants will, however, drop out of any physical quantities, and we can therefore simply ignore it.

E.3 Partition Function for Bosons

In light of quantum statistical mechanics, the partition function for a grand canonical ensemble is given by

$$Z = \operatorname{Tr} e^{-\beta(\hat{H} - \mu\hat{N})} = \int \mathcal{D}\phi_0(\mathbf{x}) \, \langle \phi_0 | \, e^{-\beta(\hat{H} - \mu\hat{N})} \, | \phi_0 \rangle \, . \tag{E.41}$$

Notice that the integrand is a matrix element that looks a lot like the transition amplitudes from the previous section, Eq. (E.40). This similarity can be exploited if we perform a so-called Wick rotation by introducing an imaginary time variable $\tau' = i\tau$ and also make the replacement

$$\mathcal{H}(\pi, \phi) \to \mathcal{H}(\pi, \phi) - \mu \mathcal{N}(\pi, \phi) \tag{E.42}$$

to account for any conserved charge. Formally, this kind of replacement of the Hamiltonian is not fully justified by our previous derivation of the path integral. It would really depend on the form of $\mathcal{N}$, but we did mention earlier that more general Hamiltonians could be considered. The matrix elements in the partition function above can now be written

$$\langle \phi_0 | \, e^{-\beta(\hat{H} - \mu\hat{N})} \, | \phi_0 \rangle = \langle \phi_0 | \, e^{-it(\hat{H} - \mu\hat{N})} \, | \phi_0 \rangle = C \int \mathcal{D}\pi(\mathbf{x}, -i\tau') \int_{\phi(\mathbf{x},0)=\phi_0(\mathbf{x})}^{\phi(\mathbf{x},-i\beta)=\phi_0(\mathbf{x})} \mathcal{D}\phi(\mathbf{x}, -i\tau')$$
$$\times \exp\left\{ \int_0^\beta d\tau' \int d^3x \left[i\pi(\mathbf{x}, -i\tau') \frac{\partial \phi(\mathbf{x}, -i\tau')}{\partial \tau'} - \mathcal{H}(\pi, \phi) + \mu \mathcal{N}(\pi, \phi) \right] \right\}. \tag{E.43}$$

Next, define primed functions $\pi'(\mathbf{x},\tau') = \pi(\mathbf{x},-i\tau')$ and $\phi'(\mathbf{x},\tau') = \phi(\mathbf{x},-i\tau')$, substitute these into the above expression and then relabel π', ϕ' and τ' to get rid of the primes. The partition function then becomes

$$\begin{aligned} Z = C \int \mathcal{D}\pi(\mathbf{x},\tau) \int_{\text{periodic}} \mathcal{D}\phi(\mathbf{x},\tau) \\ \times \exp\left\{ \int_0^\beta d\tau \int d^3x \left[i\pi(\mathbf{x},\tau) \frac{\partial\phi(\mathbf{x},\tau)}{\partial\tau} - \mathcal{H}(\pi,\phi) + \mu\mathcal{N}(\pi,\phi) \right] \right\}, \end{aligned} \tag{E.44}$$

where the term "periodic" means that we integrate over all paths in configuration space with equal endpoints. The trace operation has made it so that the integration over paths is no longer constrained to a single initial field configuration $\phi_0(x)$, though the initial and final field configuration for each path is still constrained to be equal, $\phi(\mathbf{x},0) = \phi(\mathbf{x},\beta)$, hence the use of the term periodic.

E.4 Neutral Scalar Field

Let us now consider a neutral scalar field, which describes spin-0 particles. This section will be based upon [36], but will include more details in the calculations for the sake of clarity. The most general renormalizable Lagrangian for a neutral scalar field is

$$\mathcal{L} = \frac{1}{2}\partial_\mu\phi\partial^\mu\phi - \frac{1}{2}m^2\phi^2 - U(\phi), \tag{E.45}$$

where the potential $U(\phi)$ is given by

$$U(\phi) = g\phi^3 + \lambda\phi^4, \tag{E.46}$$

with $\lambda \geq 0$ [36, p. 16]. The conjugate momentum is easily calculated from its definition, Eq. (E.25),

$$\pi = \frac{\partial\mathcal{L}}{\partial(\partial_0\phi)} = \frac{1}{2}\frac{\partial}{\partial(\partial_0\phi)}\left(\frac{\partial\phi}{\partial x^0}\right)^2 = \frac{\partial\phi}{\partial t}, \tag{E.47}$$

and the Hamiltonian is obtained by a simple Legendre transform,

$$\mathcal{H} = \pi\frac{\partial\phi}{\partial t} - \mathcal{L} = \frac{1}{2}\pi^2 + \frac{1}{2}(\nabla\phi)^2 + \frac{1}{2}m^2\phi^2 + U(\phi). \tag{E.48}$$

To compute the partition function for this system, we need to consider the discretized version of Eq. (E.44), which is given by

$$\begin{aligned} Z = \lim_{N\to\infty}\left(\frac{1}{2\pi}\right)^N \int \left(\prod_{i=0}^{N-1}\mathcal{D}\pi_i(\mathbf{x})\right)\left(\prod_{j=0}^{N-1}\mathcal{D}\phi_j(\mathbf{x})\right) \\ \times \exp\left\{ \Delta\tau \sum_{k=0}^{N-1} \int d^3x \left[i\pi_k \left(\frac{\phi_{k+1}-\phi_k}{\Delta\tau}\right) - \tfrac{1}{2}\pi_k^2 - \tfrac{1}{2}(\nabla\phi_k)^2 - \tfrac{1}{2}m^2\phi_k^2 - U(\phi_k) \right] \right\}. \end{aligned} \tag{E.49}$$

Let us now deal with the momentum integrals. By a simple rewriting of the above expression, the momentum part can be separated,

$$Z = \lim_{N\to\infty}\left(\frac{1}{2\pi}\right)^N \int\left(\prod_{j=0}^{N-1}\mathcal{D}\phi_j\right)\exp\left\{\Delta\tau\sum_{k=0}^{N-1}\int d^3x\Big[-\tfrac{1}{2}(\nabla\phi_j)^2-\tfrac{1}{2}m^2\phi_j^2 - U(\phi_j)\Big]\right\}\times\prod_{i=0}^{N-1}\int\mathcal{D}\pi_i\exp\left\{\int d^3x\Big[-\tfrac{1}{2}\Delta\tau\pi_i^2+i\pi_i(\phi_{i+1}-\phi_i)\Big]\right\}, \tag{E.50}$$

so that we can focus our attention on the integral

$$\mathcal{I}_i = \int\mathcal{D}\pi_i\exp\left\{\int d^3x\Big[-\tfrac{1}{2}\Delta\tau\pi_i^2+i\pi_i(\phi_{i+1}-\phi_i)\Big]\right\}. \tag{E.51}$$

Assume from now on that the system is placed in a fixed volume $V = L^3$ and divide it up into M^3 tiny cubical boxes with volume a^3. This implies that $L = aM$. The integral over position space in the exponential can now be written as the limit of a Riemann sum as $M\to\infty$. For convenience, define the function

$$f_i(\mathbf{x}) = -\tfrac{1}{2}\Delta\tau\pi_i(\mathbf{x})^2 + i\pi_i(\mathbf{x})\big(\phi_{i+1}(\mathbf{x})-\phi_i(\mathbf{x})\big), \tag{E.52}$$

which is nothing more than the integrand appearing in Eq. (E.51). Next, label the n-th box by B_n and form the Riemann sum

$$S_i = a^3\sum_{n=1}^{M^3} f_i(\mathbf{x}_n) = \frac{V}{M^3}\sum_{n=1}^{M^3} f_i(\mathbf{x}_n), \tag{E.53}$$

where $\mathbf{x}_n\in B_n$. We can now write

$$\mathcal{I}_i = \lim_{M\to\infty}\int\mathcal{D}\pi_i\exp\left\{\frac{V}{M^3}\sum_{n=1}^{M^3}f_i(\mathbf{x}_n)\right\} = \lim_{M\to\infty}\int\mathcal{D}\pi_i\prod_{n=1}^{M^3}\exp\left\{\frac{V}{M^3}f_i(\mathbf{x}_n)\right\}$$
$$\lim_{M\to\infty}\prod_{n=1}^{M^3}\int_{-\infty}^{\infty}d\pi_i(\mathbf{x}_n)\exp\left\{\frac{V}{M^3}\Big[-\tfrac{1}{2}\Delta\tau\pi_i(\mathbf{x}_n)^2+i\pi_i(\mathbf{x}_n)\big(\phi_{i+1}(\mathbf{x}_n)-\phi_i(\mathbf{x}_n)\big)\Big]\right\}, \tag{E.54}$$

where $\pi_i(\mathbf{x}_n)$ is viewed as an integration variable. Each integral over $\pi_i(\mathbf{x}_n)$ is just a Gaussian integral that can be solved by using Eq. (E.16). In our case $a = -\Delta\tau V/M^3$ and $J = i\big(\phi_{i+1}(\mathbf{x}_n)-\phi_i(\mathbf{x}_n)\big)V/M^3$, giving

$$\begin{aligned}\mathcal{I}_i &= \lim_{M\to\infty}\prod_{n=1}^{M^3}\sqrt{\frac{2\pi M^3}{\Delta\tau V}}\exp\left[-\frac{\Delta\tau V}{2M^3}\left(\frac{\phi_{i+1}(\mathbf{x}_n)-\phi_i(\mathbf{x}_n)}{\Delta\tau}\right)^2\right]\\ &= \lim_{M\to\infty}\left(\frac{2\pi M^3}{\Delta\tau V}\right)^{M^3/2}\exp\left[-\Delta\tau\frac{V}{M^3}\sum_{m=1}^{M^3}\frac{1}{2}\left(\frac{\phi_{i+1}(\mathbf{x}_m)-\phi_i(\mathbf{x}_m)}{\Delta\tau}\right)^2\right],\end{aligned} \tag{E.55}$$

which when substituted back into Eq. (E.50) leads to

$$\begin{aligned} Z &= \lim_{M,N\to\infty} \left(\frac{1}{2\pi}\right)^N \left(\frac{2\pi M^3}{\Delta\tau V}\right)^{M^3N/2} \int \left(\prod_{j=0}^{N-1} \mathcal{D}\phi_j\right) \\ &\times \exp\left\{\Delta\tau \sum_{k=0}^{N-1} \int d^3x \Big[-\tfrac{1}{2}(\nabla\phi_j)^2 - \tfrac{1}{2}m^2\phi_j^2 - U(\phi_j)\Big]\right\} \\ &\times \prod_{i=0}^{N-1} \exp\left[-\Delta\tau \frac{V}{M^3} \sum_{m=1}^{M^3} \frac{1}{2}\left(\frac{\phi_{i+1}(\mathbf{x}_m) - \phi_i(\mathbf{x}_m)}{\Delta\tau}\right)^2\right] \\ &= \lim_{M,N\to\infty} \left(\frac{1}{2\pi}\right)^N \left(\frac{2\pi M^3}{\Delta\tau V}\right)^{M^3N/2} \int \left(\prod_{j=0}^{N-1} \mathcal{D}\phi_j\right) \\ &\times \exp\left\{\Delta\tau \sum_{k=0}^{N-1} \left[\int d^3x \Big[-\tfrac{1}{2}(\nabla\phi_j)^2 - \tfrac{1}{2}m^2\phi_j^2 - U(\phi_j)\Big]\right.\right. \\ &\left.\left. - \frac{V}{M^3} \sum_{m=1}^{M^3} \frac{1}{2}\left(\frac{\phi_{i+1}(\mathbf{x}_m) - \phi_i(\mathbf{x}_m)}{\Delta\tau}\right)^2\right]\right\}. \end{aligned} \tag{E.56}$$

As $M \to \infty$, the sum over m reverts back to an integral over position space, while in the limit $N \to \infty$ we recover the integral over imaginary time. Taking the limits yields

$$Z = C' \int_{\text{periodic}} \mathcal{D}\phi(\mathbf{x},\tau) \exp\left\{-\int_0^\beta d\tau \int d^3x \left[\frac{1}{2}\left(\frac{\partial\phi}{\partial\tau}\right)^2 + \frac{1}{2}(\nabla\phi)^2 + \frac{1}{2}m^2\phi^2 + U(\phi)\right]\right\}. \tag{E.57}$$

The constant C' is of course highly divergent, but multiplication of Z with any constant will not change the thermodynamics. The expression in square brackets is the Lagrangian density expressed in our Wick rotated coordinate system, which we shall define as the Euclidean Lagrangian $\mathcal{L}_E$, because it looks as if we are suddenly working with a Euclidean metric. The final result can therefore be written

$$Z = C' \int_{\text{periodic}} \mathcal{D}\phi(\mathbf{x},\tau) \exp\left\{ -\int_0^\beta d\tau \int d^3x\, \mathcal{L}_E \right\} = C' \int_{\text{periodic}} \mathcal{D}\phi(\mathbf{x},\tau)\, e^S. \tag{E.58}$$

Consider now a non-interacting neutral scalar field, meaning $U(\phi) = 0$. The action in this case is given by

$$S = \int_0^\beta d\tau \int d^3x\, \mathcal{L} = -\frac{1}{2}\int_0^\beta d\tau \int d^3x \left[\left(\frac{\partial\phi}{\partial\tau}\right)^2 + (\nabla\phi)^2 + m^2\phi^2\right], \tag{E.59}$$

which can be integrated by parts, leading to

$$S = -\frac{1}{2}\int_0^\beta d\tau \int d^3x\, \phi\Big[-\frac{\partial^2}{\partial\tau^2} - \nabla^2 + m^2\Big]\phi. \tag{E.60}$$

In this step, we had to use the fact that $\phi(\mathbf{x},0)=\phi(\mathbf{x},\beta)$, which implies $\partial_\tau\phi(\mathbf{x},0)=\partial_\tau\phi(\mathbf{x},\beta)$, and we also assumed that ϕ vanishes on the boundary of V. This ensures that the boundary terms emerging from the integration by parts vanish. Furthermore, it means that ϕ is now periodic in both $\mathbf{x}$ and τ. The field can be written as a Fourier series,

$$\phi(\mathbf{x},\tau)=\sqrt{\frac{\beta}{V}}\sum_{n=-\infty}^{\infty}\sum_{\mathbf{p}}\phi_n(\mathbf{p})e^{i(\mathbf{p}\cdot\mathbf{x}+\omega_n\tau)}. \tag{E.61}$$

Here, $\omega_n=2\pi n/\beta$ and $\mathbf{p}=2\pi\mathbf{n}/L$, with $\mathbf{n}=(n_1,n_2,n_3)\in\mathbb{Z}^3$. The factor $\sqrt{\beta/V}$ has been stripped of the Fourier coefficients to make them dimensionless. The field expansion can now be substituted into the action integral, but since the field is real, one can just as well substitute in the complex conjugate of it. This leads to

$$\begin{aligned}S=&-\frac{1}{2}\frac{\beta}{V}\int_0^\beta d\tau\int d^3x\\&\times\left[\sum_n\sum_{\mathbf{p}}\phi_n(\mathbf{p})e^{i(\mathbf{p}\cdot\mathbf{x}+\omega_n\tau)}\right]\cdot\left[\sum_n\sum_{\mathbf{p}}(\omega_n^2+|\mathbf{p}|^2+m^2)\phi_n^*(\mathbf{p})e^{-i(\mathbf{p}\cdot\mathbf{x}+\omega_n\tau)}\right].\end{aligned} \tag{E.62}$$

When the infinite sums in the two sets of brackets are written out and then multiplied together, the integrand becomes an infinite sum of pairs,

$$S=-\frac{1}{2}\frac{\beta}{V}\int_0^\beta d\tau\int d^3x\sum_{n,n'}\sum_{\mathbf{p},\mathbf{p}'}(\omega_{n'}^2+|\mathbf{p}'|^2+m^2)\phi_n(\mathbf{p})\phi_{n'}^*(\mathbf{p}')e^{i(\mathbf{p}\cdot\mathbf{x}+\omega_n\tau)}e^{-i(\mathbf{p}'\cdot\mathbf{x}+\omega_{n'}\tau)}, \tag{E.63}$$

where each pair can be labeled by a tuple $(n,n',\mathbf{p},\mathbf{p}')$. Since the exponential functions are orthogonal on the domain of integration, every pair that is a cross term, meaning $n\neq n'$ or $\mathbf{p}\neq\mathbf{p}'$, will vanish when integrated. For the rest of the terms, the exponentials cancel each other, making the integration trivial. The result is

$$S=-\frac{1}{2}\beta^2\sum_n\sum_{\mathbf{p}}(\omega_n^2+\omega_{\mathbf{p}}^2)\phi_n(\mathbf{p})\phi_n^*(\mathbf{p}), \tag{E.64}$$

where we have defined $\omega_{\mathbf{p}}^2=\sqrt{|\mathbf{p}|^2+m^2}$. The partition function can now be written

$$Z=C'\int\mathcal{D}\phi(\mathbf{x},\tau)\exp\left\{-\frac{1}{2}\beta^2\sum_{n=-\infty}^{\infty}\sum_{\mathbf{p}}(\omega_n^2+\omega_{\mathbf{p}}^2)\phi_n(\mathbf{p})\phi_n^*(\mathbf{p})\right\}. \tag{E.65}$$

Before this can be taken any further, we need to take a look at the measure $\mathcal{D}\phi$. First, we note that since the field is real, the Fourier coefficients satisfy

$$\phi_n^*(\mathbf{p})=\phi_{-n}(-\mathbf{p}), \tag{E.66}$$

implying that only half of them are independent. For convenience, denote the real and imaginary parts of $\phi_n(\mathbf{p})$ as follows:

$$\phi_n(\mathbf{p})=x_n(\mathbf{p})+iy_n(\mathbf{p}). \tag{E.67}$$

We now choose all $x_n(\mathbf{p})$ and $y_n(\mathbf{p})$ with $n > 0$ as our new independent integration variables, giving us a coordinate transformation

$$\big\{\phi(\mathbf{x},\tau)\big\} \longleftrightarrow \big\{x_n(\mathbf{p}), y_n(\mathbf{p}) \mid n > 0\big\}. \tag{E.68}$$

The Jacobian matrix $\mathbf{J}$ for this transformation can be shown to be orthogonal, which further implies that $\det(\mathbf{J}) = 1$. Therefore, the measure given in terms of these new coordinates is simply

$$\mathcal{D}\phi(\mathbf{x},\tau) = \lim_{l\to 0}\prod_i d\phi(\mathbf{x}_i) = |\det(\mathbf{J})|\prod_{n>0}\prod_{\mathbf{p}} dx_n(\mathbf{p})dy_n(\mathbf{p}) = \prod_{n>0}\prod_{\mathbf{p}} dx_n(\mathbf{p})dy_n(\mathbf{p}). \tag{E.69}$$

Substituting this into Eq. (E.65) and carrying out the integration yields

$$\begin{aligned} Z &= C'\int_{-\infty}^{\infty}\left(\prod_{n>0}\prod_{\mathbf{p}} dx_n(\mathbf{p})dy_n(\mathbf{p})\right)\exp\left[-\frac{1}{2}\beta^2\sum_n\sum_{\mathbf{p}}(\omega_n^2+\omega_{\mathbf{p}}^2)|\phi_n(\mathbf{p})|^2\right] \\ &= C'\prod_{n>0}\prod_{\mathbf{p}}\int_{-\infty}^{\infty} dx_n(\mathbf{p})dy_n(\mathbf{p})\exp\left[-\frac{1}{2}\beta^2(\omega_n^2+\omega_{\mathbf{p}}^2)(x_n(\mathbf{p})^2+y_n(\mathbf{p})^2)\right] \\ &= C'\prod_{n>0}\prod_{\mathbf{p}}\sqrt{\frac{2\pi}{\beta^2(\omega_n^2+\omega_{\mathbf{p}}^2)}}\sqrt{\frac{2\pi}{\beta^2(\omega_n^2+\omega_{\mathbf{p}}^2)}} \\ &= C'\prod_{\text{all } n}\prod_{\mathbf{p}}\sqrt{\frac{2\pi}{\beta^2(\omega_n^2+\omega_{\mathbf{p}}^2)}} \end{aligned} \tag{E.70}$$

[38, p. 286]. The constants C' and $\sqrt{2\pi}$ are independent of thermodynamic quantities and can therefore simply be dropped without changing the physics. This is because to get thermodynamic quantities we use the derivative of the logarithm of Z. Thus, such constant *factors* appearing in Z or, alternatively, a similar *term* appearing in $\ln Z$ will vanish later anyway when taking derivatives.

Taking the logarithm of the expression for Z above gives

$$\ln Z = -\frac{1}{2}\sum_n\sum_{\mathbf{p}}\ln\left[\beta^2\omega_{\mathbf{p}}^2 + (2\pi n)^2\right]. \tag{E.71}$$

Next, consider the integral

$$\int_1^{\beta^2\omega_{\mathbf{p}}^2}\frac{d\theta^2}{\theta^2+(2\pi n)^2} = \ln\left[\beta^2\omega_{\mathbf{p}}^2+(2\pi n)^2\right] - \ln\left[1+(2\pi n)^2\right], \tag{E.72}$$

which lets us write

$$\ln Z = -\frac{1}{2}\sum_n\sum_{\mathbf{p}}\left\{\int_1^{\beta^2\omega_{\mathbf{p}}^2}\frac{d\theta^2}{\theta^2+(2\pi n)^2} + \ln\left[1+(2\pi n)^2\right]\right\}. \tag{E.73}$$

The remaining logarithmic term can be dropped for the same reason as above. We also do the sum over n, which evaluates to

$$\sum_{n=-\infty}^{\infty}\frac{1}{(\theta/2\pi)^2+n^2} = \frac{2\pi^2}{\theta}\coth(\theta/2) = \frac{2\pi^2}{\theta}\frac{e^\theta+1}{e^\theta-1} = \frac{2\pi^2}{\theta}\left(1+\frac{2}{e^\theta-1}\right). \tag{E.74}$$

The partition function can now be written

$$\begin{aligned}\ln Z &= -\frac{1}{2}\sum_{\mathbf{p}}\int_1^{\beta^2\omega_{\mathbf{p}}^2}\frac{d\theta^2}{(2\pi)^2}\sum_n\frac{1}{(\theta/2\pi)^2+n^2} = -\sum_{\mathbf{p}}\int_1^{\beta\omega_{\mathbf{p}}}d\theta\left(\frac{1}{2}+\frac{1}{e^\theta-1}\right)\\ &= \sum_{\mathbf{p}}\left[-\frac{1}{2}\beta\omega_{\mathbf{p}}-\ln\left(1-e^{-\beta\omega_{\mathbf{p}}}\right)\right],\end{aligned} \tag{E.75}$$

where we have dropped the irrelevant term $\ln(e-1)$. The remaining sum over $\mathbf{p}$ can be approximated by an integral if we assume the volume V to be large. Since $\mathbf{p} = 2\pi\mathbf{n}/L$, the spacing between neighboring values of $\mathbf{p} = (p_1, p_2, p_3)$ is given by

$$\Delta p_i = \frac{2\pi}{L}, \tag{E.76}$$

and, thus, we get the Riemann sum

$$\ln Z = \frac{\Delta p_1\Delta p_2\Delta p_3}{(2\pi/L)^3}\sum_{\mathbf{p}}\left[-\frac{1}{2}\beta\omega_{\mathbf{p}}-\ln\left(1-e^{-\beta\omega_{\mathbf{p}}}\right)\right]. \tag{E.77}$$

As $V\to\infty$, $\Delta p_i\to 0$, and the Riemann sum $\Delta p_1\Delta p_2\Delta p_3\sum_{\mathbf{p}}\left[\cdots\right]$ converges to an integral. Thus, in the large volume limit the partition function becomes

$$\ln Z = V\int\frac{d^3p}{(2\pi)^3}\left[-\frac{1}{2}\beta\omega_{\mathbf{p}}-\ln\left(1-e^{-\beta\omega_{\mathbf{p}}}\right)\right]. \tag{E.78}$$

We notice that the first term in the integrand is proportional to the vacuum energy $H_0 = \int\frac{d^3p}{(2\pi)^3}\frac{\omega_{\mathbf{p}}}{2}$. This term is divergent and therefore leads to the partition function becoming infinite. In the absence of gravity, one way of trying to rationalizing away the vacuum energy is by saying that only differences in energy matter, and so the vacuum energy can simply be dropped by resetting the level of origin for energy. However, the vacuum energy does indeed have consequences, such as the Casimir effect [35, p. 52]. Furthermore, in general relativity, Einstein's field equation tells us that all energy contributes to the curvature of spacetime. This makes the issue of the vacuum energy less trivial. Another way of dealing with the vacuum energy is to simply introduce an ultraviolet cutoff frequency so that the integral above becomes finite. But even when this is done, quantum field theory predicts a vacuum energy density that tremendously exceeds cosmological observations [53]. Therefore, we shall simply ignore the contribution to the partition function from the vacuum energy by dropping the first term in the integrand. What we are left with is the well-known partition function for an ideal gas of bosons with $\mu = 0$, which can be derived using completely different methods [54]. Thus, we have shown that the path integral formulation reproduces the desired result in this case.

E.5 Fermions

So far we have looked at the neutral scalar field which describes spin-0 particles. We would now like to consider particles with spin $\frac{1}{2}$. As in the previous section, we

follow the general outline of the derivation found in [36]. However, the introduction of the Grassmann algebra is inspired by [35, 55]. The starting point is the "classical" free field Dirac Lagrangian

$$\mathcal{L} = \bar{\psi}(i\gamma^\mu \partial_\mu - m)\psi \tag{E.79}$$

where $\bar{\psi} \equiv \psi^\dagger \gamma^0$ and m is understood to be multiplied by the 4×4 identity matrix. The Dirac γ-matrices satisfy the Dirac algebra

$$\{\gamma^\mu, \gamma^\nu\} = 2\eta^{\mu\nu}, \tag{E.80}$$

as well as

$$(\gamma^\mu)^\dagger = \gamma^0 \gamma^\mu \gamma^0. \tag{E.81}$$

In the Dirac-Pauli representation, they are

$$\gamma^0 = \begin{pmatrix} 1 & 0 \\ 0 & -1 \end{pmatrix}, \qquad \boldsymbol{\gamma} = \begin{pmatrix} 0 & \boldsymbol{\sigma} \\ -\boldsymbol{\sigma} & 0 \end{pmatrix}, \tag{E.82}$$

where γ^0 is a 4×4 matrix and $\boldsymbol{\gamma} = (\gamma^1, \gamma^2, \gamma^3)$ is a triplet of the remaining 4×4 matrices; a "1" denotes a unit 2×2 matrix and $\boldsymbol{\sigma}$ denotes the triplet of Pauli matrices [35, p. 168]. The conjugate momentum is given by

$$\pi = \frac{\partial \mathcal{L}}{\partial(\partial_0 \psi)} = \bar{\psi} i \gamma^0 = i\psi^\dagger, \tag{E.83}$$

which means that ψ and $\psi^\dagger$ must be treated as independent fields. The Hamiltonian density now follows from the definition, Eq. (E.25), yielding

$$\mathcal{H} = \pi \partial_0 \psi - \mathcal{L} = i\psi^\dagger \partial_0 \psi - \bar{\psi}(i\gamma^\mu \partial_\mu - m)\psi = \bar{\psi}(-i\boldsymbol{\gamma} \cdot \boldsymbol{\nabla} + m)\psi. \tag{E.84}$$

The Dirac Lagrangian has a continuous symmetry under the transformation $\psi \to \psi e^{-i\alpha}$, so by Noether's theorem there is a conserved charge density j^0, which turns out to be

$$j^0 = \psi^\dagger \psi. \tag{E.85}$$

We now quantize this "classical theory" by promoting the fields to Schrödinger picture operators, but this time we require the operators to obey the equal-time canonical *anti*commutation relations:

$$\begin{aligned} \left\{\hat{\psi}_\alpha(\mathbf{x}), \hat{\psi}^\dagger_\beta(\mathbf{y})\right\} &= \delta_{\alpha\beta}\delta^{(3)}(\mathbf{x} - \mathbf{y}), \\ \left\{\hat{\psi}_\alpha(\mathbf{x}), \hat{\psi}_\beta(\mathbf{y})\right\} &= \left\{\hat{\psi}^\dagger_\alpha(\mathbf{x}), \hat{\psi}^\dagger_\beta(\mathbf{y})\right\} = 0. \end{aligned} \tag{E.86}$$

Our goal is to find the partition function, but if we were to follow the same procedure as for a free scalar field, we would run into trouble. Because of the anticommutation relations, the eigenvalues of the field operators ψ and $\bar{\psi}$ cannot be regular scalars. Rather, they must be anticommuting "numbers". To resolve this issue, we must take a little detour into the mathematics of the *Grassmann algebra*.

Let V be an n-dimensional complex vector space. Formally, the Grassmann algebra of V is defined as the exterior algebra of V,

$$\Lambda(V) = \bigoplus_{k=0}^{n} \Lambda^k(V) = \mathbb{C} \oplus V \oplus (V \wedge V) \oplus \cdots \oplus (\underbrace{V \wedge V \wedge \cdots \wedge V}_{n \text{ times}}), \tag{E.87}$$

and the elements of this algebra are called *Grassmann numbers*. Our interest in this abstract mathematical structure comes from the fact that for any two $\zeta, \eta \in \Lambda^1(V) = V$ we have that

$$\zeta \wedge \eta + \eta \wedge \zeta = \{\zeta, \eta\} = 0. \tag{E.88}$$

This is exactly the anticommutation relation we mentioned that the eigenvalues of the quantum field operators must obey. A generating set for $\Lambda(V)$ is a set of n basis vectors $\{\theta_i\}$ of V. This simply means that any element of the algebra can be expressed as a polynomial in these θ_i, which is why they are referred to as *generators* of the algebra. The generators of a Grassmann algebra are also called *Grassmann variables*.

We now highlight a few key features of the Grassmann algebra that will be important for understanding fermionic path integrals. First and foremost, in quantum field theory, we drop the wedge product symbol and simply write

$$\theta_i \theta_j = -\theta_j \theta_i. \tag{E.89}$$

In particular, any generator squares to zero,

$$\theta_i^2 = 0. \tag{E.90}$$

Functions can be constructed from the Grassmann variables as polynomials, but they are quite limited in form, because Eq. (E.90) tells us that any term with more than one factor of a particular Grassmann variable will vanish. For example, for $n = 1$ there is only one Grassmann variable θ, which means that an arbitrary function is given by

$$f(\theta) = f_0 + f_1 \theta, \tag{E.91}$$

where f_0 and f_1 are complex numbers. Similarly, for $n = 2$ we have

$$f(\theta_1, \theta_2) = f_0 + f_1 \theta_1 + f_2 \theta_2 + f_3 \theta_1 \theta_2. \tag{E.92}$$

Analytic functions like exp and cos are defined in terms of their Taylor series, so for example

$$e^{\theta} = 1 + \theta + \tfrac{1}{2}\theta^2 + \cdots = 1 + \theta. \tag{E.93}$$

Next, let us define derivatives and integrals with respect to Grassmann variables. Starting with derivatives, we define

$$\frac{\partial}{\partial \theta_1} f(\theta_1, \theta_2) = f_1 + f_3 \theta_2, \tag{E.94}$$

which has an obvious generalization to any n. Be aware that the derivative operator acts on the left of a product of Grassmann variables, so the relative position of the variables matters,

$$\frac{\partial}{\partial\theta_1}\theta_2\theta_1 = -\frac{\partial}{\partial\theta_1}\theta_1\theta_2 = -\theta_2. \tag{E.95}$$

Somewhat strangely, we define integrals over Grassmann variables (called Berezin integrals) to be equal to the derivative operator

$$\int d\theta \equiv \frac{\partial}{\partial\theta}. \tag{E.96}$$

This has the effect of making the integration measure shift invariant,

$$\int d\theta f(\theta+\eta) = \int d\theta\,[f_0 + f_1(\theta+\eta)] = f_1 = \int d\theta f(\theta). \tag{E.97}$$

For multiple integrals, we define the usual notation

$$\int d\theta_1 d\theta_2 \equiv \int d\theta_1 \int d\theta_2, \tag{E.98}$$

which simply means that we perform the innermost integral first. The order of integration does indeed matter for these types of integrals, due to the fact that the order matters for derivatives.

Gaussian integrals are quite simple in this formalism. The case of one variable is trivial, since $e^{-\theta^2} = 1$, and for two variables we get

$$\int d\theta_1 d\theta_2 e^{-\theta_1 A_{12}\theta_2} = \int d\theta_1 d\theta_2 (1 - A_{12}\theta_1\theta_2) = A_{12}. \tag{E.99}$$

Now, say we have n θ_i and another n Grassmann variables that we denote by $\bar\theta_i$. Together they form a set of $2n$ independent Grassmann variables. Consider the integral

$$\begin{aligned}\int d\bar\theta_1 d\theta_1 \cdots d\bar\theta_n d\theta_n\, e^{-\bar\theta_i A_{ij}\theta_j} \\ = \left(\prod_i \int d\bar\theta_i d\theta_i\right)\left[1 - \bar\theta_i A_{ij}\theta_j + \frac{1}{2}(\bar\theta_i A_{ij}\theta_j)(\bar\theta_k A_{kl}\theta_l) + \cdots\right],\end{aligned} \tag{E.100}$$

where we have used the summation convention in the exponential function and in the square brackets. Only the terms in the Taylor expansion containing exactly all n θ_i and all n $\bar\theta_i$ will survive. One can quite easily show that the result is

$$\int d\bar\theta_1 d\theta_1 \cdots d\bar\theta_n d\theta_n\, e^{-\bar\theta_i A_{ij}\theta_j} = \det(A), \tag{E.101}$$

where A is the matrix whose entries are the complex numbers A_{ij}. Let us abbreviate the notation further by defining

$$\int \mathcal{D}\bar\theta\mathcal{D}\theta \equiv \int d^n\bar\theta d^n\theta \equiv \int d\bar\theta_1 d\theta_1 \ldots d\bar\theta_n d\theta_n. \tag{E.102}$$

So far only a finite set of generators have been considered, but in quantum field theory we will have to take the continuum limit, replacing the index i with a continuous variable τ, such that $\theta_i \to \theta(\tau)$.

Now, to make a long story short, it turns out that the partition function for fermions can be written in a very similar way to the partition function for bosons. The starting point is the same; one considers the transition amplitudes for a field ψ to return to its original configuration after a time t. Like before, the partition function is given by the trace of the time-evolution operator in imaginary time, which is of course the integral over the transition amplitudes. The result turns out to be

$$\begin{aligned} Z &= \int_{\text{antiperiodic}} \mathcal{D}\pi(\mathbf{x},\tau)\mathcal{D}\psi(\mathbf{x},\tau)\exp\Big(S[\pi,\psi]\Big) \\ &= \int_{\text{antiperiodic}} \mathcal{D}\pi(\mathbf{x},\tau)\mathcal{D}\psi(\mathbf{x},\tau)\exp\bigg[\int_0^\beta d\tau \int d^3x \left(i\pi\frac{\partial\psi}{\partial\tau} - \mathcal{H}(\pi,\psi) + \mu\mathcal{N}(\pi,\psi)\right)\bigg] \\ &= \int_{\text{antiperiodic}} \mathcal{D}\pi(\mathbf{x},\tau)\mathcal{D}\psi(\mathbf{x},\tau)\exp\bigg[\int_0^\beta d\tau \int d^3x\, \bar{\psi}\Big(-\gamma^0\frac{\partial}{\partial\tau} + i\boldsymbol{\gamma}\cdot\boldsymbol{\nabla} - m + \mu\gamma^0\Big)\psi\bigg], \end{aligned} \tag{E.103}$$

where "antiperiodic" means that $\psi(\mathbf{x},\beta) = -\psi(\mathbf{x},0)$ and $\pi(\mathbf{x},\beta) = -\pi(\mathbf{x},0)$. This antiperiodicity is a consequence of the anticommutation relations for the fields. Except for the fact that the fields are now antiperiodic instead of periodic, this expression is identical in form to the one for bosons, Eq. (E.44). However, this time the integral is a Berezin integral over continuous Grassmann variables.

To solve the path integral above, we start by Fourier-expanding the field,

$$\psi(\mathbf{x},\tau) = \frac{1}{\sqrt{V}}\sum_{n=-\infty}^{\infty}\sum_{\mathbf{p}}\psi_n(\mathbf{p})e^{i(\mathbf{p}\cdot\mathbf{x}+\omega_n\tau)}. \tag{E.104}$$

Since ψ is antiperiodic in τ, we must have that

$$\omega_n = (2n+1)\pi/\beta, \quad n\in\mathbb{Z}. \tag{E.105}$$

Substituting this into the action S defined in Eq. (E.103) leads to

$$\begin{aligned} S = \frac{1}{V}\int_0^\beta d\tau\int d^3x \sum_{n,n'}\sum_{\mathbf{p},\mathbf{p}'}\bar{\psi}_n(\mathbf{p})(-\gamma^0 i\omega_n - \boldsymbol{\gamma}\cdot\mathbf{p} + \mu\gamma^0 - m) \\ \times\,\psi_{n'}(\mathbf{p}')e^{i(\mathbf{p}\cdot\mathbf{x}+\omega_n\tau)}e^{-i(\mathbf{p}'\cdot\mathbf{x}+\omega_{n'}\tau)}. \end{aligned} \tag{E.106}$$

By using the same argument as was used when we dealt with Eq. (E.63), we get

$$\begin{aligned} S &= \beta\sum_n\sum_{\mathbf{p}}\bar{\psi}_n(\mathbf{p})(-\gamma^0 i\omega_n - \boldsymbol{\gamma}\cdot\mathbf{p} + \mu\gamma^0 - m)\psi_n(\mathbf{p}) \\ &= -\sum_n\sum_{\mathbf{p}}\pi_n(\mathbf{p})\Big[i\beta\big(-(i\omega_n+\mu) - \gamma^0\boldsymbol{\gamma}\cdot\mathbf{p} - m\gamma^0\big)\Big]\psi_n(\mathbf{p}) \\ &= -\sum_n\sum_{\mathbf{p}}\pi_n(\mathbf{p})D(n,\mathbf{p})\psi_n(\mathbf{p}), \end{aligned} \tag{E.107}$$

with the matrix $D(n,\mathbf{p})$ defined as

$$\begin{aligned} D(n,\mathbf{p}) &= i\beta\big(-(i\omega_n+\mu)-\gamma^0\boldsymbol{\gamma}\cdot\mathbf{p}-m\gamma^0\big) \\ &= i\beta\begin{pmatrix}-(i\omega_n+\mu)-m & -\boldsymbol{\sigma}\cdot\mathbf{p} \\ -\boldsymbol{\sigma}\cdot\mathbf{p} & -(i\omega_n+\mu)+m\end{pmatrix}. \end{aligned} \tag{E.108}$$

Inserting the action, Eq. (E.107), into the partition function, Eq. (E.103), and changing integration variables to the Fourier coefficients yields

$$\begin{aligned} Z &= \left[\prod_n\prod_{\mathbf{p}}\int d\pi_n(\mathbf{p})d\psi_n(\mathbf{p})\right]\exp\left(-\sum_n\sum_{\mathbf{p}}\pi_n(\mathbf{p})D(n,\mathbf{p})\psi_n(\mathbf{p})\right) \\ &= \prod_n\prod_{\mathbf{p}}\det D(n,\mathbf{p}), \end{aligned} \tag{E.109}$$

where we used Eq. (E.101) to perform the integral. To find the determinant of $D(n,\mathbf{p})$ we can use the following formula for the determinant of a block matrix [56]:

$$\det\begin{pmatrix}A & B\\ C & E\end{pmatrix} = \det\big(AE-BE^{-1}CE\big), \tag{E.110}$$

where A, B, C and E are blocks. In our case $B = C = -\boldsymbol{\sigma}\cdot\mathbf{p}$, $A = -(i\omega_n+\mu)-m$ and $E = -(i\omega_n+\mu)+m$. Thus, the first term in the formula above becomes

$$AE = (i\omega_n+\mu+m)(i\omega_n+\mu-m) = (i\omega_n+\mu)^2-m^2, \tag{E.111}$$

and since E is just a constant times the 2×2 identity matrix, the second term becomes

$$BE^{-1}CE = B^2E^{-1}E = (\boldsymbol{\sigma}\cdot\mathbf{p})^2. \tag{E.112}$$

Next, using the identity $(\boldsymbol{\sigma}\cdot\mathbf{p})^2 = \mathbf{p}^2$ and that the determinant of a diagonal matrix is the product of the diagonal entries gives

$$\det D(n,\mathbf{p}) = (i\beta)^4\det\big[(i\omega_n+\mu)^2-m^2-\mathbf{p}^2\big] = \beta^4\big[(i\omega_n+\mu)^2-\omega_{\mathbf{p}}^2\big]^2. \tag{E.113}$$

By applying the identity $\ln\det D = \operatorname{Tr}\ln D$, the partition function can be written

$$\begin{aligned} \ln Z &= \ln\left\{\prod_n\prod_{\mathbf{p}}\beta^4\big[(i\omega_n+\mu)^2-\omega_{\mathbf{p}}^2\big]^2\right\} = 2\sum_n\sum_{\mathbf{p}}\ln\Big\{\beta^2\big[(\omega_n+i\mu)^2+\omega^2\big]\Big\} \\ &= \sum_n\sum_{\mathbf{p}}\Big\{\ln\big[\beta^2(\omega_n^2+(\omega_{\mathbf{p}}-\mu)^2)\big]+\ln\big[\beta^2(\omega_n^2+(\omega_{\mathbf{p}}+\mu)^2)\big]\Big\}. \end{aligned} \tag{E.114}$$

From here it goes very similar to what we did for the scalar field. Consider the integral

$$\int_1^{\beta^2(\omega_{\mathbf{p}}\pm\mu)^2}\frac{d\theta^2}{\theta^2+(2n+1)^2\pi^2} = \ln\big[(2n+1)^2\pi^2+\beta^2(\omega_{\mathbf{p}}\pm\mu)^2\big]-\ln\big[1+(2n+1)^2\pi^2\big]. \tag{E.115}$$

This lets us rewrite the partition function as

$$\ln Z = \sum_{\mathbf{p}} \sum_{n=-\infty}^{\infty} \left\{ \int_1^{\beta^2(\omega_{\mathbf{p}}-\mu)^2} \frac{d\theta^2}{\theta^2 + (2n+1)^2\pi^2} + \int_1^{\beta^2(\omega_{\mathbf{p}}+\mu)^2} \frac{d\theta^2}{\theta^2 + (2n+1)^2\pi^2} \right\}, \tag{E.116}$$

where we have dropped the term $2\ln\left[1 + (2n+1)^2\pi^2\right]$, because it is independent of thermodynamic quantities and will therefore vanish later anyway when taking derivatives of $\ln Z$. By using the summation formula

$$\sum_{n=-\infty}^{\infty} \frac{1}{(n-x)(n-y)} = \frac{\pi\big[\cot(\pi x) - \cot(\pi y)\big]}{y-x}, \tag{E.117}$$

with $x = -\frac{1}{2} - \frac{\theta}{2\pi}i$ and $y = -\frac{1}{2} + \frac{\theta}{2\pi}i$, the sum over n evaluates to

$$\sum_{n=-\infty}^{\infty} \frac{1}{\theta^2 + (2n+1)^2\pi^2} = \frac{1}{4\pi^2} \sum_{n=-\infty}^{\infty} \frac{1}{(n-x)(n-y)} = \frac{1}{\theta}\left(\frac{1}{2} - \frac{1}{e^\theta + 1}\right). \tag{E.118}$$

The integrals are now easy to do, which yields

$$\begin{aligned} \ln Z &= 2\sum_{\mathbf{p}} \left[\int_1^{\beta(\omega_{\mathbf{p}}-\mu)} d\theta \left(\frac{1}{2} - \frac{1}{e^\theta + 1}\right) + \int_1^{\beta(\omega_{\mathbf{p}}+\mu)} d\theta \left(\frac{1}{2} - \frac{1}{e^\theta + 1}\right) \right] \\ &= 2\sum_{\mathbf{p}} \left[\beta\omega_{\mathbf{p}} + \ln\left(1 + e^{-\beta(\omega_{\mathbf{p}}-\mu)}\right) + \ln\left(1 + e^{-\beta(\omega_{\mathbf{p}}+\mu)}\right) \right]. \end{aligned} \tag{E.119}$$

Finally, in the large volume limit, we get

$$\ln Z = 2V \int \frac{d^3p}{(2\pi)^3} \left[\beta\omega_{\mathbf{p}} + \ln\left(1 + e^{-\beta(\omega_{\mathbf{p}}-\mu)}\right) + \ln\left(1 + e^{-\beta(\omega_{\mathbf{p}}+\mu)}\right) \right]. \tag{E.120}$$

Compared to the case of spin-0 particles, Eq. (E.78), there is an extra factor 2 in front of the integral. This is due to the fact that there are two possible spin states for fermions: "up" and "down". Or more precisely, it is because the spin space is two dimensional. The next thing we notice is the contribution from the vacuum energy, which we shall simply drop, as was argued for in the previous section. The remaining logarithmic terms are separate contributions from particles (with chemical potential μ) and antiparticles (with chemical potential $-\mu$), respectively. Fortunately, we can conclude that quantum field theory manages to reproduce the well-known partition function for an ideal Fermi gas [54].

E.6 Ideal Fermi Gases at Zero Temperature

In the previous section we found the partition function for an ideal Fermi gas, Eq. (E.120). We decided to omit the contribution from the vacuum energy, after which the partition function reads

$$\ln Z = 2V \int \frac{d^3p}{(2\pi)^3} \left[\ln\left(1 + e^{-\beta(\omega_{\mathbf{p}}-\mu)}\right) + \ln\left(1 + e^{-\beta(\omega_{\mathbf{p}}+\mu)}\right) \right]. \tag{E.121}$$

In this section, we consider the zero-temperature limit of the thermodynamics quantities resulting from the above partition function. This will yield us a simple model of the matter inside a compact star. The following derivations are inspired by [57].

Notice that at zero temperature ($\beta \to \infty$), if we use the convention that μ is positive, the term in the partition function concerning antiparticles completely vanishes. This leaves us only to consider

$$\ln Z = 2V \int \frac{d^3p}{(2\pi)^3} \ln\Big(1 + e^{-\beta(\omega_{\mathbf{p}} - \mu)}\Big). \tag{E.122}$$

Let us begin by calculating the average particle number density $\langle n \rangle$, which is given by

$$\langle n \rangle = \frac{\langle N \rangle}{V} = \frac{1}{V}\left(\frac{1}{\beta}\frac{\partial \ln Z}{\partial \mu}\right) = 2\int \frac{d^3p}{(2\pi)^3} \frac{1}{e^{\beta(\omega_{\mathbf{p}} - \mu)} + 1}. \tag{E.123}$$

Hence, the average occupation number for a single-particle state with momentum $\mathbf{p}$ is

$$\langle n_{\mathbf{p}} \rangle = \frac{2}{e^{\beta(\omega_{\mathbf{p}} - \mu)} + 1}, \tag{E.124}$$

where the factor 2 comes from the fact that a particle with momentum $\mathbf{p}$ can have two independent spin states. In the limit $\beta \to \infty$, this expression becomes the Heaviside step function

$$\lim_{\beta \to \infty} \frac{2}{e^{\beta(\omega_{\mathbf{p}} - \mu)} + 1} = 2\theta(\mu - \omega_{\mathbf{p}}). \tag{E.125}$$

Consequently, at zero temperature, only single-particle states with energy less than the chemical potential are occupied. But this is exactly the definition of the *Fermi energy*: the energy of the highest occupied single-particle energy state in a Fermi gas at zero temperature. The chemical potential therefore equals the Fermi energy E_F in the zero-temperature limit,

$$\mu(T = 0) = E_F. \tag{E.126}$$

The Fermi momentum, on the other hand, is defined implicitly by the energy-momentum relation

$$E_F = \sqrt{p_F^2 + m^2}. \tag{E.127}$$

We can now easily calculate the particle number density in terms of the Fermi momentum. Since $\omega_{\mathbf{p}}$ only depends on $|\mathbf{p}| = \mathrm{p}$, integrating over angles just gives a factor 4π. We therefore get

$$\begin{aligned} \langle n \rangle &= 2\int \frac{d^3p}{(2\pi)^3}\theta(E_F - \omega_{\mathbf{p}}) \\ &= \frac{1}{\pi^2}\int_0^\infty dp\, p^2 \theta(E_F - \omega_{\mathbf{p}}) = \frac{1}{\pi^2}\int_0^{p_F} dp\, p^2 = \frac{p_F^3}{3\pi^2}. \end{aligned} \tag{E.128}$$

Next, let us calculate the pressure P, which is given by

$$P = \frac{1}{\beta}\frac{\partial \ln Z}{\partial V} = \frac{2}{\beta}\int \frac{d^3p}{(2\pi)^3} \ln\Big(1 + e^{-\beta(\omega_{\mathbf{p}} - \mu)}\Big). \tag{E.129}$$

Integrating over angles followed by integration by parts yields

$$P = \frac{1}{\beta\pi^2}\left[\frac{1}{3}p^3 \ln\left(1+e^{-\beta(\omega_{\mathbf{p}}-\mu)}\right)\Big|_0^\infty + \frac{\beta}{3}\int_0^\infty dp\,\frac{p^4}{\sqrt{p^2+m^2}}\frac{1}{e^{\beta(\omega_{\mathbf{p}}-\mu)}+1}\right], \quad \text{(E.130)}$$

and since the boundary term vanishes, this simply reduces to

$$P = \frac{1}{3\pi^2}\int_0^\infty dp\,\frac{p^4}{\sqrt{p^2+m^2}}\frac{1}{e^{\beta(\omega_{\mathbf{p}}-\mu)}+1}. \quad \text{(E.131)}$$

We again see the appearance of the step function in the zero-temperature limit. The integral then becomes quite easy to solve, leading to

$$\begin{aligned} P &= \frac{1}{3\pi^2}\int_0^\infty dp\,\frac{p^4}{\sqrt{p^2+m^2}}\,\theta(E_F-\omega_{\mathbf{p}}) = \frac{1}{3\pi^2}\int_0^{p_F} dp\,\frac{p^4}{\sqrt{p^2+m^2}} \\ &= \frac{1}{24\pi^2}\left[p_F\sqrt{p_F^2+m^2}\left(2p_F^2-3m^2\right)+3m^4\ln\left(\frac{p_F+\sqrt{p_F^2+m^2}}{m}\right)\right] \\ &= \frac{1}{24\pi^2}\left[p_F\sqrt{p_F^2+m^2}\left(2p_F^2-3m^2\right)+3m^4\sinh^{-1}\left(\frac{p_F}{m}\right)\right]. \end{aligned} \quad \text{(E.132)}$$

The internal energy density ϵ can be calculated similarly. We first note that the average total energy in the system is given by

$$\langle E\rangle = \Big\langle \sum_{\mathbf{p}} E_{\mathbf{p}} n_{\mathbf{p}} \Big\rangle = \sum_{\mathbf{p}} \omega_{\mathbf{p}}\langle n_{\mathbf{p}}\rangle = 2V\int \frac{d^3p}{(2\pi)^3}\frac{\omega_{\mathbf{p}}}{e^{\beta(\omega_{\mathbf{p}}-\mu)}+1}. \quad \text{(E.133)}$$

Thus, in the zero-temperature limit, the energy density becomes

$$\begin{aligned} \epsilon = \frac{\langle E\rangle}{V} &= 2\int\frac{d^3p}{(2\pi)^3}\,\omega_{\mathbf{p}}\,\theta(E_F-\omega_{\mathbf{p}}) = \frac{1}{\pi^2}\int_0^{p_F} dp\,p^2\sqrt{p^2+m^2} \\ &= \frac{1}{8\pi^2}\left[p_F\sqrt{p_F^2+m^2}\left(2p_F^2+m^2\right)-m^4\ln\left(\frac{p_F+\sqrt{p_F^2+m^2}}{m}\right)\right] \\ &= \frac{1}{8\pi^2}\left[p_F\sqrt{p_F^2+m^2}\left(2p_F^2+m^2\right)-m^4\sinh^{-1}\left(\frac{p_F}{m}\right)\right]. \end{aligned} \quad \text{(E.134)}$$

The expression for the pressure, Eq. (E.132), together with the expression for the energy density, Eq. (E.134), form an equation of state for an ideal Fermi gas at zero temperature, parametrized in terms of the Fermi momentum.

Wolfram Mathematica Notebook

Quark Matter Equation of State

Massive S Quark

Setup

In[1]:=
```
L[Λ_] := 2 Log[Λ / ΛMS]
α[L_] := 4 Pi / (β0 L) * (1 - 2 β1 Log[L] / (β0^2 L))
ms[α_] := hatmS (α / Pi)^(4 / 9) (1 + 0.895062 α / Pi)
```

In[4]:=
```
ωS0[μS_, mS_] := -(μS (μS^2 - 5 mS^2/2) Sqrt[μS^2 - mS^2] + 3/2 mS^4 Log[(Sqrt[μS^2 - mS^2] + μS)/mS]) / (4 π^2)

ωS1[μS_, mS_, Λ_] := 1 / (2 Pi^3)
  (-2 (-mS^2 + μS^2)^2 + mS^2 (4 + 6 Log[Λ/mS]) (μS Sqrt[-mS^2 + μS^2] - mS^2 Log[(μS + Sqrt[-mS^2 + μS^2])/mS]) +
   3 (-μS Sqrt[-mS^2 + μS^2] + mS^2 Log[(μS + Sqrt[-mS^2 + μS^2])/mS])^2)
```

n_0:

In[6]:=
```
dωS0dmS[μS_, mS_] = D[ωS0[μS, mS], mS];
dωS1dmS[μS_, mS_, Λ_] = D[ωS1[μS, mS, Λ], mS];
dωS1dΛ[μS_, mS_, Λ_] = D[ωS1[μS, mS, Λ], Λ];
dmSdΛ[Λ_] = D[ms[α[L[Λ]]], Λ];
dαSdΛ[Λ_] = D[α[L[Λ]], Λ];
```

n_s^* (= n_s when the coupling and mass are not running):

In[11]:=
```
nSstar[μS_, mS_, Λ_] =
  Simplify[-D[ωS0[μS, mS], μS]] + Simplify[-D[ωS1[μS, mS, Λ], μS] α];
```

Output

n_s^*:

In[12]:=
```
nSstarOut = Collect[nSstar[μS, mS, Λ], α] /. Sqrt[μS^2 - mS^2] → uS
```

Out[12]=
$$\frac{\left(-mS^2+\mu S^2\right)^{3/2}}{\pi^2}-\frac{2\,uS\,\alpha\left(2\,mS^2+uS\,\mu S+3\,mS^2\,\text{Log}\left[\frac{\Lambda}{mS}\right]-3\,mS^2\,\text{Log}\left[\frac{uS+\mu S}{mS}\right]\right)}{\pi^3}$$

n_0 (The first five expressions are outputted in order. The last two end with ; :
and are therefore not outputted)

```
dωS0dmSOut = Simplify[dωS0dmS[μS, mS]] /. Sqrt[μS^2 - mS^2] → uS
dωS1dmSOut = Simplify[dωS1dmS[μS, mS, Λ]] /. Sqrt[μS^2 - mS^2] → uS
dmSdΛOut = Simplify[dmSdΛ[Λ]] /. Sqrt[μS^2 - mS^2] → uS
dωS1dΛOut = Simplify[dωS1dΛ[μS, mS, Λ]] /. Sqrt[μS^2 - mS^2] → uS
dαSdΛOut = Simplify[dαSdΛ[Λ]] /. Sqrt[μS^2 - mS^2] → uS
ωS0Out = ωS0[μS, mS] /. Sqrt[μS^2 - mS^2] → uS;
ωS1Out = ωS1[μS, mS, Λ] /. Sqrt[μS^2 - mS^2] → uS;
```

Out[14]=
$$\frac{3\,mS\left(-mS^2\,\mu S+\mu S^3+\frac{\left(mS^4-mS^2\,\mu S\,(uS+\mu S)\right)\,\text{Log}\left[\frac{uS+\mu S}{mS}\right]}{uS+\mu S}\right)}{2\,\pi^2\,\sqrt{-mS^2+\mu S^2}}$$

Out[15]=
$$\frac{1}{\pi^3\,(uS+\mu S)\,\sqrt{-mS^2+\mu S^2}}$$

Out[16]=
$$mS\left(\left(mS^2-\mu S^2\right)\left(4\,mS^2-5\,\mu S\,(uS+\mu S)\right)+\left(5\,mS^4+mS^2\,\mu S\,(uS+\mu S)-6\,\mu S^3\,(uS+\mu S)\right)\text{Log}\left[\frac{uS+\mu S}{mS}\right]+6\,mS^2\left(-mS^2+\mu S\,(uS+\mu S)\right)\text{Log}\left[\frac{uS+\mu S}{mS}\right]^2-6\,\text{Log}\left[\frac{\Lambda}{mS}\right]\left(\mu S\,(uS+\mu S)\left(mS^2-\mu S^2\right)+\left(-2\,mS^4+2\,mS^2\,\mu S\,(uS+\mu S)\right)\text{Log}\left[\frac{uS+\mu S}{mS}\right]\right)\right)$$

Out[17]=
$$\left(\text{hatmS}\left(-0.604796\,\beta0^5\,\text{Log}\left[\frac{\Lambda}{\Lambda MS}\right]^3+\beta0^2\,\beta1\,\text{Log}\left[\frac{\Lambda}{\Lambda MS}\right]\left(3.79817+10.5559\,\text{Log}\left[\text{Log}\left[\frac{\Lambda}{\Lambda MS}\right]\right]\right)+\beta0^3\,\text{Log}\left[\frac{\Lambda}{\Lambda MS}\right]^2\left(-3.51864\,\beta0+0.233629\,\beta1+1.20959\,\beta1\,\text{Log}\left[\text{Log}\left[\frac{\Lambda}{\Lambda MS}\right]\right]\right)+\beta1^2\left(-0.942147-6.2371\,\text{Log}\left[\text{Log}\left[\frac{\Lambda}{\Lambda MS}\right]\right]-7.03728\,\text{Log}\left[\text{Log}\left[\frac{\Lambda}{\Lambda MS}\right]\right]^2\right)\right)\Big/\left(\beta0^6\,\Lambda\,\text{Log}\left[\frac{\Lambda}{\Lambda MS}\right]^5\left(\frac{\beta0^2\,\text{Log}\left[\frac{\Lambda}{\Lambda MS}\right]-\beta1\,\text{Log}\left[2\,\text{Log}\left[\frac{\Lambda}{\Lambda MS}\right]\right]}{\beta0^3\,\text{Log}\left[\frac{\Lambda}{\Lambda MS}\right]^2}\right)^{5/9}\right)$$

Out[18]=
$$\frac{3\,mS^2\,uS\,\mu S-3\,mS^4\,\text{Log}\left[\frac{uS+\mu S}{mS}\right]}{\pi^3\,\Lambda}$$

Out[18]=
$$-\frac{2\,\pi\left(\beta1+\beta0^2\,\text{Log}\left[\frac{\Lambda}{\Lambda MS}\right]-2\,\beta1\,\text{Log}\left[2\,\text{Log}\left[\frac{\Lambda}{\Lambda MS}\right]\right]\right)}{\beta0^3\,\Lambda\,\text{Log}\left[\frac{\Lambda}{\Lambda MS}\right]^3}$$

Export (Expressions to .txt files)

G | Python Code

This appendix contains all the python code used to solve the numerical problems in this thesis. Notice that the code listings have automatic line breaks generated by LaTeX to fit the page. These line breaks are marked with an arrow ↪. The code is organized as such: each problem in this thesis has its own Python module with a function that gets called from main, and the settings for each problem are contained in the beginning of those functions. The module "running_combined.py" covers both Section 4.7 and 4.8. It combines the results of "running_massless_SM.py" and "running_massive_SM.py" into the same figures. Lastly, the module named starlib contains a lot of useful and shared functions and constants, e.g., an implementation of the Runge–Kutta 4 method and the structure equations.

G.1 Main

Module name: main.py

```
import incompressible_fluid
import linear_eos
import polytropic_eos
import full_ideal_fermi
import constant_massless_SM
import running_massless_SM
import running_massive_SM
import running_combined
import matplotlib.pyplot as plt

plt.rc('text', usetex=True)
plt.rc('font', family='serif')
plt.rcParams.update({'font.size': 13}) #Size guide: Three figs side by side:
↪  16, Two figs: 11, One fig: 13

KEYBOARD_INPUT = False

TASK = (
    'incompressible_fluid',
    'linear_eos',
    'polytropic_eos',
    'full_ideal_fermi',
    'constant_massless_quarks_first_order',
    'running_massless_quarks_first_order',
    'running_massive_s_quark_first_order',
    'running_combined'
)[int(input('Task number: ')) if KEYBOARD_INPUT else 7]  # <--- CHANGE TASK
↪  MANUALLY HERE
```

```
27
28
29  def main():
30
31      if TASK == 'incompressible_fluid':
32          incompressible_fluid.incompressible_fluid()
33      elif TASK == 'linear_eos':
34          linear_eos.linear_eos()
35      elif TASK == 'polytropic_eos':
36          polytropic_eos.polytropic_eos()
37      elif TASK == 'full_ideal_fermi':
38          full_ideal_fermi.full_ideal_fermi()
39      elif TASK == 'constant_massless_quarks_first_order':
40          constant_massless_SM.massless_strange_matter_constant_coupling()
41      elif TASK == 'running_massless_quarks_first_order':
42          running_massless_SM.massless_strange_matter_running_coupling()
43      elif TASK == 'running_massive_s_quark_first_order':
44          running_massive_SM.massive_strange_matter_running_coupling_and_mass()
45      elif TASK == 'running_combined':
46          running_combined.running_combined()
47
48
49  if __name__ == '__main__':
50      main()
```

G.2 Uniform Energy Density

Module name: incompressible_fluid.py

```
1   import numpy as np
2   import matplotlib.pyplot as plt
3
4
5   X_MIN = 0
6   X_MAX = 1
7   N = 1000
8   ALPHA1 = 1.15
9   ALPHA2 = 1.7
10  ALPHA3 = 60.0
11
12  FILENAME = 'incompressible_plot'
13  SAVE_FIG = True     # if set to true, plots are saved to file but not shown
14
15
16  def P_over_P_c_GR(x_list, alpha):
17      return ((1-3*np.sqrt(1-1/alpha)) / (np.sqrt(1-1/alpha)-1)) * \
18             ( ( np.sqrt(1-1/alpha) - np.sqrt(1-x_list**2 / alpha) ) / (
               ↪  np.sqrt(1-x_list**2 / alpha) - 3*np.sqrt(1-1/alpha) ) )
19
20
21  def P_over_P_c_Newton(x_list, alpha):
```

```
22      return 1/(4*alpha) * ((1-3*np.sqrt(1-1/alpha)) / (np.sqrt(1-1/alpha)-1)) *
        ↪  (1-x_list**2)
23
24
25  def incompressible_fluid():
26      plt.rcParams.update({'font.size': 16})
27
28      # ---------- Generating Data ----------
29
30      x_list = np.linspace(X_MIN, X_MAX, N)
31      y_list_GR_ax1 = P_over_P_c_GR(x_list, ALPHA1)
32      y_list_Newton_ax1 = P_over_P_c_Newton(x_list, ALPHA1)
33      y_list_GR_ax2 = P_over_P_c_GR(x_list, ALPHA2)
34      y_list_Newton_ax2 = P_over_P_c_Newton(x_list, ALPHA2)
35      y_list_GR_ax3 = P_over_P_c_GR(x_list, ALPHA3)
36      y_list_Newton_ax3 = P_over_P_c_Newton(x_list, ALPHA3)
37
38
39
40      # ---------- Plotting ----------
41
42      fig = plt.figure(figsize=(12,4))
43
44      ax = fig.add_subplot(131)
45      ax.plot(x_list, y_list_GR_ax1, label='General relativity')
46      ax.plot(x_list, y_list_Newton_ax1, label='Newtonian gravity')
47      ax.set_xlabel(r'$r/R$')
48      ax.set_ylabel(r'$P/P_c$', rotation=0)
49      ax.set_title(r'(a) $R=' + str(ALPHA1) + r'R_S$')
50      ax.yaxis.set_label_coords(-0.07, 1.01)
51      ax.legend(bbox_to_anchor=(1, 1), loc='upper right', borderaxespad=0.3)
52      ax.set_xticks(np.arange(0, 1.1, .2))
53      ax.set_yticks(np.arange(0, 1.1, .2))
54
55
56      ax = fig.add_subplot(132)
57      ax.plot(x_list, y_list_GR_ax2, label='General relativity')
58      ax.plot(x_list, y_list_Newton_ax2, label='Newtonian gravity')
59      ax.set_xlabel(r'$r/R$')
60      ax.set_ylabel(r'$P/P_c$', rotation=0)
61      ax.set_title(r'(b) $R=' + str(ALPHA2) + r'R_S$')
62      ax.yaxis.set_label_coords(-0.07, 1.01)
63      ax.set_xticks(np.arange(0, 1.1, .2))
64      ax.set_yticks(np.arange(0, 1.1, .2))
65
66      ax = fig.add_subplot(133)
67      ax.plot(x_list, y_list_GR_ax3, label='General relativity')
68      ax.plot(x_list, y_list_Newton_ax3, label='Newtonian gravity')
69      ax.set_xlabel(r'$r/R$')
70      ax.set_ylabel(r'$P/P_c$', rotation=0)
71      ax.set_title(r'(c) $R=' + str(ALPHA3) + r'R_S$')
72      ax.yaxis.set_label_coords(-0.07, 1.01)
73      ax.set_xticks(np.arange(0, 1.1, .2))
74      ax.set_yticks(np.arange(0, 1.1, .2))
75
```

```
    fig.tight_layout()


    if SAVE_FIG:
        plt.savefig(FILENAME + '.pdf')
    else:
        plt.show()
```

G.3 Linear Equation of State

Module name: linear_eos.py

```
import numpy as np
import matplotlib.pyplot as plt
import scipy.constants as sc
import starlib as sl

# P = pressure, m = mass, eps = energy_density, a = constant.
# _bar denotes nondimentionalized quantity.

SAVE_FIG = True     # if set to true, plots are saved to file but not shown
FILENAME_P_PROFILE = "linear_P_and_M_profile_plot"

def eps_bar(P_bar, gamma):
    return 1/gamma * P_bar


def P_bar(eps_bar, gamma):
    return gamma * eps_bar


# returns array of m coefficients where 0th entry is c_3, 1th entry
# is c_5 and so on up to the (m-1)th entry which is c_{2n+1}
def get_coefficients_GR(NUMBER_OF_COEFF, a, gamma, eps_bar_c):
    coeff_list = np.zeros(NUMBER_OF_COEFF)
    coeff_list[0] = eps_bar_c/3

    term_k = lambda k, n: (2*n-2*k+1)*(2*k*gamma*(gamma+3) - 4*n*gamma +
    ↪  gamma**2 + 6*gamma + 1)*coeff_list[k-1]*coeff_list[n-k-1]

    for n in range(2, NUMBER_OF_COEFF+1):
        sum = 0
        for k in range(1, n):
            sum += term_k(k, n)

        coeff_list[n-1] = -a/(2*(n-1)*(2*n+1)*gamma) * sum

    return coeff_list


def get_coefficients_newton(NUMBER_OF_COEFF, a, gamma, eps_bar_c):
```

```
    coeff_list = np.zeros(NUMBER_OF_COEFF)
    coeff_list[0] = eps_bar_c/3

    term_k = lambda k, n: (2*n-2*k+1)*coeff_list[k-1]*coeff_list[n-k-1]

    for n in range(2, NUMBER_OF_COEFF+1):
        sum = 0
        for k in range(1, n):
            sum += term_k(k, n)

        coeff_list[n-1] = -a/(2*(n-1)*(2*n+1)*gamma) * sum

    return coeff_list


def eps_bar_analytic_profile(r_values, coefficients):
    NUMBER_OF_COEFF = len(coefficients)
    energy_density_values = np.zeros(len(r_values))
    for j in range(1, NUMBER_OF_COEFF+1):
        energy_density_values += (2*j+1) * coefficients[j-1] *
        ↪  r_values**(2*j-2)
    return energy_density_values


def m_bar_analytic_profile(r_values, coefficients):
    NUMBER_OF_COEFF = len(coefficients)
    m_bar_values = np.zeros(len(r_values))
    for j in range(1, NUMBER_OF_COEFF+1):
        m_bar_values += coefficients[j-1] * r_values**(2*j+1)
    return m_bar_values


def singular_solution(r_values, a, gamma):
    return 2*gamma**2 / (a * (gamma**2 + 6*gamma + 1) * r_values**2)


def analytic_mass_and_pressure_profile(N, P_bar_c, r_bar_max, a,
↪  NUMBER_OF_COEFF, gamma):
    r_bar_list = np.linspace(0, r_bar_max, N)
    eps_bar_c = eps_bar(P_bar_c, gamma)
    coefficients_GR = get_coefficients_GR(NUMBER_OF_COEFF, a, gamma, eps_bar_c)
    coefficients_newton = get_coefficients_newton(NUMBER_OF_COEFF, a, gamma,
    ↪  eps_bar_c)
    eps_bar_array_GR = eps_bar_analytic_profile(r_bar_list, coefficients_GR)
    eps_bar_array_newton = eps_bar_analytic_profile(r_bar_list,
    ↪  coefficients_newton)
    P_bar_array_GR = gamma * eps_bar_array_GR
    P_bar_array_newton = gamma * eps_bar_array_newton
    m_bar_array_GR = m_bar_analytic_profile(r_bar_list, coefficients_GR)
    m_bar_array_newton = m_bar_analytic_profile(r_bar_list,
    ↪  coefficients_newton)

    return {'P_bar array GR': P_bar_array_GR, 'P_bar array Newton':
    ↪  P_bar_array_newton, 'm_bar array GR': m_bar_array_GR, 'm_bar array
    ↪  Newton': m_bar_array_newton, 'r_bar list': r_bar_list}
```

```
87
88
89  def plot_mass_and_pressure_profiles(numerical_data_dict, analytic_data_dict,
    ↪  P_bar_c, a, gamma):
90      y_list_TOV = numerical_data_dict['P_bar and M_bar values TOV']
91      y_list_newton = numerical_data_dict['P_bar and M_bar values Newton']
92      r_bar_list = numerical_data_dict['r_bar values']
93      radius_index_TOV = numerical_data_dict['Radius Index TOV']
94      radius_index_newton = numerical_data_dict['Radius Index Newton']
95
96      P_bar_array_GR = analytic_data_dict['P_bar array GR']
97      P_bar_array_newton = analytic_data_dict['P_bar array Newton']
98      m_bar_array_GR = analytic_data_dict['m_bar array GR']
99      m_bar_array_newton = analytic_data_dict['m_bar array Newton']
100
101     print('TOV: R=', r_bar_list[radius_index_TOV], '\tM=',
        ↪  y_list_TOV[1][radius_index_TOV])
102     print('Newton: R=', r_bar_list[radius_index_newton], '\tM=',
        ↪  y_list_newton[1][radius_index_newton])
103
104     fig = plt.figure(figsize=(7, 3))
105
106     ax = fig.add_subplot(121)
107     ax.plot(r_bar_list, y_list_TOV[0, :] / y_list_TOV[0, 0], label='General
        ↪  relativity')
108     ax.plot(r_bar_list, y_list_newton[0, :] / y_list_newton[0, 0],
        ↪  label='Newtonian gravity')
109     ax.plot(r_bar_list, P_bar_array_GR / P_bar_c, linestyle='--', color='k',
        ↪  linewidth=0.7)
110     ax.plot(r_bar_list, P_bar_array_newton / P_bar_c, linestyle='--',
        ↪  color='k', linewidth=0.7)
111     ax.plot(r_bar_list[1:], singular_solution(r_bar_list[1:], a, gamma) /
        ↪  P_bar_c, label='Singular TOV solution')
112     ax.set_xlabel(r'$r$ [km]')
113     ax.set_ylabel(r'$P(r)/P_c$', rotation=0)
114     ax.set_ylim(top=1.05, bottom=0)
115     ax.yaxis.set_label_coords(-0.05, 1.03)
116     ax.legend(bbox_to_anchor=(1, 1), loc='upper right', borderaxespad=0.3,
        ↪  fontsize=9)
117     ax.set_xticks(np.arange(0, 31, 5))
118     ax.set_xticks(np.arange(0, 31, 2.5), minor=True)
119     ax.set_yticks(np.arange(0, 1.01, 0.2))
120     ax.set_yticks(np.arange(0, 1.01, .1), minor=True)
121
122     ax = fig.add_subplot(122)
123     ax.plot(r_bar_list, y_list_TOV[1, :], label='General relativity')
124     ax.plot(r_bar_list, y_list_newton[1, :], label='Newtonian gravity')
125     ax.plot(r_bar_list, m_bar_array_GR, linestyle='--', color='k',
        ↪  linewidth=0.7)
126     ax.plot(r_bar_list, m_bar_array_newton, linestyle='--', color='k',
        ↪  linewidth=0.7)
127     ax.set_xlabel(r'$r$ [km]')
128     ax.set_ylabel(r'$m(r)/M_\odot$', rotation=0)
129     ax.set_ylim(top=6.3, bottom=0)
130     ax.yaxis.set_label_coords(-0.05, 1.03)
```

```
131     ax.set_xticks(np.arange(0, 31, 5))
132     ax.set_xticks(np.arange(0, 31, 2.5), minor=True)
133     ax.set_yticks(np.arange(0, 6.3, 1))
134     ax.set_yticks(np.arange(0, 6.3, .5), minor=True)
135 
136     fig.tight_layout()
137 
138     if SAVE_FIG:
139         plt.savefig(FILENAME_P_PROFILE + '.pdf')
140 
141 
142 def linear_eos():
143 
144     # -------------SETTINGS---------------------
145     N = 2000
146     choose_pressure = True  # Can specify either P_c or n_c
147     P_c = 3.59946e+34    # Joules/m^3
148     n_c = sl.n_saturation * 10
149 
150     gamma = 1/3
151     r_0 = 1000  # meters
152     m_0 = sl.SOLAR_MASS  # in kg
153     r_bar_max = 30
154 
155     NUMBER_OF_COEFF = 20
156     # ------------------------------------------
157     sl.set_parent(__name__)
158 
159     a = sc.G * m_0 / (r_0 * sc.c ** 2)
160     eps_0 = m_0 * sc.c ** 2 / (4 * np.pi * r_0 ** 3)
161 
162     print('eps_0 =', eps_0, '\ta =', a)
163 
164     if not choose_pressure:
165         eps_bar_c = 3*sc.hbar*sc.c/4 * (3*np.pi**2)**(1/3) * n_c**(4/3) / eps_0
166         P_bar_c = P_bar(eps_bar_c, gamma)
167         P_c = P_bar_c * eps_0
168     else:
169         P_bar_c = P_c/eps_0
170 
171     n_c_fermi = 1/(3*np.pi**2)**(1/4) * (4*P_c/(sc.hbar * sc.c))**(3/4)
172     print('P_C =', P_c, '\tNumber density UR Fermi gas =', n_c_fermi, '=',
    ↪  n_c_fermi/sl.n_saturation, 'n_sat')
173 
174     numerical_M_and_P_data_dict = sl.mass_and_pressure_profile(N, P_bar_c,
    ↪  r_bar_max, a, gamma)
175     analytic_M_and_P_data_dict = analytic_mass_and_pressure_profile(N, P_bar_c,
    ↪  r_bar_max, a, NUMBER_OF_COEFF, gamma)
176 
177     plot_mass_and_pressure_profiles(numerical_M_and_P_data_dict,
    ↪  analytic_M_and_P_data_dict, P_bar_c, a, gamma)
178 
179     if not SAVE_FIG:
180         plt.show()
```

G.4 Polytropes

Module name: polytropic_eos.py

```
import numpy as np
import matplotlib.pyplot as plt
import scipy.constants as sc
import starlib as sl
import time

SAVE_FIG = True    # if set to true, plots are saved to file but not shown
FILENAME_PM_PROFILE = "polytropic_P_and_M_profile_plot"
FILENAME_MR_RELATION = "polytropic_mass_radius_relation_plot"
FILENAME_PM_PROFILE_OF_MAX = "polytropic_P_and_M_profile_of_max_plot"

# P = pressure, m = mass, eps = energy_density, a = constant


def eps_bar(P_bar, K_bar, n):
    return (P_bar / K_bar)**(n/(n+1))


def P_bar(eps_bar, K_bar, n):
    return K_bar*eps_bar**(1+1/n)


def polytropic_eos():
    # -------------SETTINGS---------------------
    # You can either calculate the mass-radius relation
    # (which also gives the pressure and mass profile of the
    # maximum mass star) OR
    # calculate a single pressure and mass profile from either a
    # given P_c (if choose_pressure=true) or a given n_c.
    N = 5000    # number of steps used to calc a single pressure profile
    calculate_M_R_relation = True
    choose_pressure = True

    n_c = 1.0e10
    P_c = 3.59946e+34    # Joules/m^3

    m_particles = sc.neutron_mass
    n = 3/2
    r_0 = 1000  # meters
    m_0 = sl.SOLAR_MASS  # in kg
    r_bar_max_pressure_profile = 13  # should be larger than the radius of the
    # star whose P profile is to be calculated. But increasing this decreases
    ↪ resolution

    r_bar_max = 25  # should be larger than the radius of the star with largest
    ↪ radius,
    mass_radius_relation_points = 500
    n_c_max = sl.n_saturation * 1000
```

```
47      n_c_min = sl.n_saturation * 0.15
48
49      # Plotting settings
50      r_bar_limit_P_profile = 13
51      R_limit_MR_relation = 25
52      # ----------------------------------------
53      sl.set_parent(__name__)  # so that starlib can call eps_bar
54      start_time = time.time()
55
56      a = sc.G * m_0 / (r_0 * sc.c ** 2)
57      eps_0 = m_0 * sc.c ** 2 / (4 * np.pi * r_0 ** 3)
58      K = sc.hbar ** 2 / (15 * np.pi ** 2 * m_particles) * (3 * np.pi ** 2 /
        ↪  (m_particles * sc.c ** 2)) ** (5 / 3)
59      K_bar = K * eps_0 ** (1 / n)
60
61      print('eps_0=', eps_0, '\ta=', a, '\tK_bar=', K_bar, '\tK=', K)
62
63      if calculate_M_R_relation:
64          eps_bar_c_max = m_particles * n_c_max * sc.c ** 2 / eps_0
65          eps_bar_c_min = m_particles * n_c_min * sc.c ** 2 / eps_0
66          P_bar_c_max = P_bar(eps_bar_c_max, K_bar, n)
67          P_bar_c_min = P_bar(eps_bar_c_min, K_bar, n)
68          MR_relation_data_dict = sl.mass_radius_relation(N, P_bar_c_min,
            ↪  P_bar_c_max, mass_radius_relation_points, a, r_bar_max, K_bar, n)
69
70          # Calculating the mass and pressure profile of the maximum mass star
71          P_bar_c_of_max = MR_relation_data_dict['Pressure Of Max']
72          M_and_P_data_dict = sl.mass_and_pressure_profile(N, P_bar_c_of_max,
            ↪  r_bar_max, a, K_bar, n)
73
74          # ---------- Printing Specifics ----------
75          n_c_fermi = (15 * np.pi ** 2 * m_particles / sc.hbar ** 2) ** (3 / 5) /
            ↪  (3 * np.pi ** 2) * (P_bar_c_of_max * eps_0) ** (3 / 5)
76          eps_c = eps_0 * eps_bar(P_bar_c_of_max, K_bar, n)
77          speed_of_sound_max = np.sqrt((n + 1) / n * K * eps_c ** (1 / n))
78          print('Number density NR Fermi gas =', n_c_fermi, '=', n_c_fermi /
            ↪  sl.n_saturation, 'n_sat', '\teps_c =', eps_c, '\tSpeed of sound =',
            ↪  speed_of_sound_max)
79          # ----------------------------------------
80
81          sl.plot_mass_radius_relation(MR_relation_data_dict,
            ↪  R_limit_MR_relation, filename=FILENAME_MR_RELATION)
82          sl.plot_mass_and_pressure_profile(M_and_P_data_dict, eps_0,
            ↪  P_bar_c_of_max, r_bar_limit_P_profile,
            ↪  filename=FILENAME_PM_PROFILE_OF_MAX)
83      else:
84          if not choose_pressure:
85              eps_bar_c = m_particles * n_c * sc.c ** 2 / eps_0
86              P_bar_c = P_bar(eps_bar_c, K_bar, n)
87          else:
88              P_bar_c = P_c/eps_0
89
90              # ---------- Printing Specifics ----------
91              n_c_fermi = (15*np.pi**2*m_particles/sc.hbar**2)**(3/5) /
                ↪  (3*np.pi**2) * P_c**(3/5)
```

```
            eps_c = eps_0 * eps_bar(P_bar_c, K_bar, n)
            speed_of_sound_max = np.sqrt((n+1)/n * K * eps_c**(1/n))
            print('Number density NR Fermi gas =', n_c_fermi, '=',
            ↪  n_c_fermi/sl.n_saturation, 'n_sat', '\teps_c =', eps_c,
            ↪  '\tSpeed of sound =', speed_of_sound_max)
            #----------------------------------------

        M_and_P_data_dict = sl.mass_and_pressure_profile(N, P_bar_c,
        ↪  r_bar_max_pressure_profile, a, K_bar, n)
        sl.plot_mass_and_pressure_profile(M_and_P_data_dict, eps_0, P_bar_c,
        ↪  r_bar_limit_P_profile, filename=FILENAME_PM_PROFILE)

    sl.print_execution_time(start_time, time.time())

    if not SAVE_FIG:
        plt.show()
```

G.5 Ideal Fermi Gas

Module name: full_ideal_fermi.py

```
import numpy as np
import matplotlib.pyplot as plt
import scipy.constants as sc
import scipy.optimize
import starlib as sl
import time


SAVE_FIG = True    # if set to true, plots are saved to file but not shown
FILENAME_PM_PROFILE = "ideal_fermi_P_and_M_profiles_plot"
FILENAME_MR_RELATION = "ideal_fermi_MR_relation_plot"
FILENAME_PM_PROFILE_OF_MAX = "ideal_fermi_P_and_M_profiles_of_max_plot"

# P = pressure, m = mass, eps = energy_density, a = constant


def P_bar_of_xF(x_F, K_bar_P):
    return K_bar_P * (x_F*np.sqrt(x_F**2 + 1)*(2*x_F**2 - 3) +
    ↪  3*np.arcsinh(x_F))


def eps_bar_of_xF(x_F, K_bar_eps):
    return K_bar_eps * (x_F * np.sqrt(x_F**2 + 1)*(2*x_F**2 + 1) -
    ↪  np.arcsinh(x_F))


def eps_bar(P_bar, K_bar_P, K_bar_eps):
    x_F = scipy.optimize.brentq(lambda x_F: P_bar_of_xF(x_F, K_bar_P) - P_bar,
    ↪  0, 100)
    return eps_bar_of_xF(x_F, K_bar_eps)
```

```
28
29
30  def P_bar(eps_bar, K_bar_P, K_bar_eps):
31      x_F = scipy.optimize.brentq(lambda x_F: eps_bar_of_xF(x_F, K_bar_eps) -
        ↪  eps_bar, 0, 100)
32      return P_bar_of_xF(x_F, K_bar_P)
33
34
35  def full_ideal_fermi():
36
37      # -------------SETTINGS---------------------
38      # You can either calculate the mass-radius relation
39      # (which also gives the pressure and mass profile of the
40      # maximum mass star) OR
41      # calculate a single pressure and mass profile from either a
42      # given P_c (if choose_pressure=true) or a given n_c.
43      N = 4000    # number of steps used to calc a single pressure profile
44      calculate_M_R_relation = True
45      choose_pressure = True
46
47      n_c = sl.n_saturation * 0.5
48      P_c = 3.59946e+34    # Joules/m^3
49
50      m_particles = sc.neutron_mass
51      r_0 = 1000  # meters
52      m_0 = sl.SOLAR_MASS  # in kg
53      r_bar_max_pressure_profile = 13 # should be larger than the radius of the
54      # star whose P profile is to be calculated. But increasing this decreases
        ↪  resolution
55
56      # MR-relation settings
57      r_bar_max = 25  # should be larger than the radius of the star with largest
        ↪  radius,
58      mass_radius_relation_points = 400
59      n_c_max = sl.n_saturation * 100
60      n_c_min = sl.n_saturation * 0.2
61
62      # Plotting settings
63      r_bar_limit_P_profile = 13
64      R_limit_MR_relation = 25
65      # ------------------------------------------
66      sl.set_parent(__name__)  # so that starlib can call eps_bar
67      start_time = time.time()
68
69      a = sc.G * m_0 / (r_0 * sc.c ** 2)
70      eps_0 = m_0 * sc.c ** 2 / (4 * np.pi * r_0 ** 3)
71      K_bar_P = m_particles ** 4 * sc.c ** 5 / (24 * np.pi ** 2 * sc.hbar ** 3) /
        ↪  eps_0
72      K_bar_eps = 3 * K_bar_P
73
74      print('eps_0=', eps_0, '\ta=', a, '\tK_bar_P=', K_bar_P)
75
76      if calculate_M_R_relation:
77          x_F_c_max = sc.hbar / (m_particles * sc.c) * (3 * np.pi ** 2 * n_c_max)
            ↪  ** (1 / 3)
```

```
        x_F_c_min = sc.hbar / (m_particles * sc.c) * (3 * np.pi ** 2 * n_c_min)
        ↪  ** (1 / 3)
        P_bar_c_max = P_bar_of_xF(x_F_c_max, K_bar_P)
        P_bar_c_min = P_bar_of_xF(x_F_c_min, K_bar_P)
        MR_relation_data_dict = sl.mass_radius_relation(N, P_bar_c_min,
        ↪  P_bar_c_max, mass_radius_relation_points, a, r_bar_max, K_bar_P,
        ↪  K_bar_eps)

        # Calculating the mass and pressure profile of the maximum mass star
        P_bar_c_of_max = MR_relation_data_dict['Pressure Of Max']
        M_and_P_data_dict = sl.mass_and_pressure_profile(N, P_bar_c_of_max,
        ↪  r_bar_max, a, K_bar_P, K_bar_eps)

        sl.plot_mass_radius_relation(MR_relation_data_dict,
        ↪  R_limit_MR_relation, filename=FILENAME_MR_RELATION)
        sl.plot_mass_and_pressure_profile(M_and_P_data_dict, eps_0,
        ↪  P_bar_c_of_max, r_bar_limit_P_profile,
        ↪  filename=FILENAME_PM_PROFILE_OF_MAX)
    else:
        if not choose_pressure:
            x_F_c = sc.hbar / (m_particles * sc.c) * (3 * np.pi ** 2 * n_c) **
            ↪  (1 / 3)
            P_bar_c = P_bar_of_xF(x_F_c, K_bar_P)
        else:
            P_bar_c = P_c / eps_0
            x_F_c = scipy.optimize.brentq(lambda x_F: P_bar_of_xF(x_F, K_bar_P)
            ↪  - P_bar_c, 0, 100)
            n_c = (m_particles * sc.c)**3 * x_F_c**3 / (3*np.pi**2 *
            ↪  sc.hbar**3)

        print('Number density Full Fermi gas =', n_c, '=', n_c /
        ↪  sl.n_saturation, 'n_sat')

        M_and_P_data_dict = sl.mass_and_pressure_profile(N, P_bar_c,
        ↪  r_bar_max_pressure_profile, a, K_bar_P, K_bar_eps)
        sl.plot_mass_and_pressure_profile(M_and_P_data_dict, eps_0, P_bar_c,
        ↪  r_bar_limit_P_profile, filename=FILENAME_PM_PROFILE)

    sl.print_execution_time(start_time, time.time())

    if not SAVE_FIG:
        plt.show()
```

G.6 Massless Quarks with Fixed Coupling

Module name: constant_massless.py

```
import numpy as np
import matplotlib.pyplot as plt
import scipy.constants as sc
import starlib as sl
```

```
5  import time
6
7  # ------------------------------------------------------------#
8  # Massless Quarks _ First Order Corrections _ Constant Alpha #
9  # ------------------------------------------------------------#
10
11 # All quark masses are zero. This implies no electrons.
12
13 # P = pressure, m = mass, eps = energy_density, a and eps_0 are
14 # nondimensionalization constants. B = bag constant. B_bar = B/eps_0
15
16 SAVE_FIG = True  # if set to true, plots are saved to file but not shown
17 FILENAME_PM_PROFILE = "constant_massless_SM_P_and_M_profiles_plot"
18 FILENAME_MR_RELATION = "constant_massless_SM_MR_relation_plot"
19
20
21 def eps_bar(P_bar, B_bar):
22     return 3*P_bar + 4*B_bar
23
24
25 def massless_strange_matter_constant_coupling():
26
27     # -------------SETTINGS---------------------
28     # You can either calculate the mass-radius relations for
29     # several different values of B
30     # OR
31     # calculate a single pressure and mass profile from a
32     # given P_c and B.
33     N = 5000  # number of steps used to calc a single pressure profile
34     calculate_M_R_relation = True
35
36     r_0 = 1000  # meters
37     m_0 = sl.SOLAR_MASS  # in kg
38
39     B_to_the_one_fourth = 147  # If calc MR relation is false. Plots only one
       ↪  pressure profile
40     B_to_the_one_fourths = np.array([145, 147, 155, 164])  # in MeV
41
42     P_c = 3.7251e+34  # Joules/m^3
43     r_bar_max_pressure_profile = 11  # should be larger than the radius of the
44     # star whose P profile is to be calculated. But increasing this decreases
       ↪  resolution
45
46     # MR-relation settings
47     r_bar_max = 12  # should be larger than the radius of the star with largest
       ↪  radius,
48     mass_radius_relation_points = 500
49     P_c_max = 1e+35
50     P_c_min = 1e+32
51
52     # Plotting settings
53     r_bar_limit_P_profile = 12
54     R_limit_MR_relation = 13
55     M_limit_MR_relation = 2.5
56     # ------------------------------------------
```

```
    sl.set_parent(__name__)  # so that starlib can call eps_bar
    start_time = time.time()

    a = sc.G * m_0 / (r_0 * sc.c ** 2)
    eps_0 = m_0 * sc.c ** 2 / (4 * np.pi * r_0 ** 3)

    if calculate_M_R_relation:
        B_list = B_to_the_one_fourths ** 4
        B_list_SI = sl.MeV4_to_SI(B_list)
        B_bar_list = B_list_SI / eps_0

        data_dicts = [0 for i in range(len(B_to_the_one_fourths))]

        for i in range(len(B_bar_list)):
            B_bar = B_bar_list[i]

            P_bar_c_max = P_c_max / eps_0
            P_bar_c_min = P_c_min / eps_0
            data_dict = sl.mass_radius_relation(N, P_bar_c_min, P_bar_c_max,
            ↪  mass_radius_relation_points, a, r_bar_max, B_bar, mode='GR')
            B_to_the_one_fourth = sl.SI_to_MeV4(B_bar * eps_0)**(1/4)
            data_dict['Label'] = r'$B^{1/4} =$ ' +
            ↪  '{:00.0f}'.format(B_to_the_one_fourth) + ' MeV'
            data_dicts[i] = data_dict

        sl.plot_mass_radius_relation_multiple(data_dicts, R_limit_MR_relation,
        ↪  filename=FILENAME_MR_RELATION, M_limit=M_limit_MR_relation,
        ↪  plot_line=True)
    else:
        B = B_to_the_one_fourth**4
        B_bar = sl.MeV4_to_SI(B) / eps_0
        M_and_P_profile_filename = FILENAME_PM_PROFILE
        P_bar_c = P_c / eps_0

        M_and_P_data_dict = sl.mass_and_pressure_profile(N, P_bar_c,
        ↪  r_bar_max_pressure_profile, a, B_bar, mode='GR')
        sl.plot_mass_and_pressure_profile(M_and_P_data_dict, eps_0, P_bar_c,
        ↪  r_bar_limit_P_profile, filename=M_and_P_profile_filename,
        ↪  mode='GR', show_legend=False)

    sl.print_execution_time(start_time, time.time())

    if not SAVE_FIG:
        plt.show()
```

G.7 Running Mass and Coupling

Module name: running_combined.py

```
import numpy as np
import matplotlib.pyplot as plt
```

```
from matplotlib.ticker import AutoMinorLocator
import matplotlib.ticker as ticker
import scipy.optimize
import scipy.constants as sc
import starlib as sl
import running_massless_SM as massless
import running_massive_SM as massive
import time

#-----------------------------------------------------------#
#
#   This module compares the two cases massless quarks
#   and running strange quark mass. The MR relations
#   are plotted together. So is P, eps and alpha_s
#   as functions of mu
#
#-----------------------------------------------------------#

SAVE_FIG = True
FILENAME_MR = 'MR_relations_combined_plot'
FILENAME_P_EPS_ALPHA = 'P_eps_alpha_plot'


# Pressure of 3-component Fermi gas
def P_Fermi(mu):
    return 3 * mu**4 /(4*np.pi**2)


def eps_Fermi(mu):
    return 3 * 3*mu**4/(4*np.pi**2)


def get_mu_at_zero_P(B=0):
    mu_massless = scipy.optimize.brentq(
        lambda mu: massless.P(mu, B), massless.get_min_mu(),
        ↪  massless.get_max_mu())

    mu_massive = scipy.optimize.brentq(
        lambda mu: massive.P(mu, B), massive.get_min_mu(),
        ↪  massive.get_max_mu())

    return {'mu massless': mu_massless, 'mu massive': mu_massive}


def get_baryon_density(mu_massive, mu_massless):
    n_B_massless = massless.n_f(mu_massless)
    n_B_massive = massive.n_B(mu_massive)
    return {'n_B massless': n_B_massless, 'n_B massive': n_B_massive}


def print_energy_per_baryon(B=0):
    mu_values = get_mu_at_zero_P()
    mu_massless = mu_values['mu massless']
    mu_massive = mu_values['mu massive']

```

```
    baryon_densities = get_baryon_density(mu_massive, mu_massless)
    n_B_massless = baryon_densities['n_B massless']
    n_B_massive = baryon_densities['n_B massive']

    eps_massless = massless.eps(mu_massless, B)
    eps_massive = massive.eps(mu_massive, B)

    print('Energy per baryon at P=0:', '\tmassless quarks:',
    ↪  eps_massless/n_B_massless, '\trunning m_s:', eps_massive/n_B_massive)


def get_P_of_mu_data(N, mu_min_massive, mu_min_massless, mu_max = 1000, B=0):
    mu_list_massive = np.linspace(mu_min_massive, mu_max, N)
    mu_list_massless = np.linspace(mu_min_massless, mu_max, N)
    P_list_massive = np.zeros(N)
    P_list_massless = np.zeros(N)

    for i in range(N):
        P_massive = massive.P(mu_list_massive[i], B)
        P_massless = massless.P(mu_list_massless[i], B)
        P_list_massive[i] = P_massive
        P_list_massless[i] = P_massless

    return {'P list massive': P_list_massive, 'P list massless':
    ↪  P_list_massless,
            'mu list massive': mu_list_massive, 'mu list massless':
            ↪  mu_list_massless }


def get_eps_of_mu_data(N, mu_min_massive, mu_min_massless, mu_max = 1000, B=0):
    mu_list_massive = np.linspace(mu_min_massive, mu_max, N)
    mu_list_massless = np.linspace(mu_min_massless, mu_max, N)
    eps_list_massive = np.zeros(N)
    eps_list_massless = np.zeros(N)

    for i in range(N):
        eps_massive = massive.eps(mu_list_massive[i], B)
        eps_massless = massless.eps(mu_list_massless[i], B)
        eps_list_massive[i] = eps_massive
        eps_list_massless[i] = eps_massless

    return {'eps list massive': eps_list_massive, 'eps list massless':
    ↪  eps_list_massless, 'mu list massive': mu_list_massive, 'mu list
    ↪  massless': mu_list_massless }


def plot_P_eps_alpha_of_mu(pressure_data, eps_data, mu_lower_lim_eps, x_lim_P =
↪  300):
    mu_list_massive = pressure_data['mu list massive']
    mu_list_massless = pressure_data['mu list massless']

    P_list_massive = pressure_data['P list massive']
    P_list_massless = pressure_data['P list massless']
    P_list_Fermi_massive = P_Fermi(mu_list_massive) # Massless Fermi gas, but
    ↪  using massive mu_list
```

```
104     P_list_Fermi_massless = P_Fermi(mu_list_massless)
105
106     eps_list_massive = eps_data['eps list massive']
107     eps_list_massless = eps_data['eps list massless']
108     eps_list_Fermi_massive = eps_Fermi(mu_list_massive)  # Massless Fermi gas,
        ↪  but using massive mu_list
109     eps_list_Fermi_massless = eps_Fermi(mu_list_massless)
110
111     alpha_list_massless = massless.get_alpha_s(mu_list_massless)
112     alpha_list_massive = massless.get_alpha_s(mu_list_massive)
113
114     eps_lower_lim = massive.eps(mu_lower_lim_eps,
        ↪  0)/eps_Fermi(mu_lower_lim_eps)
115
116
117     fig = plt.figure(figsize=(12, 4))
118
119     ax = fig.add_subplot(131)
120     ax.plot(mu_list_massless, P_list_massless/P_list_Fermi_massless,
        ↪  label='Massless quarks')
121     ax.plot(mu_list_massive, P_list_massive/P_list_Fermi_massive,
        ↪  label=r'Running $m_s$')
122     ax.set_ylim(bottom=0)
123     ax.set_xlim(left=x_lim_P)
124     ax.set_xticks(np.arange(300, 1050, 100))
125     ax.yaxis.set_minor_locator(AutoMinorLocator(2))
126     ax.xaxis.set_minor_locator(AutoMinorLocator(2))
127     ax.set_xlabel(r'$\mu$ [GeV]')
128     ax.set_ylabel(r'$P/P_F$', rotation=0)
129     ax.yaxis.set_label_coords(-0.05, 1.01)
130     ticks = ticker.FuncFormatter(lambda x, pos: '{:0.1f}'.format(x * 1e-3))
131     ax.xaxis.set_major_formatter(ticks)
132
133     ax = fig.add_subplot(132)
134     ax.plot(mu_list_massless, eps_list_massless / eps_list_Fermi_massless,
        ↪  label='Massless quarks')
135     ax.plot(mu_list_massive, eps_list_massive / eps_list_Fermi_massive,
        ↪  label=r'Running $m_s$')
136     ax.set_ylim(bottom=eps_lower_lim)
137     ax.set_xlim(left=x_lim_P)
138     ax.set_xticks(np.arange(300, 1050, 100))
139     ax.yaxis.set_minor_locator(AutoMinorLocator(2))
140     ax.xaxis.set_minor_locator(AutoMinorLocator(2))
141     ax.set_xlabel(r'$\mu$ [GeV]')
142     ax.set_ylabel(r'$\epsilon/\epsilon_F$', rotation=0)
143     ax.yaxis.set_label_coords(-0.05, 1.01)
144     ticks = ticker.FuncFormatter(lambda x, pos: '{:0.1f}'.format(x * 1e-3))
145     ax.xaxis.set_major_formatter(ticks)
146     ax.legend(bbox_to_anchor=(1, 1), loc='upper right', borderaxespad=0.3)
147
148     ax = fig.add_subplot(133)
149     ax.plot(mu_list_massless, alpha_list_massless, label='Massless quarks')
150     ax.plot(mu_list_massless, alpha_list_massive, label='Running $m_s$')
151     ax.set_ylim(bottom=0, top=1.9)
152     ax.set_xlim(left=x_lim_P)
```

```
153     ax.set_yticks(np.arange(0, 1.9, .3))
154     ax.set_xticks(np.arange(300, 1050, 100))
155     ax.yaxis.set_minor_locator(AutoMinorLocator(3))
156     ax.xaxis.set_minor_locator(AutoMinorLocator(2))
157     ax.set_xlabel(r'$\mu$ [GeV]')
158     ax.set_ylabel(r'$\alpha_s$', rotation=0)
159     ax.yaxis.set_label_coords(-0.05, 1.01)
160     ticks = ticker.FuncFormatter(lambda x, pos: '{:0.1f}'.format(x * 1e-3))
161     ax.xaxis.set_major_formatter(ticks)
162 
163     fig.tight_layout()
164 
165     if SAVE_FIG:
166         plt.savefig(FILENAME_P_EPS_ALPHA + '.pdf')
167 
168 
169 def plot_MR_relations_and_charge_densities(N, r_bar_max, points, M_limit,
    ↪  R_limit, r_bar_limit_charge_profiles, P_c_min = 1e+32, P_c_max = 1e+35,
    ↪  B_to_the_one_fourth=0, annotate=False, plot_line=False):
170 
171     r_0 = 1000  # meters
172     m_0 = sl.SOLAR_MASS  # in kg
173 
174     # ----------------------------------------
175 
176     a = sc.G * m_0 / (r_0 * sc.c ** 2)
177     eps_0 = m_0 * sc.c ** 2 / (4 * np.pi * r_0 ** 3)
178 
179     B = B_to_the_one_fourth ** 4
180 
181     P_bar_c_max = P_c_max / eps_0
182     P_bar_c_min = P_c_min / eps_0
183 
184     sl.set_parent(massless.__name__)
185     MR_relation_data_dict_massless = sl.mass_radius_relation(N, P_bar_c_min,
    ↪  P_bar_c_max, points, a, r_bar_max, eps_0, B, mode='GR')
186     MR_relation_data_dict_massless['Label'] = 'Massless quarks'
187 
188     sl.set_parent(massive.__name__)
189     MR_relation_data_dict_massive = sl.mass_radius_relation(N, P_bar_c_min,
    ↪  P_bar_c_max, points, a, r_bar_max, eps_0, B, mode='GR')
190     MR_relation_data_dict_massive['Label'] = r'Running $m_s$'
191 
192     data_dicts = [MR_relation_data_dict_massless,
    ↪  MR_relation_data_dict_massive]
193 
194     plt.rcParams.update({'font.size': 13})
195     sl.plot_mass_radius_relation_multiple(data_dicts, R_limit, M_limit,
    ↪  'MR_relation_combined', plot_line=plot_line, annotate=annotate)
196 
197     if SAVE_FIG:
198         plt.savefig(FILENAME_MR + '.pdf')
199         massive.SAVE_FIG = True
200 
201     plt.rcParams.update({'font.size': 11})
```

```
202     P_bar_c_of_max = MR_relation_data_dict_massive['Pressure Of Max']
203     mu_and_mu_e_dict = sl.mu_and_mu_e_profiles(N, P_bar_c_of_max, r_bar_max, a,
        ↪  eps_0, eps_0, B, B=B)
204     massive.plot_electric_charge_densities(mu_and_mu_e_dict,
        ↪  r_bar_limit_charge_profiles)
205
206
207 def running_combined():
208     # -------- Settings ------------
209     N = 500
210     N_MR = 4000
211     r_bar_max_MR = 11.5
212     MR_points = 400
213
214     # Plot limits
215     M_limit_MR = 2.5
216     R_limit_MR = 14
217     r_bar_limit_charge_profiles = 11
218
219     # For MR-relation
220     P_c_min = 2e32
221     P_c_max = 1.4e35
222
223     mu_min_massless = 300
224     # ------------------------------------------
225     start_time = time.time()
226
227     # Getting the mu that gives zero pressure
228     mu_zero_P_massive = get_mu_at_zero_P()['mu massive']
229     mu_zero_P_massless = get_mu_at_zero_P()['mu massless']
230     print('Mu values that give zero P:', '\tMassless quarks:',
        ↪  mu_zero_P_massless, '\tRunning m_s:', mu_zero_P_massive)
231
232     mu_min_massive = mu_zero_P_massive
233
234     pressure_data = get_P_of_mu_data(N, mu_min_massive, mu_min_massless)
235     eps_data = get_eps_of_mu_data(N, mu_min_massive, mu_min_massless)
236     plot_P_eps_alpha_of_mu(pressure_data, eps_data, mu_zero_P_massive,
        ↪  x_lim_P=mu_min_massless)
237
238     print_energy_per_baryon()
239
240     plot_MR_relations_and_charge_densities(N_MR, r_bar_max_MR, MR_points,
        ↪  M_limit_MR, R_limit_MR, r_bar_limit_charge_profiles, P_c_min, P_c_max,
        ↪  annotate=True)
241
242
243     sl.print_execution_time(start_time, time.time())
244
245     if not SAVE_FIG:
246         plt.show()
```

Module name: running_massless_SM.py

```
import numpy as np
import matplotlib.pyplot as plt
import scipy.constants as sc
import scipy.optimize
import starlib as sl
import time

# ------------------------------------------------------------#
# Massless Quarks _ First Order Corrections _ Running Alpha #
# ------------------------------------------------------------#

# All quark masses are zero. This implies no electrons.

# P = pressure, m = mass, eps = energy_density, a and eps_0 are
# nondimensionalization constants. Phi = grand potential. B = bag constant

# NB! Most equations here are in natural units, h_bar=c=1.
# To make it work with the starlib module we convert back
# and forth between natural units and SI.
# However, m0 and r0 are given in kg and m! Using MeV as
# natural unit for energy.

SAVE_FIG = False  # if set to true, plots are saved to file but not shown
FILENAME_PM_PROFILE = "running_massless_SM_P_and_M_profiles_plot"
FILENAME_MR_RELATION = "running_massless_SM_MR_relation_plot"
FILENAME_PM_PROFILE_OF_MAX = "running_massless_SM_P_and_M_profiles_of_max_plot"


def get_mu_f(mu):
    return mu


# Quark grand potential in natural units, MeV^4.
def Phi_f(mu_f, alpha_s):
    return -mu_f**4 / (4*np.pi**2) * (1-2*alpha_s/np.pi)


# Easier to just use mu here instead of mu_f,
# although this breaks the generality of the function.
def n_f(mu):
    alpha_s = get_alpha_s(mu)
    n_f_star = mu**3 / np.pi**2 * (1-2*alpha_s/np.pi)
    n_0 = get_n_0(mu)
    n_f = n_f_star + n_0 * get_Lambda_bar_derivative()
    return n_f


# Pressure in natural units, MeV^4.
def P(mu, B):
    return - B - 3*Phi_f(get_mu_f(mu), get_alpha_s(mu))


# energy density in natural units. The parameters must be
# given in natural units!
def eps(mu, B):
```

```
56      mu_f = get_mu_f(mu)
57      return B + 3*Phi_f(mu_f, get_alpha_s(mu)) + 3*mu_f*n_f(mu)
58
59
60  def eps_bar(P_bar, eps_0, B):
61      P_SI = P_bar*eps_0
62      P_natural = sl.SI_to_MeV4(P_SI)
63
64      mu = scipy.optimize.brentq(
65          lambda mu: P(mu, B) - P_natural, get_min_mu(), get_max_mu())
66
67      eps_SI = sl.MeV4_to_SI(eps(mu, B))
68      eps_bar = eps_SI / eps_0
69      return eps_bar
70
71
72  # --------- Running coupling setup ---------
73  def get_beta_0():
74      return 9
75
76
77  def get_beta_1():
78      return 32
79
80
81  def get_Lambda_MS():
82      return 380  # MeV
83
84
85  def get_Lambda_bar(mu):
86      return 2 * mu
87
88
89  # Remember we actually take the derivative of Lambda_bar=2/3*(mu_u + mu_d +
    ↪  mu_s)
90  # and THEN substitute in mu. It is not the derivative with respect to mu.
91  def get_Lambda_bar_derivative():
92      return 2/3
93
94
95  def get_L(Lambda_bar):
96      return 2*np.log(Lambda_bar/get_Lambda_MS())
97
98
99  def get_alpha_s(mu):
100     L = get_L(get_Lambda_bar(mu))
101     beta_0 = get_beta_0()
102     beta_1 = get_beta_1()
103     return 4*np.pi/(beta_0*L) * (1-2*beta_1*np.log(L)/(beta_0**2 * L))
104
105
106 def ddx_alphaS_LambdaBar(mu):
107     Lambda_bar = get_Lambda_bar(mu)
108     L = get_L(Lambda_bar)
109     alpha_s = get_alpha_s(mu)
```

```
    beta_0 = get_beta_0()
    beta_1 = get_beta_1()
    return (-alpha_s/L - 8*np.pi*beta_1/(beta_0*L)**3 * (1-np.log(L))) *
    ↪  2/Lambda_bar


def get_n_0(mu):
    return - 3 * mu ** 4 / (2 * np.pi ** 3) * ddx_alphaS_LambdaBar(mu)


# ------- Bracketing limits ------------
def get_min_mu():
    return 0.7*get_Lambda_MS()


def get_max_mu():
    return 1000


def massless_strange_matter_running_coupling():
    # -------------SETTINGS---------------------
    # You can either calculate the mass-radius relation
    # (which also gives the pressure and mass profile of the
    # maximum mass star) OR
    # calculate a single pressure and mass profile from a
    # given P_c.
    N = 1000  # number of steps used to calc a single pressure profile
    calculate_M_R_relation = True

    r_0 = 1000  # meters
    m_0 = sl.SOLAR_MASS  # in kg

    B_to_the_one_fourth = 0  # B^(1/4) in MeV

    P_c = 3.7251e+34  # Joules/m^3
    r_bar_max_pressure_profile = 11  # should be larger than the radius of the
    # star whose P profile is to be calculated. But increasing this decreases
    ↪  resolution

    # MR-relation settings
    r_bar_max = 18  # should be larger than the radius of the star with largest
    ↪  radius,
    mass_radius_relation_points = 1000
    P_c_max = 1e+35
    P_c_min = 1e+32

    # Plotting settings
    r_bar_limit_P_profile = 18
    R_limit_MR_relation = 20
    M_limit_MR_relation = 3.5
    # ------------------------------------------
    # ------------------------------------------
    sl.set_parent(__name__)  # so that starlib can call eps_bar
    start_time = time.time()

```

```
    # These two are obviously in SI units. That is, m_0 and r_0 are
    # given in kg and m, not eV.
    a = sc.G * m_0 / (r_0 * sc.c ** 2)
    eps_0 = m_0 * sc.c ** 2 / (4 * np.pi * r_0 ** 3)

    B = B_to_the_one_fourth ** 4

    if calculate_M_R_relation:
        P_bar_c_max = P_c_max / eps_0
        P_bar_c_min = P_c_min / eps_0
        MR_relation_data_dict = sl.mass_radius_relation(N, P_bar_c_min,
        ↪  P_bar_c_max, mass_radius_relation_points, a, r_bar_max, eps_0, B,
        ↪  mode='GR')

        P_bar_c_of_max = MR_relation_data_dict['Pressure Of Max']

        sl.plot_mass_radius_relation(MR_relation_data_dict,
        ↪  R_limit_MR_relation, filename=FILENAME_MR_RELATION,
        ↪  M_limit=M_limit_MR_relation, mode='GR', show_legend=False)

        M_and_P_profile_filename = FILENAME_PM_PROFILE_OF_MAX
        P_bar_c = P_bar_c_of_max
        r_max = r_bar_max
    else:
        M_and_P_profile_filename = FILENAME_PM_PROFILE
        P_bar_c = P_c / eps_0
        r_max = r_bar_max_pressure_profile

    M_and_P_data_dict = sl.mass_and_pressure_profile(N, P_bar_c, r_max, a,
    ↪  eps_0, B, mode='GR')
    sl.plot_mass_and_pressure_profile(M_and_P_data_dict, eps_0, P_bar_c,
    ↪  r_bar_limit_P_profile, filename=M_and_P_profile_filename, mode='GR',
    ↪  show_legend=False)

    sl.print_execution_time(start_time, time.time())

    if not SAVE_FIG:
        plt.show()
```

Module name: running_massive_SM.py

```
import numpy as np
import matplotlib.pyplot as plt
from matplotlib.ticker import AutoMinorLocator
import scipy.constants as sc
import scipy.optimize
import starlib as sl
import time

# ------------------------------------------------------------#
# Massive S Quark _ First Order Corrections _ Running Alpha #
# ------------------------------------------------------------#

# Up and down quark masses are zero. Strange quark mass is nonzero and running.

```

```
# P = pressure, m = mass, eps = energy_density, a and eps_0 are
# nondimensionalization constants. Phi = grand potential. B = bag constant

# NB! Most equations here are in natural units, h_bar=c=1.
# To make it work with the starlib module we convert back
# and forth between natural units and SI.
# However, m0 and r0 are given in kg and m! Using MeV as
# natural unit for energy.

SAVE_FIG = False  # if set to true, plots are saved to file but not shown
FILENAME_PM_PROFILE = "running_massive_SM_P_and_M_profiles_plot"
FILENAME_MR_RELATION = "running_massive_SM_MR_relation_plot"
FILENAME_PM_PROFILE_OF_MAX = "running_massive_SM_P_and_M_profiles_of_max_plot"
FILENAME_CHARGE_PROFILES = "running_massive_SM_Charge_profiles_plot"


# Fermi momentum p_F_s renamed to u_s
def get_u_s(mu_s, m_s):
    return np.sqrt(mu_s**2 - m_s**2)


def electric_neutrality_condition(mu, mu_e):
    mu_u = get_mu_u(mu, mu_e)
    mu_d = get_mu_d(mu)
    mu_s = get_mu_s(mu)
    Lambda_bar = get_Lambda_bar(mu_u, mu_d, mu_s)
    L = get_L(Lambda_bar)
    alpha_s = get_alpha_s(L)
    m_s = get_m_s(alpha_s)

    n_0 = get_n_0(mu_u, mu_d, mu_s, m_s, Lambda_bar)
    return 2/3*n_f_massless(mu_u, alpha_s, n_0) - 1/3*n_f_massless(mu_d,
    ↪  alpha_s, n_0) - 1/3*n_s(mu_s, m_s, Lambda_bar, n_0) - n_e(mu_e)



# finds mu_e given mu by solving the
# electric charge neutrality equation
def get_mu_e(mu):
    mu_e = scipy.optimize.brentq(
        lambda mu_e: electric_neutrality_condition(mu, mu_e), get_min_mu_e(mu),
        ↪  get_max_mu_e(mu))
    return mu_e


def get_mu_u(mu, mu_e):
    return mu-mu_e


def get_mu_d(mu):
    return mu


def get_mu_s(mu):
    return mu
```

```
68
69
70  # ------------------ omega functions --------------------
71
72  def omega_f1_massless(mu_f):
73      return mu_f**4 / (2*np.pi**3)
74
75
76  def omega_s0(mu_s, m_s):
77      u_s = get_u_s(mu_s, m_s)
78      return -(u_s*mu_s*((-5*m_s**2)/2 + mu_s**2) + (3*m_s**4*np.log((u_s +
        ↪  mu_s)/m_s))/2)/(4*np.pi**2)
79
80
81  def omega_s1(mu_s, m_s, Lambda_bar):
82      u_s = get_u_s(mu_s, m_s)
83      return (-2*(-m_s**2 + mu_s**2)**2 + m_s**2*(4 +
        ↪  6*np.log(Lambda_bar/m_s))*(u_s*mu_s - m_s**2*np.log((u_s + mu_s)/m_s))
        ↪  + 3*(-(u_s*mu_s) + m_s**2*np.log((u_s + mu_s)/m_s))**2)/(2*np.pi**3)
84
85  # ------------------Grand potentials --------------------
86
87  # Electron grand potential in natural units, MeV^4.
88  def Phi_e(mu_e):
89      return -mu_e**4 / (12*np.pi**2)
90
91
92  # Quark grand potential in natural units, MeV^4.
93  def Phi_f_massless(mu_f, alpha_s):
94      return -mu_f**4 / (4*np.pi**2) * (1-2*alpha_s/np.pi)
95
96
97  def Phi_s(mu_s, m_s, alpha_s, Lambda_bar):
98      return omega_s0(mu_s, m_s) + alpha_s * omega_s1(mu_s, m_s, Lambda_bar)
99
100
101 # Total grand potential in natural units. The parameters must be
102 # given in natural units!
103 # Passing in mu_e to save on computation time.
104 def get_Phi(mu_e, mu_u, mu_d, mu_s, m_s, alpha_s, Lambda_bar):
105     return Phi_e(mu_e) + Phi_f_massless(mu_u, alpha_s) + \
106            Phi_f_massless(mu_d, alpha_s) + \
107            Phi_s(mu_s, m_s, alpha_s, Lambda_bar)
108
109
110 # --------------- Number densities --------------------
111
112 def n_e(mu_e):
113     return mu_e**3 / (3*np.pi**2)
114
115
116 def n_f_massless(mu_f, alpha_s, n_0):
117     n_f_star = mu_f**3 / np.pi**2 * (1-2*alpha_s/np.pi)
118     n_f = n_f_star + n_0 * get_Lambda_bar_derivative()
119     return n_f
```

```
120
121
122 def n_s(mu_s, m_s, Lambda_bar, n_0):
123     n_s_star = get_n_s_star(mu_s, m_s, Lambda_bar)
124     n_s = n_s_star + n_0 * get_Lambda_bar_derivative()
125     return n_s
126
127
128 def n_B(mu):
129     mu_e = get_mu_e(mu)
130     mu_u = get_mu_u(mu, mu_e)
131     mu_d = get_mu_d(mu)
132     mu_s = get_mu_s(mu)
133     Lambda_bar = get_Lambda_bar(mu_u, mu_d, mu_s)
134     L = get_L(Lambda_bar)
135     alpha_s = get_alpha_s(L)
136     m_s = get_m_s(alpha_s)
137     n_0 = get_n_0(mu_u, mu_d, mu_s, m_s, Lambda_bar)
138
139     n_u = n_f_massless(mu_u, alpha_s, n_0)
140     n_d = n_f_massless(mu_d, alpha_s, n_0)
141
142     n_B = 1/3 * (n_u + n_d + n_s(mu_s, m_s, Lambda_bar, n_0))
143     return n_B
144
145
146 # -------------- Pressure and Energy density -------------
147
148 # Pressure in natural units, MeV^4.
149 def P(mu, B):
150     mu_e = get_mu_e(mu)
151     mu_u = get_mu_u(mu, mu_e)
152     mu_d = get_mu_u(mu, mu_e)
153     mu_s = get_mu_u(mu, mu_e)
154
155     Lambda_bar = get_Lambda_bar(mu_u, mu_d, mu_s)
156     L = get_L(Lambda_bar)
157     alpha_s = get_alpha_s(L)
158     m_s = get_m_s(alpha_s)
159
160     Phi = get_Phi(mu_e, mu_u, mu_d, mu_s, m_s, alpha_s, Lambda_bar)
161     return - B - Phi
162
163
164 def eps(mu, B):
165     mu_e = get_mu_e(mu)
166     mu_u = get_mu_u(mu, mu_e)
167     mu_d = get_mu_u(mu, mu_e)
168     mu_s = get_mu_u(mu, mu_e)
169
170     Lambda_bar = get_Lambda_bar(mu_u, mu_d, mu_s)
171     L = get_L(Lambda_bar)
172     alpha_s = get_alpha_s(L)
173     m_s = get_m_s(alpha_s)
174
```

```
    Phi = get_Phi(mu_e, mu_u, mu_d, mu_s, m_s, alpha_s, Lambda_bar)
    n_0 = get_n_0(mu_u, mu_d, mu_s, m_s, Lambda_bar)

    return B + Phi + mu_e*n_e(mu_e) + mu_u*n_f_massless(mu_u, alpha_s, n_0) +
    ↪  mu_d*n_f_massless(mu_d, alpha_s, n_0) + mu_s*n_s(mu_s, m_s, Lambda_bar,
    ↪  n_0)


def eps_bar(P_bar, eps_0, B):
    P_SI = P_bar*eps_0
    P_natural = sl.SI_to_MeV4(P_SI)

    mu = scipy.optimize.brentq(
        lambda mu: P(mu, B) - P_natural, get_min_mu(), get_max_mu())

    eps_SI = sl.MeV4_to_SI(eps(mu, B))
    eps_bar = eps_SI / eps_0
    return eps_bar


# ---------------- n_0, n_s_star ------------------

# ddx means derivative of the word following the first underscore
# with respect to the word following the second underscore,
# e.g., ddx_omegaS0_mS means d(omegaS0)/d(mS).

# These are all from the Mathematica notebook.

def ddx_omegaS0_mS(mu_s, m_s):
    u_s = get_u_s(mu_s, m_s)
    return (3*m_s*(-(m_s**2*mu_s) + mu_s**3 + ((m_s**4 - m_s**2*mu_s*(u_s +
    ↪  mu_s))*np.log((u_s + mu_s)/m_s))/(u_s +
    ↪  mu_s)))/(2*np.pi**2*np.sqrt(-m_s**2 + mu_s**2))


def ddx_omegaS1_mS(mu_s, m_s, Lambda_bar):
    u_s = get_u_s(mu_s, m_s)
    return (m_s*((m_s**2 - mu_s**2)*(4*m_s**2 - 5*mu_s*(u_s + mu_s)) +
    ↪  (5*m_s**4 + m_s**2*mu_s*(u_s + mu_s) - 6*mu_s**3*(u_s +
    ↪  mu_s))*np.log((u_s + mu_s)/m_s) + 6*m_s**2*(-m_s**2 + mu_s*(u_s +
    ↪  mu_s))*np.log((u_s + mu_s)/m_s)**2 -
    ↪  6*np.log(Lambda_bar/m_s)*(mu_s*(u_s + mu_s)*(m_s**2 - mu_s**2) +
    ↪  (-2*m_s**4 + 2*m_s**2*mu_s*(u_s + mu_s))*np.log((u_s +
    ↪  mu_s)/m_s))))/(np.pi**3*(u_s + mu_s)*np.sqrt(-m_s**2 + mu_s**2))


def ddx_omegaS1_LambdaBar(mu_s, m_s, Lambda_bar):
    u_s = get_u_s(mu_s, m_s)
    return (3*m_s**2*u_s*mu_s - 3*m_s**4*np.log((u_s +
    ↪  mu_s)/m_s))/(np.pi**3*Lambda_bar)


def ddx_mS_LambdaBar(Lambda_bar):
    beta_0 = get_beta_0()
    beta_1 = get_beta_1()
```

```
    m_s_hat = get_m_s_hat()
    L_half = 0.5*get_L(Lambda_bar)
    return (m_s_hat*(-0.604795555*beta_0**5*L_half**3 +
    ↪  beta_0**2*beta_1*L_half*(3.798168212 + 10.555925632*np.log(L_half)) +
    ↪  beta_0**3*L_half**2*(-3.518641877*beta_0 + 0.2336291127*beta_1 +
    ↪  1.2095911112*beta_1*np.log(L_half)) + beta_1**2*(-0.94214749309 -
    ↪  6.2371049096*np.log(L_half) - 7.037283755*np.log(L_half)**2))) /
    ↪  (beta_0**6*Lambda_bar*L_half**5 * ((beta_0**2*L_half -
    ↪  beta_1*np.log(2*L_half)) / (beta_0**3*L_half**2))**(5/9))

def ddx_alphaS_LambdaBar(Lambda_bar):
    beta_0 = get_beta_0()
    beta_1 = get_beta_1()
    L_half = 0.5 * get_L(Lambda_bar)
    return (-2*np.pi*(beta_1 + beta_0**2*L_half -
    ↪  2*beta_1*np.log(2*L_half)))/(beta_0**3*Lambda_bar*L_half**3)


def get_n_0(mu_u, mu_d, mu_s, m_s, Lambda_bar):
    L = get_L(Lambda_bar)
    alpha_s = get_alpha_s(L)
    n_0 = -(ddx_omegaS0_mS(mu_s, m_s) + ddx_omegaS1_mS(mu_s, m_s, Lambda_bar) *
    ↪  alpha_s) * ddx_mS_LambdaBar(Lambda_bar) - ddx_omegaS1_LambdaBar(mu_s,
    ↪  m_s, Lambda_bar) * alpha_s - (omega_f1_massless(mu_u) +
    ↪  omega_f1_massless(mu_d) + omega_s1(mu_s, m_s,
    ↪  Lambda_bar))*ddx_alphaS_LambdaBar(Lambda_bar)
    return n_0

def get_n_s_star(mu_s, m_s, Lambda_bar):
    u_s = get_u_s(mu_s, m_s)
    alpha_s = get_alpha_s(get_L(Lambda_bar))
    return (-m_s**2 + mu_s**2)**(3/2)/np.pi**2 - (2*u_s*alpha_s*(2*m_s**2 +
    ↪  u_s*mu_s + 3*m_s**2*np.log(Lambda_bar/m_s) - 3*m_s**2*np.log((u_s +
    ↪  mu_s)/m_s)))/np.pi**3


# ------ running coupling and mass setup ---------

def get_beta_0():
    return 9


def get_beta_1():
    return 32


def get_Lambda_MS():
    return 380  # MeV


def get_m_s_hat():
    return 262  # MeV


def get_Lambda_bar(mu_u, mu_d, mu_s):
```

```
261     return 2/3 * (mu_u + mu_d + mu_s)
262
263
264 # Since Lambda_bar = 2/3 (mu_u + mu_d + mu_s), this is
265 # the same for all the quarks.
266 def get_Lambda_bar_derivative():
267     return 2/3
268
269
270 def get_L(Lambda_bar):
271     return 2*np.log(Lambda_bar/get_Lambda_MS())
272
273
274 def get_alpha_s(L):
275     beta_0 = get_beta_0()
276     beta_1 = get_beta_1()
277     return 4*np.pi/(beta_0*L) * (1-2*beta_1*np.log(L)/(beta_0**2 * L))
278
279
280 def get_m_s(alpha_s):
281     m_s_hat = get_m_s_hat()
282     return m_s_hat * (alpha_s/np.pi)**(4/9) * (1+0.895062 * alpha_s / np.pi)
283
284
285 # ------------------------------------------------
286
287
288 def plot_electric_charge_densities(mu_and_mu_e_dict, R_limit):
289     mu_list = mu_and_mu_e_dict['mu']
290     mu_e_list = mu_and_mu_e_dict['mu_e']
291     r_bar_list = mu_and_mu_e_dict['r_bar values']
292     radius_index = mu_and_mu_e_dict['Radius Index']
293     N = len(r_bar_list)
294
295     electron_profile = np.zeros(N)
296     up_profile = np.zeros(N)
297     down_profile = np.zeros(N)
298     strange_profile = np.zeros(N)
299     for i in range(0, N):
300         if i <= radius_index:
301             mu = mu_list[i]
302             mu_e = mu_e_list[i]
303             mu_u = get_mu_u(mu, mu_e)
304             mu_d = get_mu_d(mu)
305             mu_s = get_mu_s(mu)
306
307             Lambda_bar = get_Lambda_bar(mu_u, mu_d, mu_s)
308             L = get_L(Lambda_bar)
309             alpha_s = get_alpha_s(L)
310             m_s = get_m_s(alpha_s)
311             n_0 = get_n_0(mu_u, mu_d, mu_s, m_s, Lambda_bar)
312
313             electron_profile[i] = n_e(mu_e)
314             up_profile[i] = n_f_massless(mu_u, alpha_s, n_0)
315             down_profile[i] = n_f_massless(mu_d, alpha_s, n_0)
```

```
            strange_profile[i] = n_s(mu_s, m_s, Lambda_bar, n_0)

    electron_profile = -1 * 2 * sl.number_density_SI(electron_profile) /
    ↪  sl.n_saturation
    up_profile = 2/3 * 2 * sl.number_density_SI(up_profile) / sl.n_saturation
    down_profile = -1/3 * 2 * sl.number_density_SI(down_profile) /
    ↪  sl.n_saturation
    strange_profile = -1/3 * 2 * sl.number_density_SI(strange_profile) /
    ↪  sl.n_saturation

    fig = plt.figure(figsize=(8, 4))

    ax = fig.add_subplot(121)
    ax.plot(r_bar_list, up_profile, label='Up')
    ax.plot(r_bar_list, down_profile, label='Down')
    ax.plot(r_bar_list, strange_profile, label='Strange')
    ax.plot(r_bar_list, electron_profile, label='Electrons', color="C3")
    ax.set_xlabel(r'$r$ [km]')
    ax.set_ylabel(r'$n_i q_i  \ [n_{\mathrm{sat}}e/2]$')
    ax.legend(bbox_to_anchor=(1, 1), loc='upper right', borderaxespad=0.3)
    y_max = int(up_profile[0] + 2)
    y_min = int(min(down_profile[0], strange_profile[0]) - 2)
    ax.set_xlim(right=R_limit, left=0)
    ax.set_ylim(top=y_max, bottom=y_min)
    ax.yaxis.set_minor_locator(AutoMinorLocator(4))
    ax.xaxis.set_minor_locator(AutoMinorLocator(2))

    ax = fig.add_subplot(122)
    ax.plot(r_bar_list, electron_profile, label='Electrons', color="C3")
    ax.set_xlabel(r'$r$ [km]')
    ax.set_xlim(right=R_limit, left=0)
    ax.ticklabel_format(axis='y', style='sci', scilimits=(0,0))
    ax.yaxis.set_minor_locator(AutoMinorLocator(2))
    ax.xaxis.set_minor_locator(AutoMinorLocator(2))

    fig.tight_layout()

    if SAVE_FIG:
        plt.savefig(FILENAME_CHARGE_PROFILES + '.pdf')


# Use this to find the proper bracketing limits
def debug_bracketing():
    plt.figure()
    NN = 100
    mu_e_values = np.linspace(0, 150, NN)
    charge = np.zeros(NN)
    mu_values = np.linspace(390, 1000, 8)
    for mu in mu_values:
        for i in range(NN):
            charge[i] = electric_neutrality_condition(mu, mu_e_values[i])

        plt.plot(mu_e_values, charge)
    plt.axhline(y=0)

```

```
368
369 # --------------- Bracketing limits ----------------------
370
371 # These are somewhat hardcoded. Defined as functions for easy tweaking
372
373 def get_max_mu_e(mu):
374     return 100
375
376
377 def get_min_mu_e(mu):
378     return 2
379
380
381 # MeV^4. Max central chemical potential to use in
382 # bracketing solver. Raise if necessary.
383 def get_max_mu():
384     return 1000
385
386
387 def get_min_mu():
388     return 390
389
390 # ------------------------------------------------------------
391
392
393 def massive_strange_matter_running_coupling_and_mass():
394     # -------------SETTINGS---------------------
395     # You can either calculate the mass-radius relation
396     # (which also gives the pressure and mass profile of the
397     # maximum mass star) OR
398     # calculate a single pressure and mass profile from a
399     # given P_c.
400     N = 100  # number of steps used to calc a single pressure profile
401     calculate_M_R_relation = True
402
403     # Only change these if you want to scale plots
404     # differently for some reason. But then you must also
405     # change the labels in the starlib plot functions.
406     r_0 = 1000  # meters
407     m_0 = sl.SOLAR_MASS  # in kg
408
409     B_to_the_one_fourth = 0  # B^(1/4) in MeV, Bag constant
410
411     P_c = 3.7251e+34  # Joules/m^3
412     r_bar_max_pressure_profile = 20  # should be larger than the radius of the
413     # star whose P profile is to be calculated. But increasing this decreases
      ↪ resolution
414
415     # MR Relation settings
416     r_bar_max = 20  # should be larger than the radius of the star with largest
      ↪ radius,
417     mass_radius_relation_points = 30
418     P_c_max = 1e+36
419     P_c_min = 1e+34
420
```

```
421     # Plotting settings
422     r_bar_limit_P_profile = 20
423     R_limit_MR_relation = 20
424     M_limit_MR_relation = 5
425     # ----------------------------------------
426     sl.set_parent(__name__)  # so that starlib can call eps_bar
427     start_time = time.time()
428 
429     # These two are obviously in SI units. That is, m_0 and r_0 are
430     # given in kg and m, not eV.
431     a = sc.G * m_0 / (r_0 * sc.c ** 2)
432     eps_0 = m_0 * sc.c ** 2 / (4 * np.pi * r_0 ** 3)
433 
434     B = B_to_the_one_fourth**4
435 
436     if calculate_M_R_relation:
437         P_bar_c_max = P_c_max / eps_0
438         P_bar_c_min = P_c_min / eps_0
439         MR_relation_data_dict = sl.mass_radius_relation(N, P_bar_c_min,
            ↪  P_bar_c_max, mass_radius_relation_points, a, r_bar_max, eps_0, B,
            ↪  mode='GR')
440 
441         P_bar_c_of_max = MR_relation_data_dict['Pressure Of Max']
442 
443         sl.plot_mass_radius_relation(MR_relation_data_dict,
            ↪  R_limit_MR_relation, filename=FILENAME_MR_RELATION,
            ↪  M_limit=M_limit_MR_relation, mode='GR', show_legend=False)
444 
445         M_and_P_profile_filename = FILENAME_PM_PROFILE_OF_MAX
446         P_bar_c = P_bar_c_of_max
447         r_max = r_bar_max
448     else:
449         M_and_P_profile_filename = FILENAME_PM_PROFILE
450         P_bar_c = P_c / eps_0
451         r_max = r_bar_max_pressure_profile
452 
453     #debug_bracketing()
454 
455     M_and_P_data_dict = sl.mass_and_pressure_profile(N, P_bar_c, r_max, a,
    ↪  eps_0, B, mode='GR')
456     sl.plot_mass_and_pressure_profile(M_and_P_data_dict, eps_0, P_bar_c,
    ↪  r_bar_limit_P_profile, filename=M_and_P_profile_filename, mode='GR',
    ↪  show_legend=False)
457 
458     mu_and_mu_e_dict = sl.mu_and_mu_e_profiles(N, P_bar_c, r_max, a, eps_0,
    ↪  eps_0, B, B=B)
459     plot_electric_charge_densities(mu_and_mu_e_dict, r_bar_limit_P_profile)
460 
461     sl.print_execution_time(start_time, time.time())
462 
463     if not SAVE_FIG:
464         plt.show()
```

G.8 The Starlib Module

Module name: starlib.py

```
import numpy as np
import matplotlib.pyplot as plt
import scipy.constants as sc
import importlib
import datetime
import scipy.optimize
from matplotlib.ticker import AutoMinorLocator
parent_module = None

# CONSTANTS
n_saturation = 1.68e44
SOLAR_MASS = 1.988e30


# For getting access to the module (parent) that imported this module
# so that eps_bar in the parent can be called.
def set_parent(parent_module_name):
    global parent_module
    parent_module = importlib.import_module(parent_module_name)


# Converts from MeV^4 (natural units) to Joules/m^3
# (pressure/energy density)
def MeV4_to_SI(natural):
    return natural * 2.0852e25


def SI_to_MeV4(SI):
    return SI / 2.0852e25


def MeV3_to_Joules3(MeV3):
    return MeV3 * 1.6021766e-13 ** 3


def number_density_SI(n_MeV3):
    return MeV3_to_Joules3(n_MeV3) /(sc.hbar * sc.c)**3


# returns dP/dr
def TOV(P_bar, m_bar, eps_bar, a, r_bar):
    if r_bar == 0 or m_bar == 0:
        return 0
    else:
        return - a * eps_bar * m_bar / r_bar**2 * (1.0 + P_bar/eps_bar) * (1.0
        ↪  + r_bar**3 * P_bar / m_bar) / (1.0 - 2*a * m_bar/r_bar)


def newton(m_bar, eps_bar, a, r_bar):
    if r_bar == 0 or m_bar == 0:
        return 0
```

```
    else:
        return - a * eps_bar * m_bar / r_bar**2


# y = [P, m] is a vector holding the values of P and m as the solver iterates
def structure_eqs_TOV(r_bar, y, a, *args):
    P_bar, m_bar = y
    eps_bar = parent_module.eps_bar(P_bar, *args)
    dydr = np.array([TOV(P_bar, m_bar, eps_bar, a, r_bar),
    ↪  mass_continuity(eps_bar, r_bar)])
    return dydr


def structure_eqs_Newton(r_bar, y, a, *args):
    P_bar, m_bar = y
    eps_bar = parent_module.eps_bar(P_bar, *args)
    dydr = np.array([newton(m_bar, eps_bar, a, r_bar), mass_continuity(eps_bar,
    ↪  r_bar)])
    return dydr


# returns dm/dr
def mass_continuity(eps_bar, r_bar):
    return r_bar**2 * eps_bar


def RK4_single_step(t_initial, t_final, y_initial, dydt_func):

    h = t_final - t_initial
    s1 = dydt_func(t_initial, y_initial)
    if (y_initial + h/2 * s1)[0] < 0:
        return np.zeros(2), True
    else:
        s2 = dydt_func(t_initial + h/2, y_initial + h/2 * s1)
    if (y_initial + h/2 * s2)[0] < 0:
        return np.zeros(2), True
    else:
        s3 = dydt_func(t_initial + h/2, y_initial + h/2 * s2)
    if (y_initial + h * s3)[0] < 0:
        return np.zeros(2), True
    else:
        s4 = dydt_func(t_initial + h, y_initial + h * s3)

    y_final = y_initial + h/6 * (s1 + 2*s2 + 2*s3 + s4)
    return y_final, False


def RK4(derivatives_func, y_0, t_list, *args):
    points = len(t_list)
    y_list = np.zeros((2, points))
    y_list[0][0] = y_0[0]
    y_list[1][0] = y_0[1]

    radius_index = -1
    for i in range(points-1):
```

```
104         y_next, negative_pressure = RK4_single_step(t_list[i], t_list[i+1],
            ↪ np.array([y_list[0][i], y_list[1][i]]), lambda t, y:
            ↪ derivatives_func(t, y, *args))
105         if not negative_pressure:
106             y_list[0][i+1] = y_next[0]
107             y_list[1][i+1] = y_next[1]
108         else:
109             radius_index = i
110             y_list[1][i+1:] = y_list[1, radius_index]
111             break
112     return y_list, radius_index
113
114
115 # returns mass and radius for GR and Newton as two separate arrays,
116 def get_mass_and_radius(N, P_bar_c, r_bar_max, a, structure_eqs, *args):
117     y0 = [P_bar_c, 0]
118     r_bar_list = np.linspace(0, r_bar_max, N)
119     y_list, radius_index = RK4(structure_eqs, y0, r_bar_list, a, *args)
120
121     M, R = y_list[1][radius_index], r_bar_list[radius_index]
122     return M, R
123
124
125 # *args will be sent to the eps_bar function in the parent module
126 def mass_radius_relation(N, P_bar_c_min, P_bar_c_max, number_of_points, a,
↪   r_bar_max, *args, mode='Both'):
127     P_bar_c_list = np.logspace(np.log10(P_bar_c_min), np.log10(P_bar_c_max),
        ↪ number_of_points)
128     masses_and_radii_TOV = np.zeros((2, number_of_points))
129     masses_and_radii_newton = np.zeros((2, number_of_points))
130
131     for i, P_bar_c in np.ndenumerate(P_bar_c_list):
132         if mode == 'GR':
133             M_and_R_TOV = get_mass_and_radius(N, P_bar_c, r_bar_max, a,
                ↪ structure_eqs_TOV, *args)
134             print(i[0]+1, 'M and R TOV:', M_and_R_TOV, '\tP_bar_c:', P_bar_c)
135             masses_and_radii_TOV[0][i] = M_and_R_TOV[0]
136             masses_and_radii_TOV[1][i] = M_and_R_TOV[1]
137         elif mode == 'Newton':
138             M_and_R_newton = get_mass_and_radius(N, P_bar_c, r_bar_max, a,
                ↪ structure_eqs_Newton, *args)
139             print(i[0]+1, 'M and R Newton:', M_and_R_newton, '\tP_bar_c:',
                ↪ P_bar_c)
140             masses_and_radii_newton[0][i] = M_and_R_newton[0]
141             masses_and_radii_newton[1][i] = M_and_R_newton[1]
142         else:
143             M_and_R_TOV = get_mass_and_radius(N, P_bar_c, r_bar_max, a,
                ↪ structure_eqs_TOV, *args)
144             M_and_R_newton = get_mass_and_radius(N, P_bar_c, r_bar_max, a,
                ↪ structure_eqs_Newton, *args)
145             print(i[0]+1, 'M and R TOV:', M_and_R_TOV, '\tP_bar_c:', P_bar_c)
146             masses_and_radii_TOV[0][i] = M_and_R_TOV[0]
147             masses_and_radii_TOV[1][i] = M_and_R_TOV[1]
148             masses_and_radii_newton[0][i] = M_and_R_newton[0]
149             masses_and_radii_newton[1][i] = M_and_R_newton[1]
```

```
150
151     max_index = np.argmax(masses_and_radii_TOV[0])
152     max_mass = masses_and_radii_TOV[0][max_index]
153     radius_of_max = masses_and_radii_TOV[1][max_index]
154     P_bar_c_of_max = P_bar_c_list[max_index]
155     print('Max M=', max_mass, '\tR of max=', radius_of_max, '\tP_bar_c of
        ↪ max=', P_bar_c_of_max)
156
157     return {'MR TOV': masses_and_radii_TOV, 'MR Newton':
        ↪ masses_and_radii_newton,
158             'Radius of max': radius_of_max, 'Max Mass': max_mass, 'Pressure Of
                ↪ Max': P_bar_c_of_max}
159
160
161 # *args will be sent to the eps_bar function in the parent module
162 def mass_and_pressure_profile(N, P_bar_c, r_bar_max, a, *args, mode='Both'):
163     # y = [[pressure values], [mass values]]
164     y0 = [P_bar_c, 0]
165     r_bar_list = np.linspace(0, r_bar_max, N)
166
167     if mode == 'GR':
168         y_list_TOV, radius_index_TOV = RK4(structure_eqs_TOV, y0, r_bar_list,
            ↪ a, *args)
169         y_list_newton, radius_index_newton = 0, 0
170     elif mode == 'Newton':
171         y_list_newton, radius_index_newton = RK4(structure_eqs_Newton, y0,
            ↪ r_bar_list, a, *args)
172         y_list_TOV, radius_index_TOV = 0, 0
173     else:
174         y_list_TOV, radius_index_TOV = RK4(structure_eqs_TOV, y0, r_bar_list,
            ↪ a, *args)
175         y_list_newton, radius_index_newton = RK4(structure_eqs_Newton, y0,
            ↪ r_bar_list, a, *args)
176
177     return {'P_bar and M_bar values TOV': y_list_TOV, 'P_bar and M_bar values
        ↪ Newton': y_list_newton,
178             'r_bar values': r_bar_list, 'Radius Index TOV': radius_index_TOV,
179             'Radius Index Newton': radius_index_newton}
180
181
182 # Returns list of chemical potential values mu as function of radial
    ↪ coordinate.
183 # NB! Parent module must have a function P(mu) and get_mu_e(mu),
184 # as well as get_min_mu() and get_max_mu() for the bracketing.
185 def mu_and_mu_e_profiles(N, P_bar_c, r_bar_max, a, eps_0, *args, B=0):
186     y0 = [P_bar_c, 0]
187     r_bar_list = np.linspace(0, r_bar_max, N)
188     y_list, radius_index = RK4(structure_eqs_TOV, y0, r_bar_list, a, *args)
189
190     mu_list = np.zeros(N)
191     mu_e_list = np.zeros(N)
192     P_SI_list = y_list[0, :] * eps_0
193     P_natural = SI_to_MeV4(P_SI_list)
194
195     for i, P_nat in np.ndenumerate(P_natural):
```

```
196         mu = scipy.optimize.brentq(
197             lambda mu: parent_module.P(mu, B) - P_nat,
198             parent_module.get_min_mu(), parent_module.get_max_mu())
199 
200         mu_list[i] = mu
201         mu_e_list[i] = parent_module.get_mu_e(mu)
202 
203     return {'mu': mu_list, 'mu_e': mu_e_list,
204             'r_bar values': r_bar_list, 'Radius Index': radius_index}
205 
206 
207 def plot_mass_and_pressure_profile(data_dict, eps_0, P_bar_c, r_bar_limit,
    ↪  filename='', mode='Both', GR_label='General relativity',
    ↪  newton_label='Newtonian gravity', show_legend=True, m_padding=0.2):
208     y_list_TOV = data_dict['P_bar and M_bar values TOV']
209     y_list_newton = data_dict['P_bar and M_bar values Newton']
210     r_bar_list = data_dict['r_bar values']
211     radius_index_TOV = data_dict['Radius Index TOV']
212     radius_index_newton = data_dict['Radius Index Newton']
213 
214     print()
215     print('-' * 14, 'Mass and Pressure Profile Plots', '-' * 14)
216     if mode == 'GR':
217         print('TOV: R=', r_bar_list[radius_index_TOV], '\tM=',
            ↪  y_list_TOV[1][radius_index_TOV])
218     elif mode == 'Newton':
219         print('Newton: R =', r_bar_list[radius_index_newton], '\tM =',
            ↪  y_list_newton[1][radius_index_newton])
220     else:
221         print('TOV: R=', r_bar_list[radius_index_TOV], '\tM=',
            ↪  y_list_TOV[1][radius_index_TOV])
222         print('Newton: R =', r_bar_list[radius_index_newton], '\tM =',
            ↪  y_list_newton[1][radius_index_newton])
223     print('P_bar_c =', P_bar_c, '\tP_c =', P_bar_c * eps_0)
224     print('-' * 60)
225 
226 
227     fig = plt.figure(figsize=(7, 3))
228 
229     ax = fig.add_subplot(121)
230     if mode == 'GR':
231         ax.plot(r_bar_list, y_list_TOV[0, :]/y_list_TOV[0, 0], label=GR_label)
232     elif mode == 'Newton':
233         ax.plot(r_bar_list, y_list_newton[0, :]/y_list_newton[0, 0],
            ↪  label=newton_label)
234     else:
235         ax.plot(r_bar_list, y_list_TOV[0, :] / y_list_TOV[0, 0],
            ↪  label=GR_label)
236         ax.plot(r_bar_list, y_list_newton[0, :] / y_list_newton[0, 0],
            ↪  label=newton_label)
237     ax.set_xlabel(r'$r$ [km]')
238     ax.set_ylabel(r'$P(r)/P_c$', rotation=0)
239     ax.yaxis.set_label_coords(-0.05, 1.03)
240     if show_legend:
241         ax.legend(bbox_to_anchor=(1, 1), loc='upper right', borderaxespad=0.3)
```

```
    ax.set_xlim(right=r_bar_limit)
    ax.set_xticks(np.arange(0, r_bar_limit, 2))
    ax.set_xticks(np.arange(0, r_bar_limit, 1), minor=True)
    ax.set_yticks(np.arange(0, 1.1, 0.1), minor=True)

    ax = fig.add_subplot(122)
    dashedlinestyle = (0, (5, 10))
    if mode == 'GR':
        ax.plot(r_bar_list, y_list_TOV[1, :], label=GR_label)
        m_max = np.amax(y_list_TOV[1, :])
        ax.axhline(y=m_max, linestyle=dashedlinestyle, color='k',
        ↪  linewidth=0.5)
    elif mode == 'Newton':
        ax.plot(r_bar_list, y_list_newton[1, :], label=newton_label)
        m_max = np.amax(y_list_newton[1, :])
        ax.axhline(y=m_max, linestyle=dashedlinestyle, color='k',
        ↪  linewidth=0.5)
    else:
        ax.plot(r_bar_list, y_list_TOV[1, :], label=GR_label)
        ax.plot(r_bar_list, y_list_newton[1, :], label=newton_label)
        m_max_TOV = np.amax(y_list_TOV[1, :])
        m_max_newton = np.amax(y_list_newton[1, :])
        m_max = max(m_max_TOV, m_max_newton)
        ax.axhline(y=m_max_TOV, linestyle=dashedlinestyle, color='k',
        ↪  linewidth=0.5)
        ax.axhline(y=m_max_newton, linestyle=dashedlinestyle, color='k',
        ↪  linewidth=0.5)

    m_max = (m_max + m_padding)
    ax.set_xlabel(r'$r$ [km]')
    ax.set_ylabel(r'$m(r)/M_\odot$', rotation=0)
    ax.yaxis.set_label_coords(-0.05, 1.03)
    ax.set_xlim(right=r_bar_limit)
    ax.set_ylim(top=m_max)
    ax.set_xticks(np.arange(0, r_bar_limit, 2))
    ax.set_xticks(np.arange(0, r_bar_limit, 1), minor=True)
    ax.set_yticks(np.arange(0, m_max+0.1, 0.3))
    ax.yaxis.set_minor_locator(AutoMinorLocator(3))

    fig.tight_layout()

    if parent_module.SAVE_FIG:
        plt.savefig(filename + '.pdf')


def plot_mass_radius_relation(data_dict, R_limit, M_limit=1.5, filename='',
↪  mode='Both', GR_label='General relativity', newton_label='Newtonian
↪  gravity', show_legend=True):
    masses_and_radii_TOV = data_dict['MR TOV']
    masses_and_radii_newton = data_dict['MR Newton']
    radius_of_max = data_dict['Radius of max']
    max_mass = data_dict['Max Mass']

    fig = plt.figure(figsize=(6, 4))
    ax = fig.add_subplot(111)
```

```
291     if mode == 'GR':
292         ax.plot(masses_and_radii_TOV[1], masses_and_radii_TOV[0],
            ↪  label=GR_label)
293         ax.plot(np.array((radius_of_max,)), np.array((max_mass,)), marker='x',
            ↪  color='k')
294         ax.annotate('(' + '{:00.2f}'.format(radius_of_max) + ', ' +
            ↪  '{:00.3f}'.format(max_mass) + ')', xy=(radius_of_max,
            ↪  max_mass+0.05), fontsize=10, ha='center')
295     elif mode == 'Newton':
296         ax.plot(masses_and_radii_newton[1], masses_and_radii_newton[0],
            ↪  label=newton_label)
297     else:
298         ax.plot(masses_and_radii_TOV[1], masses_and_radii_TOV[0],
            ↪  label=GR_label)
299         ax.plot(masses_and_radii_newton[1], masses_and_radii_newton[0],
            ↪  label=newton_label)
300         ax.plot(np.array((radius_of_max,)), np.array((max_mass,)), marker='x',
            ↪  color='k')
301         ax.annotate('(' + '{:00.2f}'.format(radius_of_max) + ', ' +
            ↪  '{:00.3f}'.format(max_mass) + ')', xy=(radius_of_max,
            ↪  max_mass+0.05), fontsize=13, ha='center')
302     ax.set_xlabel(r'$R$ [km]')
303     ax.set_ylabel(r'$M \ [M_\odot]$')
304     ax.set_ylim(top=M_limit, bottom=0)
305     ax.set_xlim(right=R_limit, left=0)
306     ax.set_xticks(np.arange(0, R_limit+0.5, 2))
307     ax.set_xticks(np.arange(0, R_limit+0.5, 1), minor=True)
308     ax.set_yticks(np.arange(0, M_limit+0.02, 0.2))
309     ax.yaxis.set_minor_locator(AutoMinorLocator(2))
310 
311     if show_legend:
312         ax.legend(bbox_to_anchor=(1, 1), loc='upper right', borderaxespad=0.3)
313     fig.tight_layout()
314 
315     if parent_module.SAVE_FIG:
316         plt.savefig(filename + '.pdf')
317 
318 
319 def plot_mass_radius_relation_multiple(data_dicts, R_limit, M_limit=1.5,
    ↪  filename='', plot_line=False, annotate=False):
320 
321     fig = plt.figure(figsize=(6, 4))
322     ax = fig.add_subplot(111)
323 
324     if plot_line:
325         max_M_max = data_dicts[0]['Max Mass']
326         min_M_max = max_M_max
327         max_R_max = data_dicts[0]['Radius of max']
328         min_R_max = max_R_max
329         for data_dict in data_dicts:
330             M_max = data_dict['Max Mass']
331             if M_max > max_M_max:
332                 max_M_max = M_max
333             if M_max < min_M_max:
334                 min_M_max = M_max
```

```
335
336             R_max = data_dict['Radius of max']
337             if R_max > max_R_max:
338                 max_R_max = R_max
339             if R_max < min_R_max:
340                 min_R_max = R_max
341
342         slope = (max_M_max - min_M_max)/(max_R_max - min_R_max)
343         x_values = np.linspace(0, R_limit, 10)
344         y_values = min_M_max + slope*(x_values - min_R_max)
345         dashedlinestyle = (0, (5, 10))
346         ax.plot(x_values, y_values, label='{:00.2f}'.format(slope) + r'
            ↪  $M_\odot$/km', color='k', linewidth=0.5, linestyle=dashedlinestyle)
347
348     for data_dict in data_dicts:
349
350         masses_and_radii = data_dict['MR TOV']
351         radius_of_max = data_dict['Radius of max']
352         max_mass = data_dict['Max Mass']
353         label = data_dict['Label']
354
355         ax.plot(masses_and_radii[1], masses_and_radii[0], label=label)
356         ax.plot(np.array((radius_of_max,)), np.array((max_mass,)), marker='x',
            ↪  color='k')
357
358         if annotate:
359             ax.annotate('(' + '{:00.2f}'.format(radius_of_max) + ', ' +
                ↪  '{:00.2f}'.format(max_mass) + ')', xy=(radius_of_max, max_mass
                ↪  + 0.09), fontsize=13, ha='center')
360
361     ax.set_xlabel(r'$R$ [km]')
362     ax.set_ylabel(r'$M \ [M_\odot]$')
363     ax.set_ylim(top=M_limit, bottom=0)
364     ax.set_xlim(right=R_limit, left=0)
365     ax.legend(bbox_to_anchor=(0, 1), loc='upper left', borderaxespad=0.3)
366     ax.set_xticks(np.arange(0, R_limit+0.2, 2))
367     ax.set_xticks(np.arange(0, R_limit+0.2, 1), minor=True)
368     ax.set_yticks(np.arange(0, M_limit+0.03, 0.5))
369     ax.set_yticks(np.arange(0, M_limit + 0.03, 0.1), minor=True)
370
371     fig.tight_layout()
372
373     if parent_module.SAVE_FIG:
374         plt.savefig(filename + '.pdf')
375
376
377 def print_execution_time(start_time, end_time):
378     execution_time = end_time - start_time
379     time_string = str(datetime.timedelta(seconds=execution_time))
380     print("Execution time: ---- " + time_string + " ----")
```

G.9 Mathematica Expression Replacer

```
import os
from os import path
import codecs
main_folder = path.dirname(__file__)
input_folder = path.join(main_folder, 'mathematica_expressions', 'input')
output_folder = path.join(main_folder, 'mathematica_expressions', 'output')

FILENAME = 'nS1'
ALL_FILES = True

# NB! muS must be replaced before uS, ΛMS before Λ etc.!
def replace(expression):
    print(expression)

    #  -> alpha_s
    expression = expression.replace('', 'alpha_s')

    # hatmS -> m_s_hat
    expression = expression.replace('hatmS', 'm_s_hat')

    # mS -> m_s
    expression = expression.replace('mS', 'm_s')

    # muS -> mu_s
    expression = expression.replace('muS', 'mu_s')

    # Log -> np.log
    expression = expression.replace('Log', 'np.log')

    # [ -> (
    expression = expression.replace('[', '(')

    # ] -> )
    expression = expression.replace(']', ')')

    # ^ -> **
    expression = expression.replace('^', '**')

    # ΛMS -> Lambda_MS
    expression = expression.replace('ΛMS', 'Lambda_MS')

    # Λ -> Lambda_bar
    expression = expression.replace('Λ', 'Lambda_bar')

    # Pi -> np.pi
    expression = expression.replace('Pi', 'np.pi')

    # Sqrt -> np.sqrt
    expression = expression.replace('Sqrt', 'np.sqrt')

    # 1 -> beta_1
    expression = expression.replace('1', 'beta_1')
```

```
53
54      # 0 -> beta_0
55      expression = expression.replace('0', 'beta_0')
56
57      # uS -> u_s
58      expression = expression.replace('uS', 'u_s')
59
60      # S -> mu_s
61      expression = expression.replace('S', 'mu_s')
62
63      # ------------------------------------
64
65      return expression
66
67
68  def main():
69      if not ALL_FILES:
70          filepath = path.join(input_folder, FILENAME + '.txt')
71
72          with codecs.open(filepath, encoding='utf-8', mode='r') as infile:
73              expression = infile.readline()
74
75          expression = replace(expression)
76
77          outfile = open(path.join(output_folder, FILENAME + '.txt'), 'w')
78          outfile.write(expression)
79          outfile.close()
80      else:
81          for filename in os.listdir(input_folder):
82              filename = os.fsdecode(filename)
83              if filename.endswith(".txt"):
84                  with codecs.open(path.join(input_folder, filename),
                    ↪  encoding='utf-8', mode='r') as infile:
85                      expression = infile.readline()
86
87                  expression = replace(expression)
88
89                  outfile = open(path.join(output_folder, filename), 'w')
90                  outfile.write(expression)
91                  outfile.close()
92              else:
93                  continue
94
95
96  main()
```

References

[1] J. Bennett, M. Donahue, N. Schneider, and M. Voit, *The cosmic perspective* (Pearson, 2017).

[2] J. Wheeler, *Cosmic catastrophes: supernovae, gamma-ray bursts, and adventures in hyperspace* (Cambridge University Press, 2000).

[3] J. R. Oppenheimer and G. M. Volkoff, "On massive neutron cores," Phys. Rev. **55**, 374–381 (1939).

[4] B. Margalit and B. D. Metzger, "Constraining the Maximum Mass of Neutron Stars from Multi-messenger Observations of GW170817," ApJ **850**, L19, L19 (2017).

[5] M. Shibata, S. Fujibayashi, K. Hotokezaka, K. Kiuchi, K. Kyutoku, Y. Sekiguchi, and M. Tanaka, "Modeling GW170817 based on numerical relativity and its implications," Phys. Rev. D **96**, 123012, 123012 (2017).

[6] M. Ruiz, S. L. Shapiro, and A. Tsokaros, "GW170817, general relativistic magnetohydrodynamic simulations, and the neutron star maximum mass," Phys. Rev. D **97**, 021501, 021501 (2018).

[7] F. Özel and P. Freire, "Masses, Radii, and the Equation of State of Neutron Stars," ARA&A **54**, 401–440 (2016).

[8] D. D. Ivanenko and D. F. Kurdgelaidze, "Hypothesis concerning quark stars," Astrophysics **1**, 251–252 (1965).

[9] E. Annala, T. Gorda, A. Kurkela, J. Nättilä, and A. Vuorinen, "Evidence for quark-matter cores in massive neutron stars," Nature Phys. (2020).

[10] E. Annala, T. Gorda, A. Kurkela, J. Nättilä, and A. Vuorinen, "Constraining the properties of neutron-star matter with observations," Mem. Soc. Ast. It. **90**, 81 (2019).

[11] Z. G. Dai, S. Q. Wang, J. S. Wang, L. J. Wang, and Y. W. Yu, "The Most Luminous Supernova ASASSN-15lh: Signature of a Newborn Rapidly Rotating Strange Quark Star," ApJ **817**, 132, 132 (2016).

[12] J. Hartle, *Gravity: an introduction to einstein's general relativity* (Addison-Wesley, 2003).

[13] S. M. Carroll, *Spacetime and geometry: An introduction to general relativity* (Cambridge University Press, 2019).

[14] R. Wald, *General relativity* (University of Chicago Press, 1984).

[15]A. D. Rendall and B. G. Schmidt, "Existence and properties of spherically symmetric static fluid bodies with a given equation of state," Classical and Quantum Gravity **8**, 985–1000 (1991).

[16]T. Harko and M. K. Mak, "Exact power series solutions of the structure equations of the general relativistic isotropic fluid stars with linear barotropic and polytropic equations of state," Astrophysics and Space Science **361** (2016).

[17]S. Weinberg, *Gravitation and Cosmology: Principles and Applications of the General Theory of Relativity* (Wiley, New York, NY, 1972).

[18]H. L. Shipman, "Masses and radii of white-dwarf stars. III. Results for 110 hydrogen-rich and 28 helium-rich stars.," ApJ **228**, 240–256 (1979).

[19]B. Povh, K. Rith, M. Lavelle, C. Scholz, and F. Zetsche, *Particles and nuclei: an introduction to the physical concepts* (Springer, 2015).

[20]C. Mohan and A. Al-Bayaty, "Power-series solutions of the lane-emden equation," Astrophysics and Space Science **73**, 227–239 (1980).

[21]N. K. Glendenning, *Compact stars: Nuclear Physics, Particle Physics and General Relativity* (1997).

[22]S. L. Shapiro and S. A. Teukolsky, *Black holes, white dwarfs, and neutron stars : the physics of compact objects* (1983).

[23]A. S. Eddington, *The internal constitution of the stars*, Cambridge Science Classics (Cambridge University Press, 1988).

[24]H. Young, R. Freedman, and A. Ford, *University physics with modern physics* (Pearson Education, 2012).

[25]L. Neslušan, "On the global electrostatic charge of stars," A&A **372**, 913–915 (2001).

[26]W. B. Bonnor, "The equilibrium of a charged test particle in the field of a spherical charged mass in general relativity," Classical and Quantum Gravity **10**, 2077–2082 (1993).

[27]D. Bini, A. Geralico, and R. Ruffini, "Charged massive particle at rest in the field of a reissner-nordström black hole," Physical Review D **75** (2007).

[28]M. S. Bhatia, S. Bonazzola, and G. Szamosi, "Electric Field in Neutron Stars," A&A **3**, 206 (1969).

[29]S. Ray, A. L. Espíndola, M. Malheiro, J. P. S. Lemos, and V. T. Zanchin, "Electrically charged compact stars and formation of charged black holes," Physical Review D **68** (2003).

[30]A. Schmitt, "Dense matter in compact stars," Lecture Notes in Physics (2010).

[31]S. Chandrasekhar, "Dynamical Instability of Gaseous Masses Approaching the Schwarzschild Limit in General Relativity," Phys. Rev. Lett. **12**, 114–116 (1964).

[32]C. Misner, C. John Archibald Wheeler, U. Misner, K. Thorne, J. Wheeler, W. Freeman, and Company, *Gravitation*, Gravitation poeng 3 (W. H. Freeman, 1973).

[33]J. M. Bardeen, K. S. Thorne, and D. W. Meltzer, "A Catalogue of Methods for Studying the Normal Modes of Radial Pulsation of General-Relativistic Stellar Models," ApJ **145**, 505 (1966).

[34]P. Haensel, A. Potekhin, and D. Yakovlev, *Neutron stars 1: equation of state and structure*, Astrophysics and Space Science Library (Springer New York, 2006).

[35]M. D. Schwartz, *Quantum Field Theory and the Standard Model* (Cambridge University Press, 2014).

[36]J. I. Kapusta and C. Gale, *Finite-temperature field theory: Principles and applications*, Cambridge Monographs on Mathematical Physics (Cambridge University Press, 2006).

[37]E. S. Fraga and P. Romatschke, "Role of quark mass in cold and dense perturbative qcd," Physical Review D **71** (2005).

[38]M. E. Peskin and D. V. Schroeder, *An Introduction to Quantum Field Theory*, Reading, USA: Addison-Wesley (1995) 842 p (Westview Press, 1995).

[39]E. Farhi and R. L. Jaffe, "Strange matter," Phys. Rev. D **30**, 2379–2390 (1984).

[40]C. Alcock, E. Farhi, and A. Olinto, "Strange Stars," ApJ **310**, 261 (1986).

[41]C.-J. Xia and S.-G. Zhou, "Stable strange quark matter objects with running masses and coupling constant," Nuclear Physics B **916**, 669–687 (2017).

[42]P. Haensel, J. L. Zdunik, and R. Schaefer, "Strange quark stars," A&A **160**, 121–128 (1986).

[43]B. A. Freedman and L. D. McLerran, "Fermions and gauge vector mesons at finite temperature and density. i. formal techniques," Phys. Rev. D **16**, 1130–1146 (1977).

[44]B. A. Freedman and L. D. McLerran, "Fermions and gauge vector mesons at finite temperature and density. iii. the ground-state energy of a relativistic quark gas," Phys. Rev. D **16**, 1169–1185 (1977).

[45]V. Baluni, "Non-abelian gauge theories of fermi systems: quantum-chromodynamic theory of highly condensed matter," Phys. Rev. D **17**, 2092–2121 (1978).

[46]A. Kurkela, P. Romatschke, and A. Vuorinen, "Cold Quark Matter," Phys. Rev. D **81**, 105021 (2010).

[47]E. S. Fraga, R. D. Pisarski, and J. Schaffner-Bielich, "Small, dense quark stars from perturbative qcd," Physical Review D **63** (2001).

[48]D. Schroeder, *An introduction to thermal physics* (Addison Wesley, 1999).

[49]M. Blau, *Lecture Notes on General Relativity*, University of Bern. URL: `http://www.blau.itp.unibe.ch/GRLecturenotes.html`. Last visited on 02/09/2019.

[50]B. Schutz, *A first course in general relativity* (Cambridge University Press, 2009).

[51]R. Littlejohn, *The Propagator and the Path Integral*, lecture notes, Quantum Mechanics PHYSICS 221A, University of California, Berkeley. URL: `http://bohr.physics.berkeley.edu/classes/221/1920/221.html`. Last visited on 25/09/2019.

[52]R. Littlejohn, *The Quantized Electromagnetic Field*, lecture notes, Quantum Mechanics PHYSICS 221A, University of California, Berkeley. URL: http://bohr.physics.berkeley.edu/classes/221/1920/221.html. Last visited on 22/10/2019.

[53]R. J. Adler, B. Casey, and O. C. Jacob, "Vacuum catastrophe: An elementary exposition of the cosmological constant problem," American Journal of Physics **63**, 620–626 (1995).

[54]L. Landau and E. Lifshitz, *Statistical physics*, v. 5 (Elsevier Science, 2013).

[55]F. Bastianelli, *Path integrals for fermions, susy quantum mechanics, etc.*. lecture notes, Theoretical Physics 2, Istituto Nazionale di Fisica Nucleare. URL: http://www-th.bo.infn.it/people/bastianelli/ch3-FT2.pdf. Last visited on 15/12/2019.

[56]A. Schmitt, *Basics of Quantum Field Theory at Finite Temperature and Chemical Potential*, Lect. Notes Phys. 811, 123–136 (2010). URL: https://link.springer.com/content/pdf/bbm%3A978-3-642-12866-0%2F1.pdf. Last visited on 04/12/2019.

[57]J. O. Andersen, *Introduction to statistical mechanics* (Akademika forlag, 2012).

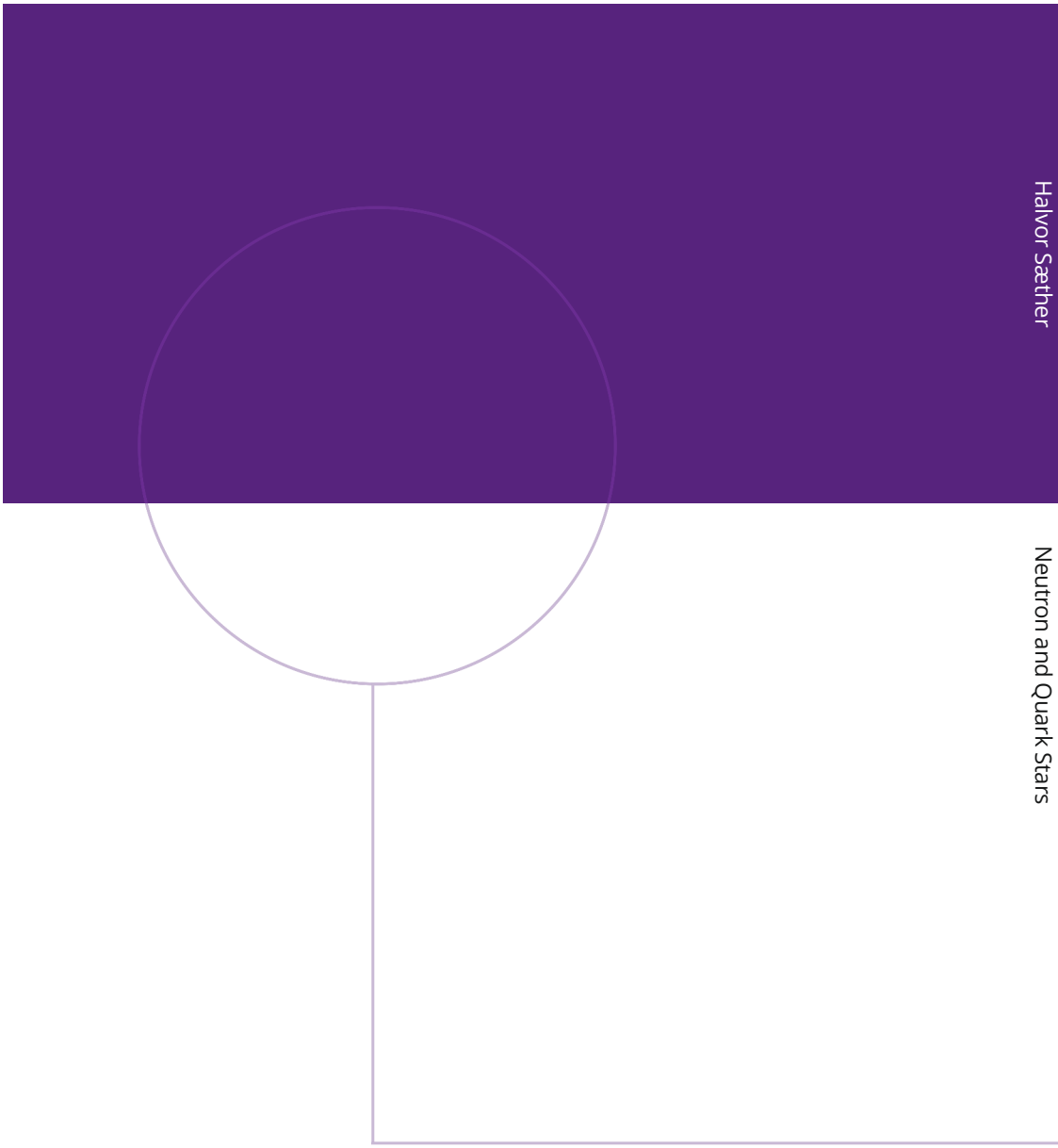

Halvor Sæther

Neutron and Quark Stars

NTNU
Norwegian University of
Science and Technology